
**Efficient and Sensitive Effect-directed Analysis
of Endocrine and Neurotoxic Effects in Aqueous Samples
Using High-performance Thin-layer Chromatography
in Combination with Effect-based Methods**

Dissertation

zur Erlangung des akademischen Grades eines
Doktors der Naturwissenschaften
– Dr. rer. nat. –

an der Fakultät für Chemie
der
Universität Duisburg-Essen

vorgelegt von
Nicolai Bätz

2024

Die vorliegende Arbeit wurde im Zeitraum von Oktober 2017 bis Mai 2022 im Arbeitskreis von Prof. Dr. Torsten C. Schmidt in der Fakultät für Chemie im Bereich Instrumentelle Analytische Chemie der Universität Duisburg-Essen durchgeführt.

Tag der Disputation: 25.07.2024

Gutachter: Prof. Dr. Torsten C. Schmidt
Prof. Dr. Dr. h.c. Henner Hollert

Vorsitzender: Prof. Dr. Maik Walpuski

DuEPublico

Duisburg-Essen Publications online

UNIVERSITÄT
DUISBURG
ESSEN

Offen im Denken

ub | universitäts
bibliothek

Diese Dissertation wird via DuEPublico, dem Dokumenten- und Publikationsserver der Universität Duisburg-Essen, zur Verfügung gestellt und liegt auch als Print-Version vor.

DOI: 10.17185/duepublico/82302

URN: urn:nbn:de:hbz:465-20240906-090153-5

Alle Rechte vorbehalten.

Erklärung

Hiermit versichere ich, dass ich die vorliegende Arbeit mit dem Titel „Efficient and Sensitive Effect-directed Analysis of Endocrine and Neurotoxic Effects in Aqueous Samples Using High-performance Thin-layer Chromatography in Combination with Effect-based Methods“ selbstständig verfasst und nur die angegebenen Hilfsmittel sowie keine anderen als die im Literaturverzeichnis angegebenen Quellen verwendet habe. Alle Stellen, die wörtlich oder sinngemäß aus veröffentlichten oder noch nicht veröffentlichten Quellen entnommen sind, sind als solche kenntlich gemacht. Die Zeichnungen und Abbildungen in dieser Arbeit sind von mir selbst erstellt worden oder mit einem entsprechenden Quellennachweis versehen. Diese Arbeit ist in gleicher oder ähnlicher Form noch bei keiner anderen Prüfungsbehörde eingereicht worden. Diese Arbeit ist auszugsweise in einer wissenschaftlichen Fachzeitschrift veröffentlicht worden.

Essen, den _____
Unterschrift

Zusammenfassung

Die stetig steigende Produktion neuer synthetischer Stoffe sowie die Nutzung und Entsorgung hunderttausender von Substanzen für unterschiedlichste Anwendungsgebiete verstärkt den weiterhin global stattfindenden Eintrag schädlicher Stoffe in die Umwelt mit entsprechenden negativen Wirkungen für Flora, Fauna und den Menschen. Dies erfordert eine umfassende Überwachung und Bewertung, die über die derzeitigen Kapazitäten der chemischen und biologischen Analytik sowie der Ökotoxikologie hinausgeht. Die effekt-dirigierte Analytik (EDA) trägt dieser Diskrepanz Rechnung, indem sie sich an Wirkungen orientiert, ein breiteres Stoffspektrum als die herkömmliche Target-Analytik abdeckt und eine zielgerichtete Analytik effektrelevanter Substanzen mit nachgeschalteten Analysemethoden ermöglicht. Eine EDA, die wirkungsbezogene Methoden mit chromatographischen Techniken kombiniert, ermöglicht eine Fokussierung auf effektrelevante Teile einer Probe.

In dieser Arbeit wurde die Hochleistungsdünnschichtchromatographie (HPTLC) mit einem innovativen transgenen Hefeassay (yeast multi-endocrine effect screen) kombiniert, der die gleichzeitige Bestimmung estrogenen, androgenen und gestagener Wirkungen auf einer HPTLC-Platte ermöglicht (HPTLC-YMEES). Zur Bestimmung von neurotoxischen Wirkungen wurde zudem ein Acetylcholinesterase-Hemmungstest mit der HPTLC verknüpft (HPTLC-AChE-I). Die Sensitivität, Präzision und Effizienz stehen bei den Untersuchungen im Mittelpunkt, um mit den optimierten Methoden einen anwendungsbezogenen effizienten Nachweis von endokrinen und neurotoxischen Umweltbelastungen zu ermöglichen. Zwei Möglichkeiten die Hefesuspension und AChE-Lösung auf HPTLC-Platten aufzutragen, Sprühen und Tauchen, wurden mittels Dosis-Wirkungs-Beziehungen von Referenzsubstanzen verglichen. Der HPTLC-AChE-I wurde um eine chemische Oxidation erweitert, um eine höhere Sensitivität gegenüber Organothiophosphaten (OTPs) zu erreichen. Abwasser-, Regenwasser- und Oberflächenwasserproben wurden mit den beiden Bioassays nach chromatographischer Auftrennung mittels HPTLC analysiert. Insbesondere der Einfluss von regenabhängigen Einleitungen wurde untersucht.

Beide Methoden ermöglichen den zuverlässigen Nachweis umweltrelevanter Konzentrationen der untersuchten Referenzhormone und OTPs. Dennoch ist eine weitere Steigerung der Sensitivität wünschenswert, um eine hohe Anreicherung zu vermeiden. Im Vergleich zur Tauchmethode wurde eine höhere Sensitivität erreicht, indem die Hefesuspension oder AChE-Lösung auf HPTLC-Platten gesprüht wurde. Ein optimiertes Sprühverfahren führte zu einer gleichmäßigeren Verteilung der Hefezellen auf der HPTLC-Platte und ergab die höchste Präzision. Aufgrund der höheren Sensitivität und Präzision wird empfohlen Hefezellen auf HPTLC-Platten zu sprühen. Im Gegensatz dazu wird trotz der etwas höheren Sensitivität der Sprühmethode aufgrund einer höheren Effizienz empfohlen, die HPTLC-Platten in die AChE-Lösung zu tauchen. Die Möglichkeit, drei endokrine Wirkungen gleichzeitig

auf einer HPTLC-Platte zu bestimmen, ist sehr effizient und daher für eine komplexe EDA besonders geeignet, erfordert jedoch weitere Anpassungen. Der HPTLC-AChE-I Ansatz wurde erfolgreich durch eine chemische Oxidation mit N-Bromsuccinimid erweitert (HPTLC-Ox-AChE-I), wodurch die Sensitivität gegenüber OTPs deutlich erhöht werden konnte.

Die Untersuchung von regenabhängigen Einleitungen ergab, dass Regenüberlaufbecken bei Regenwetter eine ähnliche oder sogar höhere endokrine Belastung des Vorfluters im Vergleich zu Kläranlagen verursachen können. Zudem wurde mit der verwendeten EDA ein AChE-I Effekt in einem an eine Autobahn angeschlossenen Regenbecken detektiert. Allerdings konnte dieser Effekt mit der verwendeten suspect- und non-target Analytik unter Verwendung der hochauflösenden Massenspektrometrie, wahrscheinlich aufgrund von störenden Substanzen und Matrixeffekten, keiner verantwortlichen Substanz zugeordnet werden.

HPTLC-YMEES und HPTLC-Ox-AChE-I eignen sich für eine EDA und ermöglichen die Detektion von mehreren endokrinen und AChE hemmenden Effekten in Oberflächen-, Regen- und Abwasser. Die HPTLC in Kombination mit wirkungsbezogener Analytik ist eine sinnvolle Methode effektrelevante Teile einer Probe zu detektieren und aufgrund der reduzierten Probenkomplexität die Wahrscheinlichkeit einer nachfolgenden Identifizierung verantwortlicher Substanzen mit weiteren analytischen Methoden zu erhöhen. Die EDA ist eine Möglichkeit die Lücke, die zwischen dem Eintrag von Substanzen in die aquatische Umwelt und dem Monitoring und der Bewertung dieser Belastungen besteht, zu verkleinern. Mit der EDA können Wirkungen und verantwortliche bekannte, aber auch unbekannte Substanzen effizient erfasst werden, um so das Wissen über Umweltbelastungen zu erweitern und eine Grundlage für geeignete Vermeidungsstrategien zu schaffen.

Summary

The constantly increasing production of new synthetic substances, as well as the use and disposal of hundreds of thousands of substances for a wide variety of applications, intensifies the ongoing global release of harmful substances into the environment, with corresponding negative effects on flora, fauna and humans. This requires comprehensive monitoring and assessment, which is beyond the current capabilities of chemical and biological analysis as well as ecotoxicology. Effect-directed analysis (EDA) takes this discrepancy into account by focusing on effects, covering a broader range of substances than conventional target analysis, and enabling the targeted analysis of effect-relevant substances with subsequent analytical methods. An EDA that combines effect-based bioanalytical methods with chromatographic techniques makes it possible to focus on the effect-relevant parts of a sample.

In this work, high-performance thin-layer chromatography (HPTLC) was combined with an innovative transgenic yeast assay (yeast multi-endocrine effect screen), which allows the simultaneous determination of estrogenic, androgenic, and gestagenic effects on one HPTLC plate (HPTLC-YMEES). To determine neurotoxic effects an acetylcholinesterase inhibition (AChE-I) assay was also coupled to HPTLC (HPTLC-AChE-I). Sensitivity, precision and efficiency are in the focus of the investigations in order to enable an application-oriented and efficient detection of endocrine and neurotoxic environmental pollution with the optimized methods. Two methods for application of the yeast suspension and AChE solution on HPTLC plates, spraying and immersion, were compared using dose-response relationships for reference substances. A chemical oxidation step was integrated in HPTLC-AChE-I to achieve higher sensitivity to organothiophosphates (OTPs). Wastewater, stormwater, and surface water samples were analyzed with the two bioassays after chromatographic separation using HPTLC. In particular, the influence of stormwater-dependent discharges was investigated.

Both methods allow reliable detection of environmentally relevant concentrations of the reference hormones and OTPs analyzed. Nevertheless, a further increase in sensitivity is desirable to avoid high enrichment. Compared to the immersion method, a higher sensitivity was achieved by spraying the yeast suspension or AChE solution onto HPTLC plates. An optimized spraying procedure resulted in a more homogeneous distribution of yeast cells on the HPTLC plate and the highest precision. Due to the higher sensitivity and precision, it is recommended to spray yeast cells onto HPTLC plates. In contrast, despite the slightly higher sensitivity of the spray method, it is recommended that the HPTLC plates be immersed in the AChE solution due to a higher efficiency. The ability to simultaneously determine three endocrine effects on one HPTLC plate is very efficient and therefore well suited for a complex EDA, but requires further adjustments. The HPTLC-AChE-I approach was successfully extended by chemical oxidation with *n*-bromosuccinimide (HPTLC-Ox-AChE-I), which significantly increased the sensitivity to OTPs.

In the study of stormwater-dependent discharges it was found that combined sewer overflows can cause similar or even greater endocrine stress to receiving waters than wastewater treatment plants. In addition, an AChE-I effect in a stormwater basin connected to a highway was detected with the EDA used. However, this effect could not be assigned to a responsible substance by suspect and non-target high resolution mass spectrometry analysis, probably due to interfering substances and matrix effects.

HPTLC-YMEES and HPTLC-Ox-AChE-I, are suitable for EDA and allow the detection of multiple endocrine and AChE inhibitory effects in surface water, stormwater and wastewater. HPTLC combined with effect-based methods is a useful method to detect effect-relevant parts of a sample and increase the probability of subsequent identification of the responsible substances by further analytical methods due to reduced sample complexity. EDA is one way to narrow the gap between inputs of substances to the aquatic environment versus the monitoring and assessment of those loads. With EDA, effects and responsible substances, both known and unknown, can be efficiently detected to increase knowledge of environmental contamination and provide the basis for appropriate mitigation strategies.

Table of Contents

Erklärung	I
Zusammenfassung.....	II
Summary	IV
Table of Contents	VI
1 General Introduction	1
1.1. Planetary boundary of novel entities.....	1
1.2. Environmental fate and (eco)toxicology – Anthropogenic contamination of the environment ..	1
1.3. The Endocrine system and its disruption – Endocrine-disruptive compounds in the aquatic environment.....	5
1.4. Neurotoxicity – Acetylcholinesterase inhibitors in the aquatic environment	13
1.5. Effect-directed analysis for comprehensive characterization of environmental samples and investigation of anthropogenic pollution.....	16
1.6. References.....	21
2 Aims and Scope	34
3 High-performance Thin-layer Chromatography in Combination with a Yeast-based Multi-effect Bioassay to Determine Endocrine Effects in Environmental Samples	36
3.1. Abstract	36
3.2. Introduction	37
3.3. Materials and methods	39
3.4. Results and discussion.....	43
3.5. Conclusion	55
3.6. Acknowledgements.....	56
3.7. Funding.....	56
3.8. References.....	56
3.9. Appendix	60
4 High-performance Thin-layer Chromatography in Combination with an Acetylcholinesterase-inhibition Bioassay with Pre-oxidation of Organothiophosphates to Determine Neurotoxic Effects in Storm, Waste, and Surface Water	70
4.1. Abstract	70
4.2. Introduction	71
4.3. Materials and methods	72
4.4. Results and discussion.....	76
4.5. Conclusion	84
4.6. Acknowledgements.....	84

4.7. Funding.....	84
4.8. Open Access	85
4.9. References.....	85
4.10. Appendix	89
5 Effect-directed Analysis of Endocrine and Neurotoxic Effects in Stormwater-Dependent Discharges.....	97
5.1. Abstract.....	97
5.2. Introduction	97
5.3. Material and methods.....	99
5.4. Results and discussion.....	105
5.5. Conclusion and Outlook.....	111
5.6. Acknowledgements.....	112
5.7. References.....	112
5.8. Appendix	117
6 General Conclusions and Outlook.....	139
6.1. References.....	149
Appendix	VIII
List of Figures.....	VIII
List of Tables.....	X
List of Abbreviations.....	XIII
List of publications.....	XV
Declaration of Scientific Contributions	XVI
Curriculum Vitae.....	XVI
Danksagung	XVII

1 General Introduction

1.1. Planetary boundary of novel entities

Chemical pollution of the environment is one of the "planetary boundaries" postulated by ROCKSTRÖM et al. (2009) in which humans can safely live and develop. In fact, ARP et al. (2023) describe that 10-20 million new substances are currently registered with the Chemical Abstract Service (CAS) each year, in addition to the more than 200 million substances already listed. According to WANG et al. (2020), more than 350,000 chemicals and mixtures are approved for use worldwide. PERSSON et al. (2022) assume that humanity has passed the planetary boundary for novel entities, as production and inputs to the environment exceed the capacity for monitoring and assessment. Safe human development would thus be jeopardized, and defined goals such as good ecological and chemical status of water bodies under the Water Framework Directive (WFD) may not be achieved (EU, 2000).

1.2. Environmental fate and (eco)toxicology – Anthropogenic contamination of the environment

The extensive production and use of chemicals, as well as the daily chemical processes in our industrialized society, cause far-reaching problems when substances do not remain in a closed system but are released into the environment. This can happen in several ways. Substances can evaporate or leach out of materials during degradation, but they can also be released directly into the environmental compartments of the geosphere as waste products, either intentionally for use or accidentally. Major pathways to the hydrosphere include discharges of untreated and treated wastewater, point and diffuse discharges of surface runoff as well as atmospheric deposition (BRUSSEAU AND ARTIOLA, 2019; WALKER et al., 2019). After a substance is released into the air, water, or soil, it undergoes various transport and transformation processes (Figure 1-1). The distribution, dilution, accumulation, transformation and degradation of a substance, as well as the temporal and spatial dimensions of these processes, are determined by abiotic and biotic factors in the respective environmental compartments, as well as by the properties of the specific substance (HEMOND AND FECHNER-LEVY, 2023).

In the environment, organic pollutants can be divided into classes based on persistence, fate, and toxicity. Persistent organic pollutants (POPs) are difficult to degrade and therefore remain in the environment for a long time. They have the potential for long-range atmospheric transport and can thus be distributed globally (EISENREICH et al., 2021). Persistent, bioaccumulative and toxic (PBT), and very persistent and very bioaccumulative (vPvB) pollutants are persistent, non-polar substances that bind to biomass and particles, accumulate in the food chain and have toxic properties. Under REACH, chemicals are evaluated according to these properties (EU, 2006). Persistent mobile organic compounds (PMOCs), on the other hand, are not yet explicitly covered under REACH but have a high

polarity and are therefore very hydrophilic, making them highly mobile in aquatic systems and capable of penetrating aquifers and endangering drinking water resources (REEMTSMA et al., 2016; JIN et al., 2020). PMOCs are difficult to remove using conventional water treatment methods and there is a need for other than the established analytical methods to detect them (KNEPPER et al., 2020). If these substances additionally exhibit toxic properties, they can be described as persistent, mobile and toxic (PMT) or very persistent and very mobile (vPvM). They may represent an equivalent level of concern as PBT and vPvB substances (HALE et al., 2020) and appear to be abundant in the aquatic environment (NEUWALD et al., 2021).

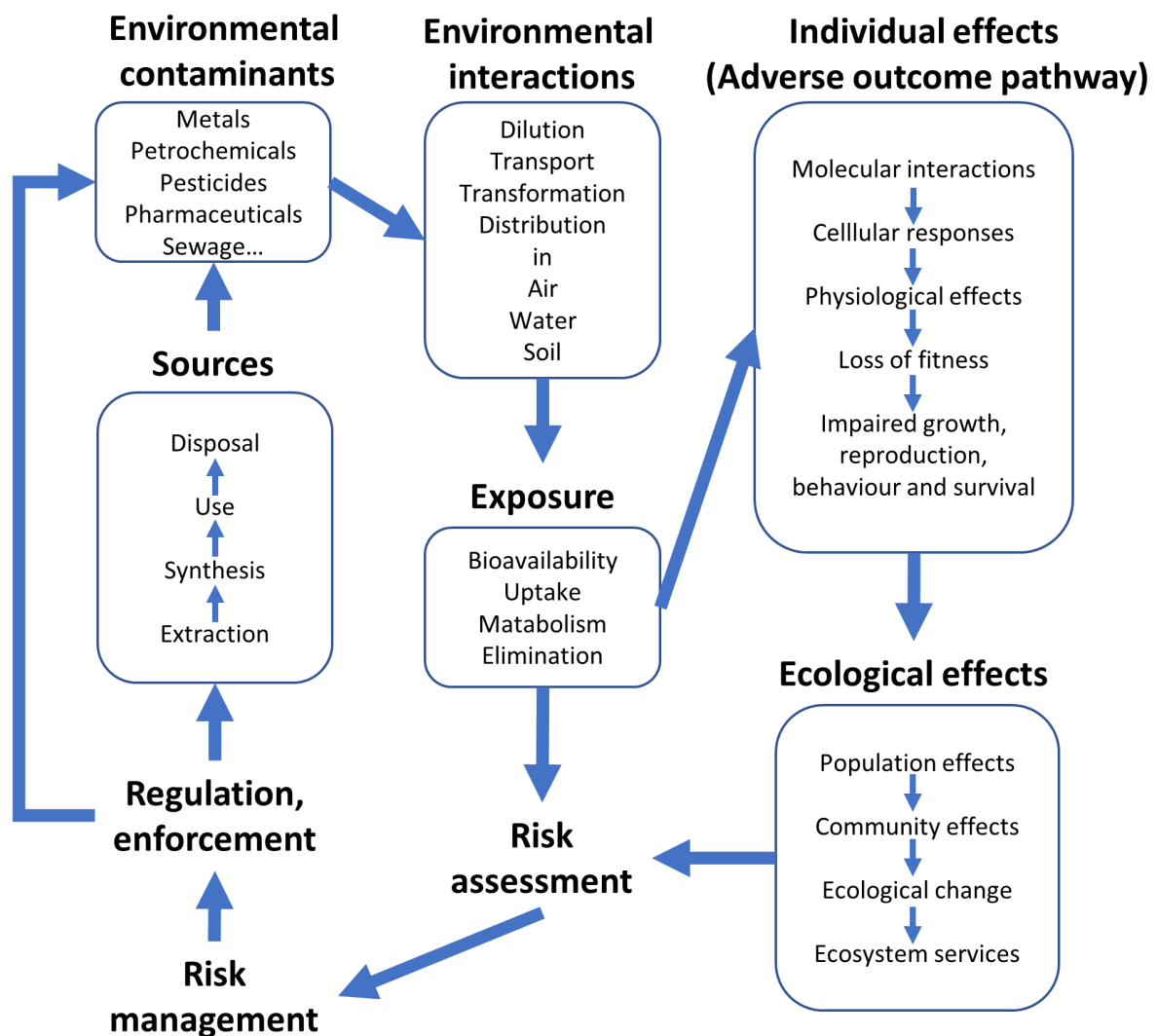


Figure 1-1 Environmental fate, ecotoxicology and risk assessment of contaminants released to the environment from anthropogenic sources. Adopted from WELBOURN AND HODSON (2022) in a modified version.

Exposure of an organism to contaminants requires that substances are bioavailable (Figure 1-1). The bioavailability of a substance depends on abiotic and biotic factors in the particular contaminated system and can change with changing conditions. Together with the properties of the substance and the concentration in the relevant medium, this determines the probability of uptake. In animals and humans, contaminants are primarily absorbed through the digestive system, the respiratory tract, i.e. lungs or gills, or the skin. In plants, this occurs through the leaves and roots. Excluding uptake processes such as endocytosis, substances are absorbed in a dissolved state. After exposure and uptake, depending on their properties, substances are distributed in the body, transported to specific areas or organs, and metabolized by the organism. Depending on their persistence and lipophilicity, substances may be stored and accumulated in tissues for shorter or longer periods of time. If a substance is very bioaccumulative, the concentration in the tissue may continue to increase with increasing trophic level. The result is biomagnification, in which the substance accumulates in the food chain. Elimination in the organism occurs either directly by excretion or by biological transformation of the substance into a subsequent product. Due to altered properties, metabolites have a different behavior and effect in the organism than their parent compounds (CAMPBELL et al., 2022).

Substances become problematic when they exhibit toxicity to organisms. The adverse outcome pathway describes the mode of action (MoA) of a substance with the respective consequences of the interlinked key events along different biological levels of organization (Figure 1-1). After exposure and uptake, a molecular initiating event occurs at the site of action (SoA), such as an interaction between a contaminant and a molecular receptor, which triggers a biochemical response. The amount of a pollutant determines the strength of the triggered signal or the achievement of an effect plateau (dose-response relationship), e.g., when all receptors are occupied. The biochemical signal triggered by a substance at the SoA leads to further effects from the cellular level through the organs/tissues to the organism itself. Exposure to contaminants can cause various physiological and developmental consequences in organisms. Growth, reproduction, and behavior may be affected, and mortality can increase. Outside the organism, the chain of effects can affect the fitness of the entire population, which in turn can affect the composition and interactions in communities and the ecosystem. Ecological structures and functions can change, and ecosystem services might be lost (HODSON AND WRIGHT, 2022a). Estimating the ecological effects of pollutants is very complex due to the various abiotic and biotic influencing factors in the contaminated ecosystem, the different MoAs and interactions in pollutant mixtures, and the increasingly complex individual and ecological effects at different biological levels (molecular to ecosystem). The significance of ecotoxicological bottom-up assessments based on individual tests of a few model species in the food web and the resulting risk assessment is thus limited in terms of ecological consequences (WINDSOR et al., 2018; HODSON AND WRIGHT, 2022a).

The interaction between changing environmental variables as a result of climate change and pollutant loads may influence toxicokinetic and -dynamic processes as well as entail altered ecological consequences. Pollution of ecosystems and the associated weakening of organisms and populations can reduce resilience to changing environmental conditions and the ability to adapt to new living conditions. Conversely, sensitivity to a chemical may increase when environmental variables reach an organism's tolerance level (HOOPER et al., 2013; WRIGHT AND CAMPBELL, 2022). A simple example of changing exposure conditions in advancing climate change is the increased frequency of prolonged droughts, which can lead to high concentrations of pollutants in water bodies with low water levels, further increasing toxic exposure to living organisms. According to DECOURTEN et al. (2019), exposure to endocrine-disruptive compounds (EDCs) and their effects on aquatic organisms may change in the context of altered abiotic factors, such as oxygen depletion, acidification, and alterations in temperature and salinity due to climate change. The global loss of biodiversity may be exacerbated by pollutant loads in conjunction with the effects of global climate change. Ultimately, exposure to pollutants can affect the entire biosphere and have global consequences.

In summary, substances introduced into the environment can have adverse effects on flora, fauna, and humans. They can alter or disrupt processes and cycles from the molecular level in organisms to the global scale along their adverse outcome pathway. Interacting with other planetary processes, such as global climate change, the effects of pollution can be amplified. In this way, the planetary boundary of novel entities can be further exceeded, accelerating other boundaries such as biodiversity loss and making human development unsafe due to lack of ecosystem services.

1.3. The Endocrine system and its disruption – Endocrine-disruptive compounds in the aquatic environment

The endocrine system is a chemical communication network that, through the specific transport and action of hormones, results in a wide range of different biological responses in vertebrates and invertebrates and controls essential physiological and developmental functions of an organism. The hypothalamic-pituitary axis regulates formation and release of hormones in vertebrates (Figure 1-2).

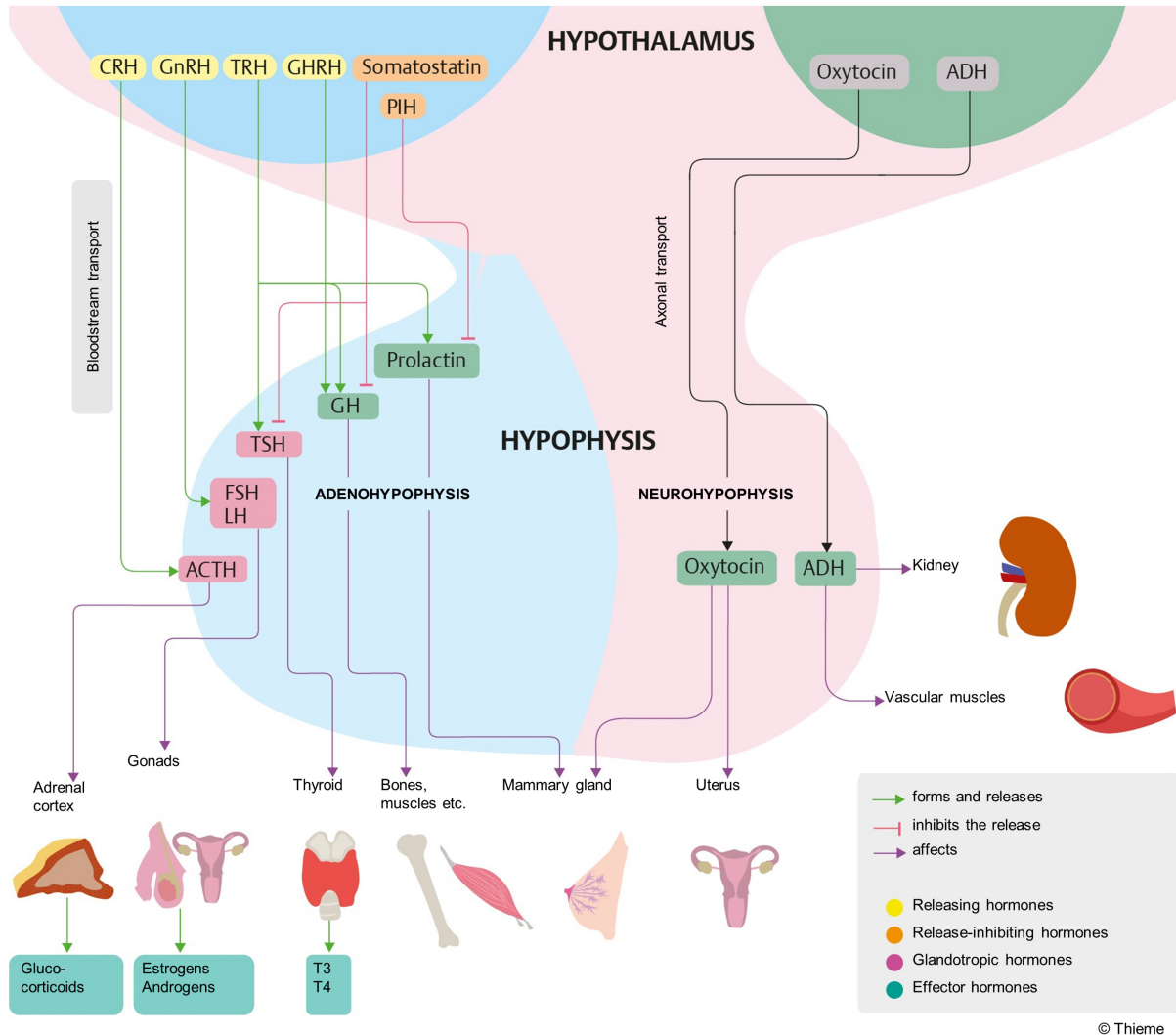


Figure 1-2 The hypothalamic-pituitary axis controls the synthesis and release of hormones. Releasing hormones (CRH, corticotropin-releasing hormone; GnRH, gonadotropin-releasing hormone; TRH, thyrotropin-releasing hormone; GHRH, growth hormone-releasing hormone) and release-inhibiting hormones (somatostatin; PIH, prolactin-inhibiting hormone) are formed in the hypothalamus, transported to the adenohypophysis and initiate or inhibit the formation and release of glandotropic (ACTH, adrenocorticotropin hormone; LH, luteinizing hormone, and FSH, follicle-stimulating hormone; TSH, thyroid-stimulating hormone) and effector (GH, growth hormone and prolactin) hormones. The effector hormones antidiuretic hormone (ADH) and oxytocin are formed in the neurohypophysis triggered by neural stimulation emanating from the hypothalamus. Effector and glandotropic hormones are transported to different target organs. ACTH, FSH and LH, and TSH stimulating the formation of glucocorticoids, estrogens and androgens, triiodothyronine (T3) and thyroxine (T4). Adopted from: I Care. Anatomie Physiologie, 2. Aufl., Stuttgart, Thieme 2020: Abb. 11.6.

In this process, neurohormones (hypophysiotropic hormones) are formed in the hypothalamus by sensory information in neurosecretory cells, transported via the bloodstream to the adenohypophysis, and act as releasing factors on tropic secreting cells, initiating or inhibiting the formation and release of tropic and effector hormones. Along the three endocrine axes hypothalamic-pituitary-adrenal (HPA), -gonadal (HPG), and -thyroid (HPT), the respective tropic hormones are transported to the adrenal cortex (adrenocorticotrop hormone, ACTH), to the gonads (luteinizing hormone, LH and follicle-stimulating hormone, FSH), and to the thyroid gland (thyroid-stimulating hormone, TSH). They stimulate the formation and release of the respective effector hormones in the target organ. HPA leads to the formation of glucocorticoids and mineralocorticoids, which regulate for example glucose level and blood pressure. HPG leads to the production of estrogens and androgens, which regulate reproduction. HPT leads to the formation of triiodothyronine (T3) and thyroxine (T4), which regulate temperature and energy balance as well as metabolism. Growth hormone (GH), which regulates growth, and prolactin (PRL), which is responsible for milk production in mammals, are formed directly in the adenohypophysis, triggered by the corresponding neurohormones from the hypothalamus, and transported as effector hormones to the corresponding organs. Neurosecretory cells connecting the hypothalamus to the neurohypophysis allow direct formation of the antidiuretic hormone (ADH), which regulates ion and water balance, as well as oxytocin, which control parturition and reproduction (METCALFE et al., 2022a).

The gonadotropins LH and FSH regulate sexual development and reproduction in mammals. They act in the ovaries and testes on estrogen and androgen production, regulating oogenesis and spermatogenesis. ACTH regulates the formation of mineralocorticoids and glucocorticoids in the adrenal cortex. Estrogens, androgens, mineralocorticoids, and glucocorticoids are steroid hormones with a similar structure based on the underlying polycyclic alcohol cholesterol. The biosynthesis of steroid hormones begins in the mitochondria with the transformation of cholesterol to the gestagen pregnenolone (Figure 1-3). Various enzymes, in particular cytochromes P450, are involved in the entire steroid hormone genesis. Starting with pregnenolone and the other gestagens, androgens, estrogens, mineralocorticoids, and glucocorticoids are formed (METCALFE et al., 2022a).

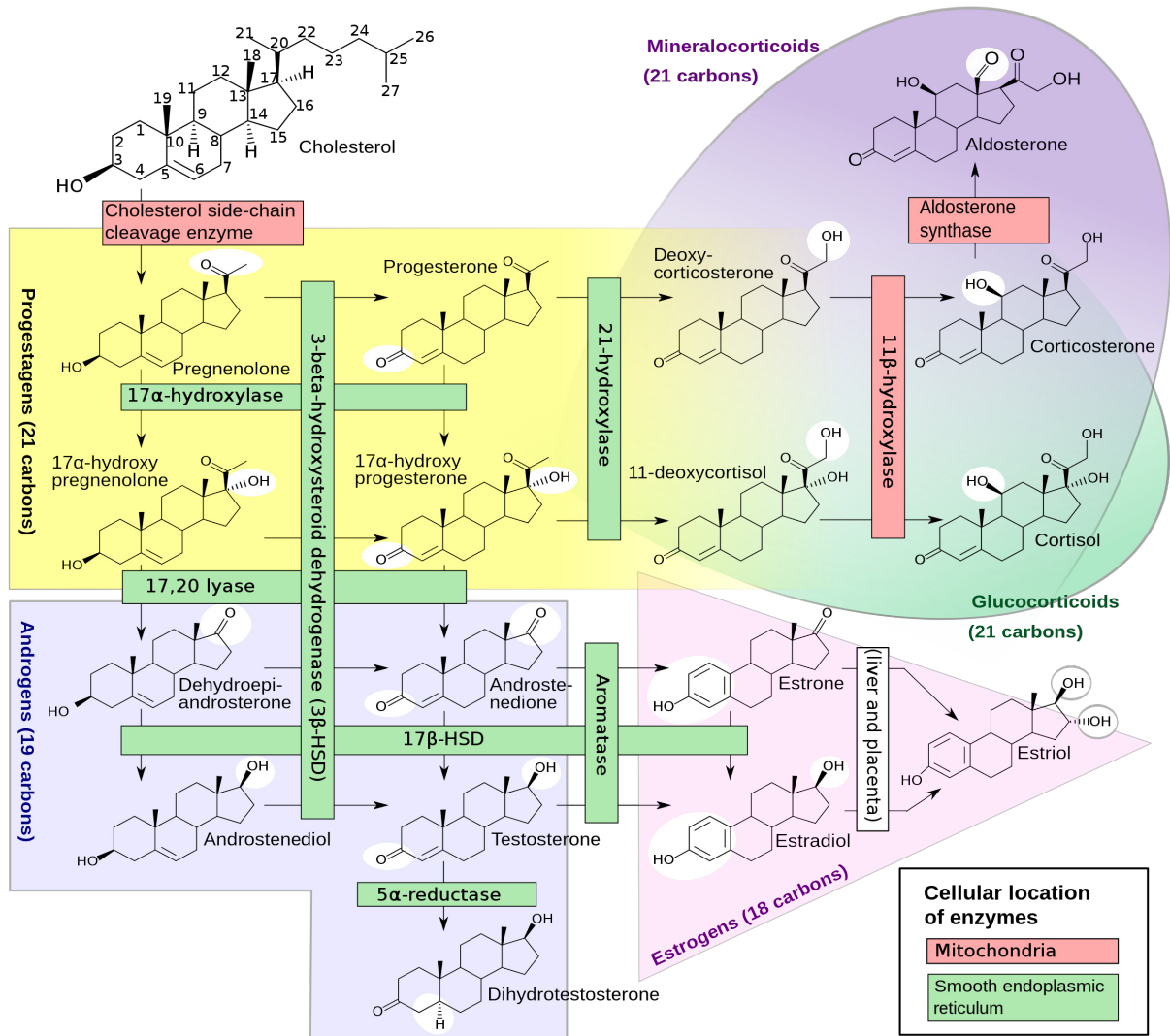


Figure 1-3 Genesis of the major classes of steroid hormones: progestagens, mineralocorticoids, glucocorticoids, androgens, and estrogens. Shown are the Enzymes involved in human steroidogenesis, their cellular location, substrates, and products. White circles indicate changes in molecular structure compared with precursors. Adopted from HÄGGSTRÖM AND RICHFIELD (2014).

“An endocrine-disrupting chemical (EDC) is an exogenous chemical, or mixture of chemicals, that can interfere with any aspect of hormone action” (ZOELLER et al., 2012). EDCs can be substances that are not hormones but, due to their structure, have the ability to bind to a hormone receptor (HR) or otherwise disrupt the hormone balance and genesis of an organism. These include substances from a wide variety of groups including heavy metals or organic pollutants such as polycyclic aromatic hydrocarbons. But also various synthetic substances from diverse groups, including pharmaceuticals such as ibuprofen and carbamazepine, personal care products containing for example parabens, plasticizers such as phthalates, flame retardants such as polybrominated diphenyl ethers (PBDEs), pesticides such as organotin and organochlorine compounds, triazines and polychlorinated dibenzofurans (PCDFs), and other industrial chemicals such as perfluorinated chemicals (PFCs), polychlorinated biphenyls (PCBs), bisphenol A and its substitutes, as well as by-products, intermediates

and degradation products such as polychlorinated dibenzodioxins (PCDDs) and nonylphenol, are among the EDCs. In addition to synthetic hormones such as 17 α -ethinylestradiol (EE2), natural steroid hormones such as estrone (E1), estradiol (E2), and estriol (E3), which enter organisms in unnatural ways and amounts and thus affect hormone balance, are also considered EDCs (ROCHESTER AND BOLDEN, 2015; KASONGA et al., 2021; PIRONTI et al., 2021; METCALFE et al., 2022a). Moreover, EDCs include transformation products (TPs) that may be formed, for example, by metabolism, biodegradation, photolytic degradation, or during various industrial processes as well as wastewater and drinking water treatment measures, but whose pathways and endocrine potential have often not yet been sufficiently investigated (KNOOP et al., 2018a; GONSIOROSKI et al., 2020; OJOGHORO et al., 2021; BRÖCKER et al., 2022; CARSTENSEN et al., 2022; KLANČIČ et al., 2022; NOWAK AND JAKOPIN, 2023).

Due to their diversity and different structures, EDCs have different MoAs in the endocrine system and along the endocrine axes. They can mimic (agonists) or inhibit (antagonists) the action of naturally occurring hormones in the organism at the molecular and cellular level, affect the biosynthesis and homeostasis of hormones and the enzymes involved, interfere with the function of hormone transport proteins or neuroendocrine axes (neuroendocrine disruption). When EDCs, as well as natural hormones, bind to corresponding nuclear HRs and activate (agonistic effect) or block (antagonistic effect) them, they affect the transcription of a gene and change gene expression (METCALFE et al., 2022a). Estrogens, androgens, gestagens, glucocorticoids, and mineralocorticoids have associated nuclear receptors that, when activated, act as transcription factors and bind to genes with the corresponding response elements in the nucleus (OJOGHORO et al., 2021; METCALFE et al., 2022a). Each individual natural and synthetic ligand has a different degree of potency toward the specific receptor (KUIPER et al., 1997; JEYAKUMAR et al., 2011). HRs in vertebrates may differ from each other, as is partially the case in humans and fish, resulting in different affinities of ligands such as gestagens to interspecific gestagen receptors, making cross-species statements not straightforward (VAN DEN BELT et al., 2004; OJOGHORO et al., 2021). EDC-induced disruption of natural hormonal communication can result in various short- and long-term toxic effects at the organism level, involving physiological homeostasis, metabolism, reproduction, development, growth, and behavior. Studies include humans and other mammals, as well as fish, amphibians, birds, reptiles, and various invertebrates (GORE et al., 2015; GONSIOROSKI et al., 2020; TRUDEAU et al., 2020; YILMAZ et al., 2020; OJOGHORO et al., 2021; METCALFE et al., 2022a). EDCs also have the ability to affect gene expression through epigenetic modification without altering the DNA sequence, allowing for effects in subsequent generations (WARNER et al., 2020). The challenge with ecotoxicological studies, which are mainly conducted at the laboratory scale, is the applicability to environmental exposure scenarios, since, among other things, the concentrations investigated in the laboratory are often higher than the detected environmental concentrations (METCALFE et al., 2022a).

The study by KIDD et al. (2007), which cannot be repeated from a bioethical point of view, is a clear demonstration of the negative effects of estrogens on a fish population in a whole-lake study. The population of *Pimephales promelas* (RAFINESQUE, 1820) was nearly extinct after chronic exposure to 5-6 ng/L of EE2. The authors observed a feminization of male fish based on the production of vitellogenin mRNA and protein, as well as a change in gonadal development and oogenesis in males and females, respectively. Because EDCs occur in mixtures in the aquatic environment, there are mixture toxicities, i.e., effects that may be different from those caused by individual substances. HAMID et al. (2021) urgently recommend intensifying research in this area for risk assessment of EDCs. According to MARLATT et al. (2022), the long-term effects of EDCs should be investigated more intensively in studies at the population level, with more attention to field observations. In addition, they suggest that interdisciplinary research is appropriate due to the multidisciplinary nature of EDCs and adverse endocrine effects with implications for humans and animals.

Endocrine changes and diseases observed in natural populations show the true ecotoxicological impact and concentrations found in various aquatic matrices, the magnitude of exposure to EDCs. EDCs have been globally dispersed in the hydrosphere by human activities and have been detected in almost all aquatic compartments, so both aquatic organisms and humans may be exposed to EDCs and their adverse effects (GONSIOROSKI et al., 2020; SACDAL et al., 2020; KASONGA et al., 2021; PIRONTI et al., 2021; DUEÑAS-MORENO et al., 2022; FINCKH et al., 2022; GOEURY et al., 2022; BALAKRISHNA et al., 2023). Although many EDCs are known, it is difficult to identify the actual endocrine disruptors because effects in aquatic environmental samples are usually caused by a mixture of various known and unknown substances (BRACK et al., 2019). Endocrine agonistic and antagonistic effects have been detected in the aquatic environment on a global scale in many surface waters, wastewaters, and in areas with different land uses without knowing the triggering substances (ITZEL et al., 2018; DE BAAT et al., 2019; ARCHER et al., 2020; STAVREVA et al., 2021; YUSUF et al., 2021; KIENLE et al., 2022). Synergistic, inhibitory and masking interactions may occur due to the different agonistic and antagonistic endocrine effects induced by different EDCs in complex aquatic samples (ITZEL et al., 2019; PANNEKENS et al., 2019). Treated and untreated wastewater and surface runoff are the main routes for EDCs to enter the aquatic environment (PIRONTI et al., 2021). Many EDCs cannot be retained or degraded in conventional wastewater treatment plants (WWTPs) and are therefore discharged into receiving waters (SPATARO et al., 2019; ITZEL et al., 2020; ZWART et al., 2020; GROBIN et al., 2023). Depending on the land use, stormwater runoff may contain various EDCs that have been washed off the surface or leached from materials and enter water bodies diffusely via surface runoff or selectively via stormwater structures (PARAJULEE et al., 2017; LAMPREA et al., 2018; MASONER et al., 2019; HAVENS et al., 2020; MÜLLER et al., 2020; WICKE et al., 2021; MÜLLER et al., 2022). During heavy rainfall that exceeds the capacity of combined sewer systems, untreated wastewater is discharged from combined sewer overflows (CSOs),

introducing wastewater-like substances into water bodies that can have endocrine disrupting effects (BOTTURI et al., 2021; SHULIAKEVICH et al., 2022; WOLF et al., 2022). With an observed increase in the frequency and intensity of heavy precipitation likely due to climate change, such loads will become more important (NISSEN AND ULBRICH, 2017; IPCC, 2023).

Due to the inadequate treatment performance of conventional wastewater treatment plants for many micropollutants, various systems are used to retain or transform them into less toxic metabolites. The performance of the various physical, chemical, electrochemical and biological treatment methods depends on the physico-chemical and biological properties of the materials, organisms and processes used, the properties of the substances, and the process conditions (temperature, pH, etc.), as well as the co-existence of process-promoting or process-inhibiting substances and matrix components (VIEIRA et al., 2021; AZIZI et al., 2022; LIM et al., 2022).

Physical treatment uses the process of adsorption to bind substances to a material. Adsorption can be improved by maximizing the surface area and by exploiting certain material properties. A wide variety of high surface area materials are used, most commonly activated carbon, but also carbon nanotubes and silicate minerals such as zeolites. Adsorption is considered to be an effective treatment method for various EDCs or the reduction of hormonal activities (VÖLKER et al., 2019; AZIZI et al., 2022). Another physical treatment technique is membrane filtration. Depending on the pore size of the membrane, this can be divided into microfiltration, ultrafiltration, nanofiltration and reverse osmosis. The key process that allows EDCs to be retained is filtration through the size of the membrane pores. The finer the pores, the more energy is required to build up the pressure necessary to push the wastewater through the membrane. Other retention processes include electrostatic, where the membrane is charged by functional groups, and physicochemical, where substances are adsorbed to the membrane (AZIZI et al., 2022). In summary, these physical treatments are technologies that retain EDCs and other contaminants. As a result, the contaminants are present in concentrated form in the adsorbent or filtrate and require further treatment.

Advanced oxidation processes (AOPs) convert contaminants into less complex TPs, allowing for easier removal with subsequent treatment steps. Some of the methods, such as ozonation, are already in full-scale operation (TUERK et al., 2016; ITZEL et al., 2017; LIM et al., 2022), while others have been studied primarily on a laboratory or pilot scale (VIEIRA et al., 2021). Processes such as photolysis, photocatalysis, ozonation, sonolysis and Fenton reaction are based on the formation of oxidizing radicals and their reaction with the target substance. Normally, toxicity is reduced by AOPs because the reaction takes place at the functional groups of the target substances. For example, the endocrine potential of TPs is usually significantly lower than that of parent estrogens (LEE et al., 2008). AOPs can achieve high efficiencies in removing micropollutants, hormonal activities, and other effluent toxicities (WESTLUND et al., 2018; VÖLKER et al., 2019; VIEIRA et al., 2021; WOLF et al., 2022).

During AOPs, toxic oxidation byproducts, such as bromates, and TPs from micropollutants, that have a new or higher toxicity than the parent compound, may be formed (LIM et al., 2022). The formation of oxidation byproducts and TPs, which can result in a change in the toxicity of the effluent, depends, among other things, on the properties and concentrations of the reactive species and organic pollutants, residual oxidants, dissolved organic matter, and the parameters set for the AOP (KHAREL et al., 2020; VIEIRA et al., 2021; WANG AND WANG, 2021). The formation of substances with genotoxic and mutagenic properties is of particular concern (MIŠÍK et al., 2020). The problem of endocrine active TPs and resulting hormonal activities after AOPs has already been documented (KNOOP et al., 2018b), but requires more intensive monitoring and further research to better determine the frequency, risks, and influencing factors.

In addition, biological aerobic and anaerobic processes such as membrane bioreactors can contribute to the reduction of EDCs mainly through biodegradation and adsorption to activated sludge. Biological methods are highly variable in their effectiveness due to species dependency and community composition and may not achieve complete degradation of EDCs. More research is needed on the efficacy and practicality of biological methods, such as the use of biofilms or approaches using microalgae, fungi and enzymes. Nevertheless, biological treatment processes promise to be a sustainable alternative to physical and chemical treatment to remove EDCs from wastewater through biodegradation (GADUPUDI et al., 2021; ROCCUZZO et al., 2021; AZIZI et al., 2022; MOUKHTARI et al., 2023). Hybrid solutions offer a good opportunity to increase treatment performance or to compensate for disadvantages of a single method. A combination of biological processes with AOPs is useful to bind or degrade TPs, e.g., from ozonation, with subsequent biological treatment steps to reduce the toxicity of the effluent and prevent for example endocrine active metabolites from entering receiving waters (ITZEL et al., 2020; WANG AND WANG, 2021). The combination of ozonation and activated carbon is also a method already in use for the reduction of reaction products (ITZEL et al., 2018; KIENLE et al., 2022). The combination of different AOPs, such as ozonation in combination with photolysis or Fenton, can increase reaction kinetics, improve pollutant degradation and mineralization, and reduce toxicity in the effluent (VIEIRA et al., 2021).

In addition to pollution from WWTPs, discharges of untreated wastewater from CSOs impacting the aquatic environment. Various nature-based solutions and technical processes can be used to treat wastewater discharged from CSOs (BOTTURI et al., 2021). Constructed wetlands, bioretention filters or retention soil filters are widely used in practice in different designs and combinations to reduce organic carbon, chemical oxygen demand, ammonium, and phosphorus but also micropollutants, such as EDCs, as well as undesired microorganisms and bacteria (SCHEURER et al., 2015; TONDERA et al., 2019; BOTTURI et al., 2021). They can be used to treat effluent from WWTPs and CSOs simultaneously, and as activated soil filters in combination with adsorbents, such as activated carbon, to enhance removal of

micropollutants from wastewater (BRUNSCH et al., 2020; BOTTURI et al., 2021). This allows EDCs such as certain phenols to be retained in case of an overflow event (WIRASNITA et al., 2018). In addition to the characteristics of the pollutant and its removal pathway, several factors play a role in removal efficiency of retention soil filters, particularly influent concentration, filter layer thickness, and filter age (TONDERA et al., 2019; RUPPELT et al., 2020).

Overall, the choice of technology is based on site conditions and must be adapted or combined accordingly. Decisive factors influencing the effectiveness of the selected process are the wastewater characteristics: general parameters, especially pH and temperature, matrix components, and possible EDCs or other micropollutants with adverse effects. In addition, retained or newly formed contaminants must be dealt with. The new process must be integrated into the existing WWTP process technology or must be adapted to the circumstances and irregular overflow events of a CSO. Accordingly, the respective treatment method should be extensively investigated and monitored analytically in the laboratory, pilot and full-scale for its performance with respect to individual EDCs, endocrine disruptive TP and hormonal activities as well as other toxic endpoints and individual substances (ITZEL et al., 2017; BOTTURI et al., 2021; BERTANZA et al., 2022).

The high variability of known and unknown substances, as well as metabolites and TPs makes the group of EDCs broadly diversified. Their ubiquitous and continuing, partly unrestricted entry into various environmental compartments, including the hydrosphere, increases the risk of exposure and thus of potential disruption of various parts of the endocrine systems of animals and humans, with consequences for reproduction, growth, development, metabolism, homeostasis and behavior. All this underscore the urgency of further interdisciplinary research, including in the fields of environmental analysis and toxicology, to enable consistent technical and regulatory measures and awareness raising to mitigate the hazards posed by EDCs.

1.4. Neurotoxicity – Acetylcholinesterase inhibitors in the aquatic environment

Endocrine disruption can also lead to neurotoxic consequences if the hormonal communication for the development of neurons is disrupted by EDCs. Neurotoxicants affect the brain, central or peripheral nervous system, or sensory organs, and can have a significant impact on development and behavior. Neurotoxic substances include pesticides, pharmaceuticals, and heavy metals, and a wide range of substances which are believed to have neurotoxic potential (LEGRADI et al., 2018; IQUBAL et al., 2020). Due to the diversity of potentially neurotoxic substances, MoAs have only been partially elucidated, mostly for a few model organisms and humans (LEGRADI et al., 2018; IQUBAL et al., 2020). In chemical evaluation and authorization under REACH and especially for pesticides, which often have a neurotoxic MoA, by the European Food and Safety Agency, the required studies are very limited. They only have to be carried out for quantities > 10 tons/year and only apply to certain mammals and birds (LEGRADI et al., 2018). Other vertebrate and invertebrate organisms and, in the case of pesticides, non-target species are excluded. In addition, monitoring with targeted instrumental analysis of a few known substances under the WFD is very limited to detect the occurrence, neurotoxic potential, and mixing effects of hundreds of thousands of registered and produced substances, as well as unknown TPs and metabolites that may be present in environmental samples (LEGRADI et al., 2018).

In particular, the developing nervous system and brain are very sensitive to toxic effects, and exposure in early life stages can lead to permanent or delayed consequences in the organism. The temporal and spatial toxicity profiles with different sensitivities depending on the developmental stage and different SoA in the complex nervous system make it challenging to determine the MoA of potentially developmental neurotoxic substances in different species. Experimental data are lacking to classify more substances as developmental neurotoxins (LEGRADI et al., 2018; CHEN et al., 2021). FRITSCHÉ et al. (2018) call for the establishment of existing *in vitro* methods and *in silico* modeling in the regulatory field to capture the unknown developmental neurotoxicity of many potentially neurotoxic substances present in the environment. To the same extent as for humans, testing with ecologically relevant model organisms should be used to investigate the diverse developmental neurotoxic MoAs and their interspecies variation for sound ecological risk assessment (LEGRADI et al., 2018). As shown by REINWALD et al. (2022), transcriptomic responses to neurotoxicants could be used as biomarker-based *in vitro* assays to predict MoAs that affect neuronal development.

Other possible, but poorly understood, MoAs of neurotoxicants include epigenetic effects (LEGRADI et al., 2018), i.e., alteration of gene expression without alteration of the DNA itself through methylation, histone modification, and non-coding RNA. Again, early life stages may be susceptible to neurotoxic stress if, for example, DNA methylation is disrupted during reprogramming stages for specific gene expression in the developing nervous system. Gene expression and thus the phenotype can be altered, resulting in altered nervous system development and potentially long-term adverse effects on the

AChE inhibitors are used for medicinal purposes, as combat agents and insecticides. Organophosphates and carbamates are the most widely used and applied AChE inhibiting insecticides (KUSHWAHA et al., 2016; DE SOUZA et al., 2020). Many organophosphates are organothiophosphates (OTPs), which are metabolically oxidized in the organism by cytochrome p450 monooxygenases and have a higher inhibitory potential than their unoxidized forms. In the oxidation process, the sulfur atom at the central phosphorus atom of OTPs is replaced by an oxygen atom. The degree of inhibition is determined by the ratio of detoxification to oxidation in the organism and is therefore species specific (LEGRADI et al., 2018).

Insecticides enter the aquatic environment primarily by diffuse pathways and pose a risk to aquatic invertebrate communities by affecting, for example, insect populations (LIESS et al., 2021). After application, they may enter the atmosphere by evaporation and be carried to water bodies by precipitation or dry deposition. Insecticides can also be washed from plants and soils by rainfall and enter waterbodies through surface runoff. Organophosphate insecticides, such as chlorpyrifos and malathion, have been detected in surface waters around the world and continue to be used worldwide (DE SOUZA et al., 2020). Due to the diffuse nature of the input of insecticides and other pesticides into surface waters, selective measures are only of limited help in achieving retention. Riparian buffer zones can help to reduce pesticide runoff into surface waters, and can also provide other benefits such as nutrient retention, erosion reduction, biodiversity enhancement, flood protection, and generally enhance the climate resilience of water bodies, e.g., by providing additional shade (ARORA et al., 2010; BUTKOVSKYI et al., 2021; WU et al., 2023). Retention efficiency depends on several factors, especially the width, continuity, and vegetation of the buffer strip (AGUIAR JR. et al., 2015; VORMEIER et al., 2023). Expanded regulatory measures, controlled sustainable use of pesticides, and increased restrictions on approvals in case of negative environmental behavior and toxic properties would go a long way toward reducing stress on aquatic systems.

1.5. Effect-directed analysis for comprehensive characterization of environmental samples and investigation of anthropogenic pollution

Endocrine and neurotoxic effects are caused by a wide variety of known and unknown EDCs and neurotoxicants that occur as mixtures in environmental samples. Comprehensive and efficient effect-directed analysis (EDA) is predestined for the identification of known and unknown substances as well as their effects, so that sources, input pathways and toxic loads can be revealed and the efficiency of treatment measures can be evaluated.

Chemical target analysis (TA), which refers only to known substances and, depending on the scope, only covers a certain group of compounds (WICKE et al., 2021; METCALFE et al., 2022b), is therefore not suitable on its own to provide sufficient information for characterizing the hazard potential of an environmental sample. Unknown and unstudied substances are not considered. At best, TA allows random identification of causative substances of possible effects among known toxic substances without knowing if there is an effect in the sample at all. In addition, low environmental concentrations of known toxic contaminants cannot always be detected with sufficient sensitivity using existing instrumental analytical methods. For a sound ecotoxicological risk assessment, it is essential to know the distribution and concentrations of substances in a contaminated ecosystem, in addition to the toxicological and ecological consequences. Therefore, detection limits must be lower than toxicity thresholds to detect potential exposure (HODSON AND WRIGHT, 2022a). For example, steroid hormones are found in the aquatic environment at very low but effect-relevant concentrations in the ng/L to pg/L range (OJOGHORO et al., 2021). Detection of concentrations in the pg/L range is partially possible for estrogens, but difficult depending on the sample matrix, so the limits of detection (LODs) of the 2018 EU watch list and environmental quality standards (EQS) of 400 pg/L for E1 and E2 and 35 pg/L for EE2 (EU, 2012, 2018) remain challenging (KÖNEMANN et al., 2018; LOOS et al., 2018; ITZEL et al., 2019; GLINEUR et al., 2020; SIMON et al., 2022). Due to the low environmental concentrations, and especially if estrogens are included as priority substances in the annex of the WFD, possibly with even lower EQS (SCHEER, 2022), so that monitoring becomes mandatory, reliable detection must be possible.

One way out is offered by effect-based methods (EBMs), which can detect the effects of substances in low concentration ranges using sensitive bioanalytical methods and enable a more holistic view on contaminations (KÖNEMANN et al., 2018; ITZEL et al., 2019; DOPP et al., 2021; SIMON et al., 2022). A variety of EBMs are available using different bioanalytical approaches, such as transgenic yeast assays for the determination of hormonal activities (Figure 1-5) or AChE inhibition (AChE-I) assays, which capture the total toxicity of a sample and thus also consider mixture toxicity (DE BAAT et al., 2019; PANNEKENS et al., 2019; YUSUF et al., 2021). They are recommended for routine water quality monitoring (BRACK et al., 2019).

However, with these methods it is not clear which substances are responsible for the detected effects and to what extent. But knowledge of the causative substances is essential in order to investigate sources, pathways, transport, transformation and degradation in the environment, (eco)toxicological MoA, regulation and technical measures for removal of pollutants.

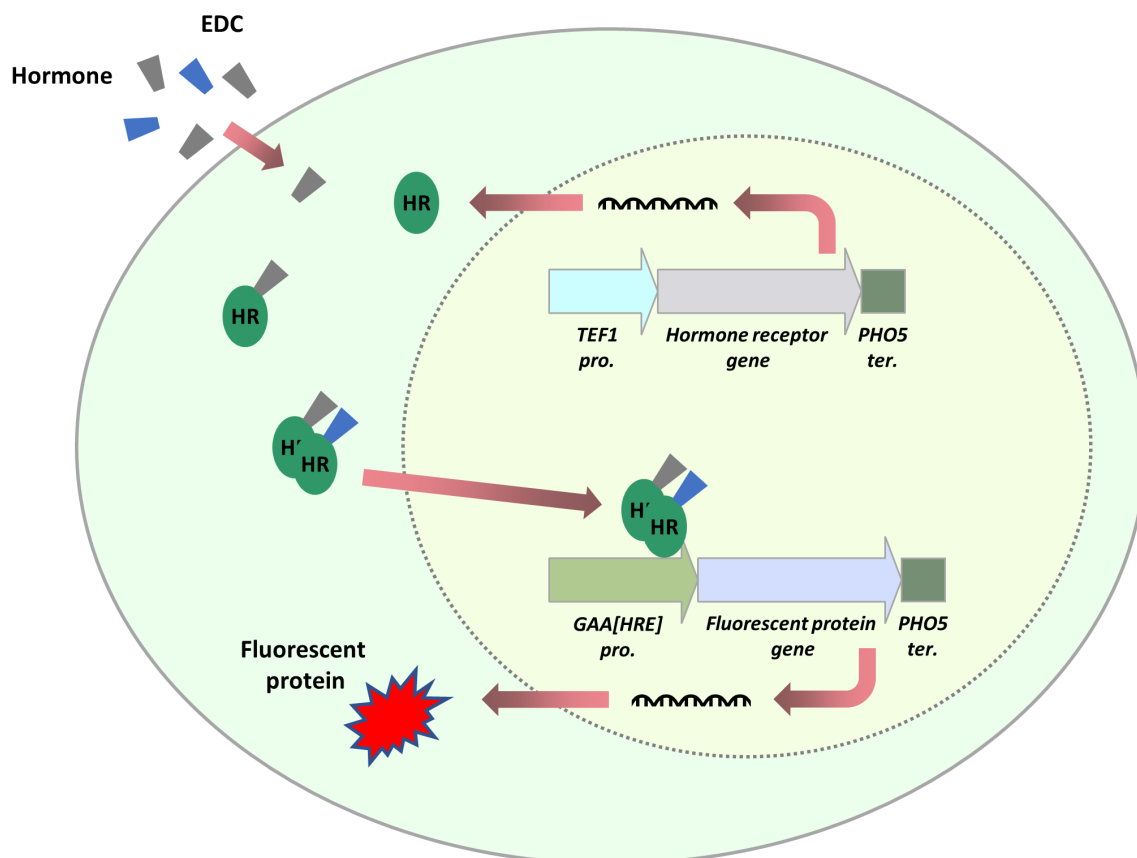


Figure 1-5 Scheme of a transgenic modified *Arxula adenivorans* cell. In the nucleus, a human hormone receptor (HR) gene is constitutively expressed. When a binding hormone or EDC is present, it can cross the yeast membrane and bind to the HR in the cytoplasm. After binding-induced receptor dimerization, this dimer can retranslocate in the nucleus and bind to the hormone response element (HRE), thus activating the GAA promoter and allowing expression of the fluorescence gene. This leads to the production of a fluorescent protein in the cytoplasm whose emission wavelength can be measured after excitation. Adopted from CHAMAS et al. (2017a) in a modified version.

Suspect and non-target screening (SNTS) approaches using high-resolution methods can be used to analyze trends, create pollution patterns, locate sources, and identify causal agents (BECKERS et al., 2020; GONZÁLEZ-GAYA et al., 2021; POSTIGO AND RICHARDSON, 2021). Although SNTS provides more information than TA, toxicological conclusions cannot be drawn from these methods and the complexity is higher (Figure 1-6). In particular, evaluation requires a lot of effort and expertise, and is not yet standardized (DOPP et al., 2019; HOHRENK et al., 2020). The probability of identifying effect-causing substances is higher with SNTS than with TA, but still very difficult to achieve due to the complexity of environmental samples and the large number of possible causative substances and the associated volume of data (Figure 1-6).

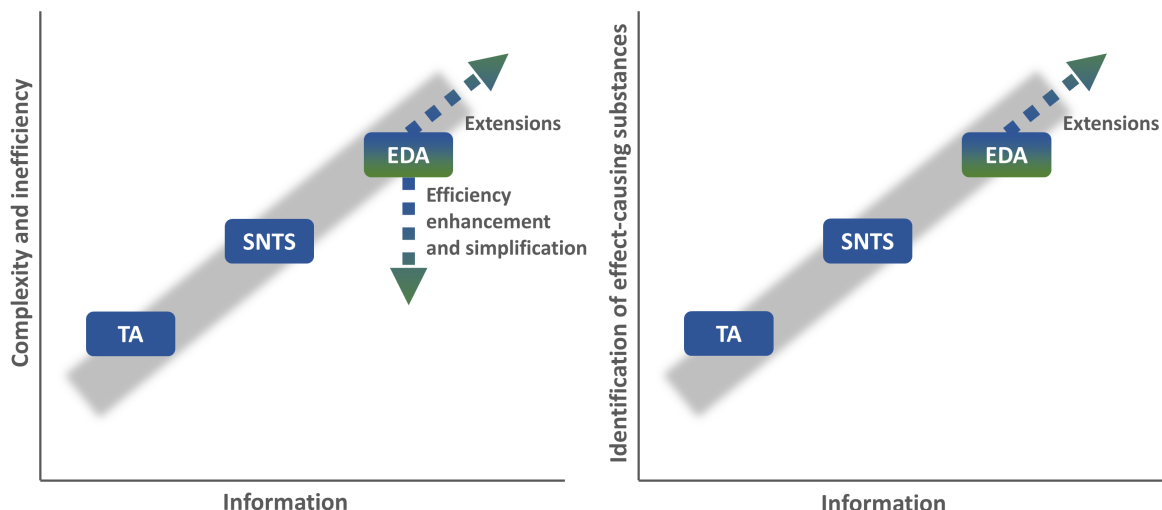


Figure 1-6 Information content of the different analytical approaches target analysis (TA), suspect and non-target screening (SNTS), and effect-directed analysis (EDA) in relation to their complexity and probability of identifying effect-causing substances. EDA is the most complex approach with the greatest risk of inefficiency, so simplification and improving efficiency are paramount. Extensions such as the integration of chromatographic methods for sample separation increase the probability of identifying toxic substances.

For more efficient evaluation and to increase the likelihood of identifying effect-causing substances, as much information as possible about the properties of the sample should be obtained. Therefore, EBMs and instrumental analysis should be combined to EDA. EDA is based on the effects investigated by *in vitro* or *in vivo* EBMs in order to integrate TA or SNTS in a targeted and efficient way to elucidate the causative substances and thus achieve a comprehensive characterization of samples and their (eco)toxicological potential (BRACK et al., 2016; DOPP et al., 2019; FINCKH et al., 2022; TIAN et al., 2023). Whole test batteries from different EBMs with different endpoints could be integrated into EDA to provide a comprehensive toxicological assessment of a sample (ALYGIZAKIS et al., 2023). In addition, other information and methods such as space, time, and type of sampling, as well as the integration of *in vivo* methods, can play an important role in EDA and contribute to the overall understanding (SONAVANE et al., 2018). Through the combination of different chemical and biological analytical methods, EDA is the most complex approach, which makes simplifying workflows and improving efficiency especially important to avoid inefficiency of the overall method (Figure 1-6). In comparison to TA and SNTS, EDA provides the most information, which in turn increases the probability of identifying effect-causing substances with SNTS integrated into EDA (Figure 1-6). More information, which can further increase the chances of identifying active compounds, can be obtained by extending EDA, e.g., by adding additional chromatographic steps. On the one hand, when a sample is fractionated, e.g., by high-performance liquid-chromatography (HPLC), and then tested for effects, synergistic or antagonistic interactions of compounds in the whole sample may not be visible anymore, i.e., mixture toxicity information might be lost.

On the other hand, fractionation of a sample can exclude components that are irrelevant to the effects being tested and also identify effects that are masked in the whole sample by other, e.g., cytotoxic, substances, by a reduced complexity of the subsamples compared to the original sample (HASHMI et al., 2020; ZWART et al., 2020; LOPEZ-HERGUEDAS et al., 2022).

Chromatographic separation within an EDA approach can also be performed using high-performance thin-layer chromatography (HPTLC), where EBMs are performed without interfering solvents from sample extracts directly on the HPTLC plate and toxic sample parts are visualized with different detection methods depending on the EBM used (WEISS et al., 2017; MORLOCK, 2021; WILSON AND POOLE, 2023). This imaging technique enables the generation of effect patterns for spatial and temporal comparison of different sampling sites or technical processes, such as treatment steps of WWTPs. The use of multiple EBMs in a test battery in combination with HPTLC enables efficient, inexpensive, rapid and robust toxicological screening, making integration into a complete EDA useful (OBERLEITNER et al., 2020; RIEGRAF et al., 2021; FINCKH et al., 2022). EBMs performed on HPTLC plates, as demonstrated by BERGMANN et al. (2020) with the planar yeast estrogen screen (p-YES), can achieve comparable or higher sensitivity than in liquid microtiter format. HPTLC has already proven its value in combination with various EBMs, such as transgenic yeast assays for the determination of different agonistic and antagonistic hormonal activities, AChE or photosystem II inhibition assays or bacterial genotoxicity bioreporters (RIEGRAF et al., 2019a; RIEGRAF et al., 2019b; SHAKIBAI et al., 2019; KLINGELHÖFER et al., 2020; RIEGRAF et al., 2022) and different technical, chemical, and biological process steps, e.g., for sensitivity enhancement and extension (SCHOENBORN et al., 2017; AZADNIYA AND MORLOCK, 2019; AZADNIYA et al., 2020; RONZHEIMER et al., 2022). With HPTLC, multi-dimensional separations as well as combinations with other chromatographic methods such as HPLC can be realized (MÓRICZ et al., 2020; STÜTZ et al., 2020). Extraction from the HPTLC plate and transfer to subsequent analytical steps, even after a bioassay has been performed, allows HPTLC-EBMs to be integrated into an EDA with TA or SNTS (FOUGÈRE et al., 2019; MEHL et al., 2021; SCHREINER AND MORLOCK, 2021). HPTLC-EDA makes it possible to examine active fractions of a total sample separately from irrelevant parts of the sample and other interfering sample matrix. The probability of identifying and quantifying known and unknown effect-causing substances with subsequent analytical methods increases because the number of features detected, e.g., by high-resolution mass spectrometry (HRMS), decreases with each additional HPTLC-EBM step, allowing to focus on the effect-relevant features with SNTS (STÜTZ et al., 2020; BELL et al., 2021; SCHREINER AND MORLOCK, 2023).

Since EDA is a combination of different analytical methods such as EBMs, TA and SNTS in conjunction with chromatographic steps for sample fractionation with HPLC or HPTLC, it has a higher information content than the individual methods can provide, but the effort required for its implementation and evaluation is much more complex (Figure 1-6). Increasing the efficiency of the implementation is

therefore particularly desirable. This opens up the possibility of integrating additional methods into the EDA, which in turn increases the information content and thus the probability of identifying effect-causing substances. In summary, a comprehensive EDA should cover a broad range of effects, be sensitive to effect-causing substances, be conducted as efficiently as possible to reduce the comparatively high effort, and provide as much information about the sample as possible to increase the likelihood of effective identification of effect-causing substances and to provide the most comprehensive characterization of a sample and possible contamination in a study area.

The transgenic yeast strains developed by CHAMAS et al. (2017a) are well suited for this purpose because they allow the simultaneous detection of multiple endocrine effects in a single workflow and do not require an additional substrate due to the direct formation of fluorescent proteins upon activation of the corresponding HR. They allow very efficient use within an EDA and have been tested in combination with HPTLC (CHAMAS et al., 2017b). However, it is necessary to further increase the sensitivity. A comparison of different application techniques for the yeast cells makes sense in this context, as it might allow a higher sensitivity, as shown by SCHOENBORN et al. (2017). In this regard, commercially available instruments that are inexpensive compared to laboratory instruments and suitable for laboratory application can be used to reduce costs and thus come closer to a simple, broadly applicable HPTLC-EDA. The AChE-I assay, already used in combination with HPTLC, is a good way to detect neurotoxic effects in separated aquatic samples (WEINS AND JORK, 1996; STÜTZ et al., 2020). The toxic activation of OTPs in organisms by enzymatic oxidation can be mimicked in AChE-I assays, increasing the sensitivity of the assay to OTPs. In an efficient EDA designed for routine use in combination with HPTLC, it makes sense to keep this oxidation simple. Chemical oxidation with *n*-bromosuccinimide is an option for this purpose, but has not yet been tested with HPTLC. In addition, a direct comparison of different application methods of the AChE solution on HPTLC plates has not yet been shown, but could point out the most sensitive approach. Stormwater-related surface water pollution due to discharges from stormwater structures or diffuse sources has not been studied to the same extent as discharges from WWTPs. Since CSOs can be expected to discharge typical wastewater substances, such as steroid hormones, from the combined sewer system during rainy weather, and since other EDCs, but also neurotoxic substances, such as pesticides and biocides, can be introduced with surface runoff, an investigation of endocrine and neurotoxic effects is necessary. The combination of HPTLC and EBMs to detect such effects in an EDA approach lends itself to a comprehensive investigation of such stresses for surface waters, but has not been done in this form before.

1.6. References

- Aguiar Jr. T. R., Bortolozzo F. R., Hansel F. A., Rasera K., Ferreira M. T., 2015. Riparian buffer zones as pesticide filters of no-till crops. *Environmental Science and Pollution Research International*, 22 (14), 10618–10626. <https://doi.org/10.1007/s11356-015-4281-5>.
- Alygizakis N., Ng K., Maragou N., Alirai S., Behnisch P., Besselink H., Oswald P., Čirka L., Thomaidis N. S., Slobodnik J., 2023. Battery of In Vitro Bioassays: A Case Study for the Cost-Effective and Effect-Based Evaluation of Wastewater Effluent Quality. *Water*, 15 (4), 619. <https://doi.org/10.3390/w15040619>.
- Archer E., Wolfaardt G. M., Van Wyk J. H., Van Blerk N., 2020. Investigating (anti)estrogenic activities within South African wastewater and receiving surface waters: Implication for reliable monitoring. *Environmental Pollution*, 263 (Pt A), 114424. <https://doi.org/10.1016/j.envpol.2020.114424>.
- Arora K., Mickelson S. K., Helmers M. J., Baker J. L., 2010. Review of Pesticide Retention Processes Occurring in Buffer Strips Receiving Agricultural Runoff. *Journal of the American Water Resources Association (JAWRA)*, 46 (3), 618–647. <https://doi.org/10.1111/j.1752-1688.2010.00438.x>.
- Arp H. P. H., Aurich D., Schymanski E. L., Sims K., Hale S. E., 2023. Avoiding the Next Silent Spring: Our Chemical Past, Present, and Future. *Environmental Science & Technology*, 57 (16), 6355–6359. <https://doi.org/10.1021/acs.est.3c01735>.
- Azadniya E. and Morlock G. E., 2019. Automated piezoelectric spraying of biological and enzymatic assays for effect-directed analysis of planar chromatograms. *Journal of Chromatography A*, 1602, 458–466. <https://doi.org/10.1016/j.chroma.2019.05.043>.
- Azadniya E., Mollergues J., Stroheker T., Billerbeck K., Morlock G. E., 2020. New incorporation of the S9 metabolizing system into methods for detecting acetylcholinesterase inhibition. *Analytica Chimica Acta*, 1129, 76–84. <https://doi.org/10.1016/j.aca.2020.06.033>.
- Azizi D., Arif A., Blair D., Dionne J., Filion Y., Ouarda Y., Pazmino A. G., Pulicharla R., Rilstone V., Tiwari B., Vignale L., Brar S. K., Champagne P., Drogui P., Langlois V. S., Blais J.-F., 2022. A comprehensive review on current technologies for removal of endocrine disrupting chemicals from wastewaters. *Environmental Research*, 207, 112196. <https://doi.org/10.1016/j.envres.2021.112196>.
- Balakrishna K., Praveenkumarreddy Y., Nishitha D.'S., Gopal C. M., Shenoy J. K., Bhat K., Khare N., Dhangar K., Kumar M., 2023. Occurrences of UV filters, endocrine disruptive chemicals, alkyl phenolic compounds, fragrances, and hormones in the wastewater and coastal waters of the Antarctica. *Environmental Research*, 222, 115327. <https://doi.org/10.1016/j.envres.2023.115327>.
- Beckers L.-M., Brack W., Dann J. P., Krauss M., Müller E., Schulze T., 2020. Unraveling longitudinal pollution patterns of organic micropollutants in a river by non-target screening and cluster analysis. *Science of the Total Environment*, 727, 138388. <https://doi.org/10.1016/j.scitotenv.2020.138388>.
- Bell A. M., Keltsch N., Schweyen P., Reifferscheid G., Ternes T., Buchinger S., 2021. UV aged epoxy coatings - Ecotoxicological effects and released compounds. *Water Research X*, 12, 100105. <https://doi.org/10.1016/j.wroa.2021.100105>.
- Bergmann A. J., Simon E., Schifferli A., Schönborn A., Vermeirssen E. L. M., 2020. Estrogenic activity of food contact materials-evaluation of 20 chemicals using a yeast estrogen screen on HPTLC or 96-well plates. *Analytical and Bioanalytical Chemistry*, 412 (19), 4527–4536. <https://doi.org/10.1007/s00216-020-02701-w>.

- Bertanza G., Steimberg N., Pedrazzani R., Boniotti J., Ceretti E., Mazzoleni G., Menghini M., Urani C., Zerbini I., Feretti D., 2022. Wastewater toxicity removal: Integrated chemical and effect-based monitoring of full-scale conventional activated sludge and membrane bioreactor plants. *Science of the Total Environment*, 851 (Pt 1), 158071. <https://doi.org/10.1016/j.scitotenv.2022.158071>.
- Botturi A., Ozbayram E. G., Tondera K., Gilbert N. I., Rouault P., Caradot N., Gutierrez O., Daneshgar S., Frison N., Akyol Ç., Foglia A., Eusebi A. L., Fatone F., 2021. Combined sewer overflows: A critical review on best practice and innovative solutions to mitigate impacts on environment and human health. *Critical Reviews in Environmental Science and Technology*, 51 (15), 1585–1618. <https://doi.org/10.1080/10643389.2020.1757957>.
- Brack W., Aissa S. A., Backhaus T., Dulio V., Escher B. I., Faust M., Hilscherova K., Hollender J., Hollert H., Müller C., Munthe J., Posthuma L., Seiler T.-B., Slobodnik J., Teodorovic I., Tindall A. J., De Aragão Umbuzeiro G., Zhang X., Altenburger R., 2019. Effect-based methods are key. The European Collaborative Project SOLUTIONS recommends integrating effect-based methods for diagnosis and monitoring of water quality. *Environmental Sciences Europe*, 31 (1), 5423. <https://doi.org/10.1186/s12302-019-0192-2>.
- Brack W., Ait-Aissa S., Burgess R. M., Busch W., Creusot N., Di Paolo C., Escher B. I., Mark Hewitt L., Hilscherova K., Hollender J., Hollert H., Jonker W., Kool J., Lamoree M., Muschket M., Neumann S., Rostkowski P., Ruttkies C., Schollee J., Schymanski E. L., Schulze T., Seiler T.-B., Tindall A. J., De Aragão Umbuzeiro G., Vrana B., Krauss M., 2016. Effect-directed analysis supporting monitoring of aquatic environments – An in-depth overview. *Science of the Total Environment*, 544, 1073–1118. <https://doi.org/10.1016/j.scitotenv.2015.11.102>.
- Bröcker J. H. L., Stone W., Carstens A., Wolfaardt G. M., 2022. Micropollutant transformation and toxicity: Electrochemical ozonation versus biological metabolism. *Toxicology Research and Application*, 6. <https://doi.org/10.1177/23978473221122880>.
- Brunsch A. F., Zubieta Florez P., Langenhoff A. A. M., Ter Laak T. L., Rijnaarts H. H. M., 2020. Retention soil filters for the treatment of sewage treatment plant effluent and combined sewer overflow. *Science of the Total Environment*, 699, 134426. <https://doi.org/10.1016/j.scitotenv.2019.134426>.
- Brusseau M. L. and Artiola J. F., 2019. Chapter 12: Chemical Contaminants. In: Brusseau M. L., Pepper I. L., Gerba C. P. (eds.), *Environmental and Pollution Science*, vol. 78, 3rd ed., pp. 175–190. Elsevier Science & Technology, San Diego.
- Butkovskiy A., Jing Y., Bergheim H., Lazar D., Gulyaeva K., Odenmarck S. R., Norli H. R., Nowak K. M., Miltner A., Kästner M., Eggen T., 2021. Retention and distribution of pesticides in planted filter microcosms designed for treatment of agricultural surface runoff. *Science of the Total Environment*, 778, 146114. <https://doi.org/10.1016/j.scitotenv.2021.146114>.
- Campbell P. G. C., Hodson P. V., Welbourn P. M., Wright D. A., 2022. Chapter 3: Contaminant uptake and bioaccumulation: mechanisms, kinetics and modelling. In: Campbell P. G. C., Hodson P. V., Welbourn P. M., Wright D. A. (eds.), *Ecotoxicology*, pp. 61–96. Cambridge University Press.
- Carstensen L., Beil S., Börnick H., Stolte S., 2022. Structure-related endocrine-disrupting potential of environmental transformation products of benzophenone-type UV filters: A review. *Journal of Hazardous Materials*, 430, 128495. <https://doi.org/10.1016/j.jhazmat.2022.128495>.
- Chamas A., Pham H. T. M., Jähne M., Hettwer K., Gehrman L., Tuerk J., Uhlig S., Simon K., Baronian K., Kunze G., 2017b. Separation and identification of hormone-active compounds using a combination of chromatographic separation and yeast-based reporter assay. *Science of the Total Environment*, 605-606, 507–513. <https://doi.org/10.1016/j.scitotenv.2017.06.077>.

- Chamas A., Pham H. T. M., Jähne M., Hettwer K., Uhlig S., Simon K., Einspanier A., Baronian K., Kunze G., 2017a. Simultaneous detection of three sex steroid hormone classes using a novel yeast-based biosensor. *Biotechnology and Bioengineering*, 114 (7), 1539–1549. <https://doi.org/10.1002/bit.26249>.
- Chen X., Guo W., Lei L., Guo Y., Yang L., Han J., Zhou B., 2021. Bioconcentration and developmental neurotoxicity of novel brominated flame retardants, hexabromobenzene and pentabromobenzene in zebrafish. *Environmental Pollution*, 268 (Pt B), 115895. <https://doi.org/10.1016/j.envpol.2020.115895>.
- De Baat M. L., Kraak M. H. S., Van der Oost R., De Voogt P., Verdonchot P. F. M., 2019. Effect-based nationwide surface water quality assessment to identify ecotoxicological risks. *Water Research*, 159, 434–443. <https://doi.org/10.1016/j.watres.2019.05.040>.
- De Souza R. M., Seibert D., Quesada H. B., De Jesus Bassetti F., Fagundes-Klen M. R., Bergamasco R., 2020. Occurrence, impacts and general aspects of pesticides in surface water: A review. *Process Safety and Environmental Protection*, 135, 22–37. <https://doi.org/10.1016/j.psep.2019.12.035>.
- DeCourten B., Romney A., Brander S., 2019. Chapter 2: The Heat Is On: Complexities of Aquatic Endocrine Disruption in a Changing Global Climate. In: Ahuja S. (ed.), *Separation Science and Technology, Evaluating water quality to prevent future disasters*, vol. 11, 1st ed., pp. 13–49. Academic Press, London, England.
- Deidda I., Russo R., Bonaventura R., Costa C., Zito F., Lampiasi N., 2021. Neurotoxicity in Marine Invertebrates: An Update. *Biology*, 10 (2), 161. <https://doi.org/10.3390/biology10020161>.
- Dopp E., Pannekens H., Gottschlich A., Schertzingler G., Gehrmann L., Kasper-Sonnenberg M., Richard J., Joswig M., Grummt T., Schmidt T. C., Wilhelm M., Tuerk J., 2021. Effect-based evaluation of ozone treatment for removal of micropollutants and their transformation products in waste water. *Journal of Toxicology and Environmental Health. Part A*, 84 (10), 418–439. <https://doi.org/10.1080/15287394.2021.1881854>.
- Dopp E., Pannekens H., Itzel F., Tuerk J., 2019. Effect-based methods in combination with state-of-the-art chemical analysis for assessment of water quality as integrated approach. *International Journal of Hygiene and Environmental Health*, 222 (4), 607–614. <https://doi.org/10.1016/j.ijheh.2019.03.001>.
- Dueñas-Moreno J., Mora A., Cervantes-Avilés P., Mahlkecht J., 2022. Groundwater contamination pathways of phthalates and bisphenol A: origin, characteristics, transport, and fate - A review. *Environment International*, 170, 107550. <https://doi.org/10.1016/j.envint.2022.107550>.
- Eisenreich S. J., Hornbuckle K., Jones K. C., 2021. The Global Legacy of POPs: Special Issue. *Environmental Science & Technology*, 55 (14), 9397–9399. <https://doi.org/10.1021/acs.est.1c03067>.
- EU, 2000. DIRECTIVE 2000/60/EC OF THE EUROPEAN PARLIAMENT AND OF THE COUNCIL of 23 October 2000 establishing a framework for Community action in the field of water policy (WFD). Official Journal of the European Communities.
- EU, 2006. REGULATION (EC) No 1907/2006 OF THE EUROPEAN PARLIAMENT AND OF THE COUNCIL of 18 December 2006 concerning the Registration, Evaluation, Authorisation and Restriction of Chemicals (REACH), establishing a European Chemicals Agency, amending Directive 1999/45/EC and repealing Council Regulation (EEC) No 793/93 and Commission Regulation (EC) No 1488/94 as well as Council Directive 76/769/EEC and Commission Directives 91/155/EEC, 93/67/EEC, 93/105/EC and 2000/21/EC (REACH). Official Journal of the European Union.
- EU, 2012. Proposal for a DIRECTIVE OF THE EUROPEAN PARLIAMENT AND OF THE COUNCIL amending Directives 2000/60/EC and 2008/105/EC as regards priority substances in the field of water policy.

- EU, 2018. COMMISSION IMPLEMENTING DECISION (EU) 2018/ 840 - of 5 June 2018 - establishing a watch list of substances for Union-wide monitoring in the field of water policy pursuant to Directive 2008/ 105/ EC of the European Parliament and of the Council and repealing Commission Implementing Decision (EU) 2015/ 495 - (notified under document C(2018) 3362) (Watch List). Official Journal of the European Union.
- Finckh S., Buchinger S., Escher B. I., Hollert H., König M., Krauss M., Leekitratapanisan W., Schiwy S., Schlichting R., Shuliakevich A., Brack W., 2022. Endocrine disrupting chemicals entering European rivers: Occurrence and adverse mixture effects in treated wastewater. *Environment International*, 170, 107608. <https://doi.org/10.1016/j.envint.2022.107608>.
- Fougère L., Da Silva D., Destandau E., Elfakir C., 2019. TLC-MALDI-TOF-MS-based identification of flavonoid compounds using an inorganic matrix. *Phytochemical Analysis*, 30 (2), 218–225. <https://doi.org/10.1002/pca.2807>.
- Fritsche E., Grandjean P., Crofton K. M., Aschner M., Goldberg A., Heinonen T., Hessel E. V. S., Hogberg H. T., Bennekou S. H., Lein P. J., Leist M., Mundy W. R., Paparella M., Piersma A. H., Sachana M., Schmuck G., Solecki R., Terron A., Monnet-Tschudi F., Wilks M. F., Witters H., Zurich M.-G., Bal-Price A., 2018. Consensus statement on the need for innovation, transition and implementation of developmental neurotoxicity (DNT) testing for regulatory purposes. *Toxicology and Applied Pharmacology*, 354, 3–6. <https://doi.org/10.1016/j.taap.2018.02.004>.
- Gadupudi C. K., Rice L., Xiao L., Kantamaneni K., 2021. Endocrine Disrupting Compounds Removal Methods from Wastewater in the United Kingdom: A Review. *Sci*, 3 (1), 11. <https://doi.org/10.3390/sci3010011>.
- Glineur A., Nott K., Carbonnelle P., Ronkart S., Purcaro G., 2020. Development And Validation Of A Method For Determining Estrogenic Compounds In Surface Water At The Ultra-Trace Level Required By The EU Water Framework Directive Watch List. *Journal of Chromatography A*, 1624, 461242. <https://doi.org/10.1016/j.chroma.2020.461242>.
- Goeury K., Munoz G., Vo Duy S., Prévost M., Sauvé S., 2022. Occurrence and seasonal distribution of steroid hormones and bisphenol A in surface waters and suspended sediments of Quebec, Canada. *Environmental Advances*, 8, 100199. <https://doi.org/10.1016/j.envadv.2022.100199>.
- Gonsioroski A., Mourikes V. E., Flaws J. A., 2020. Endocrine Disruptors in Water and Their Effects on the Reproductive System. *International Journal of Molecular Sciences*, 21 (6), 1929. <https://doi.org/10.3390/ijms21061929>.
- González-Gaya B., Lopez-Herguedas N., Bilbao D., Mijangos L., Iker A. M., Etxebarria N., Irazola M., Prieto A., Olivares M., Zuloaga O., 2021. Suspect and non-target screening: the last frontier in environmental analysis. *Analytical Methods*, 13 (16), 1876–1904. <https://doi.org/10.1039/d1ay00111f>.
- Gore A. C., Chappell V. A., Fenton S. E., Flaws J. A., Nadal A., Prins G. S., Toppari J., Zoeller R. T., 2015. EDC-2: The Endocrine Society's Second Scientific Statement on Endocrine-Disrupting Chemicals. *Endocrine Reviews*, 36 (6), E1-E150. <https://doi.org/10.1210/er.2015-1010>.
- Grobin A., Roškar R., Trontelj J., 2023. The environmental occurrence, fate, and risks of 25 endocrine disruptors in Slovenian waters. *Science of the Total Environment*, 906, 167245. <https://doi.org/10.1016/j.scitotenv.2023.167245>.
- Hägström M. and Richfield D., 2014. Diagram of the pathways of human steroidogenesis. *WikiJournal of Medicine*, 1 (1). <https://doi.org/10.15347/wjm/2014.005>.

- Hale S. E., Arp H. P. H., Schliebner I., Neumann M., 2020. Persistent, mobile and toxic (PMT) and very persistent and very mobile (vPvM) substances pose an equivalent level of concern to persistent, bioaccumulative and toxic (PBT) and very persistent and very bioaccumulative (vPvB) substances under REACH. *Environmental Sciences Europe*, 32 (1), 6856. <https://doi.org/10.1186/s12302-020-00440-4>.
- Hamid N., Junaid M., Pei D.-S., 2021. Combined toxicity of endocrine-disrupting chemicals: A review. *Ecotoxicology and Environmental Safety*, 215, 112136. <https://doi.org/10.1016/j.ecoenv.2021.112136>.
- Hashmi M. A. K., Krauss M., Escher B. I., Teodorovic I., Brack W., 2020. Effect-Directed Analysis of Progestogens and Glucocorticoids at Trace Concentrations in River Water. *Environmental Toxicology and Chemistry*, 39 (1), 189–199. <https://doi.org/10.1002/etc.4609>.
- Havens S. M., Hedman C. J., Hemming J. D. C., Mieritz M. G., Shafer M. M., Schauer J. J., 2020. Occurrence of estrogens, androgens and progestogens and estrogenic activity in surface water runoff from beef and dairy manure amended crop fields. *Science of the Total Environment*, 710, 136247. <https://doi.org/10.1016/j.scitotenv.2019.136247>.
- Hemond H. F., Fechner-Levy E. J., 2023. *Chemical fate and transport in the environment*, 4th ed. Elsevier, Academic Press, an Imprint of Elsevier, London, United Kingdom, San Diego, CA, United States, Cambridge, MA, United States, Kidlington, Oxford, United Kingdom.
- Hodson P. V. and Wright D. A., 2022b. Chapter 2: Measuring Toxicity. In: Campbell P. G. C., Hodson P. V., Welbourn P. M., Wright D. A. (eds.), *Ecotoxicology*, pp. 23–58. Cambridge University Press.
- Hodson P. V. and Wright D. W., 2022a. Chapter 4: Methods in Ecotoxicology. In: Campbell P. G. C., Hodson P. V., Welbourn P. M., Wright D. A. (eds.), *Ecotoxicology*, pp. 99–136. Cambridge University Press.
- Hohrenk L. L., Itzel F., Baetz N., Tuerk J., Vosough M., Schmidt T. C., 2020. Comparison of Software Tools for Liquid Chromatography-High-Resolution Mass Spectrometry Data Processing in Nontarget Screening of Environmental Samples. *Analytical Chemistry*, 92 (2), 1898–1907. <https://doi.org/10.1021/acs.analchem.9b04095>.
- Hooper M. J., Ankley G. T., Cristol D. A., Maryoung L. A., Noyes P. D., Pinkerton K. E., 2013. Interactions between chemical and climate stressors: a role for mechanistic toxicology in assessing climate change risks. *Environmental Toxicology and Chemistry*, 32 (1), 32–48. <https://doi.org/10.1002/etc.2043>.
- IPCC, 2023. *Climate Change 2023. Synthesis Report. Contribution of Working Groups I, II and III to the Sixth Assessment Report of the Intergovernmental Panel on Climate Change*. IPCC, Geneva, Switzerland. <https://doi.org/10.59327/IPCC/AR6-9789291691647>.
- Iqbal A., Ahmed M., Ahmad S., Sahoo C. R., Iqbal M. K., Haque S. E., 2020. Environmental neurotoxic pollutants: review. *Environmental Science and Pollution Research*, 27 (33), 41175–41198. <https://doi.org/10.1007/s11356-020-10539-z>.
- Itzel F., Baetz N., Hohrenk L. L., Gehrmann L., Antakyali D., Schmidt T. C., Tuerk J., 2020. Evaluation of a biological post-treatment after full-scale ozonation at a municipal wastewater treatment plant. *Water Research*, 170, 115316. <https://doi.org/10.1016/j.watres.2019.115316>.
- Itzel F., Gehrmann L., Bielak H., Ebersbach P., Boergers A., Herbst H., Maus C., Simon A., Dopp E., Hammers-Wirtz M., Schmidt T. C., Tuerk J., 2017. Investigation of full-scale ozonation at a municipal wastewater treatment plant using a toxicity-based evaluation concept. *Journal of Toxicology and Environmental Health. Part A*, 80 (23-24), 1242–1258. <https://doi.org/10.1080/15287394.2017.1369663>.

- Itzel F., Gehrman L., Teutenberg T., Schmidt T. C., Tuerk J., 2019. Recent developments and concepts of effect-based methods for the detection of endocrine activity and the importance of antagonistic effects. *TrAC Trends in Analytical Chemistry*, 118 (21), 699–708. <https://doi.org/10.1016/j.trac.2019.06.030>.
- Itzel F., Jewell K. S., Leonhardt J., Gehrman L., Nielsen U., Ternes T. A., Schmidt T. C., Tuerk J., 2018. Comprehensive analysis of antagonistic endocrine activity during ozone treatment of hospital wastewater. *Science of the Total Environment*, 624, 1443–1454. <https://doi.org/10.1016/j.scitotenv.2017.12.181>.
- Jeyakumar M., Carlson K. E., Gunther J. R., Katzenellenbogen J. A., 2011. Exploration of dimensions of estrogen potency: parsing ligand binding and coactivator binding affinities. *Journal of Biological Chemistry*, 286 (15), 12971–12982. <https://doi.org/10.1074/jbc.M110.205112>.
- Jin B., Huang C., Yu Y., Zhang G., Arp H. P. H., 2020. The Need to Adopt an International PMT Strategy to Protect Drinking Water Resources. *Environmental Science & Technology*, 54 (19), 11651–11653. <https://doi.org/10.1021/acs.est.0c04281>.
- Kasonga T. K., Coetzee M. A. A., Kamika I., Ngole-Jeme V. M., Benteke Momba M. N., 2021. Endocrine-disruptive chemicals as contaminants of emerging concern in wastewater and surface water: A review. *Journal of Environmental Management*, 277, 111485. <https://doi.org/10.1016/j.jenvman.2020.111485>.
- Kharel S., Stapf M., Mieke U., Ekblad M., Cimbritz M., Falås P., Nilsson J., Sehlén R., Bester K., 2020. Ozone dose dependent formation and removal of ozonation products of pharmaceuticals in pilot and full-scale municipal wastewater treatment plants. *Science of the Total Environment*, 731, 139064. <https://doi.org/10.1016/j.scitotenv.2020.139064>.
- Kidd K. A., Blanchfield P. J., Mills K. H., Palace V. P., Evans R. E., Lazorchak J. M., Flick R. W., 2007. Collapse of a fish population after exposure to a synthetic estrogen. *Proceedings of the National Academy of Sciences of the United States of America*, 104 (21), 8897–8901. <https://doi.org/10.1073/pnas.0609568104>.
- Kienle C., Werner I., Fischer S., Lüthi C., Schifferli A., Besselink H., Langer M., McArdell C. S., Vermeirssen E. L. M., 2022. Evaluation of a full-scale wastewater treatment plant with ozonation and different post-treatments using a broad range of in vitro and in vivo bioassays. *Water Research*, 212, 118084. <https://doi.org/10.1016/j.watres.2022.118084>.
- Klančič V., Gobec M., Jakopin Ž., 2022. Halogenated ingredients of household and personal care products as emerging endocrine disruptors. *Chemosphere*, 303 (Pt 1), 134824. <https://doi.org/10.1016/j.chemosphere.2022.134824>.
- Klingelhöfer I., Hockamp N., Morlock G. E., 2020. Non-targeted detection and differentiation of agonists versus antagonists, directly in bioprofiles of everyday products. *Analytica Chimica Acta*, 1125, 288–298. <https://doi.org/10.1016/j.aca.2020.05.057>.
- Knepper T. P., Reemtsma T., Schmidt T. C., 2020. Persistent and mobile organic compounds-an environmental challenge. *Analytical and Bioanalytical Chemistry*, 412 (20), 4761–4762. <https://doi.org/10.1007/s00216-020-02542-7>.
- Knoop O., Hohrenk L. L., Lutze H. V., Schmidt T. C., 2018a. Ozonation of Tamoxifen and Toremifene: Reaction Kinetics and Transformation Products. *Environmental Science & Technology*, 52 (21), 12583–12591. <https://doi.org/10.1021/acs.est.8b00996>.
- Knoop O., Itzel F., Tuerk J., Lutze H. V., Schmidt T. C., 2018b. Endocrine effects after ozonation of tamoxifen. *Science of the Total Environment*, 622–623, 71–78. <https://doi.org/10.1016/j.scitotenv.2017.11.286>.

- Könemann S., Kase R., Simon E., Swart K., Buchinger S., Schlüsener M., Hollert H., Escher B. I., Werner I., Aït-Aïssa S., Vermeirssen E., Dulio V., Valsecchi S., Polesello S., Behnisch P., Javurkova B., Perceval O., Di Paolo C., Olbrich D., Sychrova E., Schlichting R., Leborgne L., Clara M., Scheffknecht C., Marneffe Y., Chalon C., Tužil P., Soldà P., Von Danwitz B., Schwaiger J., San Martín Becares M. I., Bersani F., Hilscherová K., Reifferscheid G., Ternes T., Carere M., 2018. Effect-based and chemical analytical methods to monitor estrogens under the European Water Framework Directive. *TrAC Trends in Analytical Chemistry*, 102 (12), 225–235. <https://doi.org/10.1016/j.trac.2018.02.008>.
- Kuiper G. G., Carlsson B., Grandien K., Enmark E., Häggblad J., Nilsson S., Gustafsson J. A., 1997. Comparison of the ligand binding specificity and transcript tissue distribution of estrogen receptors alpha and beta. *Endocrinology*, 138 (3), 863–870. <https://doi.org/10.1210/endo.138.3.4979>.
- Kushwaha M., Verma S., Chatterjee S., 2016. Profenofos, an Acetylcholinesterase-Inhibiting Organophosphorus Pesticide: A Short Review of Its Usage, Toxicity, and Biodegradation. *Journal of Environmental Quality*, 45 (5), 1478–1489. <https://doi.org/10.2134/jeq2016.03.0100>.
- Lamprea K., Bressy A., Mirande-Bret C., Caupos E., Gromaire M.-C., 2018. Alkylphenol and bisphenol A contamination of urban runoff: an evaluation of the emission potentials of various construction materials and automotive supplies. *Environmental Science and Pollution Research International*, 25 (22), 21887–21900. <https://doi.org/10.1007/s11356-018-2272-z>.
- Lee Y., Escher B. I., Von Gunten U., 2008. Efficient removal of estrogenic activity during oxidative treatment of waters containing steroid estrogens. *Environmental Science & Technology*, 42 (17), 6333–6339. <https://doi.org/10.1021/es7023302>.
- Legradi J. B., Di Paolo C., Kraak M. H. S., Van der Geest H. G., Schymanski E. L., Williams A. J., Dingemans M. M. L., Massei R., Brack W., Cousin X., Begout M.-L., Van der Oost R., Carion A., Suarez-Ulloa V., Silvestre F., Escher B. I., Engwall M., Nilén G., Keiter S. H., Pollet D., Waldmann P., Kienle C., Werner I., Haigis A.-C., Knapen D., Vergauwen L., Spehr M., Schulz W., Busch W., Leuthold D., Scholz S., Vom Berg C. M., Basu N., Murphy C. A., Lampert A., Kuckelkorn J., Grummt T., Hollert H., 2018. An ecotoxicological view on neurotoxicity assessment. *Environmental Sciences Europe*, 30 (1), 46. <https://doi.org/10.1186/s12302-018-0173-x>.
- Liess M., Liebmann L., Vormeier P., Weisner O., Altenburger R., Borchardt D., Brack W., Chatzinotas A., Escher B., Foit K., Gunold R., Henz S., Hitzfeld K. L., Schmitt-Jansen M., Kamjunke N., Kaske O., Knillmann S., Krauss M., Küster E., Link M., Lück M., Möder M., Müller A., Paschke A., Schäfer R. B., Schneeweiss A., Schreiner V. C., Schulze T., Schüürmann G., Von Tümpling W., Weitere M., Wogram J., Reemtsma T., 2021. Pesticides are the dominant stressors for vulnerable insects in lowland streams. *Water Research*, 201, 117262. <https://doi.org/10.1016/j.watres.2021.117262>.
- Lim S., Shi J. L., Von Gunten U., McCurry D. L., 2022. Ozonation of organic compounds in water and wastewater: A critical review. *Water Research*, 213, 118053. <https://doi.org/10.1016/j.watres.2022.118053>.
- Loos R., Marinov D., Sanseverino I., Napierska D., Lettieri T., 2018. Review of the 1st Watch List under the Water Framework Directive and recommendations for the 2nd Watch List. In: EUR, Scientific and Technical Research Series, EUR 29173 EN. Publications Office of the European Union, Luxembourg.
- Lopez-Herguedas N., González-Gaya B., Cano A., Alvarez-Mora I., Mijangos L., Etxebarria N., Zuloaga O., Olivares M., Prieto A., 2022. Effect-directed analysis of a hospital effluent sample using A-YES for the identification of endocrine disrupting compounds. *Science of the Total Environment*, 850, 157985. <https://doi.org/10.1016/j.scitotenv.2022.157985>.

- Marlatt V. L., Bayen S., Castaneda-Cortès D., Delbès G., Grigorova P., Langlois V. S., Martyniuk C. J., Metcalfe C. D., Parent L., Rwigemera A., Thomson P., Van der Kraak G., 2022. Impacts of endocrine disrupting chemicals on reproduction in wildlife and humans. *Environmental Research*, 208, 112584. <https://doi.org/10.1016/j.envres.2021.112584>.
- Masoner J. R., Kolpin D. W., Cozzarelli I. M., Barber L. B., Burden D. S., Foreman W. T., Forshay K. J., Furlong E. T., Groves J. F., Hladik M. L., Hopton M. E., Jaeschke J. B., Keefe S. H., Krabbenhoft D. P., Lowrance R., Romanok K. M., Rus D. L., Selbig W. R., Williams B. H., Bradley P. M., 2019. Urban Stormwater: An Overlooked Pathway of Extensive Mixed Contaminants to Surface and Groundwaters in the United States. *Environmental Science & Technology*, 53 (17), 10070–10081. <https://doi.org/10.1021/acs.est.9b02867>.
- Mehl A., Schwack W., Morlock G. E., 2021. On-surface autosampling for liquid chromatography-mass spectrometry. *Journal of Chromatography A*, 1651, 462334. <https://doi.org/10.1016/j.chroma.2021.462334>.
- Metcalfe C. D., Bayen S., Desrosiers M., Muñoz G., Sauvé S., Yargeau V., 2022b. Methods for the analysis of endocrine disrupting chemicals in selected environmental matrixes. *Environmental Research*, 206, 112616. <https://doi.org/10.1016/j.envres.2021.112616>.
- Metcalfe C. D., Martyniuk C. J., Langlois V. S., Wright D. A., 2022a. Chapter 8: Endocrine Disrupting Chemicals. In: Campbell P. G. C., Hodson P. V., Welbourn P. M., Wright D. A. (eds.), *Ecotoxicology*, pp. 327–352. Cambridge University Press.
- Mišík M., Ferk F., Schaar H., Yamada M., Jaeger W., Knasmueller S., Kreuzinger N., 2020. Genotoxic activities of wastewater after ozonation and activated carbon filtration: Different effects in liver-derived cells and bacterial indicators. *Water Research*, 186, 116328. <https://doi.org/10.1016/j.watres.2020.116328>.
- Móricz Á. M., Lapat V., Morlock G. E., Ott P. G., 2020. High-performance thin-layer chromatography hyphenated to high-performance liquid chromatography-diode array detection-mass spectrometry for characterization of coeluting isomers. *Talanta*, 219, 121306. <https://doi.org/10.1016/j.talanta.2020.121306>.
- Morlock G. E., 2021. High-performance thin-layer chromatography combined with effect-directed assays and high-resolution mass spectrometry as an emerging hyphenated technology: A tutorial review. *Analytica Chimica Acta*, 1180, 338644. <https://doi.org/10.1016/j.aca.2021.338644>.
- Moukhtari F. E., Martín-Pozo L., Zafra-Gómez A., 2023. Strategies based on the use of microorganisms for the elimination of pollutants with endocrine-disrupting activity in the environment. *Journal of Environmental Chemical Engineering*, 11 (1), 109268. <https://doi.org/10.1016/j.jece.2023.109268>.
- Müller A., Österlund H., Marsalek J., Viklander M., 2020. The pollution conveyed by urban runoff: A review of sources. *Science of the Total Environment*, 709, 136125. <https://doi.org/10.1016/j.scitotenv.2019.136125>.
- Müller A., Österlund H., Marsalek J., Viklander M., 2022. Exploiting urban roadside snowbanks as passive samplers of organic micropollutants and metals generated by traffic. *Environmental Pollution*, 308, 119723. <https://doi.org/10.1016/j.envpol.2022.119723>.
- Neuwald I., Muschket M., Zahn D., Berger U., Seiwert B., Meier T., Kuckelkorn J., Strobel C., Knepper T. P., Reemtsma T., 2021. Filling the knowledge gap: A suspect screening study for 1310 potentially persistent and mobile chemicals with SFC- and HILIC-HRMS in two German river systems. *Water Research*, 204, 117645. <https://doi.org/10.1016/j.watres.2021.117645>.
- Nissen K. M. and Ulbrich U., 2017. Increasing frequencies and changing characteristics of heavy precipitation events threatening infrastructure in Europe under climate change. *Natural Hazards and Earth System Sciences*, 17 (7), 1177–1190. <https://doi.org/10.5194/nhess-17-1177-2017>.

- Nowak K. and Jakopin Ž., 2023. In silico profiling of endocrine-disrupting potential of bisphenol analogues and their halogenated transformation products. *Food and Chemical Toxicology*, 173, 113623. <https://doi.org/10.1016/j.fct.2023.113623>.
- Oberleitner D., Stütz L., Schulz W., Bergmann A., Achten C., 2020. Seasonal performance assessment of four riverbank filtration sites by combined non-target and effect-directed analysis. *Chemosphere*, 261, 127706. <https://doi.org/10.1016/j.chemosphere.2020.127706>.
- Ojogoro J. O., Scrimshaw M. D., Sumpter J. P., 2021. Steroid hormones in the aquatic environment. *Science of the Total Environment*, 792, 148306. <https://doi.org/10.1016/j.scitotenv.2021.148306>.
- Pannekens H., Gottschlich A., Hollert H., Dopp E., 2019. Evaluation of mixture effects of endocrine active substances in wastewater using CALUX reporter-gene assays. *International Journal of Hygiene and Environmental Health*, 222 (4), 670–677. <https://doi.org/10.1016/j.ijheh.2019.04.008>.
- Parajulee A., Lei Y. D., De Silva A. O., Cao X., Mitchell C. P. J., Wania F., 2017. Assessing the Source-to-Stream Transport of Benzotriazoles during Rainfall and Snowmelt in Urban and Agricultural Watersheds. *Environmental Science & Technology*, 51 (8), 4191–4198. <https://doi.org/10.1021/acs.est.6b05638>.
- Persson L., Carney Almroth B. M., Collins C. D., Cornell S., De Wit C. A., Diamond M. L., Fantke P., Hassellöv M., MacLeod M., Ryberg M. W., Søgaard Jørgensen P., Villarrubia-Gómez P., Wang Z., Hauschild M. Z., 2022. Outside the Safe Operating Space of the Planetary Boundary for Novel Entities. *Environmental Science & Technology*, 56 (3), 1510–1521. <https://doi.org/10.1021/acs.est.1c04158>.
- Pironti C., Ricciardi M., Proto A., Bianco P. M., Montano L., Motta O., 2021. Endocrine-Disrupting Compounds: An Overview on Their Occurrence in the Aquatic Environment and Human Exposure. *Water*, 13 (10), 1347. <https://doi.org/10.3390/w13101347>.
- Postigo C. and Richardson S. D., 2021. Non-target screening and novel methods based on mass spectrometry detection for identification of unknown disinfection byproducts. In: Manasfi T., Boudenne J.-L. (eds.), *Comprehensive Analytical Chemistry, Analysis and formation of disinfection byproducts in drinking water*, vol. 92, pp. 1–29. Elsevier, Amsterdam, Oxford, Cambridge, MA.
- Reemtsma T., Berger U., Arp H. P. H., Gallard H., Knepper T. P., Neumann M., Quintana J. B., De Voogt P., 2016. Mind the Gap: Persistent and Mobile Organic Compounds-Water Contaminants That Slip Through. *Environmental Science & Technology*, 50 (19), 10308–10315. <https://doi.org/10.1021/acs.est.6b03338>.
- Reinwald H., Alvincz J., Salinas G., Schäfers C., Hollert H., Eilebrecht S., 2022. Toxicogenomic profiling after sublethal exposure to nerve- and muscle-targeting insecticides reveals cardiac and neuronal developmental effects in zebrafish embryos. *Chemosphere*, 291 (Pt 1), 132746. <https://doi.org/10.1016/j.chemosphere.2021.132746>.
- Riegraf C., Bell A. M., Ohlig M., Reifferscheid G., Buchinger S., 2022. Planar chromatography-bioassays for the parallel and sensitive detection of androgenicity, anti-androgenicity and cytotoxicity. *Journal of chromatography A*, 1684, 463582. <https://doi.org/10.1016/j.chroma.2022.463582>.
- Riegraf C., Reifferscheid G., Becker B., Belkin S., Hollert H., Feiler U., Buchinger S., 2019b. Detection and Quantification of Photosystem II Inhibitors Using the Freshwater Alga *Desmodesmus subspicatus* in Combination with High-Performance Thin-Layer Chromatography. *Environmental Science & Technology*, 53 (22), 13458–13467. <https://doi.org/10.1021/acs.est.9b04634>.

- Riegraf C., Reifferscheid G., Belkin S., Moscovici L., Shakibai D., Hollert H., Buchinger S., 2019a. Combination of yeast-based in vitro screens with high-performance thin-layer chromatography as a novel tool for the detection of hormonal and dioxin-like compounds. *Analytica Chimica Acta*, 1081, 218–230. <https://doi.org/10.1016/j.aca.2019.07.018>.
- Riegraf C., Reifferscheid G., Moscovici L., Shakibai D., Hollert H., Belkin S., Buchinger S., 2021. Coupling high-performance thin-layer chromatography with a battery of cell-based assays reveals bioactive components in wastewater and landfill leachates. *Ecotoxicology and Environmental Safety*, 214, 112092. <https://doi.org/10.1016/j.ecoenv.2021.112092>.
- Rocuzzo S., Beckerman A. P., Trögl J., 2021. New perspectives on the bioremediation of endocrine disrupting compounds from wastewater using algae-, bacteria- and fungi-based technologies. *International Journal of Environmental Science and Technology*, 18 (1), 89–106. <https://doi.org/10.1007/s13762-020-02691-3>.
- Rochester J. R. and Bolden A. L., 2015. Bisphenol S and F: A Systematic Review and Comparison of the Hormonal Activity of Bisphenol A Substitutes. *Environmental Health Perspectives*, 123 (7), 643–650. <https://doi.org/10.1289/ehp.1408989>.
- Rockström J., Steffen W., Noone K., Persson Å., Chapin F. S. III, Lambin E., Lenton T. M., Scheffer M., Folke C., Schellnhuber H. J., Nykvist B., De Wit C. A., Hughes T., Van der Leeuw S., Rodhe H., Sörlin S., Snyder P. K., Costanza R., Svedin U., Falkenmark M., Karlberg L., Corell R. W., Fabry V. J., Hansen J., Walker B., Liverman D., Richardson K., Crutzen P., Foley J., 2009. Planetary Boundaries: Exploring the Safe Operating Space for Humanity. *Ecology and Society*, 14, 32. <https://www.ecologyandsociety.org/vol14/iss2/art32/>.
- Ronzheimer A., Schreiner T., Morlock G. E., 2022. Multiplex planar bioassay detecting estrogens, antiestrogens, false-positives and synergists as sharp zones on normal phase. *Phytomedicine*, 103, 154230. <https://doi.org/10.1016/j.phymed.2022.154230>.
- Ruppelt J. P., Pinnekamp J., Tondera K., 2020. Elimination of micropollutants in four test-scale constructed wetlands treating combined sewer overflow: Influence of filtration layer height and feeding regime. *Water Research*, 169, 115214. <https://doi.org/10.1016/j.watres.2019.115214>.
- Sacdal R., Madriaga J., Espino M. P., 2020. Overview of the analysis, occurrence and ecological effects of hormones in lake waters in Asia. *Environmental Research*, 182, 109091. <https://doi.org/10.1016/j.envres.2019.109091>.
- SCHEER (Scientific Committee on Health, Environmental and Emerging Risks), 2022. Preliminary Opinion on "Draft Environmental Quality Standards for Priority Substances under the Water Framework Directive". 17-alpha-ethinylestradiol (EE2), Beta-Estradiol (E2) and Estrone (E1).
- Scheurer M., Heß S., Lüddeke F., Sacher F., Güde H., Löffler H., Gallert C., 2015. Removal of micropollutants, facultative pathogenic and antibiotic resistant bacteria in a full-scale retention soil filter receiving combined sewer overflow. *Environmental Science: Processes & Impacts*, 17 (1), 186–196. <https://doi.org/10.1039/c4em00494a>.
- Schoenborn A., Schmid P., Bräm S., Reifferscheid G., Ohlig M., Buchinger S., 2017. Unprecedented sensitivity of the planar yeast estrogen screen by using a spray-on technology. *Journal of Chromatography A*, 1530, 185–191. <https://doi.org/10.1016/j.chroma.2017.11.009>.
- Schreiner T. and Morlock G. E., 2021. Non-target bioanalytical eight-dimensional hyphenation including bioassay, heart-cut trapping, online desalting, orthogonal separations and mass spectrometry. *Journal of Chromatography A*, 1647, 462154. <https://doi.org/10.1016/j.chroma.2021.462154>.
- Schreiner T. and Morlock G. E., 2023. Investigation of the estrogenic potential of 15 rosé, white and red wines via effect-directed ten-dimensional hyphenation. *Journal of Chromatography A*, 1690, 463775. <https://doi.org/10.1016/j.chroma.2023.463775>.

- Shakibai D., Riegraf C., Moscovici L., Reifferscheid G., Buchinger S., Belkin S., 2019. Coupling High-Performance Thin-Layer Chromatography with Bacterial Genotoxicity Bioreporters. *Environmental Science & Technology*, 53 (11), 6410–6419. <https://doi.org/10.1021/acs.est.9b00921>.
- Shuliakevich A., Schroeder K., Nagengast L., Wolf Y., Brückner I., Muz M., Behnisch P. A., Hollert H., Schiwy S., 2022. Extensive rain events have a more substantial impact than advanced effluent treatment on the endocrine-disrupting activity in an effluent-dominated small river. *Science of the Total Environment*, 807 (Pt 2), 150887. <https://doi.org/10.1016/j.scitotenv.2021.150887>.
- Simon E., Duffek A., Stahl C., Frey M., Scheurer M., Tuerk J., Gehrman L., Könemann S., Swart K., Behnisch P., Olbrich D., Brion F., Aït-Aïssa S., Pasanen-Kase R., Werner I., Vermeirssen E. L. M., 2022. Biological effect and chemical monitoring of Watch List substances in European surface waters: Steroidal estrogens and diclofenac - Effect-based methods for monitoring frameworks. *Environment International*, 159, 107033. <https://doi.org/10.1016/j.envint.2021.107033>.
- Sonavane M., Schollée J. E., Hidasi A. O., Creusot N., Brion F., Suter M. J.-F., Hollender J., Aït-Aïssa S., 2018. An integrative approach combining passive sampling, bioassays, and effect-directed analysis to assess the impact of wastewater effluent. *Environmental Toxicology and Chemistry*, 37 (8), 2079–2088. <https://doi.org/10.1002/etc.4155>.
- Spataro F., Ademollo N., Pescatore T., Rauseo J., Patrolecco L., 2019. Antibiotic residues and endocrine disrupting compounds in municipal wastewater treatment plants in Rome, Italy. *Microchemical Journal*, 148, 634–642. <https://doi.org/10.1016/j.microc.2019.05.053>.
- Stavreva D. A., Collins M., McGowan A., Varticovski L., Raziuddin R., Brody D. O., Zhao J., Lee J., Kuehn R., Dehareng E., Mazza N., Pegoraro G., Hager G. L., 2021. Mapping multiple endocrine disrupting activities in Virginia rivers using effect-based assays. *Science of the Total Environment*, 773, 145602. <https://doi.org/10.1016/j.scitotenv.2021.145602>.
- Stütz L., Schulz W., Winzenbacher R., 2020. Identification of acetylcholinesterase inhibitors in water by combining two-dimensional thin-layer chromatography and high-resolution mass spectrometry. *Journal of Chromatography A*, 1624, 461239. <https://doi.org/10.1016/j.chroma.2020.461239>.
- Tian Z., McMinn M. H., Fang M., 2023. Effect-directed analysis and beyond: how to find causal environmental toxicants. *Exposome*, 3 (1), osad002, 617. <https://doi.org/10.1093/exposome/osad002>.
- Tondera K., Ruppelt J. P., Pinnekamp J., Kistemann T., Schreiber C., 2019. Reduction of micropollutants and bacteria in a constructed wetland for combined sewer overflow treatment after 7 and 10 years of operation. *Science of the Total Environment*, 651 (Pt 1), 917–927. <https://doi.org/10.1016/j.scitotenv.2018.09.174>.
- Trudeau V. L., Thomson P., Zhang W. S., Reynaud S., Navarro-Martin L., Langlois V. S., 2020. Agrochemicals disrupt multiple endocrine axes in amphibians. *Molecular and Cellular Endocrinology*, 513 (4), 110861. <https://doi.org/10.1016/j.mce.2020.110861>.
- Tuerk J., Boergers A., Leonhardt J., Portner C., Gehrman L., Teutenberg T., 2016. Target Analysis, Suspected-Target, and Non-Target Screening for Evaluation and Comparison of Full-Scale Ozonation at Three Wastewater Treatment Plants. In: Drewes J. E. and Letzel T. (eds.), *ACS Symposium Ser, Assessing Transformation Products of Chemicals by Non-Target and Suspect Screening - Strategies and Workflows Volume 2*, vol. 1242, pp. 29–47. American Chemical Society, Washington, DC.
- Van den Belt K., Berckmans P., Vangenechten C., Verheyen R., Witters H., 2004. Comparative study on the in vitro/in vivo estrogenic potencies of 17beta-estradiol, estrone, 17alpha-ethynylestradiol and nonylphenol. *Aquatic Toxicology*, 66 (2), 183–195. <https://doi.org/10.1016/j.aquatox.2003.09.004>.

- Vieira W. T., De Farias M. B., Spaolonzi M. P., da Silva M. G. C., Vieira M. G. A., 2021. Latest advanced oxidative processes applied for the removal of endocrine disruptors from aqueous media – A critical report. *Journal of Environmental Chemical Engineering*, 9 (4), 105748. <https://doi.org/10.1016/j.jece.2021.105748>.
- Völker J., Stapf M., Mieke U., Wagner M., 2019. Systematic Review of Toxicity Removal by Advanced Wastewater Treatment Technologies via Ozonation and Activated Carbon. *Environmental Science & Technology*, 53 (13), 7215–7233. <https://doi.org/10.1021/acs.est.9b00570>.
- Vormeier P., Liebmann L., Weisner O., Liess M., 2023. Width of vegetated buffer strips to protect aquatic life from pesticide effects. *Water Research*, 231, 119627. <https://doi.org/10.1016/j.watres.2023.119627>.
- Walker D. B., Baumgartner D. J., Gerba C. P., Fitzsimmons K. M., 2019. Surface Water Pollution. In: Brusseau M. L., Pepper I. L., Gerba C. P. (eds.), *Environmental and Pollution Science*, 3rd ed., pp. 261–292. Elsevier Science & Technology, San Diego.
- Wang J. and Wang S., 2021. Toxicity changes of wastewater during various advanced oxidation processes treatment: An overview. *Journal of Cleaner Production*, 315 (10), 128202. <https://doi.org/10.1016/j.jclepro.2021.128202>.
- Wang Z., Walker G. W., Muir D. C. G., Nagatani-Yoshida K., 2020. Toward a Global Understanding of Chemical Pollution: A First Comprehensive Analysis of National and Regional Chemical Inventories. *Environmental Science & Technology*, 54 (5), 2575–2584. <https://doi.org/10.1021/acs.est.9b06379>.
- Warner G. R., Mourikes V. E., Neff A. M., Brehm E., Flaws J. A., 2020. Mechanisms of action of agrochemicals acting as endocrine disrupting chemicals. *Molecular and Cellular Endocrinology*, 502, 110680. <https://doi.org/10.1016/j.mce.2019.110680>.
- Weins C. and Jork H., 1996. Toxicological evaluation of harmful substances by in situ enzymatic and biological detection in high-performance thin-layer chromatography. *Journal of Chromatography A*, 750 (1-2), 403–407. [https://doi.org/10.1016/0021-9673\(96\)00601-2](https://doi.org/10.1016/0021-9673(96)00601-2).
- Weiss S. C., Egetenmeyer N., Schulz W., 2017. Coupling of In Vitro Bioassays with Planar Chromatography in Effect-Directed Analysis. *Advances in Biochemical Engineering/Biotechnology*, 157, 187–224. https://doi.org/10.1007/10_2016_16.
- Welbourn P. M. and Hodson P. V., 2022. Chapter 1: The History and Emergence of Ecotoxicology as a Science. In: Campbell P. G. C., Hodson P. V., Welbourn P. M., Wright D. A. (eds.), *Ecotoxicology*, pp. 3–20. Cambridge University Press.
- Westlund P., Isazadeh S., Therrien A., Yargeau V., 2018. Endocrine Activities of Pesticides During Ozonation of Waters. *Bulletin of Environmental Contamination and Toxicology*, 100 (1), 112–119. <https://doi.org/10.1007/s00128-017-2254-8>.
- Wicke D., Matzinger A., Sonnenberg H., Caradot N., Schubert R.-L., Dick R., Heinzmann B., Dünnbier U., Von Seggern D., Rouault P., 2021. Micropollutants in Urban Stormwater Runoff of Different Land Uses. *Water*, 13 (9), 1312. <https://doi.org/10.3390/w13091312>.
- Wilson I. D. and Poole C. F., 2023. Planar chromatography - Current practice and future prospects. *Journal of Chromatography B*, 1214, 123553. <https://doi.org/10.1016/j.jchromb.2022.123553>.
- Windsor F. M., Ormerod S. J., Tyler C. R., 2018. Endocrine disruption in aquatic systems: up-scaling research to address ecological consequences. *Biological Reviews of the Cambridge Philosophical Society*, 93 (1), 626–641. <https://doi.org/10.1111/brv.12360>.

- Wirasnita R., Mori K., Toyama T., 2018. Effect of activated carbon on removal of four phenolic endocrine-disrupting compounds, bisphenol A, bisphenol F, bisphenol S, and 4-tert-butylphenol in constructed wetlands. *Chemosphere*, 210, 717–725. <https://doi.org/10.1016/j.chemosphere.2018.07.060>.
- Wolf Y., Oster S., Shuliakevich A., Brückner I., Dolny R., Linnemann V., Pinnekamp J., Hollert H., Schiwy S., 2022. Improvement of wastewater and water quality via a full-scale ozonation plant? - A comprehensive analysis of the endocrine potential using effect-based methods. *Science of the Total Environment*, 803, 149756. <https://doi.org/10.1016/j.scitotenv.2021.149756>.
- Wright D. A. and Campbell P. G. C., 2022. Chapter 14: Emerging Concerns and Future Visions. In: Campbell P. G. C., Hodson P. V., Welbourn P. M., Wright D. A. (eds.), *Ecotoxicology*, pp. 515–550. Cambridge University Press.
- Wu S., Bashir M. A., Raza Q.-U.-A., Rehim A., Geng Y., Cao L., 2023. Application of riparian buffer zone in agricultural non-point source pollution control—A review. *Frontiers in Sustainable Food Systems*, 7, 985870, 101. <https://doi.org/10.3389/fsufs.2023.985870>.
- Yilmaz B., Terekci H., Sandal S., Kelestimur F., 2020. Endocrine disrupting chemicals: exposure, effects on human health, mechanism of action, models for testing and strategies for prevention. *Reviews in Endocrine & Metabolic Disorders*, 21 (1), 127–147. <https://doi.org/10.1007/s11154-019-09521-z>.
- Yusuf A., O'Flynn D., White B., Holland L., Parle-McDermott A., Lawler J., McCloughlin T., Harold D., Huerta B., Regan F., 2021. Monitoring of emerging contaminants of concern in the aquatic environment: a review of studies showing the application of effect-based measures. *Analytical Methods*, 13 (43), 5120–5143. <https://doi.org/10.1039/d1ay01184g>.
- Zoeller R. T., Brown T. R., Doan L. L., Gore A. C., Skakkebaek N. E., Soto A. M., Woodruff T. J., Vom Saal F. S., 2012. Endocrine-Disrupting Chemicals and Public Health Protection: A Statement of Principles from The Endocrine Society. *Endocrinology*, 153 (9), 4097–4110. <https://doi.org/10.1210/en.2012-1422>.
- Zwart N., Jonker W., Ten Broek R., De Boer J., Somsen G., Kool J., Hamers T., Houtman C. J., Lamoree M. H., 2020. Identification of mutagenic and endocrine disrupting compounds in surface water and wastewater treatment plant effluents using high-resolution effect-directed analysis. *Water Research*, 168, 115204. <https://doi.org/10.1016/j.watres.2019.115204>.

2 Aims and Scope

This work aims to provide an effect-directed analysis (EDA) of endocrine and neurotoxic effects for the characterization and evaluation of aquatic contaminations and treatment measures. The hope is to improve the monitoring and assessment of chemical pollution of the environment in order to reduce the negative impact of human activities on the livelihoods of this and future generations. The combination of high-performance thin-layer chromatography (HPTLC) and two effect-based methods should be practical, efficient, and sensitive to enable more routine use, to map effects holistically, and to increase the likelihood of identifying substances responsible for effects.

Therefore, **Chapter 3** focuses on optimizing the combination of HPTLC with the yeast multi-endocrine effect screen (HPTLC-YMEES) to provide an efficient and sensitive method that is ready for use in the simultaneous investigation of estrogenic, androgenic, and gestagenic effects in wastewater, stormwater and surface water samples on a single HPTLC plate. In **Chapter 4**, the combination of HPTLC with an acetylcholinesterase inhibition (AChE-I) assay with additional simple oxidation of organothiophosphates (HPTLC-Ox-AChE-I) is optimized to provide an efficient and sensitive method that is ready for use in the study of neurotoxic effects in stormwater and surface water samples. Two methods of applying yeast cells or the AChE solution onto HPTLC plates, spraying and immersion, are compared and prioritized based on the highest sensitivity, precision, and efficiency. Sufficient sensitivity to reference hormones and organophosphate insecticides should be achieved with regard to comparable test systems and already detected environmental concentrations or environmental quality standards (EQS).

In **Chapter 5**, discharges from a combined sewer overflow (CSO), a stormwater retention structure (SWR) and a wastewater treatment plant (WWTP) connected to the river Anger in Ratingen, Germany, and the influence of a stormwater retention basin connected to a nearby highway on the Deininghausener Bach, Deininghausen, Germany, are investigated, especially with regard to endocrine and neurotoxic effects. For this purpose, an EDA approach using the optimized HPTLC-YMEES and HPTLC-Ox-AChE-I from **Chapters 3 and 4** for the determination of estrogenic, androgenic, gestagenic, and AChE-inhibiting effects is used (Figure 2-1). Known contaminants from different groups of substances (pharmaceuticals, pesticides and industrial chemicals) and potential effect-causing estrogens are determined by accompanying target analysis with liquid chromatography and gas chromatography coupled to tandem mass spectrometry (LC-MS/MS and GC-MS/MS). High-resolution mass spectrometry (HRMS) is used to identify potential AChE inhibitors. The impact of stormwater depending discharges on surface waters and possible sources of endocrine and neurotoxic contamination should be revealed. The contribution of the CSO and SWR to the endocrine load is estimated in comparison to the WWTP.

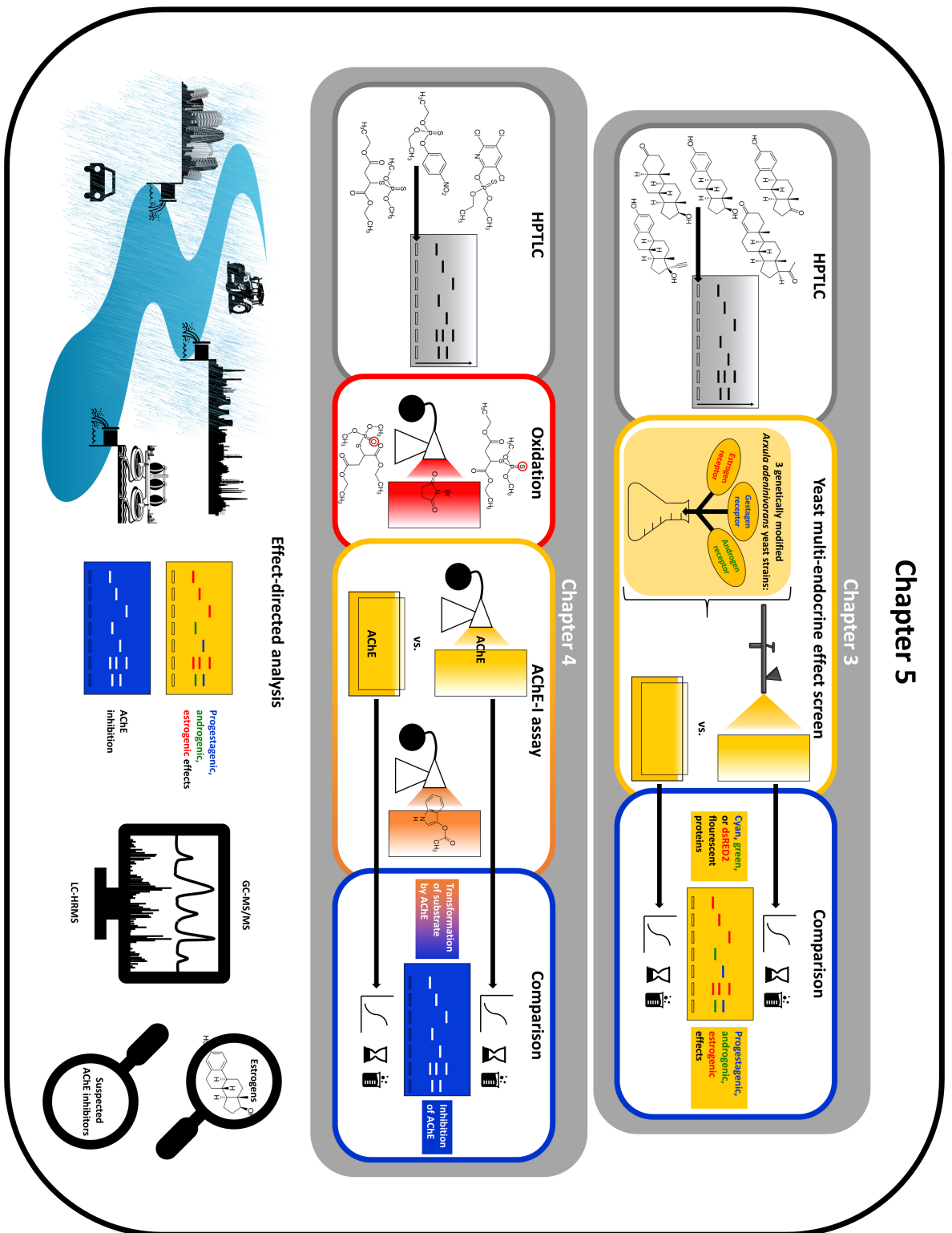


Figure 2-1 Scope and relationship of chapters 3, 4, and 5.

3 High-performance Thin-layer Chromatography in Combination with a Yeast-based Multi-effect Bioassay to Determine Endocrine Effects in Environmental Samples

This chapter is adopted from: Baetz N., Rothe L., Wirzberger V., Sures B., Schmidt T. C., Tuerk J., 2021. High-performance thin-layer chromatography in combination with a yeast-based multi-effect bioassay to determine endocrine effects in environmental samples. *Analytical and bioanalytical chemistry*, 413 (5), 1321–1335. <https://doi.org/10.1007/s00216-020-03095-5>.

3.1. Abstract

Effect-directed analysis (EDA) that combines effect-based methods (EBMs) with high-performance thin-layer chromatography (HPTLC) is a useful technique for spatial, temporal, and process-related effect evaluation and may provide a link between effect testing and responsible substance identification. In this study, a yeast multi-endocrine effect screen (YMEES) for the detection of endocrine effects is combined with HPTLC. Simultaneous detection of estrogenic, androgenic, and gestagenic effects on the HPTLC plate is achieved by mixing different genetically modified *Arxula adenivorans* (MIDDELHOVEN et al., 1984; KURTZMAN & ROBNETT, 2007) yeast strains, which contain either the human estrogen, androgen, or progesterone receptor. Depending on the yeast strain, different fluorescent proteins are formed when an appropriate substance binds to the specific hormone receptor. This allows to measure endocrine effects at different wavelengths. Two yeast cell application approaches, immersion and spraying, are compared. The sensitivity and reproducibility of the method are shown by dose-response investigations for reference compounds. The spraying approach indicated similar sensitivities and higher precisions for the tested hormones compared to immersion. The EC_{10S} for estrone (E1), 17β -estradiol (E2), 17α -ethinylestradiol (EE2), 5α -dihydrotestosterone (DHT), and progesterone (P4) were 95, 1.4, 10, 7.4, and 15 pg/spot, respectively. Recovery rates of E1, E2, EE2, DHT, and P4 between 88 and 120% show the usability of the general method in combination with sample enrichment by solid phase extraction (SPE). The simultaneous detection of estrogenic, androgenic, and gestagenic effects in wastewater and surface water samples demonstrates the successful application of the YMEES in such matrices. This promising method allows us to identify more than one endocrine effect on the same HPTLC plate, which saves time and material. The method could be used for comparison, evaluation, and monitoring of different river sites and wastewater treatment steps and should be tested in further studies.

3.2. Introduction

Pollution of surface waters with endocrine-disruptive compounds (EDCs) from wastewater treatment plants (WWTPs) and diffusive inputs are an emerging problem (ROGOWSKA et al., 2020). Besides estrogenic and androgenic effects, which could be analyzed in surface water and wastewater (HENNEBERG et al., 2014; GEHRMANN et al., 2018; HARTH et al., 2018; ITZEL et al., 2018), also gestagenic effects play an important role in the aquatic environment (FENT, 2015). According to CHANG et al. (2011), androgen (60%) and gestagen (24%) active compounds account for a substantially higher proportion of the total hormone concentration in the effluent of seven WWTPs in China than estrogens (16%). Even if nine androgens, nine gestagens, and only five estrogens were investigated in that study, it still highlights the importance to take other hormones into account, in addition to estrogens. Such results are not yet represented by the European Water Framework Directive (WFD), which considered only the natural estrogens E2 and E1 as well as the synthetic analog EE2 at the watch list (EU, 2018). However, many more known and unknown compounds have the potential to bind to a receptor in the endocrine system. Effects of natural and synthetic hormones as well as byproducts and compounds that are designed for another purpose, but have the potential to be endocrinologically active, could already be observed at very low concentrations (pg/L – ng/L). Described effects mainly relate to reproduction, development, and behavior of aquatic organisms and populations such as fish, gastropods, and amphibians (DUFT et al., 2003; JOBLING et al., 2003; KIDD et al., 2007; ARIS et al., 2014; ORLANDO AND ELLESTAD, 2014; ÖRN et al., 2016; RIVERO-WENDT et al., 2016; ŽIKOVÁ et al., 2017; KUCKELKORN et al., 2018). Moreover, endocrine effects in the aquatic environment caused by transformation products, generated during advanced treatment processes such as ozonation, are hardly known yet (KNOOP et al., 2018b; KNOOP et al., 2018a).

EBMs focus on identification of effects in environmental samples, including all responsible compounds. Therefore, they are recommended for the monitoring of water quality (BRACK et al., 2019). The next step is to link EBMs with chemical and instrumental analysis to receive more information on the sample composition regarding effects and responsible compounds. An EDA is an expanded approach, combining EBMs with chromatographic techniques, enabling a more specific instrumental analysis afterward (SCHUETZLE AND LEWTAS, 1986; BRACK, 2003, 2011; WELLER, 2012; BRACK et al., 2016). A fractionation by high-performance liquid chromatography (HPLC) in combination with EBMs and high-resolution mass spectrometry (HRMS) seems to be a promising tool to evaluate advanced treatment measures, to monitor surface waters, and to identify more effectively effect-relevant substances (ITZEL et al., 2018; MUSCHKET et al., 2018; HASHMI et al., 2020). Nevertheless, this type of EDA is time-consuming when testing the bioactivity of all fractions with a standard microtiter plate bioassay. Complementary to HPLC separations, HPTLC can also be used in combination with EBMs (MORLOCK AND SCHWACK, 2010; BUCHINGER et al., 2013; CHAMAS et al., 2017a; WEISS et al., 2017). Although the

separation is not as effective as the fractionation by HPLC, EBMs can be performed directly on the HPTLC plates. Thus, an opportunity is offered for an all-in-one effect analysis, which includes all separated fractions of a sample. A 2D separation by HPTLC combined with a bioassay is also possible (STÜTZ et al., 2017; STÜTZ et al., 2020). The solvents used for HPTLC are evaporated and therefore do not influence the subsequently performed bioassays. Besides the possible more effective identification of effect-relevant substances after using EDA, an HPTLC-EBM approach can be used to evaluate temporal, spatial, or process-related changes of bioactivity by comparing the effect pattern of a set of samples.

This study addresses a combination of HPTLC and a yeast reporter gene bioassay to detect estrogenic, androgenic, and gestagenic effects simultaneously and directly on the HPTLC plate. This multi-endocrine effect screen (YMEES) is based on genetically modified *Arxula adenivorans* yeast strains that form different fluorescent proteins, if an appropriate substance binds to the inserted human estrogen, androgen, or progesterone receptors (CHAMAS et al., 2017b). This allows the simultaneous detection of more than one endocrine effect in a sample when using a mixture of the yeast strains. In comparison to bioassays where an enzyme is formed by yeast cells, which transforms a substrate into a photometrically detectable product, the present approach does not require an additional substrate. SCHOENBORN et al. (2017) address the problem of lower sensitivity and blurred peaks when immersing HPTLC plates into the yeast suspension. Reversed-phase HPTLC plates, such as RP-18W, can be used, which may reduce the elution of applied samples by the wet yeast suspension (KLINGELHÖFER AND MORLOCK, 2014). Another approach to gain higher sensitivities is to spray the yeast cells onto the HPTLC plates (SCHOENBORN et al., 2017). The authors described higher sensitivities and sharper bands for the used planar yeast estrogen screen (p-YES). CHAMAS et al. (2017a) immersed the HPTLC plates into the yeast suspension. Therefore, the reproducibility and sensitivity of the two yeast cell application methods, immersion and spraying, are compared in this study. Furthermore, the analysis of wastewater and surface water SPE extracts is supposed to demonstrate the detection of estrogenic, androgenic, and gestagenic effects in such matrices when using a spraying approach.

3.3. Materials and methods

3.3.1. Chemicals

The hormones E1, E2, EE2, DHT, and P4 were all purchased from Sigma-Aldrich GmbH (Steinheim, Germany). They were solubilized in methanol at a stock concentration of 1 mg/mL. Methanol (LC-MS grade), acetone (LC-MS grade), dichloromethane (LC-MS grade), and water (LC-MS grade) were all purchased from Th. Geyer GmbH & Co. KG (Renningen, Germany). Cyclohexane (LC-MS grade) was purchased from LGC Standards GmbH (Wesel, Germany). The following chemicals were used for yeast minimal medium supplemented with glucose (cultivation medium) or maltose (test medium): maltose and glucose were purchased from Carl Roth GmbH & Co. KG (Karlsruhe, Germany). NaNO_3 , KH_2PO_4 , and $\text{MgSO}_4 \times \text{H}_2\text{O}$ were purchased from Sigma-Aldrich (Steinheim, Germany). Furthermore, salts, trace elements, and vitamins were purchased from new_diagnostics (Berlin, Germany).

3.3.2. High-performance thin-layer chromatography

The automatic TLC Sampler 4 (ATS 4, CAMAG, Muttenz, Switzerland) was used for sample application. The desired sample volumes were sprayed as 6 mm bands, 8 mm from the bottom and 15 mm from the side, on the plate with an application speed of 300 nL/s. Methanol was used as the rinsing solvent. The following further application parameters were used: filling speed 15 $\mu\text{L/s}$, predosage volume 200 nL, retraction volume 200 nL, rinsing vacuum time 4 s, filling vacuum time 0 s, rinsing cycles 2, and filling cycle 1. The rinsing and filling cycles were varied for the environmental samples to prevent a possible carryover to following samples. For the first two samplings, the filling cycles were set to 2 to wash the syringe with the sample extracts. For the additional river sample, the filling cycles were set to 1 and the rinsing cycles were increased to 3 to save sample extract. Overall, carryover effects were not observed in this study and therefore the settings of rinsing and filling cycle had no influence on the results. The development was realized by the Automated Multiple Development 2 (AMD 2, CAMAG, Muttenz, Switzerland) containing the eluent mixture dichloromethane, cyclohexane, and acetone in different proportions and with increasing migration distances (Figure 3-6 and Figure 3-7). Once the set migration distance was reached, the development stopped and a drying step of 2–3 min under vacuum followed. The final migration distance was 80 mm.

3.3.2.1. Stationary phase

Three different types of thin-layer chromatography plates with a size of 200 × 100 mm were used. The first plate is a SIL G-25 (Macherey-Nagel, Düren, Germany) with a 250 μm silica gel layer, which has a specific surface area of 500 m^2/g , a mean pore size of 60 Å, a specific pore volume of 0.75 mL/g, and a particle size of 5–17 μm . The second plate is an RP-18W (Macherey-Nagel, Düren, Germany) with a 250 μm octadecyl-modified silica gel layer. The plate has the same specifications as the first plate except for a particle size of 2–10 μm . The third plate is a LiChrospher HPTLC silica gel 60 F254s

(Merck, Darmstadt, Germany) with a layer thickness of 170–190 μm and spherical silica particles. The particle size is 7 μm . The plates were washed with methanol, dried for 20 min at room temperature, heated at 105 $^{\circ}\text{C}$ for 20 min, and stored in a desiccator for further use.

3.3.2.2. Separation of hormones

On the three different plate types (3.3.2.1), 5 μL of E1, E2, EE2, DHT, and P4 was applied as single compounds and in an overall mixture. The concentration of each substance in methanol also within the mixture was 100 $\mu\text{g}/\text{mL}$, which corresponds to 500 ng on the plate. For an optical analysis without using the YMEES, the developed plates were sprayed with 8% sulfuric acid in ethanol and incubated for 10 min at 105 $^{\circ}\text{C}$. Then, the absorbance of each track was scanned at 310 nm using the TLC Scanner 3 (CAMAG, Muttenz, Switzerland). The CAMAG-embedded software, Wincats (vers. 1.4.9), was used to provide chromatograms of each track and to evaluate the absorbing zones. Experiments with each plate type were performed in triplicate. The mean of the substance's retardation factor (R_F) was calculated and compared with the mean of the substance's R_F from the different concentrations of the dose-response investigations (3.3.3.4).

3.3.2.3. Multiple application procedure

Three spots of E2 with a concentration of 100 $\mu\text{g}/\text{mL}$ dissolved in methanol were applied on a SIL G-25 plate. The application volume was 25 μL , resulting in 2500 ng/spot. On the same plate, three spots of E2 with a concentration of 50 $\mu\text{g}/\text{mL}$ were applied two times in succession resulting also in 2500 ng/spot. Moreover, 25 $\mu\text{g}/\text{mL}$ was applied four times and 12.5 $\mu\text{g}/\text{mL}$ eight times. The plate was not developed, because the focus was the multiple application of E2. The optical analysis was the same as described before (3.3.2.2). After the scan, the peak areas of the different application numbers were compared. For this purpose, the mean values of the three spots were calculated with Excel 2013 (vers. 15.0.5172.1000, Microsoft, Redmond, USA).

3.3.3. Yeast multi-endocrine effect screen

3.3.3.1. Strains and cultivation conditions

In this study, the yeast strains *Arxula adenivorans* G1212/YRC102-hPR-CFP (gestagen), G1212/YRC102-hAR-GFP (androgen), and G1212/YRC102-hER-DsRed2 (estrogen) described by CHAMAS et al. (2017b) and provided by new_diagnostics (Berlin, Germany) were used. For the detection of gestagenic, androgenic, and estrogenic effects on HPTLC plates, each strain was cultivated in yeast minimal media supplemented with glucose at 30 $^{\circ}\text{C}$ for approximately 24 h. During incubation, the yeast cells were shaken at 350 rpm using a Vibramax 100 platform shaker (orbit: 3 mm; Heidolph Instruments GmbH & Co. KG, Schwabach, Germany).

After incubation, the OD_{620 nm} of each yeast strain was measured with the absorbance microplate reader Sunrise (Tecan Trading AG, Switzerland) and should be between 3 and maximal 4. The cells were centrifuged at 4000×g for 10 min at 25 °C. The pellets were resuspended in yeast minimal media supplemented with maltose. The composition of both test media is shown in Table 3-4. After resuspension, the OD_{620 nm} of each yeast strain was checked again. If it was between 2.5 and 3.5, the three individual yeast suspensions were mixed 1:1:1 by volume to receive *A. adenivorans* G1212/YRC102-hHR-fluo at a final total OD_{620 nm} of approximately 3.

3.3.3.2. Experimental procedure

The mixed yeast suspension was applied on the HPTLC plates either by immersion or by spraying. For the immersion approach, the Chromatogram Immersion Device 3 (CID 3, CAMAG, Muttenz, Switzerland) was used. The plates were immersed into approximately 200 mL yeast suspension with a speed of 2.5 cm/s for 5 s. Excessive cell suspension was removed on the sides and the surface of the plates with a clean paper towel. For the spraying approach, a conventional double-action airbrush gun (AFC-101A, Conrad Electronics SE, Hirschau, Germany) with a 0.35 mm nozzle was used. Instead of air, nitrogen serves as the carrier gas. The spraying was carried out under a fume hood. The HPTLC plates were placed on a stainless-steel rack in an upright position. The distance between the plate and sprayer was approximately 30 cm. Approximately 14 mL of the yeast suspension was sprayed in a steady and repeatable way by spraying from left to right and bottom to top (Figure 3-8). The optimized spraying procedure includes an additional 180° rotation of the plate (Figure 3-9). The spraying scheme was repeated until the whole volume of the yeast suspension was used up. After the application of the yeast suspension, the HPTLC plates were put into plastic boxes, which contained wet paper towels to achieve a humidity of 100%. The closed boxes were incubated for 18 h at 30 °C. After incubation, the plates were scanned with the TLC Scanner 3 and following excitation wavelengths/emission filters: 445/K460 nm, 475/K500 nm and 542/K560 nm to determine the fluorescence of the cyan fluorescent protein (CFP, gestagen), green fluorescent protein (GFP, androgen), and DsRed2 protein (estrogen), respectively. Wincats (vers. 1.4.9) was used to provide chromatograms of each track and to evaluate the fluorescent zones.

3.3.3.3. Dispersion of the yeast cells

Twenty spots of E2 with a concentration of 1 ng/mL were applied on SIL G-25 plates. The application volume was 25 µL, resulting in 25 pg E2 per spot. Five tracks were applied, each including four spots that were sprayed 10, 30, 50, and 70 mm from the bottom. The plates were not developed. The YMEES was performed as described in 3.3.3.2. Three plates per yeast cell application approach were tested. Another three plates were tested with the optimized spraying method.

After the scan, the relative standard deviation of the peak areas from all spots was calculated for every single plate using Microsoft Excel.

3.3.3.4. Dose-response relationship

The optimized spraying and the immersion method were used to establish dose-response curves of E1, E2, EE2, DHT, and P4. Dilution series of an estrogen mixture (E1, E2, EE2) were applied on SIL G-25 and RP-18W plates (Table 3-5). Dilution series of a mixture of DHT and P4 were only applied on SIL G-25 plates (Table 3-6). Additionally, a methanol blank and the single substances were applied. The application volume was 25 μ L. After development (3.3.2), the YMEES was performed as described in 3.3.3.2. The statistic program Prism (version 5.00, GraphPad Software, San Diego, USA) was used to generate four parametric dose-response curves from the peak areas and to determine effect doses (EDs) for the five substances.

3.3.4. Analysis of environmental samples

3.3.4.1. Sampling sites

Two samplings were performed in June and July 2019 at the municipal WWTP Schwerte in Germany (Figure 3-10), which is operated by the water association Ruhrverband (Essen, Germany). The WWTP is equipped with two completely separated treatment lines: the first line operates only with the conventional treatment steps (mechanical, biological, and chemical treatment) and the second one with ozonation as an additional advanced treatment step for micropollutant removal (GRÜNEBAUM et al., 2014). The ozonated water from the secondary clarifier is recirculated into the biological treatment step to enable a subsequent degradation of possibly formed transformation products. Grab samples were taken from the effluent of the conventional treatment line, from the advanced treatment line after biological post treatment, and from the receiving river Ruhr upstream of the WWTP. In addition, grab samples were taken directly after the ozonation. Another grab sample was taken in March 2020 at the Anger in Ratingen, Germany. During this third sampling, also a sampling blank, containing water (LC-MS grade), was opened at the sampling point and also used to wash the sampling vessel. The hydraulic retention time of the different treatment steps and the flow rate of the rivers were not considered during sampling. The samples were cooled during transport and stored < 8 °C until further sample preparation.

3.3.4.2. Sample preparation

The samples were enriched by SPE within 24 h after sampling. Moreover, the sampling blank, water for a SPE blank, and water spiked with a mixture of estrogens and a mixture of DHT and P4 for two SPE quality controls (SPE QC) were enriched in the same way.

The cartridges (150 mg, Oasis HLB 6 cc, Waters GmbH, Eschborn, Germany) were conditioned with methanol (2 × 3 mL) and equilibrated with water (2 × 3 mL), before being loaded with 1000 ± 5 mL sample (the exact volume was determined by weighting) through a polytetrafluoroethylene tube. After drying the cartridges under vacuum, they were stored at -18 °C until further usage. The cartridges were eluted with methanol (5 × 5 mL) that was evaporated afterward at 60 °C under a gentle nitrogen gas stream. The dried extracts were redissolved in 1 mL methanol to achieve a nominal 1000-fold enrichment.

3.3.4.3. HPTLC and yeast multi-endocrine effect screen

The extracts were applied on SIL G-25 plates. In addition, a methanol blank, the SPE blank, two positive controls (PC1: E1, E2, EE2, and PC2: DHT, P4), and the two SPE QCs were applied. The applied absolute amounts for PCs and SPE QCs are 1000/5000 pg E1, 25 pg E2, 100 pg EE2, 250/100 pg DHT, and 250 pg P4 (first sampling/second sampling). The application volume was 25 µL. After development (3.3.2), the plates were scanned at the specific wavelengths of the YMEES that was performed as described in 3.3.3.2. In this case, the optimized spraying method was used for yeast application. Peaks that are visible when scanning at the three wavelengths before applying the YMEES were considered as no endocrine effects. Effect peaks in the samples, which showed the same R_F as peaks in the SPE blank or in the sampling blank of the third sampling, were not used for evaluation. Effect peaks with a peak area lower than 1000 AU were not used for further evaluation. Recovery rates were calculated by relating the peak areas of E1, E2, EE2, DHT, and P4 in the SPE QCs to the peak areas in the PCs.

3.4. Results and discussion

The separation of five hormones on three different HPTLC plate types was compared. The automated eight-step HPTLC development process (Figure 3-6) showed the following separation order: E2, DHT, EE2, P4, and E1 (Table 3-1 and Figure 3-1). The different HPTLC plate types did not affect this aspect, but they influenced the separation quality. While the substances' migration distances were the lowest on the LiChrospher plate, the peak width was much narrower than on the other plates. This led to a similar separation quality as on the RP-18W plate, where the peaks were a bit wider, but the R_F s and particularly the distance between DHT and EE2 were higher. The poorest separation quality was observed at the SIL G-25 plate because the distances between the hormones were not sufficient for a clear differentiation, especially for P4 and E1. The silica particles, which are spherical on the LiChrospher plate and smaller on the RP-18W plate than on the SIL G-25 plate, might be one reason for this result. The higher R_F s on the RP-18W plate are a consequence of the C18 modification. However, a dose-response investigation, which was implemented with the same concentrations as on SIL G-25 plates (Table 3-5) showed substantially lower sensitivities for E1, E2, and EE2 on the RP-18W plate. Klingelhöfer and Morlock (2014), who applied yeast cells by immersion and used the

RP-18W plate, showed lower sensitivities for E1, E2, EE2, and estriol (E3) than Schoenborn et al. (2017), who applied yeast cells by spraying and used normal phase silica gel plates. Although the sensitivity might be higher on the LiChrospher plate than on the SIL G 25, it was not tested with the YMEES due to delivery problems. Nevertheless, the following dose-response investigations with the SIL G-25 plate are appropriate to show the differences between the yeast cell applications by immersion and spraying. Because of the better hormone separation, it would make sense to analyze environmental samples with the LiChrospher plate. However, to provide a realistic proof of concept for the general method, using the optimized spraying approach instead of immersion in contrast to Chamas et al. (2017a), the results with the SIL G-25 plate should be sufficient. Except for DHT, all substances migrated a little further when using the YMEES on the SIL G-25 plate, which can be seen in the slightly higher R_F s in comparison to the results of the optical analysis (Table 3-1). DHT showed the same R_F of 0.22 for the optical analysis and optimized spraying approach. Only with the immersion method, DHT migrated to a R_F of 0.24, but otherwise no significant differences could be observed between the two yeast application methods. The results indicated that the application of yeast suspension results in a slight shift of the substances. However, all the observed differences could be due to variability of the plate's surface or the chromatographic process with the AMD 2. The resulting peaks of the YMEES had not clear and sharp peak forms as with the optical analysis. The reasons are probably the indirect effect detection by the formation of fluorescent proteins and the wet application of the yeast suspension instead of a chemical pretreatment as with the optical analysis. Differences between the two application methods regarding the peak shape and width as described by Schoenborn et al. (2017) were not observed in this study.

Table 3-1 The mean retardation factors (R_F s) \pm standard deviations (SDs) of E2, DHT, EE2, P4, and E1 on different HPTLC plate types, measured with optical analysis after chromatographic separation, are shown on the left side ($n = 3$). The absorbance of each track was scanned at 310 nm. The mean R_F s \pm SDs of E2, DHT, EE2, P4, and E1 on SIL G-25 plates, measured with the yeast multi-endocrine effect screen (YMEES) after similar chromatographic separation by HPTLC, are shown on the right side for both yeast cell application methods (immersion and optimized spraying). The mean R_F s and SDs are calculated from the different tested concentrations of the dose-response investigations ($n = 27$).

Method	Optical analysis			Immersion	Optimized spraying
	RP18-W	LiChrospher	SIL G-25	SIL G-25	SIL G-25
Substance					
E2	0.23 \pm 0.03	0.14 \pm 0.01	0.18 \pm 0.01	0.20 \pm 0.01	0.21 \pm 0.01
DHT	0.27 \pm 0.02	0.17 \pm 0.01	0.22 \pm 0.01	0.24 \pm 0.01	0.22 \pm 0.01
EE2	0.35 \pm 0.03	0.21 \pm 0.03	0.25 \pm 0.01	0.29 \pm 0.01	0.29 \pm 0.02
P4	0.40 \pm 0.02	0.25 \pm 0.02	0.32 \pm 0.01	0.34 \pm 0.02	0.34 \pm 0.02
E1	0.43 \pm 0.02	0.27 \pm 0.04	0.34 \pm 0.01	0.40 \pm 0.01	0.39 \pm 0.01

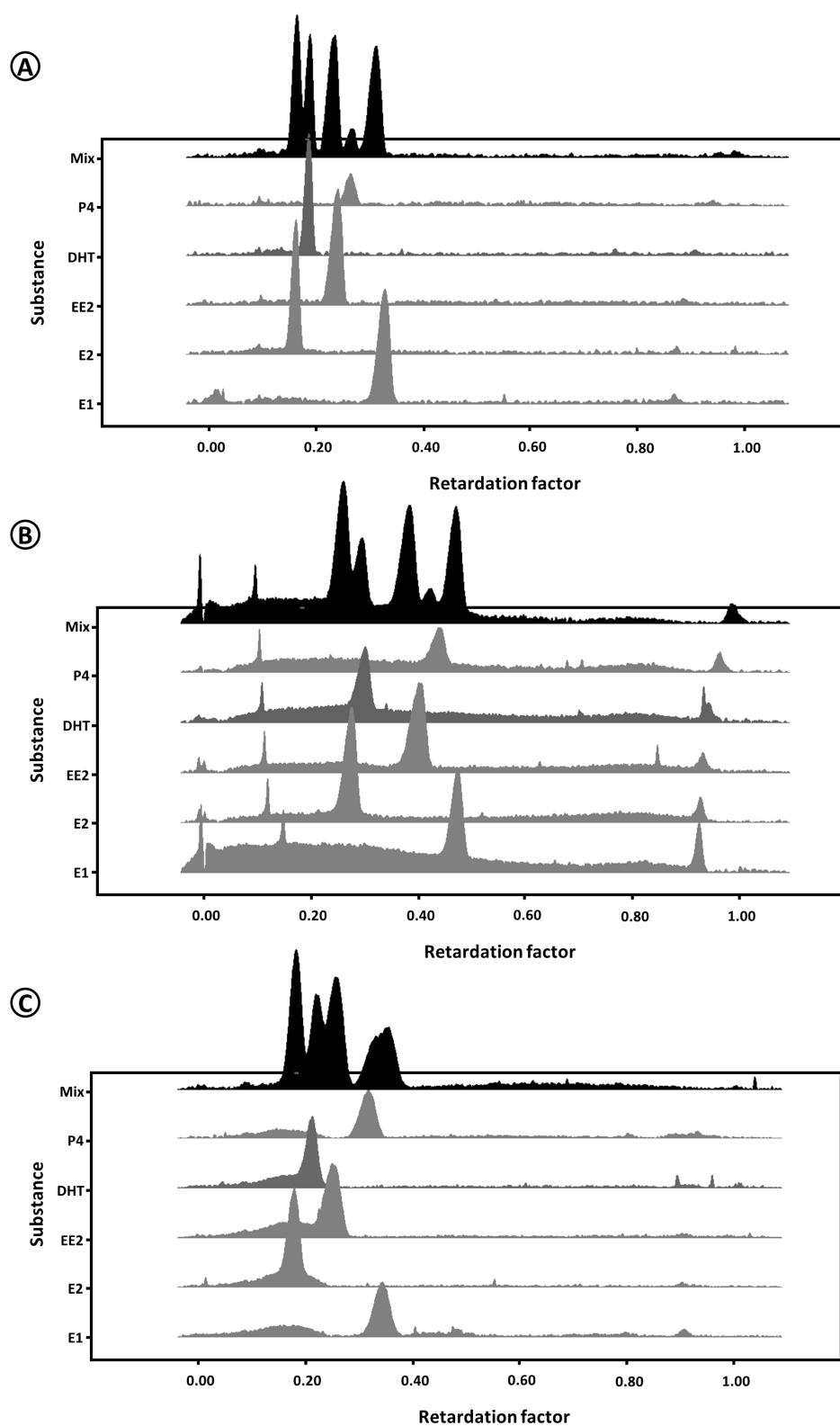


Figure 3-1 Separation of E2, DHT, EE2, P4, and E1 on LiChrospher (A), RP-18W (B), and SIL G-25 (C) plates. The application volume was 5 μ L and the concentration of each substance in methanol also within the mixture was 100 μ g/mL, which corresponds to 500 ng on the HPTLC plates. After chromatographic separation, the plates were sprayed with 8% sulfuric acid in ethanol and incubated for 10 min at 105 $^{\circ}$ C. The absorbance of each track was measured at 310 nm. The y-axis shows the tracks of the different hormones and the mixture. The x-axis shows the retardation factor.

When comparing the two yeast application methods, one aspect should be the dispersion of the yeast cells on the HPTLC plate. A spraying approach with a conventional airbrush gun is sensitive to an inhomogeneous dispersion of the yeast suspension because it depends on the user where the spray mist reaches the plate. The plates were sprayed in a steady and repeatable way by spraying from left to right and bottom to top (Figure 3-8). However, this approach showed a slightly more inhomogeneous result than immersion (Table 3-7). The peak areas of the E2 signals decreased from bottom to top (Figure 3-11). More yeast suspension seems to reach the lower end than the top of the plate because of gravity. SCHOENBORN et al. (2017) also applied yeast suspension onto HPTLC plates in upright position by spraying with a glass reagent sprayer. They described an opposite result because the signals at the bottom of the plate were significantly lower than the highest signals they tested. For this reason, an optimized spraying approach, which included an additional repeated 180° rotation of the plate (Figure 3-9), was applied to guarantee a more consistent dispersion of the yeast cells. The relative standard deviation (RSD) of peak areas from 60 E2 spots indicated a better RSD of 13% than for immersion and the first spraying approach (Table 3-7). Moreover, the optimized spraying method showed a more consistent distribution than the first spraying method (Figure 3-11). As an alternative to manual spraying, other studies used an automatic TLC derivatizer to spray yeast cells onto HPTLC plates (BERGMANN et al., 2020).

The determined dose-response relations for the estrogens indicated the following order of decreasing sensitivity: E2, EE2, and E1 (Figure 3-2 and Table 3-2). This is not surprising because studies such as KLINGELHÖFER AND MORLOCK (2014) and VAN DEN BELT et al. (2004) showed the same receptor affinity order for these estrogens. The best fit ED_{10S} for E2 with 2.0 and 1.4 pg/spot were more than six times lower than the results for EE2 with 13 and 10 pg/spot for immersion and spraying, respectively. The ED_{10S} for E1 were much higher: for immersion, 173 and for spraying, 95 pg/spot. SCHOENBORN et al. (2017) described lower sensitivity levels for these estrogens. However, a comparison with these results should be taken with caution because other yeast strains were used. Moreover, the signal to noise ratio was used to define detection limits. CHAMAS et al. (2017a) showed a first detectable peak at 7.5 pg/spot. They also presented a dose-response relation of the amounts of E2 and the tested peak areas, but unfortunately did not indicate EDs, neither for E2 nor for DHT and P4. The linear section of the dose-response curve between ED₂₀ and ED₈₀ could be used for quantification of these estrogens or to give equivalent concentrations of unknown estrogenic effects. The linear ranges for the immersion and spraying procedure are shown in Figure 3-2 and Table 3-2.

The DHT dose-response relations showed a similar result. For the estrogens, the spraying approach was more sensitive than immersion. The best fit ED_{10S} for DHT with 8.6 and 7.4 pg/spot for immersion and spraying, respectively, also indicated a better sensitivity for the spraying method (Table 3-2). RIEGRAF et al. (2019) showed an ED₁₀ of 46 pg with the p-YAS using a spraying approach.

CHAMAS et al. (2017a) detected the first DHT peak at 25 pg/spot. The immersion approach showed a flatter curve progression for DHT, which could be seen in the higher ED₅₀. The linear ranges of the dose-response curves were between 22 and 506 pg/spot for immersion and 17 and 295 pg/spot for spraying.

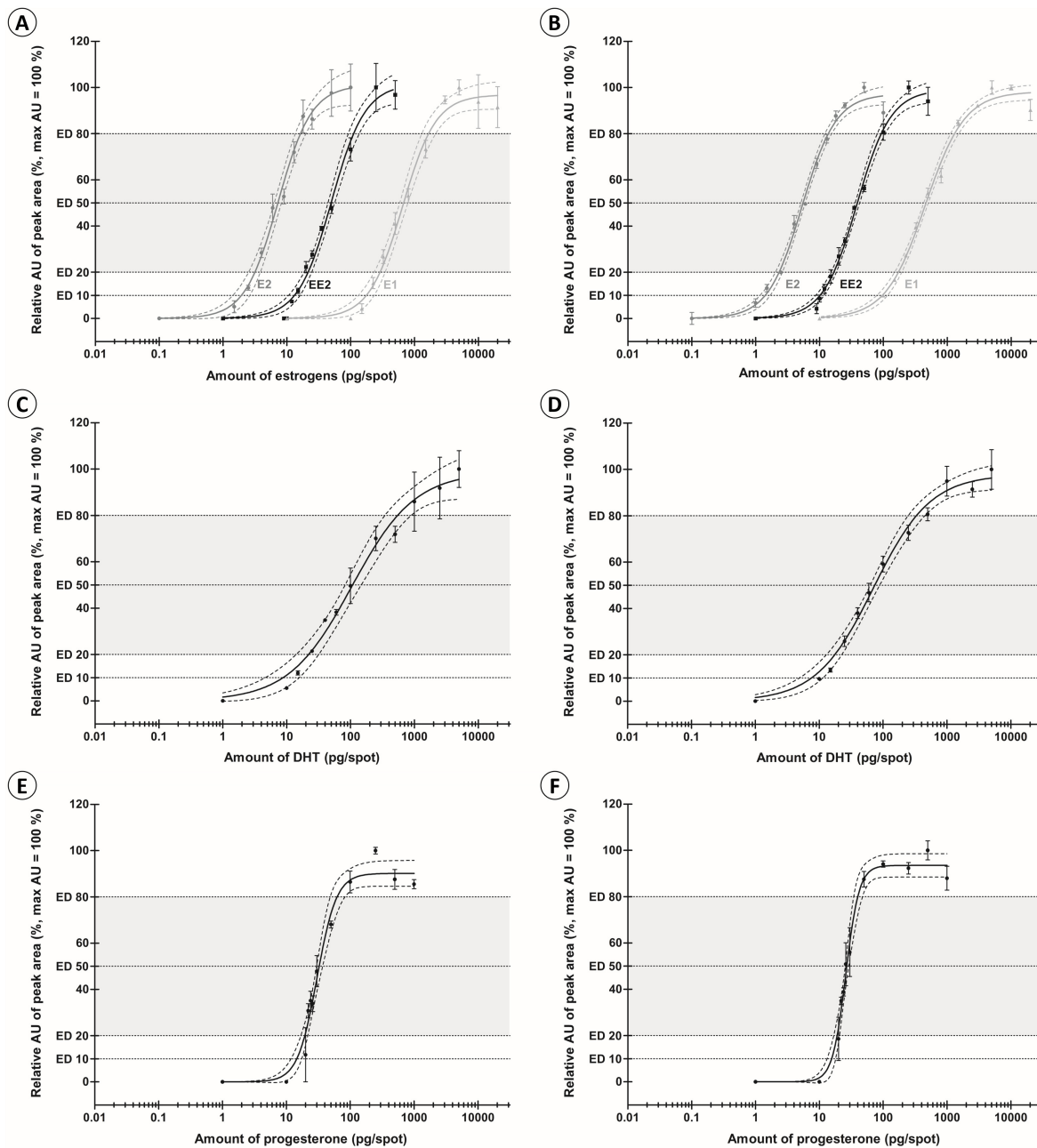


Figure 3-2 Dose-response curves (4-PL fit) of E1, E2, EE2, DHT, and P4. A mix of the estrogens and a mix of DHT and P4 were applied with different concentrations on SIL G-25 plates. The application volume was 25 μ L. After chromatographic separation by HPTLC the yeast multi-endocrine effect screen (YMEES) for the detection of estrogenic, androgenic, and gestagenic effects was performed. The HPTLC plates were either immersed (A, C, and E) into the yeast suspension or the cells were sprayed (B, D, and F) onto the plates by airbrush. The gray, black, and light gray curves (A and B) indicate E2, EE2, and E1, respectively. C, D: Dose-response curves for DHT. E, F: Dose-response curves for P4. The dots represent the relative AUs of the mean peak areas ($n = 3$) at a specific hormone amount on the HPTLC plate (pg/spot). The highest mean peak areas define 100%. The dashed lines show the 95% confidence intervals and the error bars the standard deviations. The dotted lines indicate ED₁₀, ED₂₀, ED₅₀, and ED₈₀. The gray-colored area between ED₂₀ and ED₈₀ shows the linear range.

Table 3-2 Results of dose-response investigations. A mix of E1, E2, and EE2, and a mix of DHT and P4 were applied with different concentrations on SIL G-25 plates. The application volume was 25 μ L. After chromatographic separation by HPTLC the yeast multi-endocrine effect screen (YMEES) for the detection of estrogenic, androgenic, and gestagenic effects was performed. The HPTLC plates were either immersed (left side) into the yeast suspension or the cells were sprayed (right side) onto the plates by airbrush. The best fit 10, 20, 50, and 80% effect doses (ED) in pg/spot and 95% confidence intervals (95% ci) of the dose-response curves (4-PL fit) are shown.

Method	Immersion				Optimized spraying			
	ED ₁₀	ED ₂₀	ED ₅₀	ED ₈₀	ED ₁₀	ED ₂₀	ED ₅₀	ED ₈₀
Substance								
E1								
Best fit	173	282	649	1497	95	169	453	1216
95% ci	130–231	231–344	542–778	1077–2080	79–114	149–192	407–505	990–1493
E2								
Best fit	2.0	3.2	7.3	17	1.4	2.3	5.3	13
95% ci	1.5–2.6	2.6–3.9	6.1–8.8	12–24	1.2–1.7	2.0–2.6	4.8–5.9	10–15
EE2								
Best fit	13	22	50	116	10	17	39	90
95% ci	11–16	19–25	42–60	84–161	8.8–12	15–18	34–44	73–112
DHT								
Best fit	8.6	22	105	506	7.4	17	71	295
95% ci	4.9–15	15–32	65–170	206–1244	4.9–11	13–22	55–91	179–487
P4								
Best fit	14	19	30	49	15	19	26	36
95% ci	11–17	16–21	27–34	39–62	13–18	17–21	24–28	31–43

The P4 dose-response relations indicated a slightly better sensitivity for immersion with an ED₁₀ of 14 pg/spot (Table 3-2). The ED₁₀ for spraying was 15 pg/spot. CHAMAS et al. (2017a) showed a lower sensitivity of 25 pg/spot. HASHMI et al. (2020) detected P4 in surface water with a concentration of 3.3 ng/L. Thus, it is possible to detect such concentrations with this method after a 1000-fold enrichment. Both curves showed a steep progression. The ED₅₀s were 30 and 26 pg/spot for immersion and spraying, respectively. The precision was slightly higher for the spraying method. The results showed a narrow quantifiable range compared with the other tested substances. It was between 19 and 49 pg/spot for immersion and 19 and 36 pg/spot for spraying. Overall, the evaluation of gestagenic effects is more difficult than for the other endocrine effects because of unclear peak forms and low peak heights. This complicates the peak identification in low concentration ranges. Peaks at higher concentrations become wider but are still much lower than estrogenic or androgenic effect peaks in high concentration ranges (Figure 3-12). Thus, P4 results are less reliable than results for DHT and estrogens and the identification of gestagenic effects in environmental samples becomes less likely with this method.

Overall, the sensitivity of both methods, spraying and immersion, is similar for all hormones tested. CHAMAS et al. (2017a) showed lower sensitivities for E2, DHT, and P4. In contrast to this study, they immersed polyester sheets precoated with 0.2 mm silica gel into the individual yeast strain suspensions to investigate the sensitivity for E2, DHT, and P4 without prior chromatography. The higher precision of the spraying approach is shown by the 95% confidence intervals. In summary, these facts, the reduced consumption of yeast suspension, and the better distribution of the yeast cells when using the optimized spraying procedure lead to a promising alternative to the immersion method. Therefore, the optimized spraying approach was used in the following environmental measurements.

The results demonstrated the possibility to detect E2 within the recommended environmental quality standard (EQS) of 0.4 ng/L (EU, 2018), provided that for example a prior sample enrichment by SPE of 1000-fold is achieved and a volume of 6 µL extract is applied on the HPTLC plate. The recommended EQS for EE2 of 0.035 ng/L (EU, 2018) can be detected, for example if 1000 mL of a sample is reduced via SPE to 100 µL extract and a volume of 50 µL is applied. However, due to matrix effects when analyzing for example wastewater samples, the high enrichment factor of 10,000 could affect the chromatography and following bioassay. Higher application volumes on an HPTLC plate allow lower sample volumes for SPE or a higher overall enrichment. A higher enrichment makes sense because of predicted low sensitivities for hormones and other unknown EDCs in surface water and wastewater matrices. Multiple applications are suitable to achieve higher application volumes. A multiple application of methanol samples spiked with E2 showed recovery rates on the HPTLC plate between 85 and 117% in relation to a one-time application (Figure 3-13). Moreover, multiple applications enable

the direct application of aqueous samples on HPTLC plates. SCHOENBORN et al. (2017) mention a possible application of aqueous samples with a volume of up to 1.5 mL. KLINGELHÖFER AND MORLOCK (2015) applied 1 mL of double-distilled water, spiked with E1, E2, and EE2. The recovery rates were all above 80%, but the detection limits were higher than for extracted samples. The needed application volume with the method used in this study would be at least 3.5 mL to achieve 0.4 ng/L, due to the ED_{10} of 1.4 pg/spot for E2 (Table 3-2). The application of 25 μ L takes up to 3 min, depending on the number of rinsing steps and application speed, which was 300 nL/s. Therefore, 420 min would be necessary to apply 3.5 mL on an HPTLC plate. Long application times might lead to a loss of already-applied substances. A lower limit of detection and adjusted application settings, described by KLINGELHÖFER AND MORLOCK (2015) for the application of aqueous samples, would reduce the procedure time. To apply native water samples directly on the HPTLC plate, a subsequent centrifugation might be required because particulate material could block the syringe or disturb the chromatography and following measurements. High amounts of particulate material could also block SPE cartridges but this was not observed in this study. Besides the enrichment and long-term stability before analysis, SPE allows the application and elution of a whole native water sample, including particle-bound substances (GÜNTER et al., 2016). This shows the advantage to integrate SPE in the workflow, even though the recovery of unknown effect causing substances might be insufficient.

A problem of the used yeast strains is the fact that estrogenic effects can also be detected when scanning for androgenic effects (GFP, excitation 475 nm/emission filter K500) (Figure 3-14). The peak areas in the androgen scan were slightly lower than those in the estrogen scan. This problem was also observed and explained by CHAMAS et al. (2017a). The reason is probably a second excitation peak of the DsRED protein in the range of the GFP's excitation wavelength so that DsRED is induced simultaneously. The emission light of both proteins is above 500 nm. Only the wavelengths below 500 nm are filtered by the K500 emission filter, which results in the measurement of both emission wavelengths when scanning for androgenic effects. A differentiation between estrogenic and androgenic effects is possible because androgenic effects are not visible when scanning for estrogenic effects (DsRED2, excitation 542 nm/emission filter K560) (Figure 3-15). This is also shown when comparing androgenic and estrogenic effects of the wastewater sample taken from the outlet of ozonation during the second sampling (Figure 3-3). Two estrogenic effect peaks with a R_F between 0.36 and 0.46 appeared also in the androgen scan, but with another peak directly adjoining left of them (R_F range: 0.46–0.51), which was not visible in the estrogen scan. Thus, the latter must be a true androgenic effect. The occurrence of both effects at the same spot would complicate the evaluation. Only an explicitly higher peak in the androgen than in the estrogen scan would be a hint for the presence of both effects.

When scanning for gestagenic effects (CFP, excitation 445 nm/emission filter K460), estrogenic and androgenic effects can also be visible, but with much lower peak areas and heights than in the actual estrogen or androgen scan (Figure 3-14 and Figure 3-15). The reason could be an additional binding to the progesterone receptor in the yeast cells so that estrogen active compounds also cause gestagenic effects. Androgenic effects may occur in the gestagenic scan because of a simultaneous excitation of the GFP at 445 nm. This wavelength is probably part of the GFP excitation peak, but not the maximum, which would explain the lower intensities (COTLET et al., 2006).

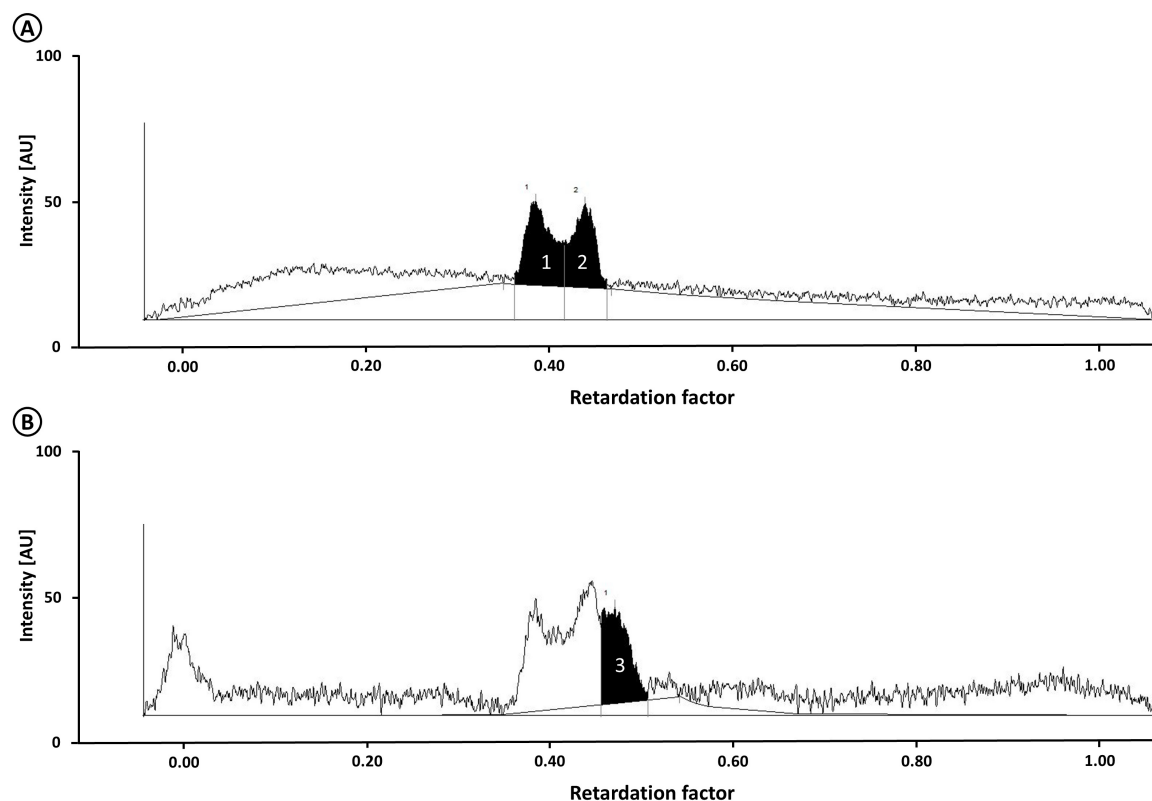


Figure 3-3 Chromatogram of estrogenic (A) and androgenic (B) effects in the outlet of the ozonation (second sampling). The application volume of the 1000-fold enriched sample (SPE) was 25 μ L. The sample was separated by HPTLC and measured with the yeast multi-endocrine effect screen (YMEES) for the detection of estrogenic, androgenic, and gestagenic effects. Estrogenic effect peaks (A) 1 and 2 and an androgenic effect peak (B) 3 are shown.

However, the simultaneous formation and direct measuring of different fluorescent proteins on the same HPTLC plate lead to fewer steps and substances, such as a substrate, needed for the workflow. Moreover, it allows the analysis of more than one endocrine effect, which is a big advantage, because of substantial time and material savings. Nevertheless, the strength of this method is weakened when effects are detectable not only in their specific scan. The use of other fluorescent proteins or a genetic modification of the used fluorescent proteins are two possibilities to overcome this problem. Another possibility is the use of bandpass filters to exclude emission wavelengths outside the maximum emission ranges of the individual fluorescent proteins, which is strongly recommended for further

studies with this method. Moreover, a reduced incubation time other authors used for the p-YES (BUCHINGER et al., 2013; SCHICK AND SCHWACK, 2017) would result in a 1-day analysis and should be tested with the yeast cells used in this study.

Some endocrine effects could be detected in samples from different treatment measures of a municipal WWTP and the receiving river Ruhr (Figure 3-4). Gestagenic effects could not be detected in the first measurements of both samplings because of methodical problems in the workflow. A remeasurement with the original extracts (stored at -18 °C), 4–6 months later, showed no definite gestagenic effects because a clear differentiation between two detected gestagenic effects in the samples of the second sampling and effects in the SPE blank was not possible. Estrogenic effects found in samples of the second sampling in the range of E2 (R_f 0.42) were possibly a result of contaminations during sample preparation. First, they were detected in the SPE blank. Second, the effect intensities in the ozonation sample were similar to the ones in the other samples, although E2 was shown to be removed during ozonation (NAKADA et al., 2007). However, good recoveries of E1, E2, EE2, DHT, and P4 were observed in the SPE QCs in relation to the PCs. The recovery rates were between 93 and 112% and 88 and 120%, first and second samplings, respectively (Table 3-3), which showed the principle feasibility of the method and sample preparation, although recoveries in native samples might be lower because of the matrix. However, CHAMAS et al. (2017a) showed that tap water, source, river, and WWTP effluent samples spiked with E2, DHT, and P4 had similar peak areas as the positive controls.

Table 3-3 Recovery rates of E1, E2, EE2, DHT, and P4 in the SPE quality controls (QCs) in relation to the positive controls (PCs). The QCs were 1000-fold enriched by SPE. The application volume on the HPTLC plate was 25 μ L. The SPE QCs and PCs contain a mix of 1000/5000 pg E1 (40/200 μ g/L), 25 pg E2 (1 μ g/L), and 100 pg EE2 (4 μ g/L), and a mix of 250/100 pg DHT (10/4 μ g/L) and 250 pg P4 (10 μ g/L) (first/second sampling). The samples were separated by HPTLC and measured with the yeast multi-endocrine effect screen (YMEEES) for the detection of estrogenic, androgenic, and gestagenic effects. P4 was measured one-time in both samplings. DHT could not be evaluated in the second sampling. The tested peak areas of the SPE QCs were divided by the peak areas of the PCs (100%). The recovery rates \pm standard deviations (%) are shown

Sampling	Recovery rate \pm standard deviation (%)	
	First	Second
Substance		
E1	112 \pm 18 (n = 3)	105 (n = 1)
E2	109 \pm 18 (n = 3)	103 \pm 24 (n = 2)
EE2	112 \pm 19 (n = 3)	120 \pm 32 (n = 2)
DHT	99 \pm 3 (n = 3)	-
P4	93 (n = 1)	88 (n = 1)

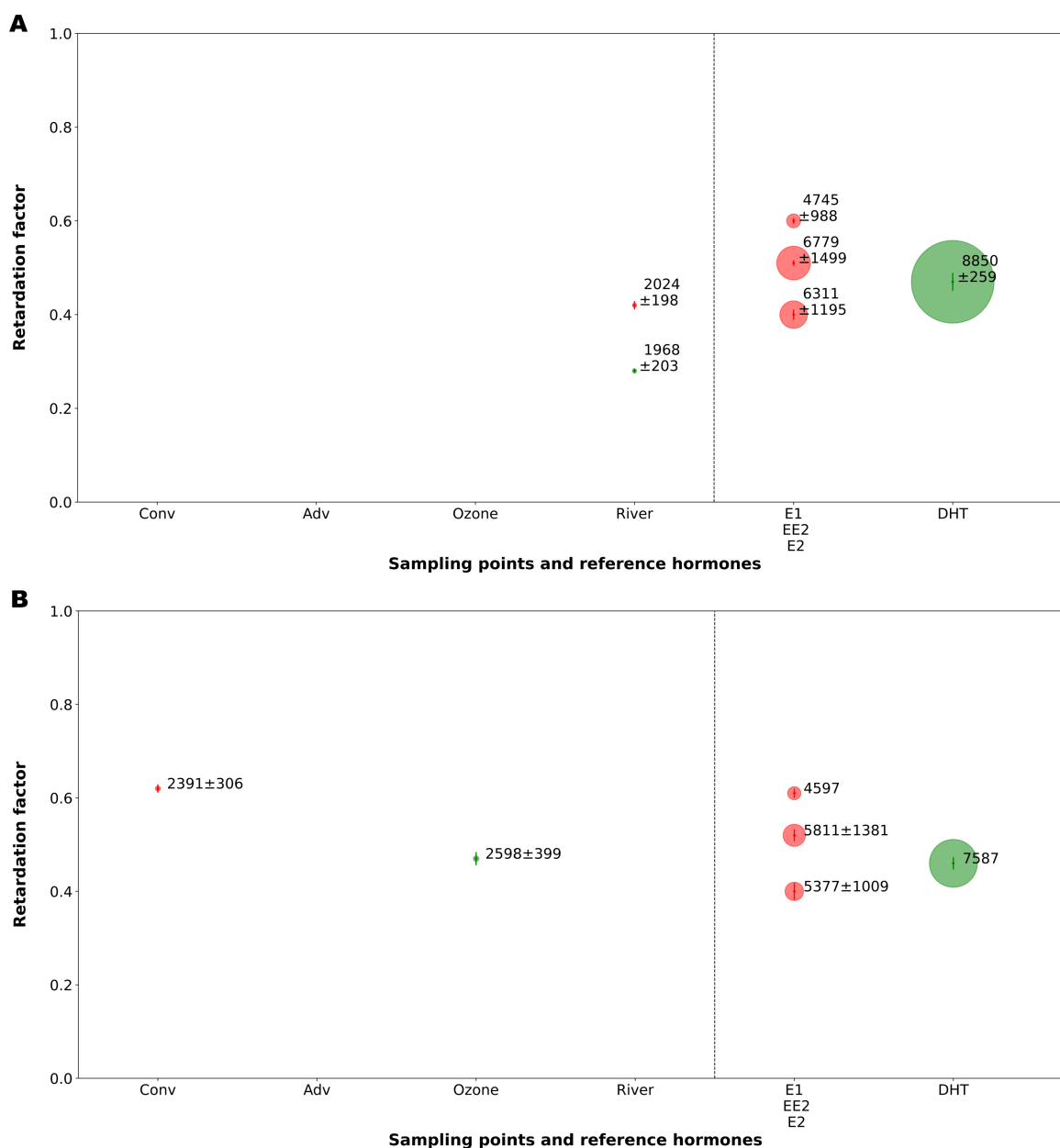


Figure 3-4 Estrogenic and androgenic effects detected in samples from the municipal WWTP in Schwerte, Germany. Two samplings were performed in June (A) and July (B) 2019. The samples were taken from a conventional treatment line (Conv), an advanced treatment line (Adv), which includes an ozonation step, the outlet of the ozonation (Ozone), and the receiving river Ruhr (River). A mix of 1000/5000 pg E1 (40/200 µg/L), 25 pg E2 (1 µg/L), and 100 pg EE2 (4 µg/L), and a mix of 250/100 pg DHT (10/4 µg/L) were applied (first/second sampling) (right side). The red and green dots represent estrogenic and androgenic effects, respectively. The mean peak area (AU) ± standard deviation of the effects ($n = 4$) and the reference hormones (first sampling: $n = 3$; second sampling: E2 and EE2 $n = 2$, E1 and DHT $n = 1$) are presented next to the dots. The size of the dots also represents the peak area. The y-axis shows the retardation factor (R_F). The position of the dots highlights the mean R_F s and the error bars show the standard deviations of the effects ($n = 4$) and the reference hormones (first sampling: $n = 3$; second sampling: $n = 2$). The samples were 1000-fold enriched by SPE. The application volume on the HPTLC plate was 25 µL. The samples were separated by HPTLC and measured with the yeast multi-endocrine effect screen (YMEES) for the detection of estrogenic, androgenic, and gestagenic effects.

When comparing different treatment steps at a WWTP, the retention and flow time of the different steps must be considered, which is at least very difficult with grab samples. Thus, a time- or flow rate-dependent sampling over a longer period is reasonable for further studies. Some of the detected effects showed similar R_F ranges as reference hormones. E2 (R_F 0.4) was detected in the same fraction as an effect (R_F 0.42) observed in the river sample of the first sampling (Figure 3-4A). DHT (R_F 0.46) showed a similar R_F range as an androgenic effect (R_F 0.47) found in the ozonation sample of the second sampling (Figure 3-4B). Nevertheless, it is rather unlikely that DHT occurs in the outlet of an ozonation. For this reason, transformation products (TPs) might be responsible, which were probably removed in the subsequent biological treatment. ITZEL et al. (2020) showed a removal of potential TPs by a biological post-treatment in another municipal WWTP. E1 (R_F 0.62) migrates to a position of an estrogenic effect (R_F 0.63) in the conventional sample of the second sampling (Figure 3-4B). Responsible substances seem to be removed by the advanced treatment process. In conclusion, the separation by HPTLC and following YMEES provide first information of potential effect causing substances when they are detected in the same fraction. Nevertheless, one has to keep in mind that tested effect bands could be caused by other unknowns and more than one substance.

Another sampling was performed at the Anger in Ratingen, Germany. The results of this river sample substantiate the possibility to detect estrogenic and androgenic effects in surface water with the introduced method. An estrogenic and androgenic effect was detected in the fraction of E2 (R_F 0.42) and DHT (R_F 0.48), respectively (Figure 3-5). The results demonstrate that it is also possible to detect gestagenic effects in river samples with this method. A gestagenic effect was detected in the range of P4 (R_F 0.61) (Figure 3-5). All these results must be seen as a proof of concept for the general method. Grab samples marginally reflect the real conditions. A more extensive study, which includes a continuous sampling over a longer period by automatic sampling or passive samplers, would increase the significance of such process-related and spatial effect evaluations. However, the presented results already show the usability of the introduced method and sample preparation regarding the recovery of reference hormones and in contrast to CHAMAS et al. (2017a) who spiked hormones in their environmental samples, the detection of estrogenic, androgenic, and gestagenic effects in native water samples.

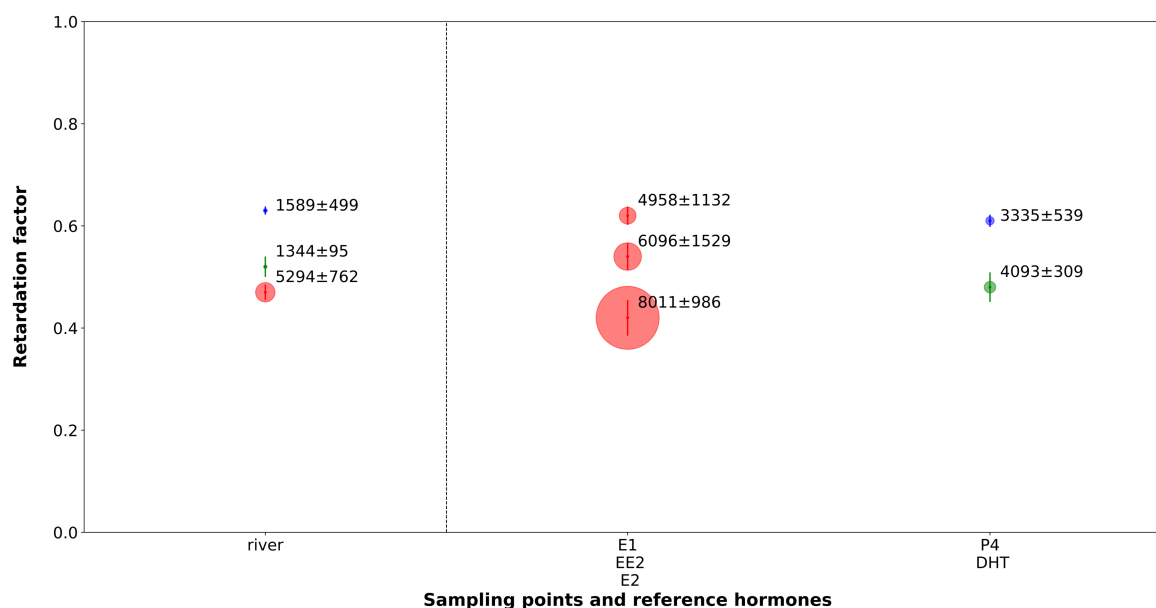


Figure 3-5 Estrogenic, androgenic, and gestagenic effects detected in a sample from the Anger in Ratingen, Germany (left side). The sampling was performed in March 2020. A mix of 1000 pg E1 (40 µg/L), 100 pg E2 (4 µg/L), and 100 pg EE2 (4 µg/L), and a mix of 100 pg DHT (4 µg/L) and 250 pg P4 (10 µg/L) were applied (right side). The red, green, and blue dots represent estrogenic, androgenic, and gestagenic effects, respectively. The mean peak area (AU) ± standard deviation of the effects (n = 4) and the reference hormones (n = 4) are presented next to the dots. The size of the dots also represents the peak area. The y-axis shows the retardation factor (R_F). The position of the dots highlights the mean R_F s and the error bars show the standard deviations of the effects (n = 4) and the reference hormones (n = 4). The samples were 1000-fold enriched by SPE. The application volume on the HPTLC plate was 25 µL. The samples were separated by HPTLC and measured with the yeast multi-endocrine effect screen (YMEES) for the detection of estrogenic, androgenic, and gestagenic effects.

3.5. Conclusion

In conclusion, the combination of HPTLC with the presented YMEES is suitable for the direct and simultaneous measurement of estrogenic, androgenic, and gestagenic effects on the HPTLC plate and thus saves material and time although a shorter incubation time would be beneficial. In comparison to an immersion of the HPTLC plates into the yeast suspension, spraying the yeast cells onto the HPTLC plates is an adequate alternative with similar sensitivities, but higher precisions and less needed yeast suspension. The general method in combination with SPE allows the whole unfiltered water sample analysis for E2 within the recommended EQS of 0.4 ng/L. Even though the effect evaluation is difficult when effects are visible in the scan for one of the other effects, it is possible to detect estrogenic, androgenic, and gestagenic effects in wastewater or surface water samples. Nevertheless, the use of bandpass filters in future studies is recommended to guarantee a specific measurement of the formed fluorescent proteins. An integration into an effect-directed approach should be tested in a comprehensive study for the evaluation of different wastewater treatment steps, analysis of substance discharges into receiving waters, or monitoring investigations in surface waters.

3.6. Acknowledgements

Financial support for the graduate program Future Water by the Ministry of Culture and Science of the Federal State of North Rhine-Westphalia (MKW NRW, Düsseldorf, Germany) is gratefully acknowledged. Gratefully acknowledged is also the support of the Ruhrverband (Essen, Germany) especially Prof. Dr. Grünebaum and the team from the WWTP Schwerte. Special thanks also go to new_diagnostics (Berlin, Germany) and especially Martin Jähne for providing the yeast strains and fruitful discussions. Further thanks also go to the reviewers of this work, who really helped to improve the manuscript and conclusions with their comments.

3.7. Funding

This study received funding from the graduate program Future Water by the Ministry of Culture and Science of the Federal State of North Rhine-Westphalia (MKW NRW, Düsseldorf, Germany).

3.8. References

- Aris A. Z., Shamsuddin A. S., Praveena S. M., 2014. Occurrence of 17 α -ethynylestradiol (EE2) in the environment and effect on exposed biota: a review. *Environment International*, 69, 104–119. <https://doi.org/10.1016/j.envint.2014.04.011>.
- Bergmann A. J., Simon E., Schifferli A., Schönborn A., Vermeirssen E. L. M., 2020. Estrogenic activity of food contact materials-evaluation of 20 chemicals using a yeast estrogen screen on HPTLC or 96-well plates. *Analytical and Bioanalytical Chemistry*, 412 (19), 4527–4536. <https://doi.org/10.1007/s00216-020-02701-w>.
- Brack W., 2003. Effect-directed analysis: a promising tool for the identification of organic toxicants in complex mixtures? *Analytical and Bioanalytical Chemistry*, 377 (3), 397–407. <https://doi.org/10.1007/s00216-003-2139-z>.
- Brack W., 2011. Effect-Directed Analysis of Complex Environmental Contamination. In: *The handbook of environmental chemistry*, vol. 15. Springer, Berlin, Heidelberg.
- Brack W., Aissa S. A., Backhaus T., Dulio V., Escher B. I., Faust M., Hilscherova K., Hollender J., Hollert H., Müller C., Munthe J., Posthuma L., Seiler T.-B., Slobodnik J., Teodorovic I., Tindall A. J., De Aragão Umbuzeiro G., Zhang X., Altenburger R., 2019. Effect-based methods are key. The European Collaborative Project SOLUTIONS recommends integrating effect-based methods for diagnosis and monitoring of water quality. *Environmental Sciences Europe*, 31 (1), 5423. <https://doi.org/10.1186/s12302-019-0192-2>.
- Brack W., Ait-Aissa S., Burgess R. M., Busch W., Creusot N., Di Paolo C., Escher B. I., Mark Hewitt L., Hilscherova K., Hollender J., Hollert H., Jonker W., Kool J., Lamoree M., Muschket M., Neumann S., Rostkowski P., Ruttkies C., Schollee J., Schymanski E. L., Schulze T., Seiler T.-B., Tindall A. J., De Aragão Umbuzeiro G., Vrana B., Krauss M., 2016. Effect-directed analysis supporting monitoring of aquatic environments--An in-depth overview. *Science of the Total Environment*, 544, 1073–1118. <https://doi.org/10.1016/j.scitotenv.2015.11.102>.
- Buchinger S., Spira D., Bröder K., Schlüsener M., Ternes T., Reifferscheid G., 2013. Direct coupling of thin-layer chromatography with a bioassay for the detection of estrogenic compounds: applications for effect-directed analysis. *Analytical Chemistry*, 85 (15), 7248–7256. <https://doi.org/10.1021/ac4010925>.

- Chamas A., Pham H. T. M., Jähne M., Hettwer K., Gehrman L., Tuerk J., Uhlig S., Simon K., Baronian K., Kunze G., 2017a. Separation and identification of hormone-active compounds using a combination of chromatographic separation and yeast-based reporter assay. *Science of the Total Environment*, 605-606, 507–513. <https://doi.org/10.1016/j.scitotenv.2017.06.077>.
- Chamas A., Pham H. T. M., Jähne M., Hettwer K., Uhlig S., Simon K., Einspanier A., Baronian K., Kunze G., 2017b. Simultaneous detection of three sex steroid hormone classes using a novel yeast-based biosensor. *Biotechnology and Bioengineering*, 114 (7), 1539–1549. <https://doi.org/10.1002/bit.26249>.
- Chang H., Wan Y., Wu S., Fan Z., Hu J., 2011. Occurrence of androgens and progestogens in wastewater treatment plants and receiving river waters: comparison to estrogens. *Water Research*, 45 (2), 732–740. <https://doi.org/10.1016/j.watres.2010.08.046>.
- Cotlet M., Goodwin P. M., Waldo G. S., Werner J. H., 2006. A comparison of the fluorescence dynamics of single molecules of a green fluorescent protein: one- versus two-photon excitation. *ChemPhysChem*, 7 (1), 250–260. <https://doi.org/10.1002/cphc.200500247>.
- Duft M., Schulte-Oehlmann U., Tillmann M., Markert B., Oehlmann J., 2003. Toxicity of triphenyltin and tributyltin to the freshwater mud snail *Potamopyrgus antipodarum* in a new sediment biotest. *Environmental Toxicology and Chemistry*, 22 (1), 145–152. <https://doi.org/10.1002/etc.5620220119>.
- EU, 2018. COMMISSION IMPLEMENTING DECISION (EU) 2018/ 840 - of 5 June 2018 - establishing a watch list of substances for Union-wide monitoring in the field of water policy pursuant to Directive 2008/ 105/ EC of the European Parliament and of the Council and repealing Commission Implementing Decision (EU) 2015/ 495 - (notified under document C(2018) 3362) (Watch List). Official Journal of the European Union.
- Fent K., 2015. Progestins as endocrine disrupters in aquatic ecosystems: Concentrations, effects and risk assessment. *Environment International*, 84, 115–130. <https://doi.org/10.1016/j.envint.2015.06.012>.
- Gehrman L., Bielak H., Behr M., Itzel F., Lyko S., Simon A., Kunze G., Dopp E., Wagner M., Tuerk J., 2018. (Anti-)estrogenic and (anti-)androgenic effects in wastewater during advanced treatment: comparison of three in vitro bioassays. *Environmental Science and Pollution Research International*, 25 (5), 4094–4104. <https://doi.org/10.1007/s11356-016-7165-4>.
- Grünebaum T., Jardin N., Lübken M., Wichern M., Lyko S., Rath L., Thöle D., Türk J., 2014. Untersuchung verschiedener Verfahren zur weitergehenden Spurenstoffelimination auf kommunalen Kläranlagen im großtechnischen Maßstab. *KA Korrespondenz Abwasser, Abfall*, 61 (10), 876–884. <https://doi.org/10.3242/kae2014.10.002>.
- Günter A., Balsaa P., Werres F., Schmidt T. C., 2016. Influence of the drying step within disk-based solid-phase extraction both on the recovery and the limit of quantification of organochlorine pesticides in surface waters including suspended particulate matter. *Journal of Chromatography A*, 1450, 1–8. <https://doi.org/10.1016/j.chroma.2016.03.073>.
- Harth F. U. R., Arras C., Brettschneider D. J., Misovic A., Oehlmann J., Schulte-Oehlmann U., Oetken M., 2018. Small but with big impact? Ecotoxicological effects of a municipal wastewater effluent on a small creek. *Journal of Environmental Science and Health, Part A*, 53 (13), 1149–1160. <https://doi.org/10.1080/10934529.2018.1530328>.
- Hashmi M. A. K., Krauss M., Escher B. I., Teodorovic I., Brack W., 2020. Effect-Directed Analysis of Progestogens and Glucocorticoids at Trace Concentrations in River Water. *Environmental Toxicology and Chemistry*, 39 (1), 189–199. <https://doi.org/10.1002/etc.4609>.

- Henneberg A., Bender K., Blaha L., Giebner S., Kuch B., Köhler H.-R., Maier D., Oehlmann J., Richter D., Scheurer M., Schulte-Oehlmann U., Sieratowicz A., Ziebart S., Triebkorn R., 2014. Are in vitro methods for the detection of endocrine potentials in the aquatic environment predictive for in vivo effects? Outcomes of the Projects SchussenAktiv and SchussenAktivplus in the Lake Constance Area, Germany. *PLOS ONE*, 9 (6), e98307. <https://doi.org/10.1371/journal.pone.0098307>.
- Itzel F., Baetz N., Hohrenk L. L., Gehrmann L., Antakyali D., Schmidt T. C., Tuerk J., 2020. Evaluation of a biological post-treatment after full-scale ozonation at a municipal wastewater treatment plant. *Water Research*, 170, 115316. <https://doi.org/10.1016/j.watres.2019.115316>.
- Itzel F., Jewell K. S., Leonhardt J., Gehrmann L., Nielsen U., Ternes T. A., Schmidt T. C., Tuerk J., 2018. Comprehensive analysis of antagonistic endocrine activity during ozone treatment of hospital wastewater. *Science of the Total Environment*, 624, 1443–1454. <https://doi.org/10.1016/j.scitotenv.2017.12.181>.
- Jobling S., Casey D., Rodgers-Gray T., Oehlmann J., Schulte-Oehlmann U., Pawlowski S., Baunbeck T., Turner A. P., Tyler C. R., 2003. Comparative responses of molluscs and fish to environmental estrogens and an estrogenic effluent. *Aquatic Toxicology*, 65 (2), 205–220. [https://doi.org/10.1016/s0166-445x\(03\)00134-6](https://doi.org/10.1016/s0166-445x(03)00134-6).
- Kidd K. A., Blanchfield P. J., Mills K. H., Palace V. P., Evans R. E., Lazorchak J. M., Flick R. W., 2007. Collapse of a fish population after exposure to a synthetic estrogen. *Proceedings of the National Academy of Sciences of the United States of America*, 104 (21), 8897–8901. <https://doi.org/10.1073/pnas.0609568104>.
- Klingelhöfer I. and Morlock G. E., 2014. Sharp-bounded zones link to the effect in planar chromatography-bioassay-mass spectrometry. *Journal of Chromatography A*, 1360, 288–295. <https://doi.org/10.1016/j.chroma.2014.07.083>.
- Klingelhöfer I. and Morlock G. E., 2015. Bioprofiling of Surface/Wastewater and Bioquantitation of Discovered Endocrine-Active Compounds by Streamlined Direct Bioautography. *Analytical Chemistry*, 87 (21), 11098–11104. <https://doi.org/10.1021/acs.analchem.5b03233>.
- Knoop O., Hohrenk L. L., Lutze H. V., Schmidt T. C., 2018a. Ozonation of Tamoxifen and Toremifene: Reaction Kinetics and Transformation Products. *Environmental Science & Technology*, 52 (21), 12583–12591. <https://doi.org/10.1021/acs.est.8b00996>.
- Knoop O., Itzel F., Tuerk J., Lutze H. V., Schmidt T. C., 2018b. Endocrine effects after ozonation of tamoxifen. *Science of the Total Environment*, 622-623, 71–78. <https://doi.org/10.1016/j.scitotenv.2017.11.286>.
- Kuckelkorn J., Redelstein R., Heide T., Kunze J., Maletz S., Waldmann P., Grummt T., Seiler T.-B., Hollert H., 2018. A hierarchical testing strategy for micropollutants in drinking water regarding their potential endocrine-disrupting effects-towards health-related indicator values. *Environmental Science and Pollution Research International*, 25 (5), 4051–4065. <https://doi.org/10.1007/s11356-017-0155-3>.
- Morlock G. and Schwack W., 2010. Hyphenations in planar chromatography. *Journal of Chromatography A*, 1217 (43), 6600–6609. <https://doi.org/10.1016/j.chroma.2010.04.058>.
- Muschket M., Di Paolo C., Tindall A. J., Touak G., Phan A., Krauss M., Kirchner K., Seiler T.-B., Hollert H., Brack W., 2018. Identification of Unknown Antiandrogenic Compounds in Surface Waters by Effect-Directed Analysis (EDA) Using a Parallel Fractionation Approach. *Environmental Science & Technology*, 52 (1), 288–297. <https://doi.org/10.1021/acs.est.7b04994>.

- Nakada N., Shinohara H., Murata A., Kiri K., Managaki S., Sato N., Takada H., 2007. Removal of selected pharmaceuticals and personal care products (PPCPs) and endocrine-disrupting chemicals (EDCs) during sand filtration and ozonation at a municipal sewage treatment plant. *Water Research*, 41 (19), 4373–4382. <https://doi.org/10.1016/j.watres.2007.06.038>.
- Orlando E. F. and Ellestad L. E., 2014. Sources, concentrations, and exposure effects of environmental gestagens on fish and other aquatic wildlife, with an emphasis on reproduction. *General and Comparative Endocrinology*, 203, 241–249. <https://doi.org/10.1016/j.ygcen.2014.03.038>.
- Örn S., Holbech H., Norrgren L., 2016. Sexual disruption in zebrafish (*Danio rerio*) exposed to mixtures of 17 α -ethinylestradiol and 17 β -trenbolone. *Environmental Toxicology and Pharmacology*, 41, 225–231. <https://doi.org/10.1016/j.etap.2015.12.010>.
- Riegraf C., Reifferscheid G., Belkin S., Moscovici L., Shakibai D., Hollert H., Buchinger S., 2019. Combination of yeast-based in vitro screens with high-performance thin-layer chromatography as a novel tool for the detection of hormonal and dioxin-like compounds. *Analytica Chimica Acta*, 1081, 218–230. <https://doi.org/10.1016/j.aca.2019.07.018>.
- Rivero-Wendt C. L. G., Oliveira R., Monteiro M. S., Domingues I., Soares A. M. V. M., Grisolia C. K., 2016. Steroid androgen 17 α -methyltestosterone induces malformations and biochemical alterations in zebrafish embryos. *Environmental Toxicology and Pharmacology*, 44, 107–113. <https://doi.org/10.1016/j.etap.2016.04.014>.
- Rogowska J., Cieszynska-Semenowicz M., Ratajczyk W., Wolska L., 2020. Micropollutants in treated wastewater. *Ambio*, 49 (2), 487–503. <https://doi.org/10.1007/s13280-019-01219-5>.
- Schick D. and Schwack W., 2017. Planar yeast estrogen screen with resorufin- β -d-galactopyranoside as substrate. *Journal of Chromatography A*, 1497, 155–163. <https://doi.org/10.1016/j.chroma.2017.03.047>.
- Schoenborn A., Schmid P., Bräm S., Reifferscheid G., Ohlig M., Buchinger S., 2017. Unprecedented sensitivity of the planar yeast estrogen screen by using a spray-on technology. *Journal of Chromatography A*, 1530, 185–191. <https://doi.org/10.1016/j.chroma.2017.11.009>.
- Schuetzle D. and Lewtas J., 1986. Bioassay-Directed Chemical Analysis in Environmental Research. *Analytical Chemistry*, 58 (11), 1060A-1075A. <https://doi.org/10.1021/ac00124a714>.
- Stütz L., Schulz W., Winzenbacher R., 2020. Identification of acetylcholinesterase inhibitors in water by combining two-dimensional thin-layer chromatography and high-resolution mass spectrometry. *Journal of Chromatography A*, 1624, 461239. <https://doi.org/10.1016/j.chroma.2020.461239>.
- Stütz L., Weiss S. C., Schulz W., Schwack W., Winzenbacher R., 2017. Selective two-dimensional effect-directed analysis with thin-layer chromatography. *Journal of Chromatography A*, 1524, 273–282. <https://doi.org/10.1016/j.chroma.2017.10.009>.
- Van den Belt K., Berckmans P., Vangenechten C., Verheyen R., Witters H., 2004. Comparative study on the in vitro/in vivo estrogenic potencies of 17 β -estradiol, estrone, 17 α -ethinylestradiol and nonylphenol. *Aquatic Toxicology*, 66 (2), 183–195. <https://doi.org/10.1016/j.aquatox.2003.09.004>.
- Weiss S. C., Egetenmeyer N., Schulz W., 2017. Coupling of In Vitro Bioassays with Planar Chromatography in Effect-Directed Analysis. *Advances in Biochemical Engineering/Biotechnology*, 157, 187–224. https://doi.org/10.1007/10_2016_16.
- Weller M. G., 2012. A unifying review of bioassay-guided fractionation, effect-directed analysis and related techniques. *Sensors*, 12 (7), 9181–9209. <https://doi.org/10.3390/s120709181>.

Ziková A., Lorenz C., Hoffmann F., Kleiner W., Lutz I., Stöck M., Kloas W., 2017. Endocrine disruption by environmental gestagens in amphibians - A short review supported by new in vitro data using gonads of *Xenopus laevis*. *Chemosphere*, 181, 74–82. <https://doi.org/10.1016/j.chemosphere.2017.04.021>.

3.9. Appendix

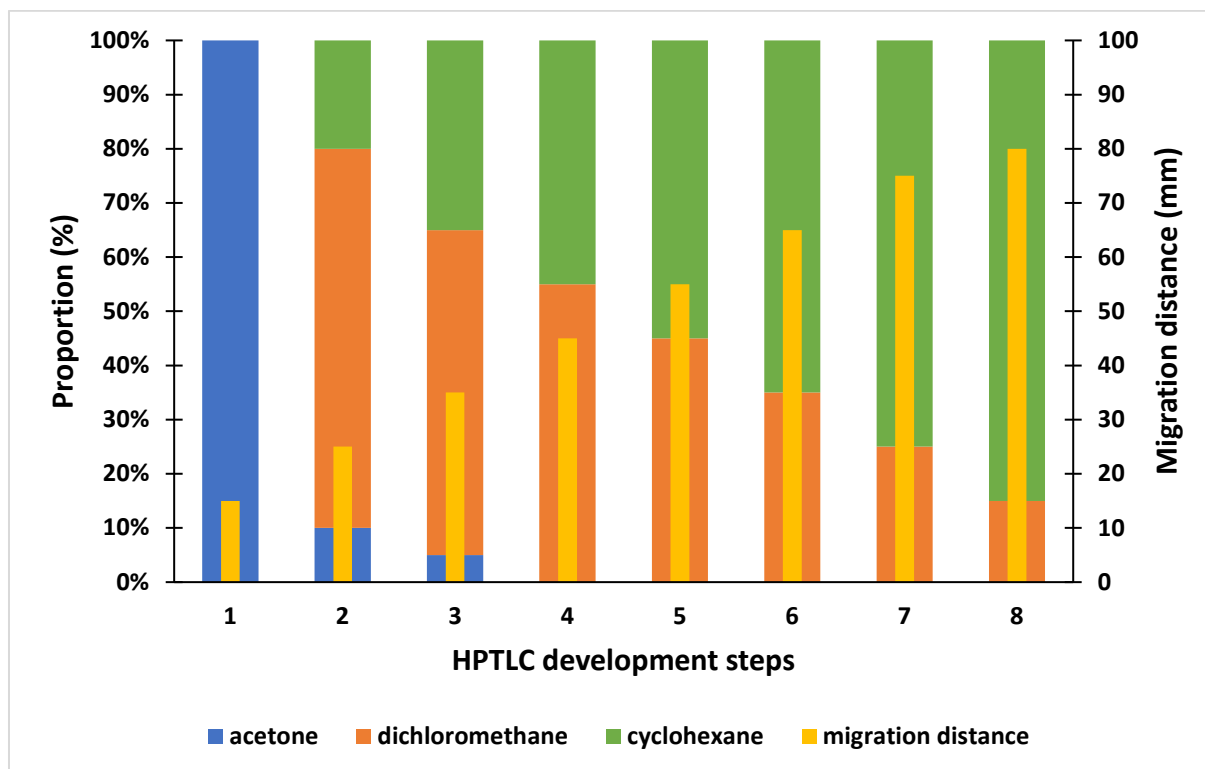


Figure 3-6 The automated eight-step HPTLC development process for separation of E1, E2, EE2, DHT, and P4 on SIL G-25, RP-18W and LiChrospher HPTLC plates. This development process was also used for the dose-response investigations of E1, E2, EE2, DHT, and P4 on SIL G-25 plates. Every step contains another amount of the used solvents. The blue bars represent acetone, the orange bars dichloromethane, the green bars cyclohexane. The yellow bars show the increasing migration distances. Final migration distance was 80 mm.

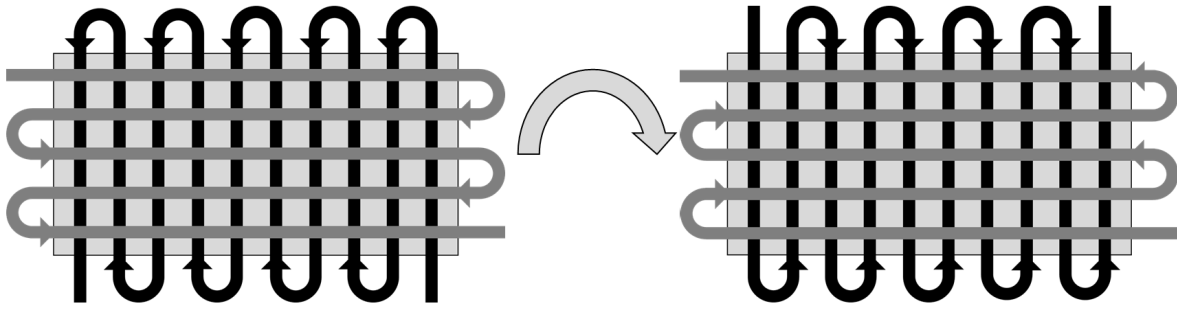


Figure 3-9 The used optimized spraying scheme for yeast cell application on HPTLC plates. The airbrush gun was moved from left to right and bottom to top. Then the plate was rotated by 180° and sprayed again. The spraying course and the rotation were repeated until a yeast suspension volume of approximately 14 mL was sprayed onto the plate.

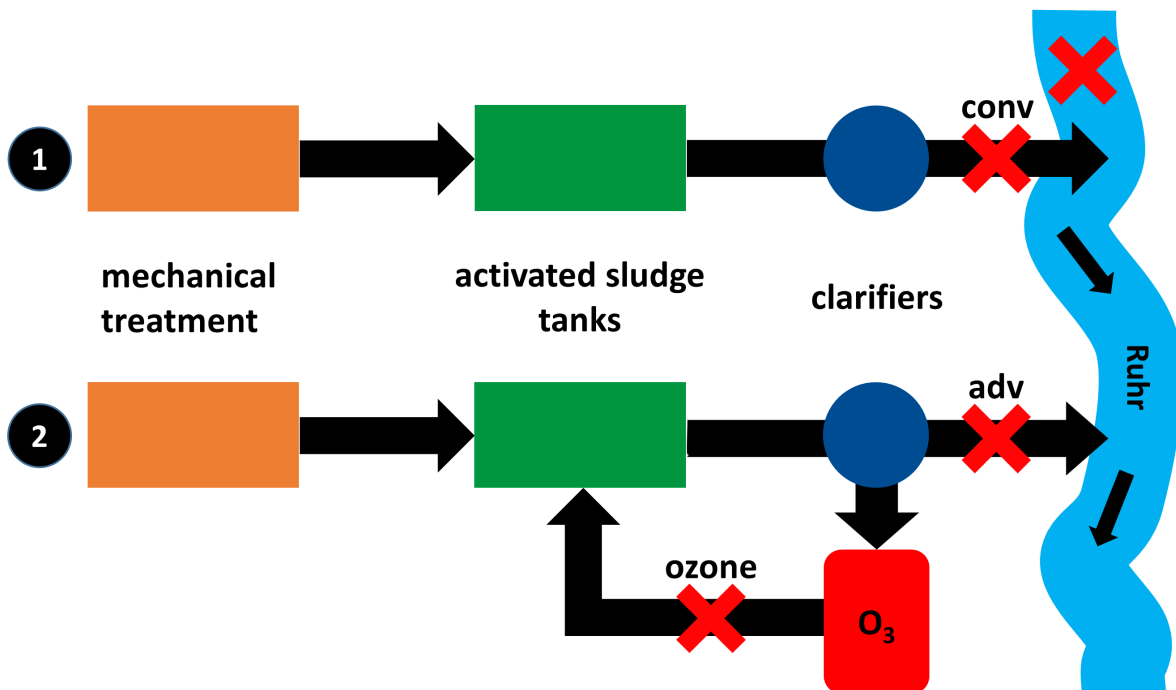


Figure 3-10 Scheme of the municipal WWTP in Schwerte, Germany. The WWTP operates two treatment lines: line 1 only with the conventional treatment steps (mechanical and biological) and line 2 with an ozonation as an additional advanced treatment step. The ozonated water is recirculated into the biological treatment step. Grab samples were taken from the outlet of treatment line 1 (conv) and 2 (adv). Moreover, samples were taken from the outlet of the ozonation (ozone) and the receiving river Ruhr upstream WWTP. The red crosses represent the sampling points and the small arrows label the flow direction of the river.

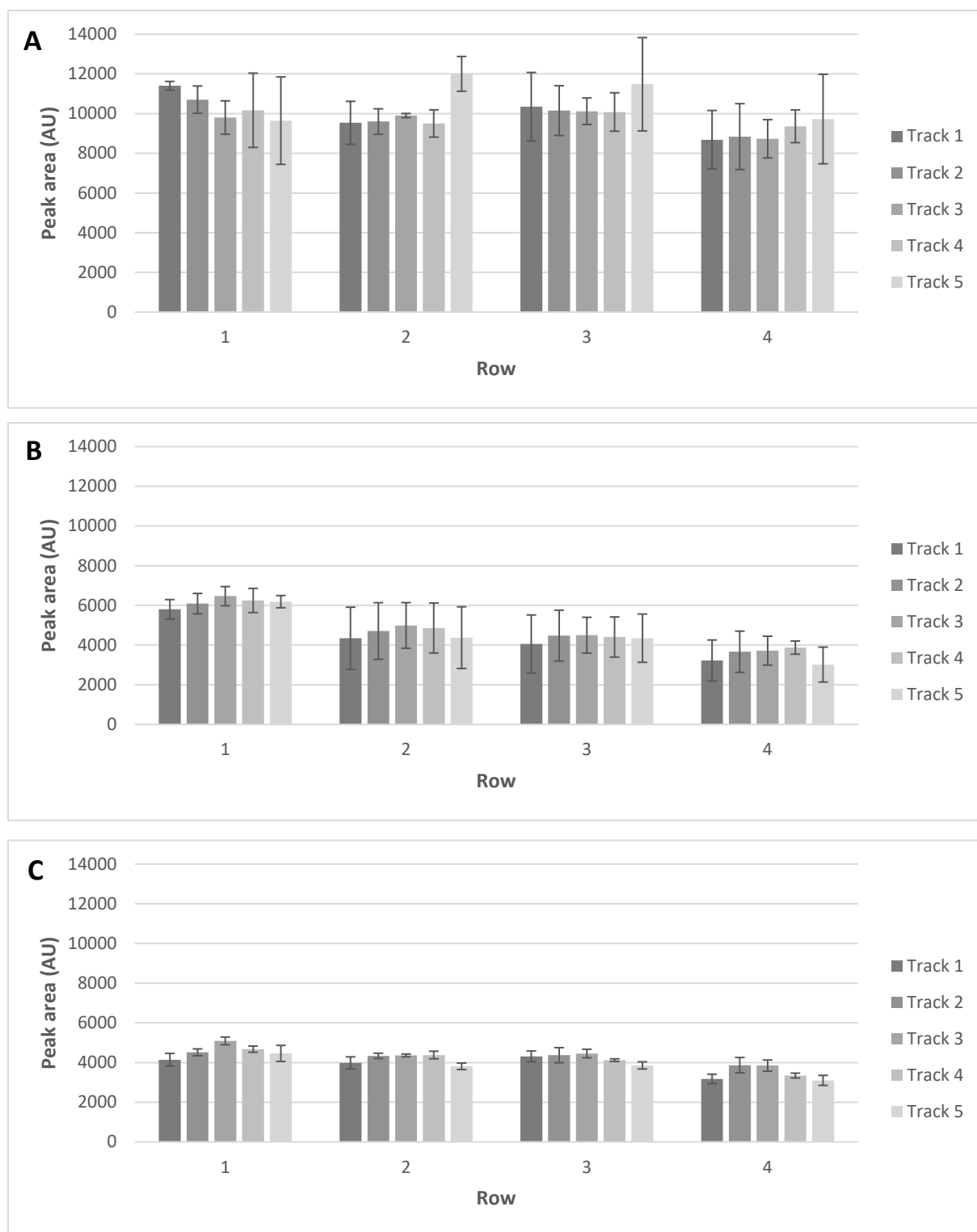


Figure 3-11 Comparison of immersion (A), spray (B), and optimized spray (C) application regarding the yeast cell dispersion of 20 evenly distributed E2 spots on SIL G-25 plates. The mean (bars) and the standard deviation (error bars) of the peak areas are shown for each track and row ($n = 3$). The yeast multi-endocrine effect screen (YMEES) was performed without prior chromatographic separation by HPTLC.

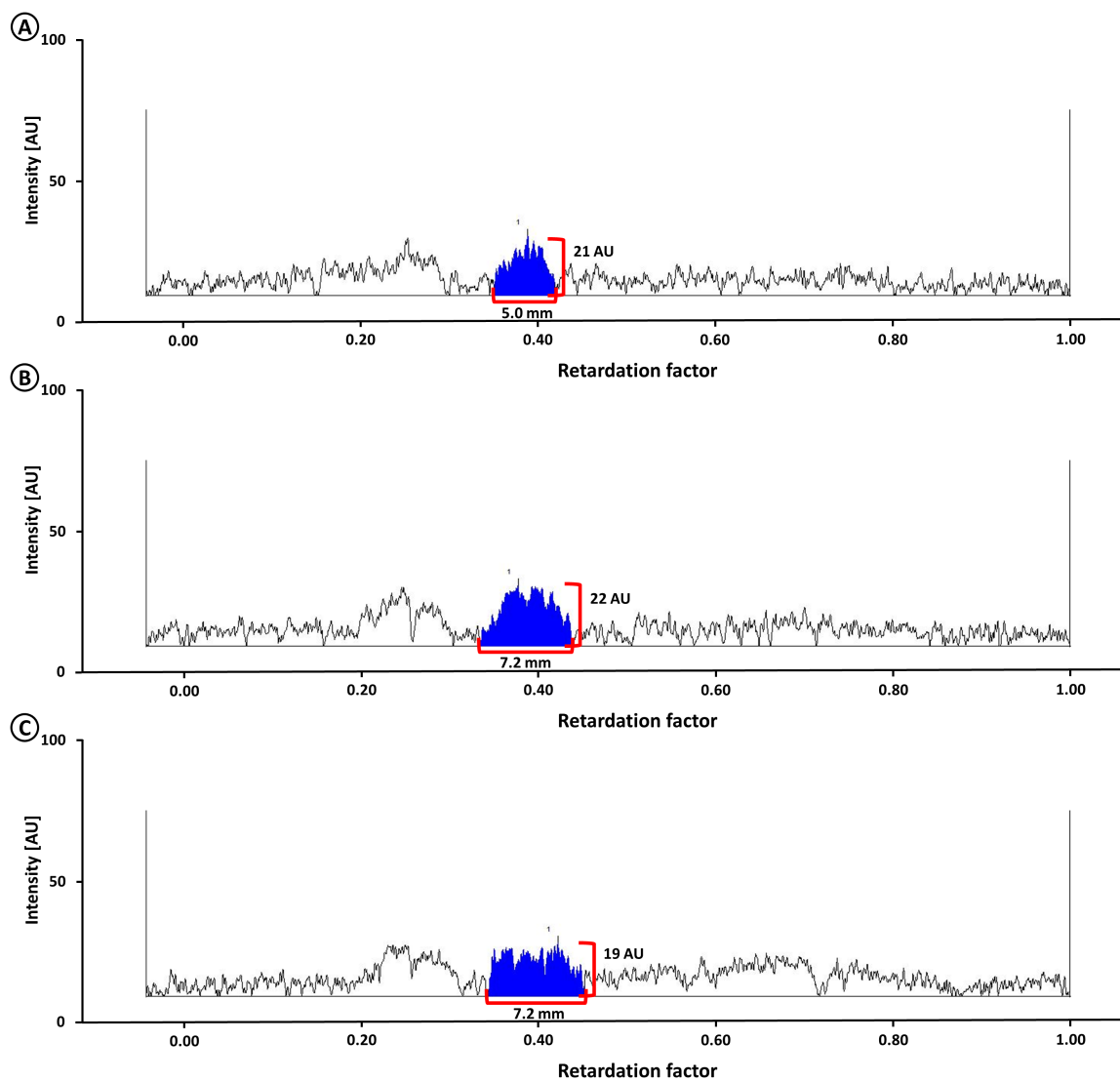


Figure 3-12 Effects of 30 pg (A), 100 pg (B), and 250 pg (C) P4 on a SIL G-25 plate. The peak width (mm) is shown under and the peak height (AU) next to the peaks. The application volume was 25 μ L. The yeast multi-endocrine effect screen (YMEES) was performed after chromatographic separation by HPTLC.

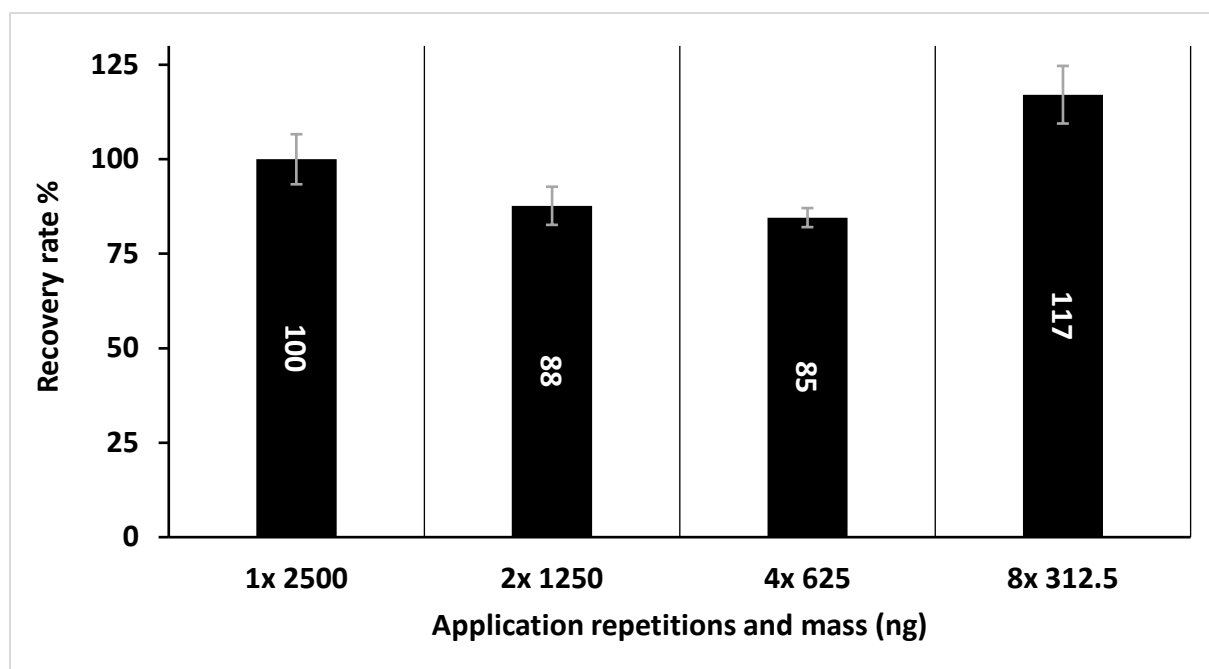


Figure 3-13 Recovery rates and standard deviations (error bars) of E2 after multiple application in comparison to a one-time application on a SIL G-25 plate. The application volume was 25 μ L. The application repetitions were doubled, and the applied concentrations halved, which resulted in equal applied masses ($n = 3$). The plate was sprayed with 8% sulfuric acid in ethanol and incubated for 10 min at 105 $^{\circ}$ C. The absorbance of each track was scanned at 310 nm. No chromatographic separation was performed.

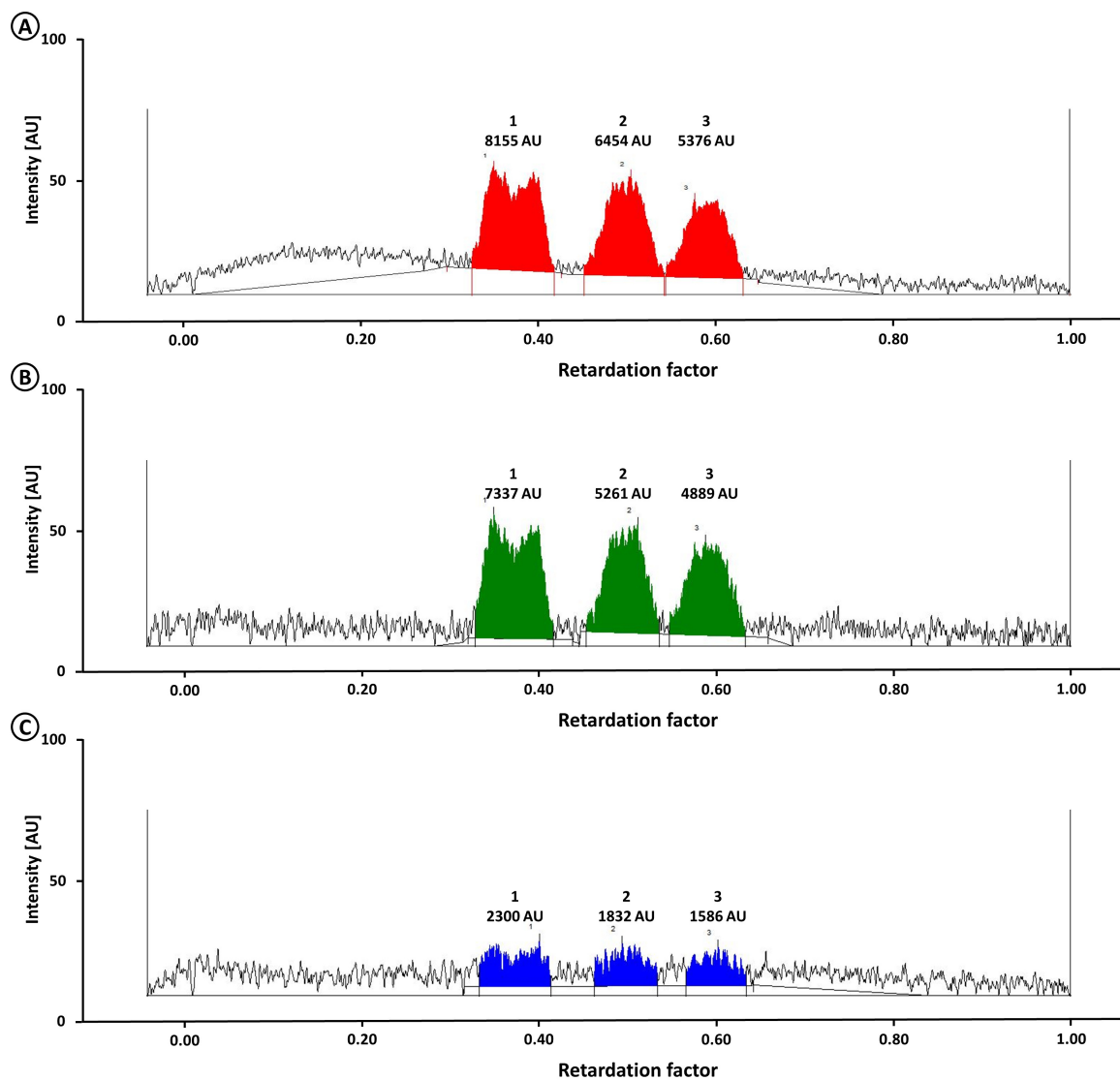


Figure 3-14 Effects of E2 (100 pg) (1), EE2 (100 pg) (2), and E1 (1000 pg) (3) in the estrogen scan (DsRED2, excitation 542 nm/emission filter K560) (A), androgen scan (GFP, excitation 475 nm/emission filter K500) (B), and gestagen scan (CFP, excitation 445 nm/emission filter K460) (C) on a SIL G-25 plate. The peak area is shown above the peaks. The application volume was 25 μ L. The yeast multi-endocrine effect screen (YMEES) was performed after chromatographic separation by HPTLC.

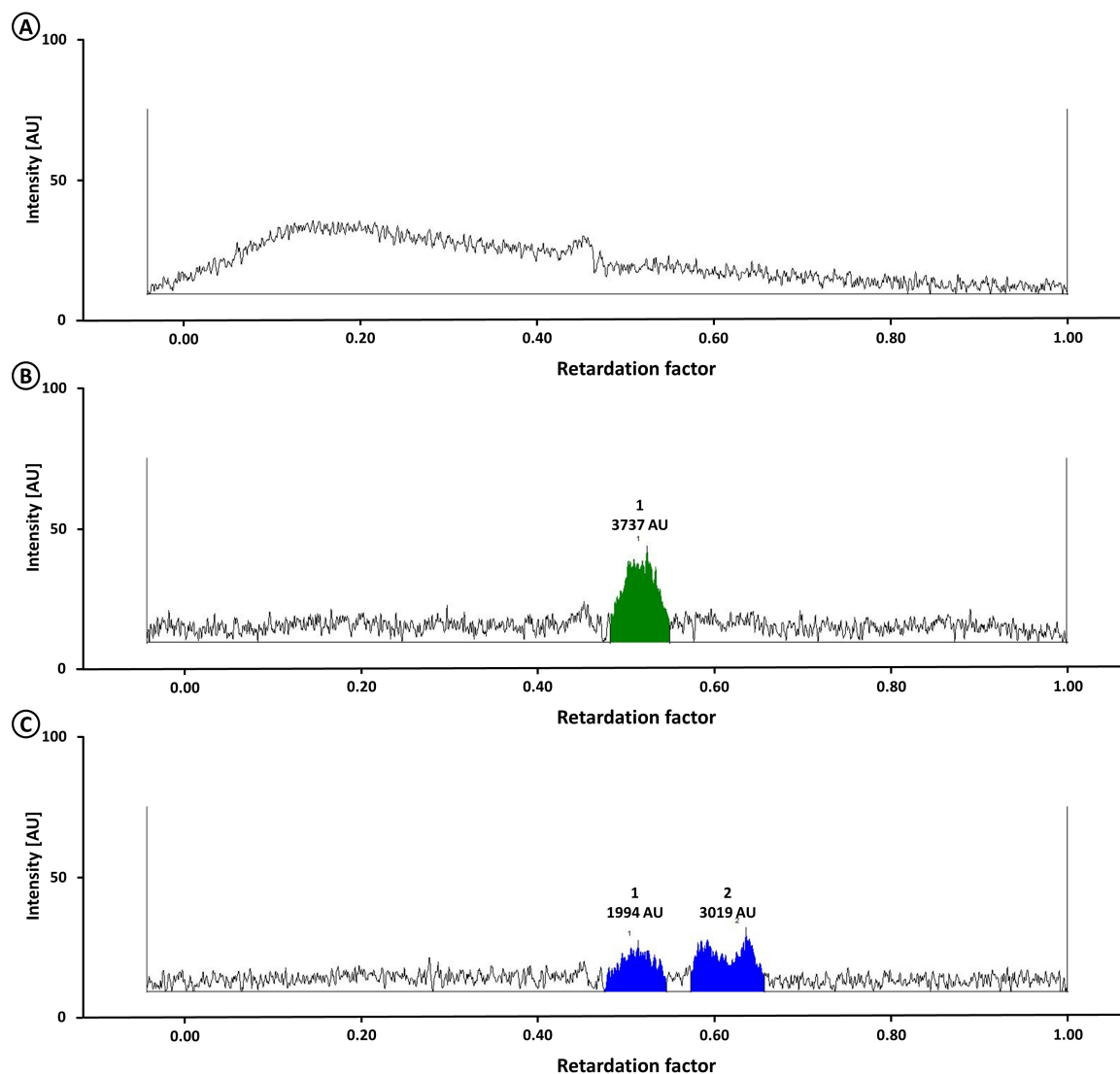


Figure 3-15 Effects of DHT (100 pg) (1) and P4 (250 pg) (2) in the estrogen scan (DsRED2, excitation 542 nm/emission filter K560) (A), androgen scan (GFP, excitation 475 nm/emission filter K500) (B), and gestagen scan (CFP, excitation 445 nm/emission filter K460) (C) on a SIL G-25 plate. The peak area is shown above the peaks. The application volume was 25 μ L. The yeast multi-endocrine effect screen (YMEEs) was performed after chromatographic separation by HPTLC.

Table 3-4 Composition of the used cultivation medium (supplemented with glucose) and test medium (supplemented with maltose) for the yeast multi-endocrine effect screen (YMEES).

Substance	Concentration (g/L)
Glucose	100
Maltose	100
NaNO ₃	17.85
KH ₂ PO ₄	40.53
MgSO ₄ x H ₂ O	2.41
H ₃ BO ₃	0.0025
CuSO ₄ x 5H ₂ O	0.0005
KI	0.0005
MnSO ₄ x H ₂ O	0.002
ZnSO ₄ x 7H ₂ O	0.002
Na ₂ MoO ₄ x 2H ₂ O	0.001
CoCl ₂	0.0005
FeCl ₃ x 6H ₂ O	0.05
Ca(NO ₃) ₂	5
Ca-D-Panthenat	0.01
Thiamin-Hydrochlorid	0.01
Niacin	0.0025
Biotin	0.001
Pyridoxin-Hydrochlorid	0.01
Inositol	0.1

Table 3-5 Concentrations and applied masses of E1, E2, and EE2 used for the dose-response investigations. The estrogens were applied on SIL G-25 plates. The application volume was 25 µL. The yeast multi-endocrine effect screen (YMEES) was performed after chromatographic separation by HPTLC. The HPTLC plates were either immersed into the yeast suspension or the cells were sprayed onto the plates by airbrush.

Mass (pg)			Concentration (µg/L)		
E1	E2	EE2	E1	E2	EE2
10	0.1	1	0.4	0.004	0.04
100	1	9	4	0.04	0.36
150	1.5	10	6	0.06	0.4
225	2.5	12	9	0.1	0.48
325	4	15	13	0.16	0.6
500	6	20	20	0.24	0.8
800	9	25	32	0.36	1
1,500	13	35	60	0.52	1.4
3,000	18	50	120	0.72	2
5,000	25	100	200	1	4
10,000	50	250	400	2	10
20,000	100	500	800	4	20

Table 3-6 Concentrations and applied masses of DHT and P4 used for the dose-response investigations. The hormones were applied on SIL G-25 plates. The application volume was 25 μ L. The yeast multi-endocrine effect screen (YMEES) was performed after chromatographic separation by HPTLC. The HPTLC plates were either immersed into the yeast suspension or the cells were sprayed onto the plates by airbrush.

Mass (μ g)		Concentration (μ g/L)	
DHT	P4	DHT	P4
10	0.1	0.4	0.004
100	1	4	0.04
150	1.5	6	0.06
225	2.5	9	0.1
325	4	13	0.16
500	6	20	0.24
800	9	32	0.36
1,500	13	60	0.52
3,000	18	120	0.72
5,000	25	200	1
10,000	50	400	2
20,000	100	800	4

Table 3-7 Comparison of immersion, spray, and optimized spray application regarding the yeast cell dispersion using the relative standard deviation (RSD) of the peak areas of 20 evenly distributed E2 spots on SIL G-25 plates. Three plates were tested. The total RSD of 60 spots is shown. For the spray approach also the RSD of two plates is shown. The yeast multi-endocrine effect screen (YMEES) was performed without prior chromatographic separation by HPTLC.

Method	Relative standard deviation (RSD) (%)		
	Immersion	Spraying	Optimized spraying
Amount E2 spots			
Plate 1 (n = 20)	16	16	11
Plate 2 (n = 20)	12	18	14
Plate 3 (n = 20)	10	45	13
3 plates (n = 60)	16	31	13
2 plates (n = 40)	-	17	-

4 High-performance Thin-layer Chromatography in Combination with an Acetylcholinesterase-inhibition Bioassay with Pre-oxidation of Organothiophosphates to Determine Neurotoxic Effects in Storm, Waste, and Surface Water

This chapter is adopted from: Baetz N., Schmidt T. C., Tuerk J., 2022. High-performance thin-layer chromatography in combination with an acetylcholinesterase-inhibition bioassay with pre-oxidation of organothiophosphates to determine neurotoxic effects in storm, waste, and surface water. *Analytical and bioanalytical chemistry*, 414 (14), 4167–4178. <https://doi.org/10.1007/s00216-022-04068-6>.

4.1. Abstract

Pesticides such as organothiophosphates (OTPs) are neurotoxically active and enter the aquatic environment. Bioassays, using acetylcholinesterase (AChE), a suitable substrate and reactant, can be applied for the photometric detection of AChE inhibition (AChE-I) effects. The oxidized forms of OTPs, so-called oxons, have higher inhibition potentials for AChE. Therefore, a higher sensitivity is achieved for application of oxidized samples to the AChE assay. In this study, the oxidation of malathion, parathion, and chlorpyrifos by *n*-bromosuccinimide (NBS) was investigated in an approach combining high-performance thin-layer chromatography (HPTLC) with an AChE-I assay. Two AChE application approaches, immersion and spraying, were compared regarding sensitivity, precision, and general feasibility of the OTP effect detection. The oxidation by NBS led to an activation of the OTPs and a strong increase in sensitivity similar to the oxons tested. The sensitivity and precision of the two application techniques were similar, although the spray method was slightly more sensitive to the oxidized OTPs. The 10% inhibition concentrations (IC_{10}) for the spray approach were 0.26, 0.75, and 0.35 ng/spot for activated malathion, parathion, and chlorpyrifos, respectively. AChE-I effect recoveries in samples from a stormwater retention basin and receiving stream were between 69 and 92% for malathion, parathion, and chlorpyrifos. The overall workflow, including sample enrichment by solid-phase extraction, HPTLC, oxidation of OTPs, and AChE-I assay, was demonstrated to be suitable for the detection of AChE-I effects in native water samples. An effect of unknown origin was found in a sample from a stormwater retention basin.

4.2. Introduction

The worldwide use of pesticides has caused a contamination of the environment in all compartments such as water bodies, soil, and air. Pesticides and biocides can harm and alter organisms, populations, and entire food webs in several ways. Some compounds are suspected of being carcinogenic or influencing hormone balance, so that residues in food and ground and drinking water can also pose a risk for humans (SHARMA et al., 2019). Pesticides and biocides are introduced into the aquatic environment via runoff from agricultural areas, discharges from combined or separate sewer systems and wastewater treatment plants (SINGER et al., 2010; WITTMER et al., 2010; BOLLMANN et al., 2014; PIETRZAK et al., 2019). Biocides used in non-agricultural sectors can enter the environment, for example, when they evaporate or leach from facade painting (BURKHARDT et al., 2011; BOLLMANN et al., 2016). In addition, pesticide residues are found in food (CHAWLA et al., 2018).

Organophosphates and carbamates are two widespread pesticide groups and have been analyzed in different matrices all the way from plants and soils to the aquatic system (SIDHU et al., 2019; DE SOUZA et al., 2020). These two groups of pesticides inhibit AChE, which occurs in the nervous system of mammals, birds, fish, reptiles, and insects (FUKUTO, 1990; SULTATOS, 1994; CROUCHER AND JEWESS, 1999). Enzyme based biosensors were used for neurotoxicity testing of pesticides in the environment (SONGA AND OKONKWO, 2016). The AChE activity can be measured by well-established AChE assays (ELLMAN et al., 1961; DOCTOR et al., 1987; VAN DYK AND PLETSCHKE, 2011; WOREK et al., 2012). The combination of HPTLC with AChE-I assays has been successfully demonstrated and used for effect-directed analysis (EDA) of environmental, food, and plant samples (ACKERMANN, 1968; MENDOZA et al., 1968; AKKAD AND SCHWACK, 2010; STÜTZ et al., 2017; WEISS et al., 2017; CORNI et al., 2020; OBERLEITNER et al., 2020; SOBSTYL et al., 2020; STÜTZ et al., 2020; CHANDANA AND MORLOCK, 2021). OTPs, such as chlorpyrifos and malathion, become stronger AChE inhibitors when the sulfur atom in the phosphorus-sulfur bond is replaced biologically (metabolic or microbiological actions) or chemically (chemical or photo-oxidation) by an oxygen atom (ACKERMANN, 1968; FUKUTO, 1990; SULTATOS, 1994; CROUCHER AND JEWESS, 1999; SINGH AND WALKER, 2006; VAN DYK AND PLETSCHKE, 2011). The OTPs are not always completely oxidized to the respective oxons, but other products or a further transformation may take place (SHEMER AND LINDEN, 2006; KRALJ et al., 2007). Higher inhibition sensitivities can be achieved by a pre-oxidation of OTPs whereby bromine is used by several authors before applying an AChE-I assay on HPTLC plates (ACKERMANN, 1968; MENDOZA et al., 1969; AKKAD AND SCHWACK, 2011). Other studies presented a biological activation of OTPs (SCHULZE et al., 2004; ROEPCKE et al., 2010; AZADNIYA et al., 2020). OTPs in lower inhibition concentrations are detectable and most important the metabolic OTP activation in organisms can be simulated in this way. NBS is an alternative bromine containing oxidizing agent that is used in AChE-I assays and has proven to be suitable for a complete oxidation of OTPs in water samples (DIN, 1995; KRALJ et al., 2006).

Two methods, immersion and spraying, for the application of biosensors on HPTLC plates have been used in a study by AZADNIYA AND MORLOCK (2019). MENDOZA et al. (1968) and STÜTZ et al. (2020) used, as in this study, indoxyl acetate as an esterase substrate but each of them employed a different method to apply the esterase solution on thin-layer plates: immersion or spraying. In a previous work, an immersion and a spray method for application of yeast suspension on HPTLC plates were compared whereas a similar sensitivity and a better precision of the spraying approach were observed (BAETZ et al., 2021). SCHOENBORN et al. (2017) sprayed yeast cells onto HPTLC plates and observed an unprecedented sensitivity of the planar yeast estrogen screen (p-YES) compared to immersion.

This study aims to demonstrate that oxidation of OTPs by NBS is successful not only in an AChE-I microtiter assay but also in a combination of HPTLC, oxidation, and AChE-I assay (HPTLC-Ox-AChE-I). An expected increase in sensitivity will be demonstrated by investigating dose-response relations of malathion, parathion, chlorpyrifos, and related oxons either with or without oxidation by NBS after chromatographic separation. Moreover, it is interesting to ask whether differences in sensitivity, precision, and general feasibility can be observed in an HPTLC-Ox-AChE-I approach when the enzyme is sprayed onto the HPTLC plates or the plates were immersed into the enzyme solution. As a proof of concept, native water samples from a stream and connected stormwater retention basin were investigated with the HPTLC-Ox-AChE-I method after enrichment by solid-phase extraction (SPE).

4.3. Materials and methods

4.3.1. Chemicals

The pesticides parathion, chlorpyrifos, and malathion as well as the oxons paraoxon and malaoxon were purchased from Sigma-Aldrich GmbH (Steinheim, Germany). Chlorpyrifosoxon was purchased from LGC standards GmbH (Wesel, Germany). All standards had a purity of > 95%. AChE from electric eel (*Electrophorus electricus*), acetylthiocholine (ATCL), NBS, 5,5'-dithiobis(2-nitrobenzoic acid) (DTNB), ascorbic acid, and bovine serum albumin (BSA) were purchased from Sigma-Aldrich GmbH (Steinheim, Germany). Tris(hydroxymethyl)aminomethane (TRIS) was purchased from Carl Roth GmbH + Co. KG (Karlsruhe, Germany). HCl was purchased from Merck (Darmstadt, Germany). Indoxyl acetate was purchased from Thermo Fisher Scientific (Geel, Belgium). Methanol (LC-MS grade), acetone (LC-MS grade), dichloromethane (LC-MS grade), and water (LC-MS grade) were all purchased from Th. Geyer GmbH & Co. KG (Renningen, Germany). Cyclohexane (LC-MS grade) was purchased from LGC Standards GmbH (Wesel, Germany).

4.3.2. AChE-inhibition microtiter assay

Stock solutions (1 mg/mL) of NBS and ascorbic acid were each freshly prepared before the test and then diluted to 10 µg/mL and 100 µg/mL, respectively. The assay was performed with modifications according to Ellman's method (ELLMAN et al., 1961).

OTPs, oxons, water, and methanol blanks (15 μL) were each mixed with 15 μL of NBS (10 $\mu\text{g}/\text{mL}$) in a 96-well plate. After an incubation at room temperature for 5 min, the reaction was stopped by adding 15 μL ascorbic acid (100 $\mu\text{g}/\text{mL}$). For the test setup without oxidation, OTPs, oxons, water, and methanol blanks (15 μL) were mixed with 30 μL water per well. Subsequently, 200 μL of a DTNB solution (0.15 mM), buffered in TRIS/HCl at a pH of 7.4, was added to each well of both test setups. Then, 20 μL of an AChE solution (0.5 U/mL), also buffered in TRIS/HCl at a pH of 7.4, was added. An incubation at 30 °C for 30 min without shaking followed. An ATCL solution (0.8 mM) was freshly prepared with water and 30 μL per well was added after incubation. During another incubation at room temperature for 30 min, ATCL was cleaved by AChE into thiocholine and acetic acid. Thiocholine reacts with DTNB to 2-nitro-5-thiobenzoate (ELLMAN et al., 1961). The absorbance of the yellow-colored anion was photometrically measured at 405 nm (Sunrise Remote, Tecan Group AG, Männedorf, Schweiz). A flow chart of the used procedure is shown in Figure 4-4.

4.3.2.1. Dose-response relationship

Dilution series with eight concentrations of the three OTPs and related oxons (Table 4-3) were freshly prepared from stock solutions (1 – 10 mg/mL) in methanol. The OTPs and oxons were tested in duplicates with and without prior oxidation in two measurements as described in 4.3.2. Eight water and eight methanol blanks were tested per test setup (oxidation and no oxidation). Of these, two were tested without AChE and two without ATCL. The mean AChE activity (absorption at 405 nm, $n = 4$) was related to the specific inhibitor dose. The statistic program Prism (version 5.00, Graph Pad Software, San Diego, USA) was used to generate dose-response curves (4-PL fit) and to determine ICs for the three OTPs and related oxons. The 95% confidence intervals of the curves and the standard deviations of the mean AChE activity were also calculated. The lower boundary of the curves is fixed to 0 and the highest mean activity defines 100%.

4.3.3. Combination of HPTLC and AChE-inhibition assay

4.3.3.1. HPTLC

LiChrospher 10 \times 20 cm HPTLC Silica gel 60 F254s plates (Merck, Darmstadt, Germany) with a layer thickness of 170 – 190 μm and spherical silica particles with a size of 7 μm were used. The HPTLC plates were immersed twice in 2-propanol for 20 min, each time followed by a drying step at room temperature for 20 min. The plates then were pre-developed with methanol, dried for 20 min at room temperature, heated at 105 °C for 20 min, and stored in a desiccator for further use. The automatic TLC Sampler 4 (ATS 4, CAMAG AG, Muttenz, Switzerland) was used for sample application. The desired sample volumes were sprayed as 6 mm wide bands onto the HPTLC plates with an application speed of 300 nL/s. The distances of the exterior bands from the edges of the plates were 15 mm. The distance from the bottom edge was 8 mm for all bands. Methanol was used as rinsing solvent. The following

further application parameters were used: filling speed 15 $\mu\text{L/s}$, pre-dosage volume 200 nL, retraction volume 200 nL, rinsing vacuum time 4 s, filling vacuum time 0 s, rinsing cycles 2, and filling cycles 1. The development of the HPTLC plates was realized by the Automated Multiple Development 2 (AMD 2, CAMAG, Muttenz, Switzerland). The OTPs, their oxons, and environmental samples were separated with an eluent mixture of cyclohexane, dichloromethane, and acetone in different proportions and with increasing migration distances (Figure 4-5). After each development step, a drying step of 3 min under vacuum followed. The final migration distance was 80 mm and the whole procedure took approximately 45 min. In addition, a simpler development process was used containing only the last step of the previous described method.

4.3.3.2. Chemical oxidation of OTPs and AChE-inhibition assay

After chromatographic development, 10 mL of freshly prepared NBS (100 $\mu\text{g/mL}$) was sprayed onto the HPTLC plates with a glass reagent sprayer, followed by a 5 min incubation at room temperature. The following AChE-I assay was performed in parts according to MENDOZA et al. (1968), STÜTZ et al. (2017), and WEINS AND JORK (1996). AChE was buffered in TRIS/HCl at a pH of 7.8 (2.5 U/mL). The AChE solution was either sprayed onto the HPTLC plates with a glass reagent sprayer until the plates were evenly moist (approx. 10 mL) or the plates were immersed in the AChE solution using the Chromatogram Immersion Device 3 (CID 3, CAMAG, Muttenz, Switzerland). The immersion volume, speed, time, and depth were approx. 200 mL, 2.5 cm/s, 2 s, and approx. 85 mm, respectively. Afterward, the plates were placed separately in closed plastic boxes, which contained paper towels moistened with water to gain a saturated atmosphere. An incubation at 37 °C for 5 min followed. The substrate indoxyl acetate was freshly prepared in methanol at a concentration of 20 mg/mL and 5 mL was sprayed onto the HPTLC plates with a glass reagent sprayer. During 45 min incubation time at room temperature, AChE cleaves the substrate into indoxyl and acetate. The indoxyl reacts with oxygen to the blue indigo dye. When AChE was inhibited, no indigo was produced and the spot stayed white. The TLC Scanner 3 (CAMAG, Muttenz, Switzerland) was used to scan each track on the plates at 670 nm using the fluorescence mode without optical filter. The CAMAG-embedded software Wincats (Vers. 1.4.9) was used to provide chromatograms of each track and to evaluate inhibition zones.

4.3.3.3. Separation of organothiophosphates and oxons by HPTLC

The mean retardation factors (R_f s) and standard deviations (SDs) ($n = 18$) of the OTPs and oxons were calculated using Excel 2013 (vers. 15.0.5172.1000, Microsoft, Redmond, USA). For the four-step development process, the R_f s and SDs from the different tested amounts of the dose-response investigations (4.3.3.4) were used ($n = 18$). The separation of OTPs and oxons with the single-step development was done in duplicate on two HPTLC plates ($n = 4$).

The influence of the single- and four-step development on the migration of sample matrix was investigated by using a SPE extract from a combined sewer overflow.

4.3.3.4. Dose-response relationship

Several amounts of an OTP mix and an oxon mix were applied on HPTLC plates (Table 4-4) and tested as described in 4.3.3. Three plates were used for each dilution series. The application volume was 10 μ L for investigating OTPs with following oxidation and 100 μ L for testing OTPs without following oxidation. The application volume for the oxons was 10 μ L. They were tested without oxidation step also in triplicates. The peak heights were used for evaluation. Only peaks that have a signal-to-noise ratio ≥ 3 were considered in the evaluation. The height next to the respective peak defines the noise. The first detected peak at one of the applied concentrations with a signal to noise ratio ≥ 3 defines the limit of detection (LOD) for the specific substance and the respective application method. The mean AChE-I (mean peak height, AU at 670 nm, $n = 3$) was related to the inhibitor amounts. Prism was used to generate dose-response curves (4-PL fit) and to determine ICs for the three OTPs (oxidized and unoxidized) and related oxons. The 95% confidence intervals of the curves and the SDs of the mean peak heights were also calculated. The lower boundary of the curves is fixed to 0 and the highest mean peak height defines 100%.

4.3.4. Proof of concept using environmental samples

4.3.4.1. Sampling

Grab samples were taken in March and August 2020 from a stormwater retention basin, which is connected to a highway nearby, and up- and downstream the receiving stream Deininghauser Bach near Deininghausen, Germany. A field blank was prepared with LC-MS grade water, which was used to wash the sampling vessel and opened at the sampling points. The samples were cooled during transport and stored < 8 °C until further sample preparation.

4.3.4.2. Sample preparation

The samples were enriched by SPE within 24 h after sampling. Moreover, the field blank and water for a SPE blank were enriched in the same way. For additional matrix investigations, 1 mL malathion, parathion, and chlorpyrifos (100 ng/mL in methanol) were spiked into native samples taken in August 2020 and a water control before being loaded on the SPE cartridges. The cartridges (150 mg, Oasis HLB 6 cc, Waters GmbH, Eschborn, Germany) were conditioned with methanol (2×5 mL) and equilibrated with water (2×5 mL), before being loaded with 1000 ± 5 mL sample (the exact volume was determined by weighting) through a polytetrafluoroethylene tube. After drying the cartridges under vacuum, they were stored at -18 °C until further usage. The cartridges were eluted with methanol (5×5 mL) that

was evaporated afterward at 60 °C under a gentle nitrogen gas stream. The dried extracts were redissolved in 1 mL methanol to achieve a nominal 1000-fold enrichment.

4.3.4.3. HPTLC and AChE-inhibition assay

The extracts, spiked samples, positive controls (PC: mix of malathion, parathion, and chlorpyrifos), and blanks were tested with the HPTLC-Ox-AChE-I method as described in 4.3.3. Each sample was tested in duplicates on two HPTLC plates ($n = 4$). The application volume was 100 μ L resulting in a PC of 2000 ng/spot. The resulting amounts for the matrix investigation were 1000 and 10 ng/spot for the PCs and 10 ng/spot for the spiked samples. The matrix investigation was performed with and without the oxidation step. Excel was used to relate the peak areas of the spiked samples to the peak areas of the PCs (10 ng/spot). Differences between both approaches (oxidation and no oxidation) were shown by comparing the results of the spiked samples and PCs.

4.4. Results and discussion

4.4.1. AChE-inhibition microtiter assay

In a preliminary experiment using microtiter plates, it was confirmed that oxidation with NBS is suitable to increase the AChE-I potential of the tested OTPs, and in this way, the sensitivity of AChE assays to OTPs as shown in other studies (BARBER et al., 1999; SCHULZE et al., 2004). Although concentrations up to 500 μ g/mL were used, the inhibition intensities of the unoxidized OTPs were not high enough to generate full sigmoidal dose-response curves in contrast to oxidized OTPs (Figure 4-1). The observed differences of the ICs between oxons and oxidized OTPs could be due to an incomplete oxidation of OTPs to their corresponding oxons, a formation of other non-active products, or a decay of formed oxons. KRALJ et al. (2006) showed that with an increasing NBS concentration formed oxons could not be detected or the signals decreased, which could be an indication for a further transformation of the oxons. In a further study by KRALJ et al. (2007), it is shown that several transformation products were formed during photolysis or photocatalysis of malathion. The increase in toxicity of OTPs due to biotransformation during natural metabolism can be mimicked in a simple way by using NBS for chemical oxidation. Biological activation of OTPs with cytochrome P450 proteins is maybe closer to the metabolism in vivo. However, in vivo metabolism depends on different cytochrome P450 types and differs between organisms and could be even sex-specific (SAMS et al., 2000; TANG et al., 2001). Studies often used one enzyme for activation of OTPs such as a genetically engineered P450 or chloroperoxidase (HERNANDEZ et al., 1998; SCHULZE et al., 2004; ROEPCKE et al., 2010).

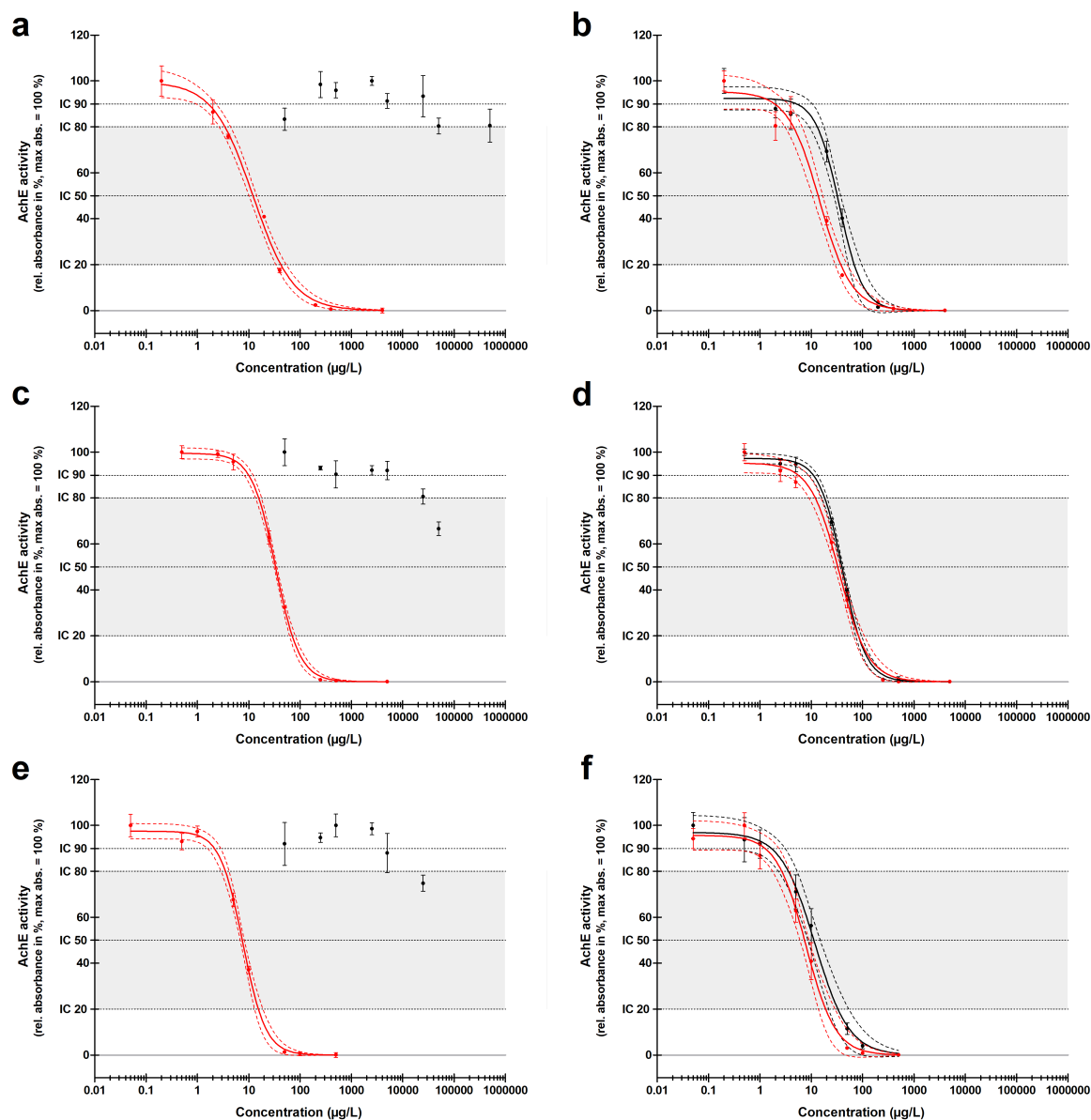


Figure 4-1 Dose-response curves (4-PL fit) of malathion (a, b), parathion (c, d), and chlorpyrifos (e, f) (black dots and curves), and malaoxon (a, b), paraoxon (c, d), and chlorpyrifos-oxon (e, f) (red dots and curves). An AChE inhibition assay for the detection of inhibition effects was performed in 96-well plates (AChE-I microtiter assay) either without (left side: a, c, and e) or after oxidation by *n*-bromosuccinimide (right side: b, d, and f). Acetylthiocholine (ATCL) was used as substrate and DTNB as reactant for thiocholine. The AChE activity (relative absorbance in %) is shown on the y-axis and the specific substance concentration ($\mu\text{g/L}$) on the x-axis ($n = 4$). The lower boundary of the curves is fixed to 0. The highest mean absorbance defines 100%. The dashed lines show the 95% confidence intervals, and the error bars the standard deviations. The dotted lines indicate the inhibition concentration (IC) for 90, 80, 50 and 20% AChE activity. The grey colored area between IC₈₀ and IC₂₀ shows the linear range.

In comparison, the chemical oxidation process presented is much less demanding in terms of preparation, chemicals, and materials. In addition, biological activation requires a buffer with a pH value that is within the optimum of the enzyme used for oxidation which does not necessarily match a subsequent AChE-I microtiter assay. Thus, the used oxidation method is a simpler and more robust procedure for testing native water samples. The sensitivity of the following HPTLC-Ox-AChE-I approach was in a comparable range to the AChE-I microtiter assay. However, the application volume of the HPTLC-Ox-AChE-I approach is decisive, so that better sensitivities can also be achieved. The IC_{50} s of malathion, parathion, and chlorpyrifos for the microtiter assay were 35, 41, and 12 $\mu\text{g/L}$, respectively (Table 4-5). In comparison, when 100 μL sample was applied onto the HPTLC plate, the IC_{50} s of malathion, parathion, and chlorpyrifos were 14, 42, and 15 $\mu\text{g/L}$, respectively.

4.4.2. High-performance thin-layer chromatography

For the dose-response investigations and following analysis of environmental samples, a development method was needed that is able to separate malathion, parathion, chlorpyrifos, and the related oxons on the HPTLC plate. With the four-step development (Figure 4-5), it was possible to separate all three OTPs and the oxons to a sufficient extent for the following investigations (Table 4-1 and Figure 4-7).

Table 4-1 The mean retardation factor (R_F), standard deviation (SD), calculated relative R_F , and resolution (R) of malaoxon, paraoxon, chlorpyrifos-oxon, malathion, parathion, and chlorpyrifos on the LiChrospher HPTLC plate. After chromatographic separation, using a four step HPTLC development process, and oxidation by n-bromosuccinimide (NBS), the plates were measured with an AChE inhibition assay using indoxyl acetate as substrate. The HPTLC plates were either immersed in AChE solution (left side) or AChE was sprayed onto the plates (right side). The plates were scanned at 670 nm. The mean R_F s and SDs were calculated from the different tested amounts (1-250 ng/spot) of the dose-response investigations ($n = 18$).

Substance	Immersion				Spraying			
	Mean R_F	SD	rel. R_F	R	Mean R_F	SD	rel. R_F	R
Malaoxon	0.22	0.04			0.21	0.02		
Paraoxon	0.31	0.04	1.4	1.0	0.29	0.02	1.4	1.1
Chlorpyrifos-oxon	0.50	0.07	1.6	1.9	0.47	0.03	1.6	2.2
Malathion	0.74	0.06	1.5	2.2	0.67	0.03	1.4	2.1
Parathion	0.85	0.03	1.2	1.3	0.78	0.04	1.2	1.3
Chlorpyrifos	0.93	0.02	1.1	1.0	0.85	0.05	1.1	1.0

The single-step method allowed a separation of all 6 compounds with reduced time, cost, and solvent consumption (Table 4-7). In addition, attempts were made to better separate polar matrix of environmental samples from non-polar fractions. For this purpose, an unconventional approach, the four-step HPTLC development procedure with increasing migration distance and increasing elution power (Figure 4-5), was compared to the single-step development method.

A sample extract from a combined sewer overflow (CSO) was separated by the four-step and the single-step development procedures. The four-step development showed less migration of visible sample components in comparison to the single-step method before applying the AChE-I assay (Figure 4-8). Using the four-step development, the sample matrix had less influence on at least the last third of the solvent migration distance in contrast to the single-step development. Whether matrix retention on a HPTLC plate can actually be achieved with such a development and what benefit it has over single-step or multi-step development with increasing migration distance and decreasing elution power should be determined in further, more in-depth studies. However, the four-step development was used for the following dose-response experiments and analysis of water samples because a sufficient separation of the OTPs was achieved and an influence of the separation method on the results of dose-response investigations is rather unlikely.

4.4.3. Oxidation on high-performance thin-layer plates

The dose-response relations of malathion, parathion, chlorpyrifos, and the related oxons were used to evaluate the oxidation by NBS on the HPTLC plate. In Figure 4-2, Table 4-6, and Table 4-8, it is obvious that the oxidation of the three OTPs on HPTLC plates can be applied as expected. The sensitivity of the HPTLC-AChE-I assay can be increased dramatically for the detection of OTPs by oxidation with NBS. Differences between the AChE-I potential and thus the ICs of the tested oxons and the activated OTPs (Figure 4-2, Figure 4-7, and Table 4-6) could be due to an insufficient oxidation of the OTPs on the HPTLC plate. Another possibility is, as discussed for the AChE-I microtiter assay, a formation of other OTP products or a partial decay of the formed oxons during the following incubation times. The final scan of the HPTLC plate takes place about an hour after the application of NBS. AKKAD AND SCHWACK (2011) used bromine for oxidation before applying a HPTLC esterase inhibition assay and showed an increase of the inhibition potential of OTPs. They also observed differences of the esterase inhibition between the activated OTPs and corresponding oxons. AZADNIYA et al. (2020) used a S9 mixture to metabolize OTPs successfully on HPTLC plates. After sample application, a pre-wetting step follows before they applied the S9 mixture. An incubation of 30 min followed. The benefit of the here presented oxidation method with NBS is its simplicity: one application step followed by an incubation of 5 min. For a further increase of the sensitivity, a higher amount of NBS for oxidation could be reasonable. However, a concentration of 1 mg/mL NBS was tested, resulting in a lower activity or inhibition of AChE. Less indoxyl acetate seemed to be cleaved by AChE, and therefore, less indigo was formed. The HPTLC plate only became a blue tinge instead of a stronger blue color.

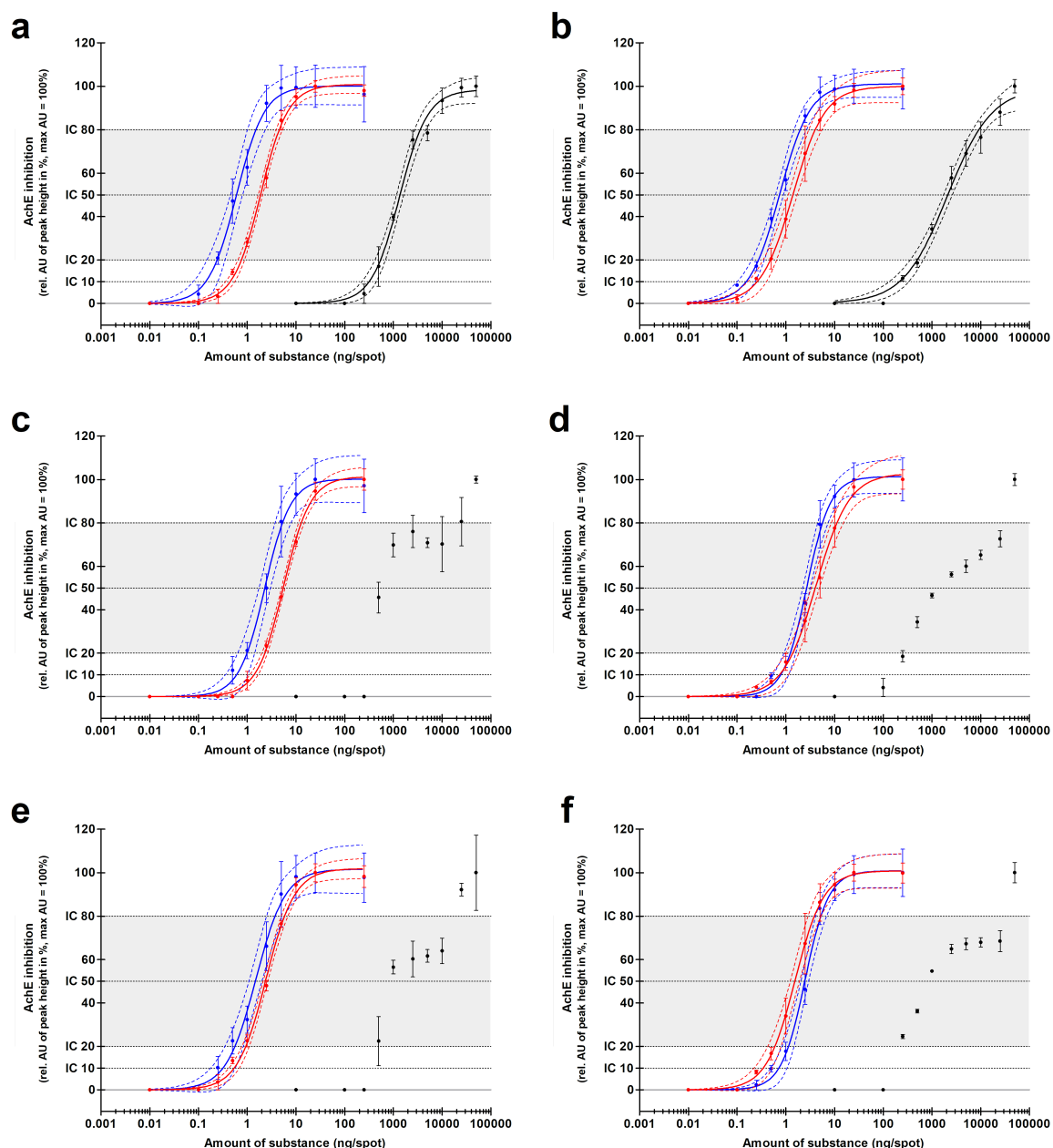


Figure 4-2 Dose-response curves (4-PL fit) of different organothiophosphates (OTPs) and their oxons. An OTP mix and an oxon mix were applied with different concentrations on LiChrosphere HPTLC plates. The application volume was 10 μL for the oxons and OTPs with following oxidation and 100 μL for the OTPs without following oxidation. After chromatographic separation by HPTLC, an AChE inhibition (AChE-I) assay either with or without prior oxidation by *n*-bromosuccinimide (NBS) was performed (HPTLC-Ox-AChE-I). The HPTLC plates were either immersed in AChE solution (a, c, e) or AChE was sprayed onto the plates (b, d, f). The black, red, and blue dots and curves represent the AChE-I by malathion, oxidized malathion, and malaoxon (a, b), parathion, oxidized parathion and paraoxon (c, d), and chlorpyrifos, oxidized chlorpyrifos, and chlorpyrifos-oxon (e, f), respectively. The peak heights were used for evaluation. Only peaks that have a signal-to-noise ratio ≥ 3 were considered in the evaluation. The heights next to the respective peak define the noise. The AChE-I is shown on the y-axis as the relative AU of the mean peak heights ($n = 3$) at a specific amount of substance on the HPTLC plate (x-axis). The lower boundary of the curves is fixed to 0. The highest mean peak height defines 100%. The dashed lines show the 95% confidence intervals and the error bars the standard deviations. The dotted lines indicate the inhibition concentration (IC) for 10, 20, 50, and 80% AChE-I. The grey colored area between IC_{20} and IC_{80} shows the linear range.

4.4.4. Comparison between immersion and spray method

The comparison between the immersion and the spray approach revealed that when using the immersion method to apply AChE on the HPTLC plates, the OTPs showed significantly higher R_F s than using the spray approach (D'Agostino and Pearson omnibus normality test and Mann–Whitney test) (Table 4-1). A reason could be that the immersion method influences the migration retrospectively. However, this assumption is counteracted by the fact that the R_F s of the oxons do not differ significantly from each other. Notable differences in the effect peaks' width were not observed between the immersion and spray method, which would have to be assumed if the immersion method had an influence. Since the immersion line (85 mm) is quite close to the solvent front (80 mm) and the OTPs again have very high R_F values, a shift of the OTPs may have occurred in the upper part of the plate near the immersion line. After using a combination of HPTLC and enzyme inhibition assay in which plates were immersed in the enzyme solution, AKKAD AND SCHWACK (2010) showed that some OTP spots with very high R_F values were more blurred than compounds with R_F values less than 0.5.

The comparison between the immersion and the spray approach with the dose-response investigations showed that the spray method had a slightly better sensitivity to all tested activated OTPs (Figure 4-2, Table 4-6, and Table 4-8). Low concentrations are thus more likely to be detected. The IC_{10} s substantiate that. In another study, the application of yeast cells on HPTLC plates for the detection of endocrine effects was compared (BAETZ et al., 2021). An overall similar sensitivity was shown between spray and immersion approaches. SCHOENBORN et al. (2017) observed a better sensitivity of the p-YES by spraying yeast suspension onto HPTLC plates. One reason for a better sensitivity of spray methods is maybe that substances could be extracted to a small extent from the HPTLC plates during the immersion process. SCHOENBORN et al. (2017) obtained a higher peak quality with the spray method and blurred peaks with the immersion approach. A difference in the peak quality such as wider peaks with the immersion than with the spray method could not be observed in this study. The linear ranges between IC_{20} and IC_{80} are suitable for calibration. A comparison of the precision between the two application methods does not give a consistent picture. The 95% confidence intervals of the dose-response curves were narrower for the activated OTPs when using the immersion method, but wider for the oxons, in comparison to the spray method (Figure 4-2, Table 4-6). In a previous study, investigating the application of a yeast suspension, the spray approach was slightly more precise than the immersion method (BAETZ et al., 2021). Differences were the use of airbrush to apply the yeast suspension onto the HPTLC plate until it was evenly moist. In this study, a glass reagent sprayer was used to spray the AChE solution onto the HPTLC plate until it was evenly wet, almost as with the immersion method, to guarantee an even distribution. AZADNIYA AND MORLOCK (2019) compared immersion and piezoelectric spraying for application of cholinesterase and substrate

solutions on HPTLC plates. Besides many advantages of the spray method, they reported that the main argument in favor of the immersion method is its simplicity. This was also the case in this study because complete wetting of the HPTLC plates took much longer than it did with the immersion method. The spraying method was therefore less user-friendly, which could be counteracted by automatic spraying methods (AZADNIYA AND MORLOCK, 2019; BERGMANN et al., 2020). Despite the slight differences in sensitivity, precision, and handling, both application methods behave very similar and can be used for the detection of AChE-I effects in an HPTLC-Ox-AChE-I approach. The spray approach was used for the following proof of concept with environmental samples because of the slightly higher sensitivity and the associated higher probability of detecting effects in low concentration ranges.

4.4.5. Environmental samples

Samples taken from a stream and a connected stormwater retention basin (4.3.4.1) were analyzed using the developed HPTLC-Ox-AChE-I method including an enrichment by SPE. Besides the investigation of unknown AChE-I effects, the samples taken in August 2020 were spiked with malathion, parathion, and chlorpyrifos to show the recovery of the effects triggered by the OTPs. No notable differences between the stream and stormwater basin matrix were observed (Table 4-2).

Table 4-2 Recovery rates of the effect peak area of malathion, parathion, and chlorpyrifos. Native water samples and a water control sample were spiked with 100 ng of each organothiophosphate (OTP). The samples were taken at the Deininghauser Bach near Deininghausen next to the highway A42 from a rainwater retention basin, and up- and downstream the outlet of the rainwater retention basin in August 2020. After enrichment by solid phase extraction (SPE), 100 μ L of the extracts and the positive control (mix of the OTPs) were applied on LiChrosphere HPTLC plates, resulting in an OTP amount of 10 ng/spot. After chromatographic separation by HPTLC, an AChE inhibition assay with prior oxidation by n-bromosuccinimide (NBS) was performed. AChE was sprayed onto the HPTLC plates. The mean peak areas of the spiked samples were related to the mean peak areas of the positive controls (100%). The recovery rates \pm standard deviations (%) are shown (n = 4).

Substance	Recovery rate \pm standard deviation (%)		
	Malathion	Parathion	Chlorpyrifos
Sample			
Upstream	92 \pm 11	82 \pm 10	78 \pm 7
Stormwater basin	81 \pm 8	75 \pm 9	74 \pm 5
Downstream	87 \pm 12	79 \pm 13	69 \pm 5
Spiked water	85 \pm 6	74 \pm 3	63 \pm 4

Malathion showed the highest recovery of the effect peak area related to the tested positive control. The recoveries in comparison to the positive control were between 81 and 92% for malathion after SPE and HPTLC-Ox-AChE-I. The recoveries of parathion and chlorpyrifos were between 75–82% and 69–78%, respectively. A study by AKKAD AND SCHWACK (2011), who combined HPTLC with a multi-enzyme inhibition assay with prior oxidation of organophosphates, showed recoveries of 91 – 106% for parathion, chlorpyrifos, and paraoxon in apple juice and tap water samples.

No notable matrix effects of the native samples could be shown in comparison to an ultrapure water sample spiked with the OTPs (Table 4-2). A reason for partly lower recoveries in the ultrapure water sample could be the organic material in the native samples that was retained in the cartridge and to which additional molecules bound. The spiked samples were also tested without oxidation. Neither the spiked water samples nor the positive control (10 ng/spot) showed any effect peaks. Thus, the oxidation by NBS works with native surface water sample extracts on HPTLC plates. If the samples were oxidized, the PC concentration (1000 ng/spot) is in the maximum inhibition plateau (Figure 4-2). At this level, the peak heights do not increase but the areas continue to increase. Therefore, the peak area was used for evaluation. Only the positive control with 1000 ng/spot showed peaks for all three OTPs, but with lower intensities than the same positive control tested with oxidation step. The peak areas differed by a factor of 5 – 8 (Figure 4-6). This shows that the chemical oxidation by NBS on HPTLC plates is a robust way to mimic the natural activation of OTPs by biotransformation.

The results showed that the overall workflow with prior sample enrichment by SPE is suitable to detect AChE-I effects caused by OTPs in surface water samples. This was confirmed by an AChE-I effect detected in an unspiked stormwater basin sample taken in March 2020 caused by unknown substances (Figure 4-3). The samples taken in August 2020 showed no AChE-I effects. The presented HPTLC-Ox-AChE-I approach should facilitate subsequent analysis, because the complexity of the sample is reduced by HPTLC and information about the effect type are available, which reduces the number of possible responsible substances.

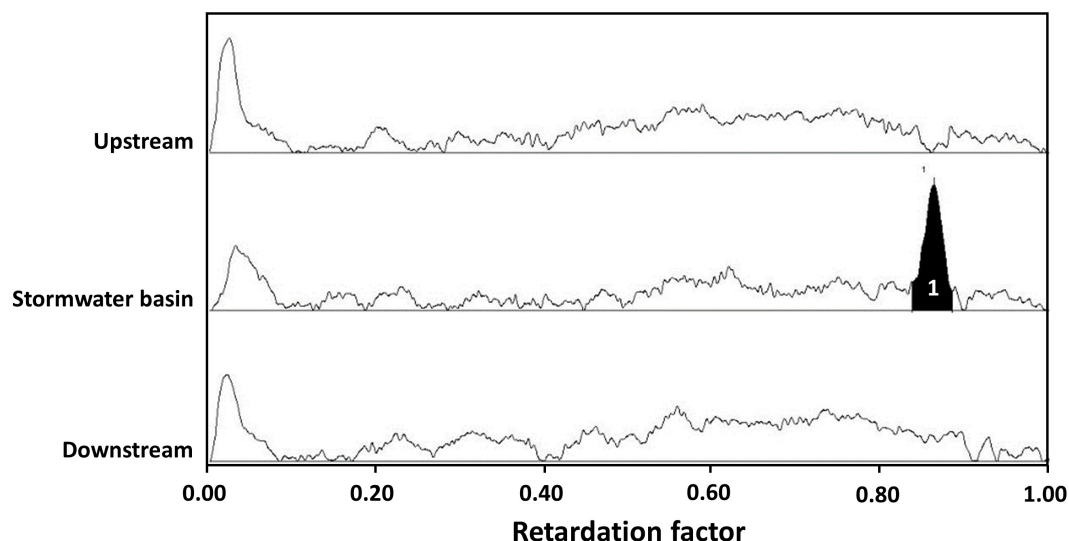


Figure 4-3 AChE inhibition (AChE-I) effect (1) in the sample of a stormwater retention basin. The samples were taken at the Deininghauser Bach near Deininghausen, Germany next to the highway A42 from a stormwater retention basin, and up- and downstream the outlet of the stormwater basin in March 2020. After enrichment by solid phase extraction (SPE), 100 μ L of the extracts were applied on LiChrosphere HPTLC plates. As a positive control a mix of malathion, parathion, and chlorpyrifos (each 2000 ng/spot) were also applied. After chromatographic separation by HPTLC, an AChE-I assay with prior oxidation by n-bromosuccinimide (NBS) was performed. AChE was sprayed onto the HPTLC plates. The sampling points are shown on the y-axis and the retardation factor on the x-axis.

4.5. Conclusion

This study demonstrates that an oxidation of OTPs by NBS can be applied in an HPTLC-Ox-AChE-I approach and leads to a strong increase of the substances' inhibition potential and therefore a better sensitivity of the method. Chemical oxidation by NBS mimics the natural activation of OTPs in a more simple and robust manner than biological approaches, which allows a rapid investigation of neurotoxicity. The formation of different products than the corresponding oxons and the temporal processes and pathways during the oxidation should be investigated in detail for example by comparing dose-response relations of oxons that undergo the oxidation process or not. The comparison of the two main application methods for AChE on HPTLC plates, immersion and spraying, showed slight differences in sensitivity and precision. Both methods are suitable for the presented HPTLC-Ox-AChE-I approach. The potential of the spray approach for higher sensitivities should be refined. It may be reasonable to replace the manual spray approach by an automated device. The automation of the entire workflow may increase the reproducibility and comparability and in addition could save time and material. In conclusion, the combination of sample enrichment by SPE, separation by HPTLC, oxidation of possible OTPs, and AChE-I effect testing can be used to investigate neurotoxic activities in surface water samples. The overall workflow should be used to monitor these effects in the aquatic environment in more extensive studies and for the clarification of unknown effect-responsible substances in combination with further instrumental analysis.

4.6. Acknowledgements

Financial support for the graduate program Future Water by Ministry of Culture and Science of the Federal State of North Rhine-Westphalia (MKW NRW, Düsseldorf, Germany) is gratefully acknowledged. Gratefully acknowledged is the support of Prof. Dr. Grünebaum from the Ruhrverband (Essen, Germany). We would like to thank also Max Jochums, Martin Kläßen, and Dr. Thorsten Teutenberg (all also from IUTA, Duisburg, Germany) for their inspiration in coming up with ideas for the oxidation process and especially Max Jochums for carrying out initial investigations in the not reported assay format.

4.7. Funding

Open Access funding enabled and organized by Projekt DEAL. This study received funding from the graduate program Future Water by the Ministry of Culture and Science of the Federal State of North Rhine-Westphalia (MKW NRW, Düsseldorf, Germany).

4.8. Open Access

This article is licensed under a Creative Commons Attribution 4.0 International License, which permits use, sharing, adaptation, distribution and reproduction in any medium or format, as long as you give appropriate credit to the original author(s) and the source, provide a link to the Creative Commons license, and indicate if changes were made. The images or other third party material in this article are included in the article's Creative Commons license, unless indicated otherwise in a credit line to the material. If material is not included in the article's Creative Commons license and your intended use is not permitted by statutory regulation or exceeds the permitted use, you will need to obtain permission directly from the copyright holder. To view a copy of this license, visit <http://creativecommons.org/licenses/by/4.0/>.

4.9. References

- Ackermann H., 1968. Dünnschichtchromatographisch-enzymatischer Nachweis Phosphororganischer Insektizide. Aktivierung schwacher Esterasehemmer. *Journal of Chromatography*, 36, 309–317.
- Akkad R. and Schwack W., 2010. Multi-enzyme inhibition assay for the detection of insecticidal organophosphates and carbamates by high-performance thin-layer chromatography applied to determine enzyme inhibition factors and residues in juice and water samples. *Journal of Chromatography B*, 878 (17-18), 1337–1345. <https://doi.org/10.1016/j.jchromb.2009.12.021>.
- Akkad R. and Schwack W., 2011. Effect of bromine oxidation on high-performance thin-layer chromatography multi-enzyme inhibition assay detection of organophosphates and carbamate insecticides. *Journal of Chromatography A*, 1218 (19), 2775–2784. <https://doi.org/10.1016/j.chroma.2011.02.029>.
- Azadniya E. and Morlock G. E., 2019. Automated piezoelectric spraying of biological and enzymatic assays for effect-directed analysis of planar chromatograms. *Journal of Chromatography A*, 1602, 458–466. <https://doi.org/10.1016/j.chroma.2019.05.043>.
- Azadniya E., Mollergues J., Stroheker T., Billerbeck K., Morlock G. E., 2020. New incorporation of the S9 metabolizing system into methods for detecting acetylcholinesterase inhibition. *Analytica Chimica Acta*, 1129, 76–84. <https://doi.org/10.1016/j.aca.2020.06.033>.
- Baetz N., Rothe L., Wirzberger V., Sures B., Schmidt T. C., Tuerk J., 2021. High-performance thin-layer chromatography in combination with a yeast-based multi-effect bioassay to determine endocrine effects in environmental samples. *Analytical and Bioanalytical Chemistry*, 413 (5), 1321–1335. <https://doi.org/10.1007/s00216-020-03095-5>.
- Barber D., Correll L., Ehrich M., 1999. Comparison of two in vitro activation systems for protoxicant organophosphorous esterase inhibitors. *Toxicological Sciences*, 47 (1), 16–22. <https://doi.org/10.1093/toxsci/47.1.16>.
- Bergmann A. J., Simon E., Schifferli A., Schönborn A., Vermeirssen E. L. M., 2020. Estrogenic activity of food contact materials-evaluation of 20 chemicals using a yeast estrogen screen on HPTLC or 96-well plates. *Analytical and Bioanalytical Chemistry*, 412 (19), 4527–4536. <https://doi.org/10.1007/s00216-020-02701-w>.
- Bollmann U. E., Minelgaite G., Schlüsener M., Ternes T., Vollertsen J., Bester K., 2016. Leaching of Terbutryn and Its Photodegradation Products from Artificial Walls under Natural Weather Conditions. *Environmental Science & Technology*, 50 (8), 4289–4295. <https://doi.org/10.1021/acs.est.5b05825>.

- Bollmann U. E., Tang C., Eriksson E., Jönsson K., Vollertsen J., Bester K., 2014. Biocides in urban wastewater treatment plant influent at dry and wet weather: concentrations, mass flows and possible sources. *Water Research*, 60, 64–74. <https://doi.org/10.1016/j.watres.2014.04.014>.
- Burkhardt M., Zuleeg S., Vonbank R., Schmid P., Hean S., Lamani X., Bester K., Boller M., 2011. Leaching of additives from construction materials to urban storm water runoff. *Water Science and Technology*, 63 (9), 1974–1982. <https://doi.org/10.2166/wst.2011.128>.
- Chandana N. G. A. S. S. and Morlock G. E., 2021. Comprehensive bioanalytical multi-imaging by planar chromatography in situ combined with biological and biochemical assays highlights bioactive fatty acids in abelmosk. *Talanta*, 223 (Pt 1), 121701. <https://doi.org/10.1016/j.talanta.2020.121701>.
- Chawla P., Kaushik R., Shiva Swaraj V. J., Kumar N., 2018. Organophosphorus pesticides residues in food and their colorimetric detection. *Environmental Nanotechnology, Monitoring & Management*, 10 (1–3), 292–307. <https://doi.org/10.1016/j.enmm.2018.07.013>.
- Corni G., Brighenti V., Pellati F., Morlock G. E., 2020. Effect-directed analysis of bioactive compounds in *Cannabis sativa* L. by high-performance thin-layer chromatography. *Journal of Chromatography A*, 1629, 461511. <https://doi.org/10.1016/j.chroma.2020.461511>.
- Croucher L., Jewess P., 1999. *Metabolic pathways of agrochemicals. Part 2 Insecticides and fungicides.* The Royal Society of Chemistry, Cambridge.
- De Souza R. M., Seibert D., Quesada H. B., De Jesus Bassetti F., Fagundes-Klen M. R., Bergamasco R., 2020. Occurrence, impacts and general aspects of pesticides in surface water: A review. *Process Safety and Environmental Protection*, 135, 22–37. <https://doi.org/10.1016/j.psep.2019.12.035>.
- Deutsches Institut für Normung (DIN), 1995. German standard methods for the examination of water, waste water and sludge - sub-animal testing (group T) - part 1: determination of cholinesterase inhibiting organophosphorus and carbamate pesticides (cholinesterase inhibition test) (T 1). Beuth, Berlin. DIN 38415–1.
- Doctor B. P., Toker L., Roth E., Silman I., 1987. Microtiter assay for acetylcholinesterase. *Analytical Biochemistry*, 166 (2), 399–403. [https://doi.org/10.1016/0003-2697\(87\)90590-2](https://doi.org/10.1016/0003-2697(87)90590-2).
- Ellman G. L., Courtney D., Andres V., Featherstone R. M., 1961. A new and rapid colorimetric determination of acetylcholinesterase activity. *Biochemical Pharmacology*, 7 (2), 88–95. [https://doi.org/10.1016/0006-2952\(61\)90145-9](https://doi.org/10.1016/0006-2952(61)90145-9).
- Fukuto T. R., 1990. Mechanism of action of organophosphorus and carbamate insecticides. *Environmental Health Perspectives*, 87, 245–254. <https://doi.org/10.1289/ehp.9087245>.
- Hernandez J., Robledo N. R., Velasco L., Quintero R., Pickard M. A., Vazquez-Duhalt R., 1998. Chloroperoxidase-Mediated Oxidation of Organophosphorus Pesticides. *Pesticide Biochemistry and Physiology*, 61 (2), 87–94. <https://doi.org/10.1006/pest.1998.2351>.
- Kralj M. B., Cernigoj U., Franko M., Trebse P., 2007. Comparison of photocatalysis and photolysis of malathion, isomalathion, malaaxon, and commercial malathion--products and toxicity studies. *Water Research*, 41 (19), 4504–4514. <https://doi.org/10.1016/j.watres.2007.06.016>.
- Kralj M. B., Trebse P., Franko M., 2006. Oxidation as a pre-step in determination of organophosphorus compounds by the AChE-TLS bioassay. *Acta Chimica Slovenica*, 53 (1), 43–51.
- Mendoza C. E., Wales P. J., Grant D. L., McCully K. A., 1969. Effect of bromine and ultraviolet light on eight pesticides detected with liver esterases of five species. *Journal of Agricultural and Food Chemistry*, 17 (6), 1196–1198. <https://doi.org/10.1021/jf60166a046>.
- Mendoza C. E., Wales P. J., McLeod H. A., McKinley W. P., 1968. Enzymatic detection of ten organophosphorus pesticides and carbaryl on thin-layer chromatograms: an evaluation of indoxyl, substituted indoxyl and 1-naphthyl acetates as substrates of esterases. *Analyst*, 93, 34–38. <https://doi.org/10.1039/AN9689300034>.

- Oberleitner D., Stütz L., Schulz W., Bergmann A., Achten C., 2020. Seasonal performance assessment of four riverbank filtration sites by combined non-target and effect-directed analysis. *Chemosphere*, 261, 127706. <https://doi.org/10.1016/j.chemosphere.2020.127706>.
- Pietrzak D., Kania J., Malina G., Kmiecik E., Wątor K., 2019. Pesticides from the EU First and Second Watch Lists in the Water Environment. *CLEAN - Soil Air Water*, 47 (7), 1800376. <https://doi.org/10.1002/clen.201800376>.
- Roepcke C. B. S., Muench S. B., Schulze H., Bachmann T. T., Schmid R. D., Hauer B., 2010. Analysis of phosphorothionate pesticides using a chloroperoxidase pretreatment and acetylcholinesterase biosensor detection. *Journal of Agricultural and Food Chemistry*, 58 (15), 8748–8756. <https://doi.org/10.1021/jf1013204>.
- Sams C., Mason H. J., Rawbone R., 2000. Evidence for the activation of organophosphate pesticides by cytochromes P450 3A4 and 2D6 in human liver microsomes. *Toxicology Letters*, 116 (3), 217–221. [https://doi.org/10.1016/s0378-4274\(00\)00221-6](https://doi.org/10.1016/s0378-4274(00)00221-6).
- Schoenborn A., Schmid P., Bräm S., Reifferscheid G., Ohlig M., Buchinger S., 2017. Unprecedented sensitivity of the planar yeast estrogen screen by using a spray-on technology. *Journal of Chromatography A*, 1530, 185–191. <https://doi.org/10.1016/j.chroma.2017.11.009>.
- Schulze H., Schmid R. D., Bachmann T. T., 2004. Activation of phosphorothionate pesticides based on a cytochrome P450 BM-3 (CYP102 A1) mutant for expanded neurotoxin detection in food using acetylcholinesterase biosensors. *Analytical Chemistry*, 76 (6), 1720–1725. <https://doi.org/10.1021/ac035218t>.
- Sharma A., Kumar V., Shahzad B., Tanveer M., Sidhu G. P. S., Handa N., Kohli S. K., Yadav P., Bali A. S., Parihar R. D., Dar O. I., Singh K., Jasrotia S., Bakshi P., Ramakrishnan M., Kumar S., Bhardwaj R., Thukral A. K., 2019. Worldwide pesticide usage and its impacts on ecosystem. *SN Applied Sciences*, 1 (11), 1446. <https://doi.org/10.1007/s42452-019-1485-1>.
- Shemer H. and Linden K. G., 2006. Degradation and by-product formation of diazinon in water during UV and UV/H₂O₂ treatment. *Journal of Hazardous Materials*, B136 (3), 553–559. <https://doi.org/10.1016/j.jhazmat.2005.12.028>.
- Sidhu G. K., Singh S., Kumar V., Dhanjal D. S., Datta S., Singh J., 2019. Toxicity, monitoring and biodegradation of organophosphate pesticides: A review. *Critical Reviews in Environmental Science and Technology*, 49 (13), 1135–1187. <https://doi.org/10.1080/10643389.2019.1565554>.
- Singer H., Jaus S., Hanke I., Lück A., Hollender J., Alder A. C., 2010. Determination of biocides and pesticides by on-line solid phase extraction coupled with mass spectrometry and their behaviour in wastewater and surface water. *Environmental Pollution*, 158 (10), 3054–3064. <https://doi.org/10.1016/j.envpol.2010.06.013>.
- Singh B. K. and Walker A., 2006. Microbial degradation of organophosphorus compounds. *FEMS Microbiology Reviews*, 30 (3), 428–471. <https://doi.org/10.1111/j.1574-6976.2006.00018.x>.
- Sobstyl E., Szopa A., Ekiert H., Gnat S., Typek R., Choma I. M., 2020. Effect directed analysis and TLC screening of Schisandra chinensis fruits. *Journal of Chromatography A*, 1618, 460942. <https://doi.org/10.1016/j.chroma.2020.460942>.
- Songa E. A. and Okonkwo J. O., 2016. Recent approaches to improving selectivity and sensitivity of enzyme-based biosensors for organophosphorus pesticides: A review. *Talanta*, 155, 289–304. <https://doi.org/10.1016/j.talanta.2016.04.046>.
- Stütz L., Schulz W., Winzenbacher R., 2020. Identification of acetylcholinesterase inhibitors in water by combining two-dimensional thin-layer chromatography and high-resolution mass spectrometry. *Journal of Chromatography A*, 1624, 461239. <https://doi.org/10.1016/j.chroma.2020.461239>.

- Stütz L., Weiss S. C., Schulz W., Schwack W., Winzenbacher R., 2017. Selective two-dimensional effect-directed analysis with thin-layer chromatography. *Journal of Chromatography A*, 1524, 273–282. <https://doi.org/10.1016/j.chroma.2017.10.009>.
- Sultatos L. G., 1994. Mammalian toxicology of organophosphorus pesticides. *Journal of Toxicology and Environmental Health*, 43 (3), 271–289. <https://doi.org/10.1080/15287399409531921>.
- Tang J., Cao Y., Rose R. L., Brimfield A. A., Dai D., Goldstein J. A., Hodgson E., 2001. Metabolism of chlorpyrifos by human cytochrome P450 isoforms and human, mouse, and rat liver microsomes. *Drug Metabolism and Disposition*, 29, 1201–1204.
- Van Dyk J. S. and Pletschke B., 2011. Review on the use of enzymes for the detection of organochlorine, organophosphate and carbamate pesticides in the environment. *Chemosphere*, 82 (3), 291–307. <https://doi.org/10.1016/j.chemosphere.2010.10.033>.
- Weins C. and Jork H., 1996. Toxicological evaluation of harmful substances by in situ enzymatic and biological detection in high-performance thin-layer chromatography. *Journal of Chromatography A*, 750 (1-2), 403–407. [https://doi.org/10.1016/0021-9673\(96\)00601-2](https://doi.org/10.1016/0021-9673(96)00601-2).
- Weiss S. C., Egetenmeyer N., Schulz W., 2017. Coupling of In Vitro Bioassays with Planar Chromatography in Effect-Directed Analysis. *Advances in Biochemical Engineering/Biotechnology*, 157, 187–224. https://doi.org/10.1007/10_2016_16.
- Wittmer I. K., Bader H.-P., Scheidegger R., Singer H., Lück A., Hanke I., Carlsson C., Stamm C., 2010. Significance of urban and agricultural land use for biocide and pesticide dynamics in surface waters. *Water Research*, 44 (9), 2850–2862. <https://doi.org/10.1016/j.watres.2010.01.030>.
- Worek F., Eyer P., Thiermann H., 2012. Determination of acetylcholinesterase activity by the Ellman assay: a versatile tool for in vitro research on medical countermeasures against organophosphate poisoning. *Drug Testing and Analysis*, 4 (3-4), 282–291. <https://doi.org/10.1002/dta.337>.

4.10. Appendix

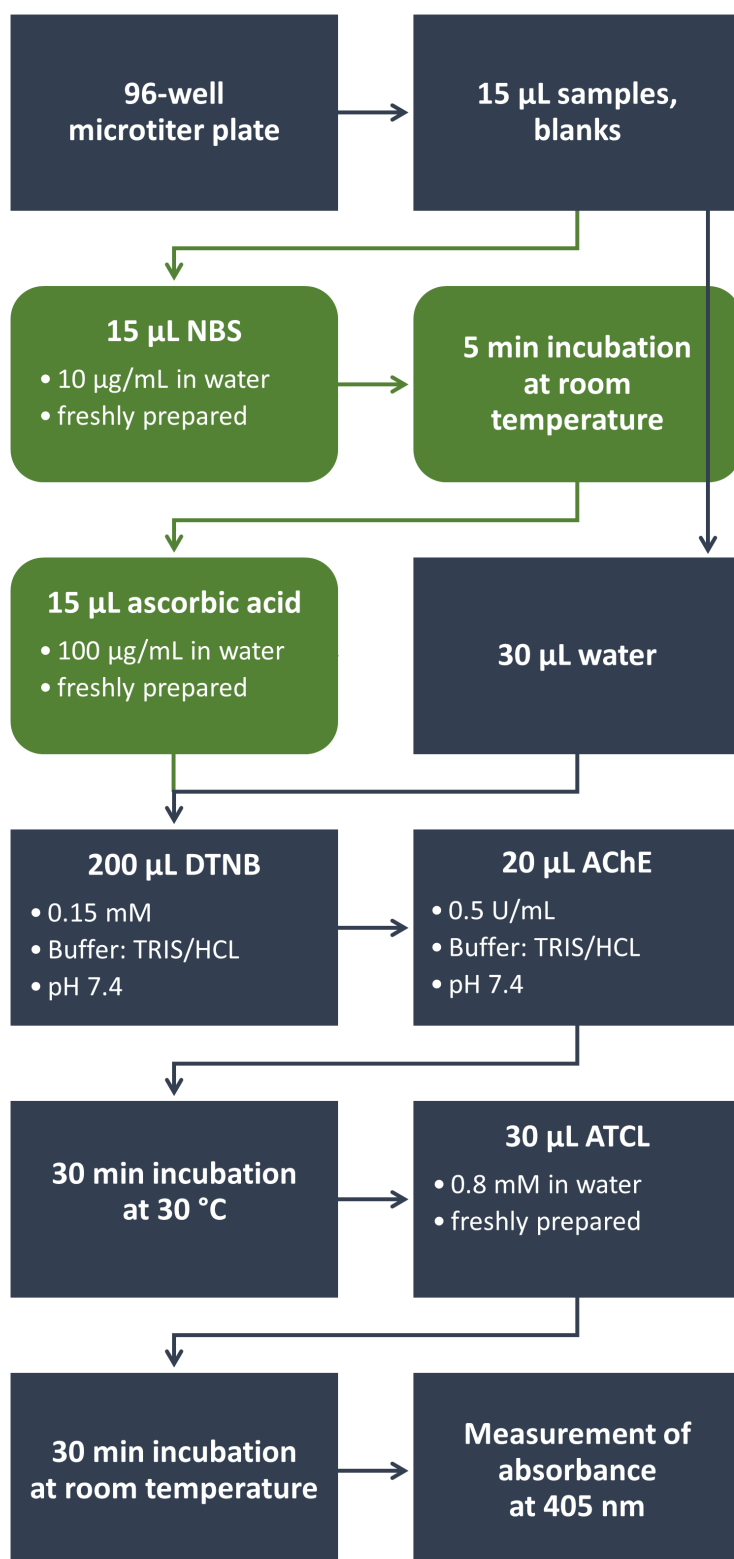


Figure 4-4 Flow chart of the acetylcholinesterase inhibition (AChE-I) assay in microtiter plates. The green steps show the additional oxidation with n-bromosuccinimide (NBS). Ascorbic acid stops the oxidation. Acetylthiocholine (ATCL) is cleaved by AChE into thiocholine and acetic acid. Thiocholine reacts with 5,5'-dithiobis (2-nitrobenzoic acid) (DTNB) to the yellow colored 2-nitro-5-thiobenzoate.

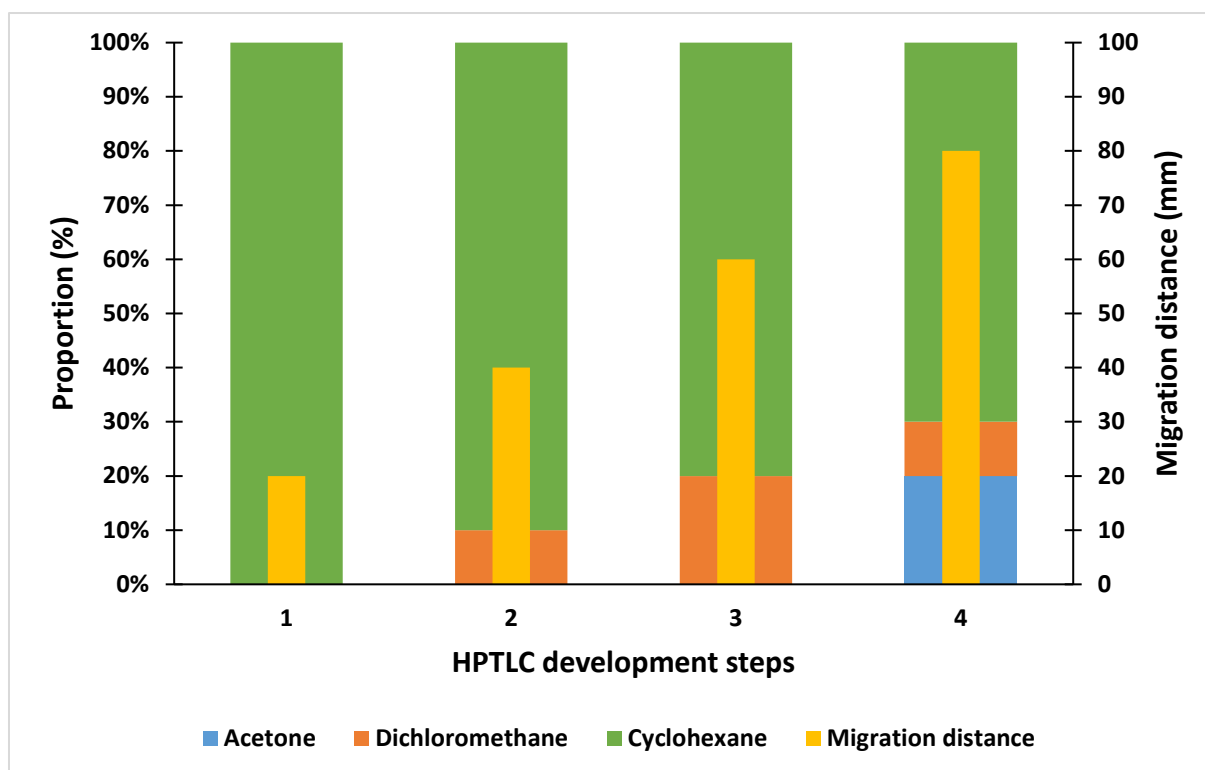


Figure 4-5 The automated four-step HPTLC development process for separation of organothiophosphates (OTPs) and their oxons on LiChrospher HPTLC plates. Every step contains another amount of the used solvents. First step: 100% cyclohexane, second step: 90% cyclohexane and 10% dichloromethane, third step: 80% cyclohexane and 20% dichloromethane, and fourth step: 70% cyclohexane, 10% dichloromethane, and 20% acetone. The green bars represent cyclohexane, the orange bars dichloromethane, and the blue bar acetone. The small yellow bars show the increasing migration distances. Final migration distance was 80 mm.

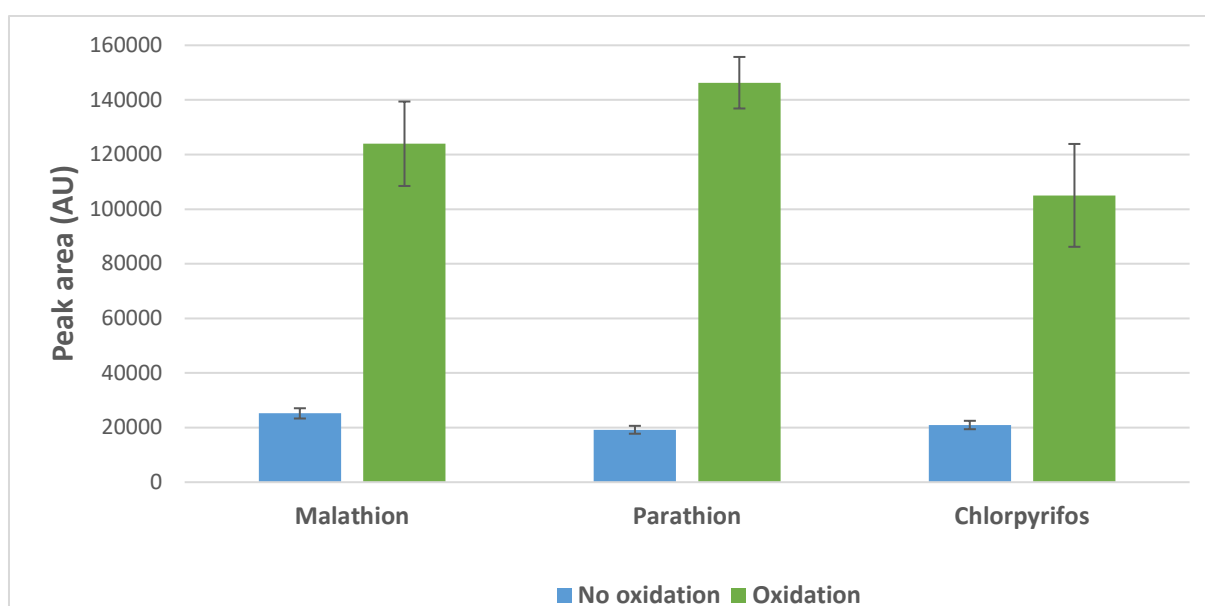


Figure 4-6 Peak areas (AU) of positive controls containing malathion, parathion, and chlorpyrifos. After chromatographic separation by HPTLC, an AChE inhibition assay with (green bars) and without (blue bars) prior oxidation by *n*-bromosuccinimide (NBS) was performed. AChE was sprayed onto the HPTLC plates. 10 μ L of the positive control was applied in duplicates on two LiChrosphere HPTLC plates per method, resulting in 1000 ng/spot. The error bars represent the standard deviations.

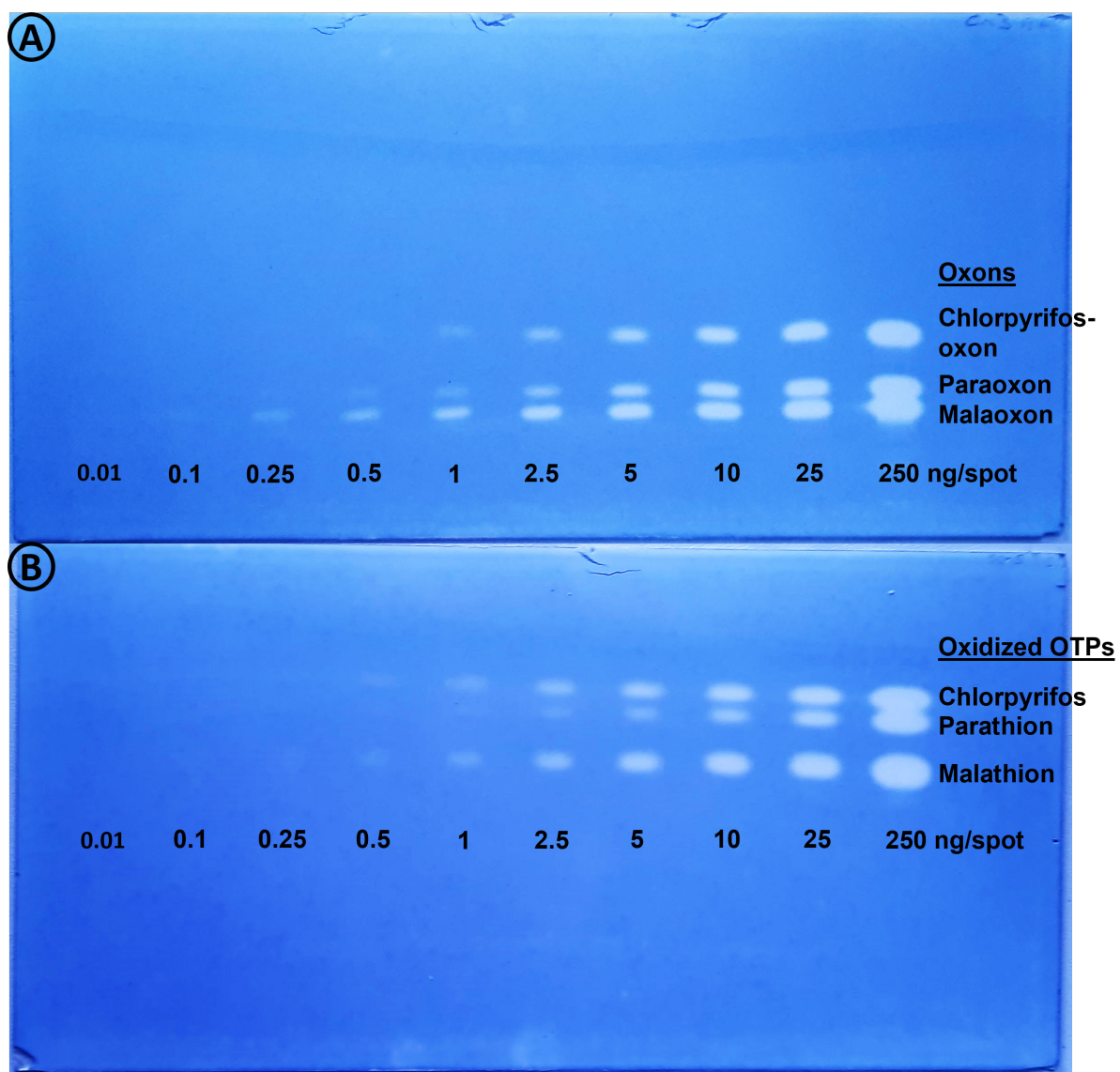


Figure 4-7 Results of dose-response investigations for malathion, malaoxon, parathion, paraoxon, chlorpyrifos, and chlorpyrifos-oxon. An oxon mix (A) and an organothiophosphate (OTP) mix (B) were applied with amounts between 250 and 0.01 ng/spot on LiChrosphere HPTLC plates. The application volume was 10 μ L. After chromatographic separation by HPTLC, an AChE inhibition assay with prior oxidation by n-bromosuccinimide (NBS) was performed. AChE was sprayed onto the plates.

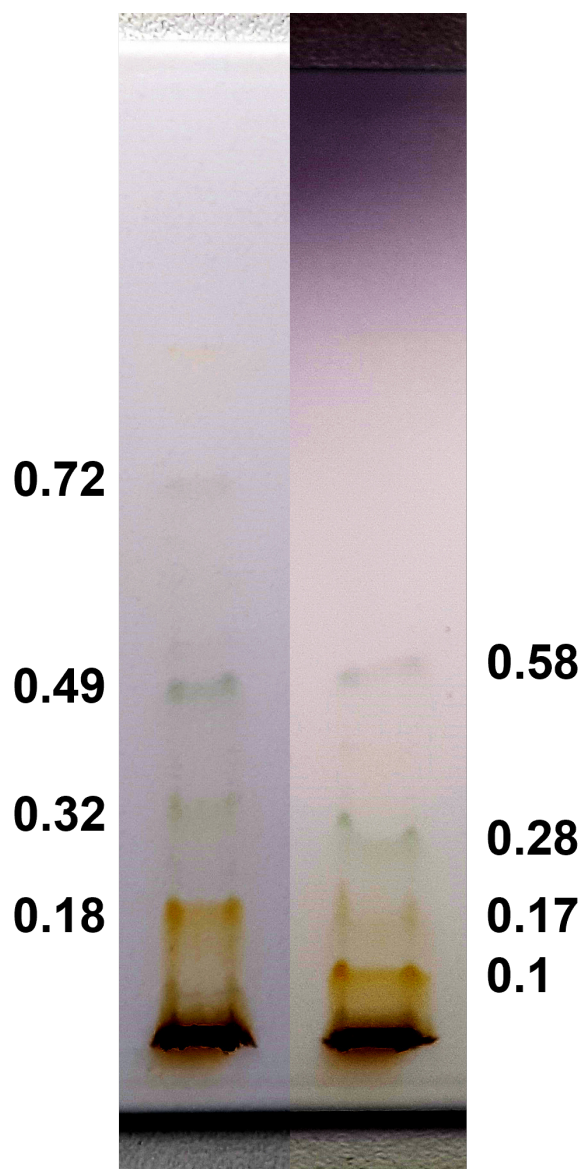


Figure 4-8 Separation of an enriched combined sewer overflow sample with HPTLC on LiChrosphere plates. The application volume was 100 μL . Two automatic development procedures were used: A four-step development with increasing migration distance and elution power (right side), and a single-step development only using the last step of the four-step development (left side). Every step contains another amount of the used solvents. First step: 100% cyclohexane, second step: 90% cyclohexane and 10% dichloromethane, third step: 80% cyclohexane and 20% dichloromethane, and fourth step: 70% cyclohexane, 10% dichloromethane, and 20% acetone. Final migration distance was 80 mm. R_F values of separated bands are shown next to the images.

Table 4-3 Concentrations ($\mu\text{g/L}$) of parathion, chlorpyrifos, and malathion used for dose-response investigations. The same concentrations as for the oxidized organothiophosphates were used for the specific oxons. An AChE assay for the detection of inhibition effects was performed in 96-well plates either without or with prior oxidation by n-bromosuccinimide (NBS). Acetylthiocholine (ATCL) was used as substrate and DTNB as reactant for thiocholine.

Parathion ($\mu\text{g/L}$)		Chlorpyrifos ($\mu\text{g/L}$)		Malathion ($\mu\text{g/L}$)	
Non-oxidized	Oxidized	Non-oxidized	Oxidized	Non-oxidized	Oxidized
50	0.5	50	0.05	50	0.2
250	2.5	250	0.5	250	2
500	5	500	1	500	4
2,500	25	2,500	5	2,500	20
5,000	50	5,000	10	5,000	40
25,000	250	25,000	50	25,000	200
50,000	500	50,000	100	50,000	400
500,000	5,000	500,000	500	500,000	4,000

Table 4-4 Concentrations (ng/spot) of parathion, chlorpyrifos, malathion, paraoxon, chlorpyrifos-oxon, and malaoxon used for dose-response investigations. An organothiophosphate (OTP) mix and an oxon mix were applied with different concentrations on LiChrosphere HPTLC plates. The application volume was 10 μL for the oxons and OTPs with following oxidation and 100 μL for the OTPs without following oxidation. After chromatographic separation by HPTLC, an AChE inhibition assay either with or without prior oxidation by n-bromosuccinimide (NBS) was performed. The HPTLC plates were either immersed in AChE solution or AChE was sprayed onto the plates.

Organothiophosphates (ng/spot)		Oxons (ng/spot)
Non-oxidized	Oxidized	
10	0.01	0.01
100	0.10	0.10
250	0.25	0.25
500	0.50	0.50
1,000	1.0	1.0
2,500	2.5	2.5
5,000	5.0	5.0
10,000	10	10
25,000	25	25
50,000	250	250

Table 4-5 Results of dose-response investigations for malathion, malaoxon, parathion, paraoxon, chlorpyrifos, and chlorpyrifos-oxon. An AChE assay for the detection of inhibition effects was performed in 96-well plates either without (left side) or with (right side) prior oxidation by n-bromosuccinimide (NBS). Acetylthiocholine (ATCL) was used as substrate and DTNB as reactant for thiocholine. The best-fit inhibition concentrations (IC) in $\mu\text{g/L}$ for 90, 80, 50 and 20% AChE activity and the 95% confidence intervals (95% ci) of the dose-response curves (4-PL fit) are shown. The used concentrations of malathion, parathion, and chlorpyrifos were not sufficient for full dose-response curves without oxidation. No IC values could be calculated.

Method	No oxidation				Oxidation			
	IC ₉₀	IC ₈₀	IC ₅₀	IC ₂₀	IC ₉₀	IC ₈₀	IC ₅₀	IC ₂₀
Inhibition concentration ($\mu\text{g/L}$)								
Substance								
Malathion								
Best fit	n/a	n/a	n/a	n/a	11	17	35	72
95% ci	n/a	n/a	n/a	n/a	7.0–17	12–23	30–41	52–100
Malaoxon								
Best fit	1.7	3.5	12	42	3.0	5.4	15	39
95% ci	0.98–2.9	2.3–5.4	9.6–16	34–53	1.5–6.1	3.2–9.2	11–19	30–51
Parathion								
Best fit	n/a	n/a	n/a	n/a	13	20	41	84
95% ci	n/a	n/a	n/a	n/a	11–16	17–23	38–44	74–96
Paraoxon								
Best fit	10	16	34	71	8.4	14	35	86
95% ci	8.2–13	14–19	31–36	62–80	5.4–13	10–19	30–40	68–109
Chlorpyrifos								
Best fit	n/a	n/a	n/a	n/a	2.2	4.1	12	34
95% ci	n/a	n/a	n/a	n/a	1.1–4.4	2.5–6.8	8.6–16	21–55
Chlorpyrifos-oxon								
Best fit	2.5	3.8	7.7	16	1.8	3.1	7.9	20
95% ci	1.9–3.3	3.1–4.6	7.0–8.5	13–19	0.97–3.5	2.0–4.9	6.3–9.8	13–29

Table 4-6 Results of dose-response investigations for malathion, malaoxon, parathion, paraoxon, chlorpyrifos, and chlorpyrifos-oxon. An organothiophosphate (OTP) mix and an oxon mix were applied with different concentrations on LiChrosphere HPTLC plates. The application volume was 10 μ L for the oxons and OTPs with following oxidation and 100 μ L for the OTPs without following oxidation. After chromatographic separation by HPTLC, an AChE inhibition (AChE-I) assay either with or without prior oxidation by n-bromosuccinimide (NBS) was performed. The HPTLC plates were either immersed in AChE solution (left side) or AChE was sprayed onto the plates (right side). The peak heights were used for evaluation. Only peaks that have a signal-to-noise ratio ≥ 3 were considered in the evaluation. The heights next to the respective peak define the noise. The best-fit inhibition concentrations (IC) in ng/spot for 10, 20, 50, and 80% AChE-I and the 95% confidence intervals (95% ci) of the dose-response curves (4-PL fit) are shown.

Method	Immersion				Spraying			
	IC ₁₀	IC ₂₀	IC ₅₀	IC ₈₀	IC ₁₀	IC ₂₀	IC ₅₀	IC ₈₀
Substance								
Malathion								
Best fit	313	536	1343	3363	212	493	2096	8910
95% ci	221–443	418–686	1,088–1,657	2,334–4,846	138–325	365–666	1,474–2,980	4,715–16,837
Oxidized malathion								
Best fit	0.45	0.76	1.9	4.7	0.26	0.48	1.4	4.0
95% ci	0.36–0.56	0.66–0.89	1.7–2.1	3.8–5.8	0.17–0.40	0.35–0.66	1.1–1.8	2.5–6.4
Malaoxon								
Best fit	0.14	0.24	0.60	1.5	0.16	0.28	0.75	2.0
95% ci	0.08–0.26	0.16–0.37	0.44–0.83	0.85–2.7	0.10–0.24	0.21–0.37	0.60–0.94	1.4–3.1
Oxidized parathion								
Best fit	1.4	2.3	5.6	13	0.75	1.4	4.2	13
95% ci	1.2–1.7	2.0–2.7	5.0–6.2	11–16	0.49–1.2	1.1–1.9	3.2–5.5	7.8–20
Paraoxon								
Best fit	0.60	0.99	2.3	5.4	0.79	1.2	2.7	5.9
95% ci	0.34–1.1	0.66–1.5	1.7–3.2	3.1–9.2	0.53–1.2	0.94–1.7	2.2–3.3	4.2–8.4
Oxidized chlorpyrifos								
Best fit	0.55	0.95	2.4	6.2	0.35	0.60	1.6	4.0
95% ci	0.43–0.69	0.80–1.1	2.1–2.8	4.9–7.9	0.22–0.53	0.44–0.82	1.2–2.0	2.5–6.2
Chlorpyrifos-oxon								
Best fit	0.32	0.57	1.5	4.0	0.72	1.1	2.5	5.4
95% ci	0.17–0.59	0.36–0.88	1.0–2.2	2.1–7.4	0.49–1.1	0.86–1.5	2.0–3.1	3.8–7.7

Table 4-7 The mean retardation factor (R_F), standard deviation (SD), calculated relative R_F , and resolution (R) of malaoxon, paraoxon, chlorpyrifos-oxon, malathion, parathion, and chlorpyrifos on the LiChrospher HPTLC plate ($n = 4$). After chromatographic separation, using a one-step HPTLC development process, and oxidation by n-bromosuccinimide (NBS), the plates were measured with an AChE inhibition assay using indoxyl acetate as substrate. AChE was sprayed onto the plates. The plates were scanned at 670 nm.

Substance	Mean R_F	SD	rel. R_F	R
Malaoxon	0.18	0.02		
Paraoxon	0.26	0.03	1.0	1.5
Chlorpyrifos-oxon	0.47	0.04	2.2	1.8
Malathion	0.59	0.05	1.1	1.3
Parathion	0.69	0.06	1.1	1.2
Chlorpyrifos	0.82	0.05	1.4	1.2

Table 4-8 Limits of detection (LOD) for malathion, oxidized malathion, malaoxon, chlorpyrifos, oxidized chlorpyrifos, chlorpyrifos-oxon, parathion, oxidized parathion, and paraoxon. An organothiophosphate (OTP) mix and an oxon mix were applied with different concentrations on LiChrosphere HPTLC plates. The application volume was 10 μL for the oxons and OTPs with following oxidation and 100 μL for the OTPs without following oxidation. After chromatographic separation by HPTLC, an AChE inhibition assay either with or without prior oxidation by n-bromosuccinimide (NBS) was performed. The HPTLC plates were either immersed in AChE solution (left side) or AChE was sprayed onto the plates (right side). The peak heights were used for evaluation. The first detected peak at one of the applied concentrations with a signal-to-noise ratio ≥ 3 defines the LOD for the specific substance and respective method. The heights next to the respective peak define the noise.

Method	Limit of detection (LOD) (ng/spot)	
	Immersion	Spraying
Substance		
Malathion	250	250
Oxidized malathion	0.25	0.1
Malaoxon	0.1	0.1
Chlorpyrifos	500	250
Oxidized chlorpyrifos	0.25	0.25
Chlorpyrifos-oxon	0.25	0.25
Parathion	500	100
Oxidized parathion	1.0	0.25
Paraoxon	0.5	0.5

5 Effect-directed Analysis of Endocrine and Neurotoxic Effects in Stormwater-Dependent Discharges

This chapter is submitted: Baetz N., Cunha J. R., Itzel F., Schmidt T. C., Tuerk J., 2024. Effect-directed analysis of endocrine and neurotoxic effects in stormwater depending discharges. Water Research.

5.1. Abstract

The investigation of pollutant inputs via stormwater runoff and subsequent effects in receiving waters is becoming increasingly urgent in view of climate change with accompanying extreme weather situations such as heavy rainfall events. In this study, two sampling areas, one urban and one rural but dominated by a highway, were investigated using effect-directed analysis (EDA) to identify endocrine and neurotoxic effects and potentially responsible substances in stormwater structures and receiving waters. For this purpose, a transgenic yeast cell assay for the simultaneous detection of estrogenic, androgenic, and gestagenic effects (YMEES) was performed directly on high-performance thin-layer chromatography (HPTLC) plates. Concomitantly, estrogens were analyzed by gas chromatography coupled to tandem mass spectrometry (GC-MS/MS) and other micropollutants typical for wastewater and stormwater by liquid chromatography coupled to tandem mass spectrometry (LC-MS/MS). Discharges from a combined sewer overflow (CSO) contribute a large portion of the endocrine load to the studied water body, even surpassing the load from a nearby wastewater treatment plant (WWTP). An effect pattern similar to the CSO sample was shown downstream in the receiving water with lower intensities, consisting of an estrogenic, androgenic, and gestagenic effect. In contrast, after the WWTP, only one estrogenic effect with a lower intensity was detected. Concentrations of estrone (E1), 17 α -estradiol (17 α -E2), 17 β -estradiol (17 β -E2), 17 α -ethinylestradiol (EE2), and estriol (E3) in the CSO sample were 2.0, 0.41, 1.1, 0.56, and 2.7 ng/L, respectively. HPTLC-YMEES and GC-MS/MS complement each other very well and help to elucidate endocrine stresses. An acetylcholinesterase (AChE) inhibitory effect could not be assigned to a causative compound by suspect and non-target analysis using liquid chromatography coupled to high-resolution mass spectrometry (LC-HRMS). However, the workflow showed how information from HPTLC separation, effect-based methods (EBMs), and other meta-information on the sampling area and substance properties can contribute to an identification of effect-responsible substances. Overall, the study demonstrated that EBMs in combination with HPTLC and instrumental analysis can be implemented to investigate pollution by stormwater run-off particularly regarding heavy rain events due to climate change.

5.2. Introduction

The IPCC has highlighted that human-induced climate change is likely responsible for the increasing frequency and intensity of precipitation observed since 1950 (IPCC, 2021). Heavy rainfall events with an associated increased runoff can lead to a higher pollution of receiving waters

(NISSEN AND ULBRICH, 2017; IPCC, 2022). A wide variety of substances are carried along in the stormwater depending on the catchment area, land use, and existing development (WICKE et al., 2021). Runoff from agricultural areas can contain pesticides (LEFRANCO et al., 2017) and stormwater that runs off impervious surfaces such as streets, roofs, and facades transports substances deposited on or contained in the respective surface and washed out by rain (MÜLLER et al., 2020; SPAHR et al., 2020; PAIJENS et al., 2021). Additional substances such as pharmaceuticals or hormones contained in the mixed water (storm- and wastewater) are discharged from CSOs without regular treatment in WWTPs in case of heavy rainfall events that exceed the hydraulic capacity of the combined sewer system (PHILLIPS et al., 2012; KAY et al., 2017; WOLF et al., 2022). According to various studies, CSO pollutant discharge is comparable to or, depending on substances, even higher than the pollution caused by WWTPs (WEYRAUCH et al., 2010; PHILLIPS et al., 2012; KAY et al., 2017; SHULIAKEVICH et al., 2022). Stormwater from the separate sewer system enters the aquatic environment either completely untreated or after simple sedimentation. Loads from WWTPs, stormwater structures and diffusive inputs can have various toxic effects. Substances such as carbamates and organophosphates (OPs) that are mainly used as pesticides have a neurotoxic potential and inhibit AChE (DE SOUZA et al., 2020). Hormonal effects can be triggered by endocrine disruptive compounds (EDCs) that bind to an appropriate hormone receptor. These substances range from actual natural hormones, synthetic representatives such as EE2 to various substances such as plasticizers, pharmaceuticals, pesticides, industrial chemicals, and heavy metals (KASONGA et al., 2021; PIRONTI et al., 2021).

Up to now, rain induced surface water pollution has been characterized primarily by means of the detection of known individual substances (KAY et al., 2017; MASONER et al., 2019; WICKE et al., 2021). Decisive questions, however, are which effects can emanate from these inputs, to what extent are investigated target substances responsible for the effects, and which causative agents remain unknown. EBMs could provide an overall effect picture that also reveals effects of unknown substances and covers mixing effects (BRACK et al., 2019; ITZEL et al., 2019; ITZEL et al., 2020; NEALE et al., 2020; ALYGIZAKIS et al., 2023). Nevertheless, it is of great interest to also identify effect-responsible known and unknown substances to name sources and develop mitigation measures. Therefore, EDA has proven to be suitable in toxicity assessment by linking chromatographic techniques, EBMs and instrumental analysis to gain a focused and more efficient identification of toxic substances (DOPP et al., 2019; HASHMI et al., 2020; ZWART et al., 2020; TIAN et al., 2023). Several studies have already used a combination of HPTLC and EBMs with different endpoints, such as inhibition of AChE (AChE-I) or different endocrine effects, to investigate a wide variety of samples and matrices (STÜTZ et al., 2020; BAETZ et al., 2021; MORLOCK, 2021; RIEGRAF et al., 2022). The possibility of applying EBMs directly on HPTLC plates allows the characterization of stormwater-dependent discharges to receiving waters regarding certain effects and the comparison of different sites based on the effect pattern.

Moreover, the probability of identifying causative compounds with subsequent instrumental analysis is increased since effect information is available and the complexity of a sample is reduced by HPTLC separation.

In this study, stormwater-dependent pollution of streams was investigated using an EDA approach. Endocrine and neurotoxic effects in samples from stormwater retention and overflow structures and receiving waters were identified using a combination of HPTLC and two EBMs. An identification of possible effect-responsible substances was done by accompanying and subsequent instrumental analysis. The continued diffuse and point source input of known micropollutants in the sampling area is demonstrated. The impact of a CSO on the endocrine load of the receiving stream is presented, including a comparison to a WWTP. LC-HRMS and a specific evaluation workflow were used to gain information in a critical pre-treated sample about substances or substance groups responsible for a stormwater induced AChE-I effect.

5.3. Material and methods

5.3.1. Chemicals and cells

Methanol (MeOH), acetone, dichloromethane, hexane, ethyl acetate, acetonitrile (ACN) and water (all LC-MS grade) were purchased from Th. Geyer GmbH & Co. KG (Renningen, Germany). Cyclohexane (LC-MS grade) was purchased from LGC Standards GmbH (Wesel, Germany). Hydrochloric and formic acid were purchased from Merck (Darmstadt, Germany). General information of all used standards is given in Table 5-2. Parathion, chlorpyrifos, malathion, E1, 17 α -E2, 17 β -E2, EE2, E3, 5 α -dihydrotestosterone (DHT), progesterone (P4), estron-d4 (E1-d4), 17 β -estradiol-d3 (17 β -E2-d3), 17 α -ethinyloestradiol-d4 (EE2-d4), tris(2-ethylhexyl)phosphat (TEHP), 2-ethylhexyldiphenylphosphat (EHDPP), AChE, n-bromosuccinimide (NBS), bovine serum albumin (BSA), N,O-bis(trimethylsilyl)trifluoroacetamide (BSTFA), trimethylchlorosilane (TMCS) and pyridine were purchased from Sigma Aldrich GmbH (Steinheim, Germany). All standards had a purity of at least 95% and they were solubilized in methanol at stock concentrations of 1 mg/mL. Standards for the LC-MS/MS analysis were purchased from different suppliers, had a purity of at least 95% and were solubilized in ACN/water (v/v) at stock concentrations of 1 mg/mL. Tris(hydroxymethyl)aminomethane (TRIS) was purchased from Carl Roth GmbH + Co. KG (Karlsruhe, Germany). Indoxyl acetate was purchased from Thermo Fisher Scientific (Geel, Belgium). The yeast cell strains *Arxula adenivorans* G1212/YRC102-hPR-CFP, G1212/YRC102-hAR-GFP and G1212/YRC102-hER-DsRed2 were provided by new_diagnostics GmbH (Berlin, Germany). Following chemicals were used for yeast minimal medium supplemented with glucose (cultivation medium) or maltose (test medium): Maltose and glucose were purchased from Carl Roth GmbH & Co. KG (Karlsruhe, Germany). NaNO₃, KH₂PO₄ and MgSO₄ x H₂O

were purchased from Sigma Aldrich (Steinheim, Germany). Further salts, trace elements and vitamins were purchased from new_diagnostics GmbH (Berlin, Germany).

5.3.2. HPTLC-EBM

5.3.2.1. Sample preparation

Samples, the field blank and quality controls (QC) spiked with mixtures of estrogens (E1, α -E2, β -E2, EE2, and E3), DHT, and P4 were enriched by solid phase extraction (SPE) within 24 h after sampling. After conditioning of the cartridges (150 mg, Oasis HLB 6 cc, Waters GmbH, Eschborn, Germany) with methanol (2 x 5 mL) and equilibrating with water (2 x 5 mL) they were loaded with 1000 \pm 5 mL water sample (the exact volume was determined by weighting) through a polytetrafluoroethylene tube. The cartridges were dried under vacuum and stored at -18 °C until further usage. Elution was done with methanol (5 x 5 mL) that was evaporated afterwards at 60 °C under a gentle nitrogen gas stream. The dried extracts were redissolved in 1 mL methanol to achieve a nominal 1000-fold enrichment. The extracts were analyzed with the HPTLC-YMEES (5.3.2.3) and HPTLC-Ox-AChE-I (5.3.2.4).

5.3.2.2. HPTLC

SIL G-25 plates (Macherey-Nagel, Düren, Germany) were used as stationary phase for the HPTLC-YMEES and LiChrospher HPTLC Silica gel 60 F254s plates (Merck, Darmstadt, Germany) for the HPTLC-Ox-AChE-I. The further preparation, HPTLC settings for the Automatic TLC Sampler 4 (ATS 4, CAMAG AG, Muttenz, Switzerland) and Automated Multiple Development 2 (AMD 2, CAMAG, Muttenz, Switzerland), and the development process are described in previous studies (BAETZ et al., 2021; BAETZ et al., 2022).

5.3.2.3. Yeast multi-endocrine effect screen (YMEES)

The HPTLC-YMEES procedure is described in detail in a previous study (BAETZ et al., 2021). The *Arxula adenivorans* yeast strains G1212/YRC102-hPR-CFP, G1212/YRC102-hAR-GFP and G1212/YRC102-hER-DsRed2, described by CHAMAS et al. (2017), were cultivated separately in cultivation medium and were mixed equally in test medium with a final total OD_{620 nm} of approximate 3 to detect gestagenic, androgenic and estrogenic effects by scanning different wavelengths according to the three fluorescent proteins. The YMEES was performed after application of samples, blanks, positive controls (PCs: mix of 1000 pg E1 (40 μ g/L), 100 pg EE2 (4 μ g/L), and 100 pg 17 β -E2 (4 μ g/L), mix of 100 pg (4 μ g/L) (first sampling) or 250 pg (10 μ g/L) (second sampling) 17 α -E2 and 1000 pg (40 μ g/L) (first sampling) or 250 pg (10 μ g/L) (second sampling) E3, and mix of 250 pg P4 (10 μ g/L) and 100 pg DHT (4 μ g/L)), and SPE QCs and following chromatographic development. Samples from the first sampling were distributed on three plates and measured two times (six plates). Samples from the second sampling were distributed on three plates and measured one time (three plates).

Samples were applied in duplicates and PCs and QCs were applied once per plate. Results were summarized by calculating mean values and standard deviations (first sampling: samples: $n = 4$, PCs: $n = 6$; second sampling: samples: $n = 2$, PCs: $n = 3$). Effect recoveries of the hormones in the QCs in relation to the PCs are shown in Table 5-3. The application volume was 25 μL . The yeast suspension was sprayed in a steady and repeatable way onto the HPTLC plates by airbrush (0.35 mm nozzle, AFC-101A, Conrad Electronics SE, Hirschau, Germany). The TLC Scanner 3 (CAMAG, Muttenz, Switzerland) and the CAMAG-embedded software, Wincats (Vers. 1.4.9) was used for evaluation.

5.3.2.4. AChE-inhibition assay

After application of 100 μL of samples, blanks, and PCs (mix of 2000 ng (20 $\mu\text{g}/\text{mL}$) malathion, parathion, and chlorpyrifos) and following chromatographic development, the AChE-I assay with prior oxidation step with NBS (HPTLC-Ox-AChE-I) was performed as described in a previous study (BAETZ et al., 2022). Each sample was tested in duplicates on two HPTLC plates ($n = 4$). The PCs were tested once per plate ($n = 2$). The TLC Scanner 3 was used to scan each track on the plates at 670 nm using the fluorescence mode without optical filter. Wincats (Vers. 1.4.9) was used to evaluate the inhibition zones.

For identification of suspect effect-responsible substances after suspect and non-target screening, 1000 and 100 ng of TEHP and EHDPP were applied on HPTLC plates and the AChE-I assay was performed. The R_f s of both substances were compared with the R_f of an unknown effect.

5.3.2.5. Extraction from HPTLC plates

Relevant spots were extracted from the HPTLC plate by scraping off the silica material with a scalpel into a glass vial via a glass funnel. The funnel was flushed with 25 mL MeOH to rinse remaining silica particles into the vial. Afterward, the funnel was cleaned with MeOH. The extracts were stored in a freezer at $-18\text{ }^\circ\text{C}$. Before analysis, the extracts were shaken at 500 rpm for 20 h. After deposition of the silica material the supernatant was taken off. The extracts were filtered through a 0.20 μm syringe filter. 5 mL of the extracts were evaporated under a gentle nitrogen stream at $60\text{ }^\circ\text{C}$ and redissolved in 1 mL water for following LC-HRMS analysis.

5.3.3. Instrumental analysis

5.3.3.1. Estrogens (GC-MS/MS)

The analysis of estrogens was performed with modifications according to the method of TERNES et al. (1999). After sampling, the samples were stored at $\leq 8\text{ }^\circ\text{C}$ for not more than four days. For SPE, the samples, field blank, SPE blank and a water QC were spiked with 1 ng of the internal standards E1-d4, 17 β -E2-d3, and EE2-d4 (Table 5-2). The QC sample was also spiked with 1 ng of E1, 17 α -E2, 17 β -E2, EE2, and E3. BAKERBOND Speedisks (C18, 50 mm, Avantor, Center Valley, USA) were conditioned with

10 mL MeOH and equilibrated with 10 mL water before one liter of each sample, blank and QC was extracted. Then the disks were dried for 20 min. The disks were combined with activated trimethylsilanol cartridges and 25 mL ethyl acetate:hexane (50:50, v:v) were used for elution. The extracts were evaporated at 60 °C under a gentle nitrogen stream. The residues were derivatized with 50 µL pyridine and 50 µL BSTFA at 70 °C for 30 min. The calibration was prepared in ethyl acetate:hexane (50:50, v:v) and derivatized in the same way. The parameters for the analysis with the TQ8040 GC-MS/MS system (Shimadzu, Kyōto, Japan) are shown in Table 5-4 and Table 5-5. A Zebron ZB-5MSi Capillary GC Column (30 m x 0.25 mm x 0.25 µm with 10 m additional Guard Column, Phenomenex, Torrance, USA) was used. The software GCSolutions Insight (Shimadzu, Kyōto, Japan) was used for peak identification and quantification. Quality data of the measurements is given in Table 5-6 and Table 5-7.

5.3.3.2. Pharmaceuticals, Pesticides, and Industrial Chemicals (LC-MS/MS)

The analytes and internal standards of this method are shown in Table 5-2. After sampling the samples were stored at ≤ 8 °C for not more than ten days. Samples and blanks were spiked with internal standards. The samples were filtered with a 0.45 µm syringe filter. The calibration was prepared in water/acetonitrile (99:1, v/v + 0.1 % formic acid). The parameters for the analysis with LC-MS/MS (1200 Series, Agilent Technologies, Santa Clara, USA; QTRAP 6500+, SCIEX, Framingham, USA) are shown in Table 5-8 and Table 5-9. As stationary phase a Raptor ARC-18 (50 x 2.1 mm, 2.7 µm, Restek GmbH, Bad Homburg, Germany) was used. Water (+ 0.1% formic acid) was used as mobile phase A and acetonitrile (+ 0.1 % formic acid) as mobile phase B.

5.3.3.3. Suspect and non-target screening

An extract with potential neurotoxic compounds was taken from an inhibition zone of an enriched sample from the retention basin at the second sampling site after HPTLC-Ox-AChE-I (5.3.2.4 and 5.3.2.5). Moreover, a blank sample was extracted from the solvent blank track on the same HPTLC plate. Samples were measured in triplicate. A quality control with reference compounds was also measured (Table 5-2 and Figure 5-8). A solution with internal standards (10 ng/mL) was spiked into the samples during injection (Table 5-2 and Figure 5-9). Representative phosphorous insecticides, flame retardants/plasticizers, and carbamates (Table 5-13) were measured at different concentrations (0.1 – 100 ng/mL) to gain insight into limits of detection (Table 5-14) and to acquire retention time values and MS² data for supporting identification (SCHYMANSKI et al., 2014) during suspect screening. The identification categories are described in Table Table 5-15. A requisite for all categories is the *m/z* matching which should be within 5 ppm deviation from the expected mass.

The differentiation of the identification levels is then performed according a predefined ruleset, following the criteria stipulated by SCHYMANSKI et al. (2014). The identification workflow was adapted from the framework of patRoan (HELMUS et al., 2021).

For the reversed-phase chromatography an XSelect HSS T3 3.5 μm column (2.1 x 75 mm) and a standard gradient (i.e., water-acetonitrile both with 0.1% formic acid) were used. The data was acquired with a high-resolution 6560 Ion Mobility LC/Q-TOF (Agilent, Santa Clara, USA). The positive ionization mode was used for measurements. MS^1 data from m/z 50 to 1,200 was acquired at 5 spectra/s. MS^2 was acquired at the same rate via data dependent acquisition (DDA). The AutoMS mode from the Mass Hunter software (Agilent) was used. Per cycle (maximum of 0.9 s), three MS^1 precursors with intensity above 5000 counts were selected with an isolation window of 1.3 Da (i.e., 0.65 Da were added and subtracted to the target m/z of a given precursor ion for isolation in the quadrupole) and fragmented at 10 and 35 eV. A maximum of 25,000 counts per spectrum were acquired to shorten the acquisition time window, maximizing both MS^1 and MS^2 data.

Suspect and non-target screening (SNTS) was performed for all samples following the workflow shown in Figure 5-1. Data evaluation for each step of the SNTS workflow was performed in R (R Core Team, 2020) using self-assembled scripts and in particular the package patRoan (HELMUS et al., 2021). Prioritization of features was performed by blank subtraction (i.e., intensity sample > 3x blank intensity), replicate deviation (i.e., standard deviation of intensity between replicates < 0.4), minimum intensity of 600 counts, and minimum signal-to-noise ratio of 3. To filter effect relevant features and assign them to possible substances, a suspect fragment list (Table 5-12) and a suspect list of carbamates and phosphorous insecticides, flame retardants and plasticizers (Table 5-13) were used.

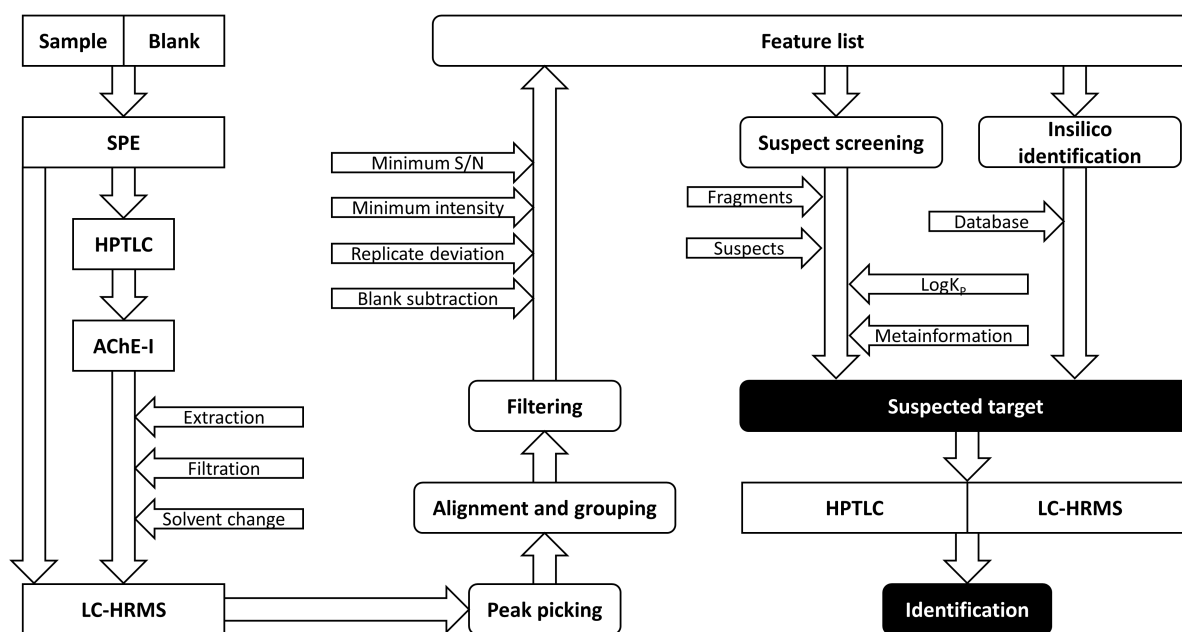


Figure 5-1 Workflow of the HPTLC-Ox-AChE-I analysis with subsequent suspect and non-target screening with LC-HRMS of suspect effect-responsible substances.

5.3.4. Sampling and sampling site

The sampling was performed in March and August 2020 at two sampling sites. Site 1 is at the river Anger in Ratingen, Germany (Figure 5-4). Qualified grab samples were taken at site 1 from a CSO, downstream the CSO and upstream storm sewer outlets (A1), a stormwater retention structure (SWR) connected to the storm sewer, downstream the storm sewer outlets (A2), and downstream the WWTP Ratingen, Germany (A3). Site 2 is at the creek Deininghauser Bach in Deininghausen, Germany next to the highway A42 (Figure 5-5). Qualified grab samples were taken at site 2 from a stormwater retention basin (RB), which is connected to a highway nearby, and up- and downstream the receiving creek Deininghauser Bach (US and DS).

The combined sewer, to which the CSO is connected, drains an area of approx. 1.6 km². The area drained by the storm sewer, to which the SWR is connected, has a size of approx. 1 km². Residential as well as commercial and small industry units are located in both areas. The CSO is connected parallel to the combined sewer. The dry weather flow is completely piped to the WWTP Ratingen. When the capacity of the sewer is reached during a rain event, the overflow is discharged into a sedimentation tank via a separating structure. After passing the sedimentation tank the wastewater is discharged into a retention basin. Depending on the load, the wastewater is either pumped into the Anger or back to the combined sewer and the WWTP Ratingen. The SWR is located at the end of a storm sewer. The stormwater is treated mechanically in a sedimentation tank and is discharged in a stormwater retention tank and a connected retention basin. The stormwater is pumped into the Anger with a discharge adapted to the inflow and the capacity of the retention structures. Samples were taken at the outlets of the retention structures in front of the pumping stations. The RB at the second sampling site receives stormwater from the adjacent highway. The stormwater is then discharged into the Deininghauser Bach, which is a small creek with low flow rates.

A qualified grab sample is a special form of a composite sample that consists of several individual grab samples. At least five individual grab samples must be taken. The grab samples were taken with consistent volume at least two minutes apart and mixed until the desired total volume was achieved. A field blank was prepared with LC-MS grade water, which was used to wash the sampling vessel and opened at the sampling points. The samples were cooled during transport and stored < 8 °C until further sample preparation.

5.4. Results and discussion

5.4.1. Target analysis of micropollutants

The target analysis revealed storm- and wastewater dependent pollution by micropollutants from point and diffuse sources. The pollution of the Anger with wastewater from CSO and WWTPs is demonstrated since pharmaceuticals as wastewater indicators (BRÜCKNER et al., 2020) were detected in all samples, except in the SWR sample, with comparable concentrations above 1,000 ng/L (Figure 5-2, Table 5-10, and Table 5-11).

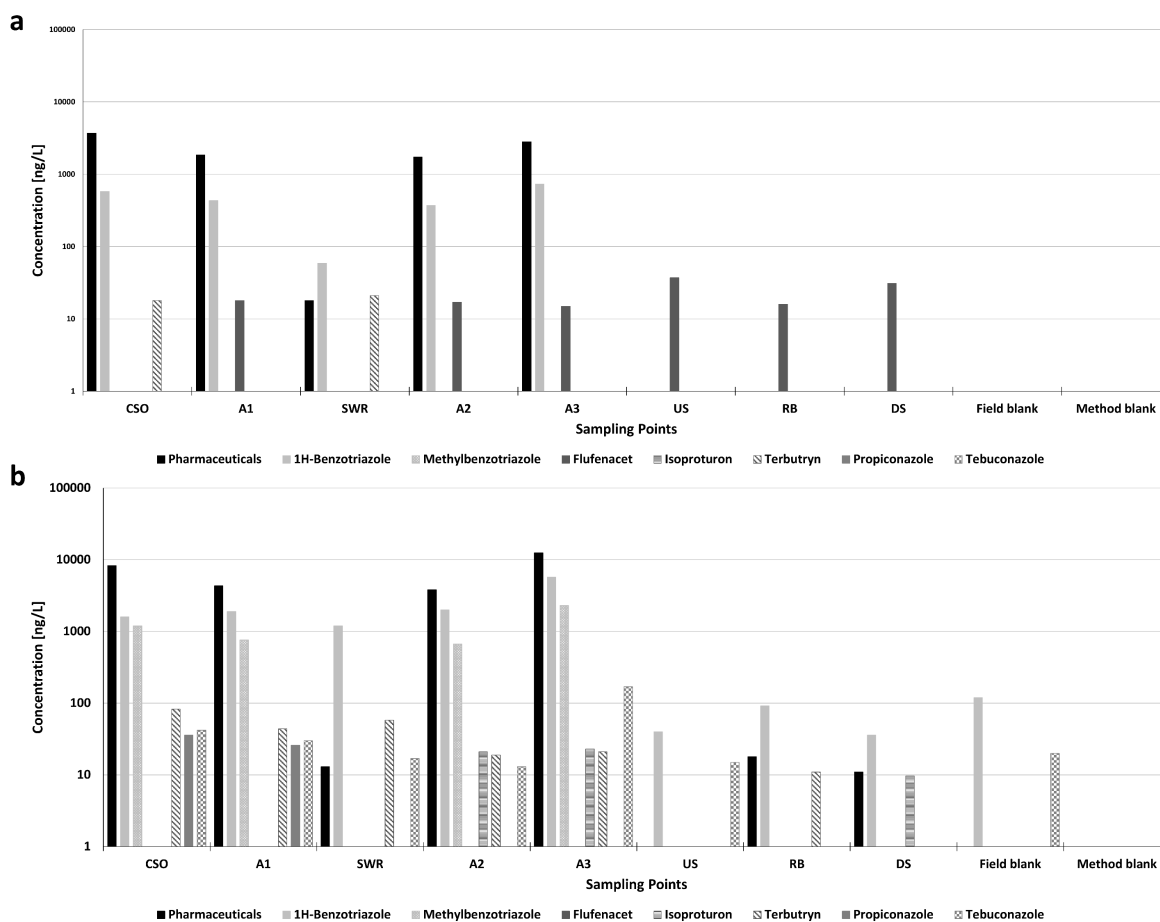


Figure 5-2 Concentrations of substances detected with LC-MS/MS in samples from stormwater structures and the receiving river Anger in Ratingen, Germany (first sampling site) and from a stormwater retention basin, draining a highway, and the receiving small stream Deininghauser Bach near Deininghausen, Germany (second sampling site). The sampling was performed in March 2020 during rainy weather conditions (a) and in August 2020 during dry weather conditions (b). At the first sampling site the samples were taken from a combined sewer overflow (CSO), downstream the CSO and upstream storm sewer outlets (A1), a stormwater retention structure connected to the storm sewer (SWR), downstream the storm sewer outlets (A2), and downstream the wastewater treatment plant Ratingen, Germany (A3). At the second sampling site the samples were taken from a stormwater retention basin (RB), which is connected to a highway nearby, and up- and downstream the receiving creek Deininghauser Bach (US and DS). The concentrations of the pharmaceuticals are shown as one summed concentration (black bars). The sampling points are shown on the x-axis and the concentrations (ng/L) are shown on the y-axis in logarithmic scaling.

KAY et al. (2017) suggest that discharges from CSOs may be as relevant to the input of pharmaceuticals as WWTPs. The herbicide terbutryn demonstrates surface water pollution from stormwater discharges, as the WWTP does not appear to have a significant effect on downstream concentrations. It was found in the CSO and, as also reported by BURKHARDT et al. (2011), in stormwater from the separate sewer system and the related SWR. Diffusive exposure during wet weather originated from agricultural sources becomes apparent by the detection of the pre-emergence herbicide flufenacet at all sampling points in both streams and the RB but not in the CSO and SWR. WILLKOMMEN et al. (2019) showed that flufenacet and other pesticides are released into streams via drainage from fields in a time-varying dependence on weather conditions, application, and substance properties. The detection of methylbenzotriazoles and 1*H*-benzotriazole in the CSO and after the WWTP indicates that loads in the Anger originated mostly from mixed water, but since 1*H*-benzotriazole was also present in the SWR, an occurrence in stormwater runoff as described by PARAJULEE et al. (2017) is additionally possible. They noticed that beside WWTP effluents and deicing activities on airports also vehicular emissions may play a major role in pollution of surface waters. Methylbenzotriazoles are more likely to occur in wastewater, as they were not detected in the SWR sample or during rainy weather.

5.4.2. EDA of Endocrine effects and Estrogens

The results of the target analysis of micropollutants provide preliminary evidence that discharges from stormwater retention and overflow structures in the sampling area contribute to receiving water pollution by EDCs during wet weather. The first sampling during rainy weather reveals endocrine effects in the samples from all sampling points in Ratingen, Germany with the used HPTLC-YMEES (Figure 5-3). Especially estrogenic effects in the range of α - and β -E₂ (E₂-range) were found. Shifts in R_F values on the HPTLC plates when comparing the CSO, A1, and SWR sample to the A2 and A3 sample occurred because the samples were analyzed on different plates. For the reference standards an average R_F value of all used plates is shown. The influence of the CSO on the endocrine load in the receiving river is demonstrated by the most intense estrogenic effects in the E₂-range, androgenic effects in the range of DHT, and gestagenic effects possibly triggered by P4. All these effects were found in both the CSO and the A1 sample taken downstream the CSO. The intensities in A1 are about half as high as in the outlet of the CSO, which indicates dilution effects during wet weather and related high flow rates. Additional estrogenic effects in the range of E₁ and E₃ as in the CSO sample would also be expected in the A1 sample with about half the intensity. The concentrations in the water sample were probably too low for an effect detection, because of a lower binding affinity of these estrogens to the estrogen receptor than E₂. The estrogens E₁, α - and β -E₂, and E₃ could be identified by target analysis with GC-MS/MS in the CSO and A1 sample (Table 5-1), which supports the assumption that these hormones may be at least partially responsible for the tested effects. EE₂ could also be measured by GC-MS/MS in the CSO sample at a low concentration that was undetectable by HPTLC-YMEES.

The concentration of EE2 is 0.56 ng/L so that the amount on the HPTLC plate with the enrichment used (1 L sample was enriched to 1 mL extract and 25 µL of the extract was applied on the HPTLC plate) is 14 pg. The amount is in the range of the ED₁₀ as shown in a previous publication (BAETZ et al., 2021). It is possible that no effect of EE2 could be detected in this case due to deviations of the biological test system. A higher application volume on the HPTLC plate would lower the detectable concentration of an extract. However, this shows how important the combination of effect testing and target analysis is and how well both methods complement each other. FINCKH et al. (2022) also used a combination of EBM and chemical target analysis to determine endocrine stress in several effluents from WWTPs. They were able to demonstrate a good correlation between the results of the two methods, which were compared using bioanalytical equivalent concentrations (BEQs). Estrogens that could be responsible for the endocrine effects tested in the CSO outlet possibly originated from wastewater as part of the mixed water. Only one estrogenic effect with a very low intensity in the E2-range is detected in the stormwater sampled in the outlet of the SWR during wet weather. Although the influence of the WWTP is evident from the estrogen concentrations (Table 5-1), only one estrogenic effect in the E2-range was detected in A3 with a smaller intensity than downstream of the CSO (A1) (Figure 5-3).

Table 5-1 Concentrations of E1, 17α-E2, 17β-E2, EE2, and E3 detected with GC-MS/MS in samples from stormwater structures and the receiving river Anger in Ratingen, Germany (first sampling site) and from a stormwater retention basin, draining a highway, and the receiving small stream Deininghauser Bach near Deininghausen, Germany (second sampling site). The sampling was performed in March 2020 during rainy weather conditions. At the first sampling site the samples were taken from a combined sewer overflow (CSO), downstream the CSO and upstream storm sewer outlets (A1), a stormwater retention structure (SWR) connected to the storm sewer, downstream the storm sewer outlets (A2), and downstream the wastewater treatment plant Ratingen, Germany (A3). At the second sampling site the samples were taken from a stormwater retention basin (RB), which is connected to a highway nearby, and up- and downstream the receiving stream Deininghauser Bach (US and DS). The LOD, LOQ and substance concentrations are shown in ng/L. The substance concentrations are shown with a confidence interval (95%).

Substance	Concentration (ng/L)				
	E1	17α-E2	17β-E2	EE2	E3
Sample					
CSO	2.0 ± 0.2	0.41 ± 0.05	1.1 ± 0.1	0.56 ± 0.24	2.7 ± 0.2
A1	0.47 ± 0.17	0.09 ± 0.05	0.16 ± 0.07	< 0.34*	0.57 ± 0.15
SWR	0.31 ± 0.17	0.13 ± 0.05	< 0.035*	0.41 ± 0.24	< 0.066*
A2	0.27 ± 0.17	0.067 ± 0.049	0.038 ± 0.072	< 0.34*	< 0.066*
A3	0.76 ± 0.16	0.19 ± 0.05	0.23 ± 0.07	0.49 ± 0.24	2.0 ± 0.2
US	0.32 ± 0.17	0.117 ± 0.049	< 0.035*	< 0.34*	< 0.066*
RB	0.32 ± 0.17	0.125 ± 0.049	< 0.035*	0.49 ± 0.24	< 0.066*
DS	0.33 ± 0.17	0.103 ± 0.049	< 0.035*	0.48 ± 0.24	< 0.066*
LOQ	0.006	0.009	0.005	0.006	0.003
LOD	0.002	0.003	0.002	0.002	0.001

* Sample specific LOD (S/N = 3)

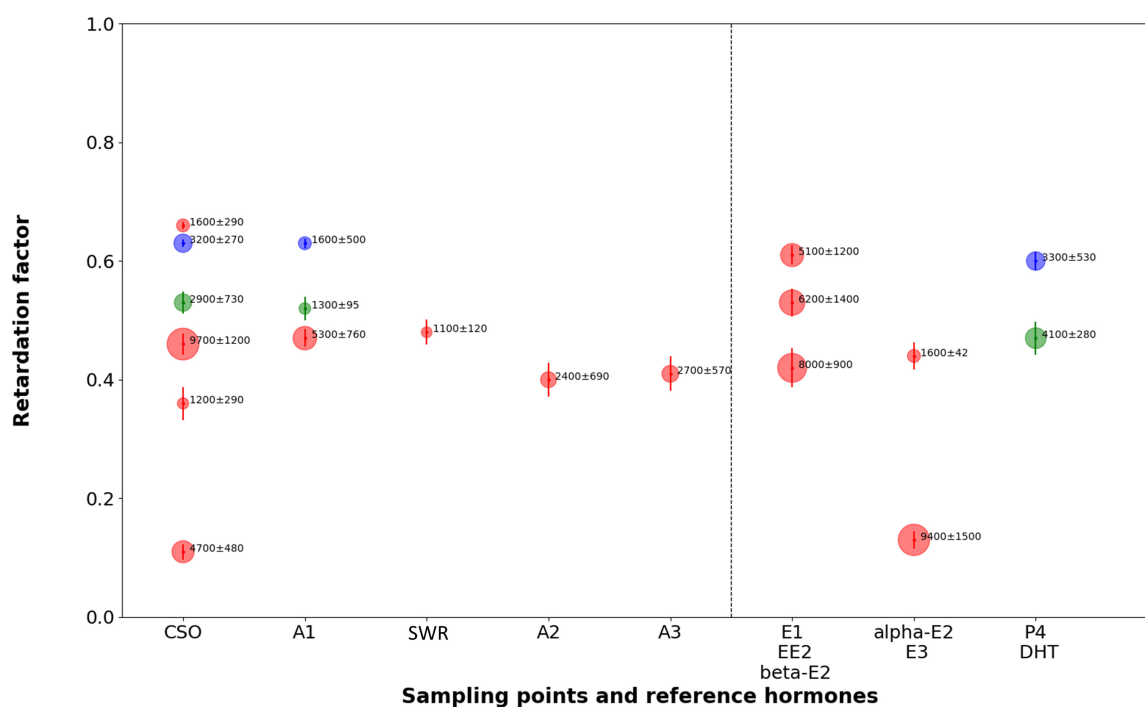


Figure 5-3 Estrogenic, androgenic, and gestagenic effects detected in samples from stormwater structures and the receiving river Anger in Ratingen, Germany (first sampling site). The sampling was performed in March 2020 during rainy weather conditions. The samples were taken from a combined sewer overflow (CSO), downstream the CSO and upstream storm sewer outlets (A1), a stormwater retention structure (SWR) connected to the storm sewer, downstream the storm sewer outlets (A2), and downstream the wastewater treatment plant Ratingen, Germany (A3). A mix of 1000 pg E1 (40 µg/L), 100 pg 17β-E2 (4 µg/L), and 100 pg EE2 (4 µg/L), a mix of 100 pg 17α-E2 (10 µg/L), and 1000 pg E3 (10 µg/L), and a mix of 100 pg DHT (4 µg/L), and 250 pg P4 (10 µg/L) were applied (right side). The red, green, and blue dots represent estrogenic, androgenic, and gestagenic effects, respectively. The mean peak area (AU) ± standard deviation of the effects (n = 4) and the reference hormones (n = 4; α-E2: n = 2) are presented next to the dots. The size of the dots also represents the peak area. The y-axis shows the retardation factor (R_F). The position of the dots highlights the mean R_F s and the error bars show the standard deviations of the effects (n = 4) and the reference hormones (n = 4). The samples were 1000-fold enriched by SPE. The application volume on the HPTLC plate was 25 µL. The samples were separated by HPTLC and measured with the yeast multi-endocrine effect screen (YMEES) for the detection of estrogenic, androgenic, and gestagenic effects.

In comparison to the three different endocrine effects tested in A1, the HPTLC-YMEES results suggest a higher input of EDCs by the CSO than by the WWTP. PHILLIPS et al. (2012) have shown that a CSO can contribute a significant proportion to the hormone load in a lake compared to treated effluent from a wastewater treatment plant. Since other studies showed a reduction of EDCs and endocrine activities during wastewater treatment processes, with or without advanced treatment, lower endocrine loads from a wastewater treatment plant than from a CSO, containing raw wastewater, is possible (KIRK et al., 2002; JANEX-HABIBI et al., 2009; GEHRMANN et al., 2018; ITZEL et al., 2020).

The effect pattern and detected estrogens in the samples of the CSO and downstream of its outlet (A1) stand out, which confirm the assumption that discharges by a CSO can lead to observable endocrine loads during wet weather. The effects caused in this way are in any case in addition to the endocrine effects normally already present in surface waters, e.g. caused by discharges from WWTPs.

Two estrogenic effects were detected in the CSO sample of the second sampling in the range of E1 and E2 (Figure 5-6). There was no discharge to the receiving water on this day. Two endocrine effects were detected in the RB and DS sample of the second sampling site (Figure 5-7). The origin is unknown, because in this rural area and from the highway no direct wastewater inputs are expected. The samples of the first sampling in this area show no effects at all and the estrogen concentrations were in the range of the tested blanks (Table 5-1 and Table 5-6). Due to the few low intensity effects and low estrogen concentrations, these results were not pursued further.

HPTLC-YMEES and accompanying GC-MS/MS allow to assign detected estrogenic effects to possibly responsible estrogens. In conjunction with HPTLC-YMEES, further target analysis with the additional inclusion of known androgens and gestagens may contribute to extensive characterization of samples and sites in future studies. Sample preparation via SPE for the HPTLC-YMEES and GC-MS/MS was performed without a prior filtration to also capture the endocrine active portion of the samples bound to suspended solids. ARGOLLO et al. (2021) have shown that estrogenic activities originate to a significant extent from the solid phase. For the validated GC-MS/MS method, a C18 Speeddisk was used for optimal detection of the target estrogens, which additionally allows a rapid sample application. Since the HPTLC-YMEES method is also concerned with the detection of effects triggered by unknown substances, an HLB cartridge was used that covers a broader polarity range.

5.4.3. Workflow for identification of AChE inhibitors by HRMS

The neurotoxicity assessment yielded one positive result by HPTLC-Ox-AChE-I in the RB sample of the first sampling during rainy weather at the second sampling site and has been shown in a previous study (BAETZ et al., 2022). The effect and a blank spot with the same R_F were extracted from the HPTLC plate on which the actual AChE-I assay and a previous oxidation step were performed. In this way, difficulties could be avoided that were described by STÜTZ et al. (2020) regarding the localization of relevant zones on a second developed HPTLC plate on which no bioassay was performed. In addition, material, solvents, sample extract, and time could be saved. However, the pre-oxidation and AChE-I assay on the HPTLC plate promotes potential complications for subsequent detection of effect relevant substances by HRMS. The predominantly inadequate recovery of the internal standards (Figure 5-9) suggests that certain transformation processes or a signal suppression have occurred in the extracts from the HPTLC plate. A continuing oxidation of substances after extraction, possibly triggered by the oxidant NBS still contained in the extracts, is one possible explanation. Another possibility is a signal suppression by bromide and chloride ions originating from the NBS and TRIS/HCl buffer of the AChE

solution. In the original SPE extract of the RB sample 4885 and in the extract from the HPTLC plate 2474 features were found after subtraction of the respective blanks. The number of features that were detected in both samples was 100. As shown by STÜTZ et al. (2020), the number of effect-irrelevant substances in a sample could be reduced by HPTLC separation, allowing for a focused subsequent analysis in active HPTLC extracts. The high number of new features in the HPTLC extract of the RB sample indicates that in addition to added substances, transformation processes may also have taken place either already on the HPTLC plate or after extraction. Therefore, it is possible that the substance responsible for the AChE-I effect was subjected to transformation and degradation processes. It was assumed that transformation fragments (TFs) of the original effect-responsible substance may be present in the HPTLC extract after these processes. A suspect TF list was used to examine the HRMS results (Table 5-12). The TF list contains the basic structures of OPs and carbamates such as the phosphate group and carbamate group. Meta-information about the sampling area was included to specify the fragment list. KIEFER et al. (2021) classified their samples by urban or agricultural origin of target substances and were thus able to prioritize in HRMS analysis. In our case, the sampling site is in a rural area which suggest insecticides, such as OPs or carbamates known to be AChE inhibitors, responsible for the found effect. Since OP insecticides are rarely allowed in Germany and the retention basin is connected to the storm drainage of the highway nearby, it may rather be OPs used as plasticizers or flame retardants. They are possibly released to the RB via runoff from the highway as they are used in different materials for vehicles. Therefore, various molecule groups specific for different OP flame retardants and plasticizers, which are normally bound to the phosphate group of the parental compound, were included in the suspect TF list. The evaluation revealed several possible suspect TF candidates that could be contained in the samples (Table 5-16). However, only one TF (TEHP fragment 3) matched a feature found in the HPTLC extract and could be confirmed up to category 2 (SCHYMANSKI et al., 2014) using the feature MS² data and in silico fragmentation with SIRIUS (DÜHRKOP et al., 2019) through the patRoon platform. The matching TF has the molecular formula C₁₆H₃₅PO₄ and could therefore be part of tris(2-ethylhexyl)phosphate (TEHP), since the TF could consist of the phosphate group and two of the three molecular groups actually attached to TEHP (formula: C₂₄H₅₁PO₄). Both features indicative of the TEHP fragment 3 have their highest intensity in the HPTLC extract (Table 5-16). Unfortunately, they also occur with lower intensities in the HPTLC blank. A contamination of the blank during extraction procedure or following evaporation step is possible. The next step was to match the data with a suspect target list, which contains several OP pesticides, flame retardants, and plasticizers as well as some carbamates (Table 5-13). The calibration of reference standards showed that the OP flame retardant/plasticizer tris(2-chlorisopropyl)phosphat (TCIPP) could be detected with a LOD of 0.74 µg/L (Table 5-14), which gives confidence to the detection of this substance group.

The mass of a feature could be assigned to TEHP but no further information could be generated (Table 5-17). However, the analysis of the HRMS data and the sampling area information have provided an indication of a possible effect-responsible substance. HPTLC results were used to provide further clarification. The detected AChE-I effect showed a mean $R_F \pm$ standard deviation of 0.91 ± 0.05 , which was higher than the R_F of chlorpyrifos ($R_F = 0.85 \pm 0.07$), used as a positive control. Chlorpyrifos has a logP of 5.11 (NORMAN, 2023). The logP of the effect-responsible substance should accordingly be at least above 5. TEHP has a logP of 9.49. However, SHI et al. (2021) showed that alkyl organophosphate flame retardants such as TEHP did not inhibit AChE, whereas aryl ones did. A suspect TF (EHDPP fragment 4) of 2-Ethylhexyl diphenyl phosphate (EHDPP) with the formula $C_8H_{19}PO_4$ could be assigned to two features but either with a high deviation or low intensities in the samples (Table 5-16). Nevertheless, EHDPP (formula: $C_{20}H_{27}PO_4$) has one alkyl- and two aryl-groups attached to PO_4 which makes it an interesting substance for AChE-I investigation. In addition, the logP of EHDPP is 6.3 and thus could fit to the R_F of the detected effect in the RB sample. HPTLC-Ox-AChE-I was carried out for TEHP and EHDPP, under the same conditions as for the measurement of the RB sample, to obtain possible AChE-I effects and to compare the R_F s with the detected unknown effect. The two OPs show a clear inhibition of AChE at a concentration of 1000 ng/spot (no inhibition at 100 ng/spot), but not the same R_F as the detected AChE-I effect in the RB sample. The R_F s were 0.52 ± 0.02 and 0.48 ± 0.02 for TEHP and EHDPP, respectively. Thus, the logP is not decisive for the R_F and TEHP seems to have an inhibitory potential against AChE after all.

Probably due to contamination during the extraction process from the HPTLC plate and matrix components in the extract originated from the oxidation and AChE-I assay with associated changes in the extract and signal suppression in HRMS analysis, it was not possible to determine an effect-responsible substance with the used workflow. The method should be used with an optimized maybe automated sample extraction (STÜTZ et al., 2020; BELL et al., 2021; MEHL et al., 2021; WILSON AND POOLE, 2023), to reduce contamination and substance losses in the extracts. When samples are extracted directly from the same HPTLC plate on which an oxidation step was performed, ongoing oxidation in the extracts should be avoided. A suppression of ions in the subsequent HRMS by high matrix loads from previous HPTLC steps and assays should be prevented for example using methodologies shown by SCHREINER AND MORLOCK (2021) that, in combination with an optimized HRMS workflow (MENGER et al., 2022), can increase the probability of identifying effect-causing substances.

5.5. Conclusion and Outlook

If a direct extraction from a HPTLC plate, on which an EBM has been performed, is desired to save resources, attention should be paid on possible steps of the EBM that could change the extract afterward or involves a high load of matrix components that interfere with subsequent analysis. Optimized HPTLC extraction and extract clean-up before HRMS is required to facilitate subsequent

identification by suspect and non-target methods. Even if the two suspect substances are not responsible for the detected inhibition of AChE in the stormwater retention basin sample investigated here, the HRMS workflow, the search for suspect fragments, results from HPTLC-Ox-AChE-I, and meta information on the sampling site may help to elucidate effect-causing loads in surface waters and treatment structures in future studies.

HPTLC-YMEES and accompanying target analysis of estrogens by GC-MS/MS allows comprehensive investigation of endocrine effects and responsible estrogens for characterization of the pollution of receiving waters by stormwater structures and WWTPs. Both methods complement each other by generating information that would not have been visible with one single method. This allows a better understanding of the situation on site and reveals the influence of the CSO on the endocrine load of the receiving water. The results show that a CSO can contribute to a large portion of the EDC pollution and corresponding effects in receiving waters during wet weather conditions, even when compared to a nearby WWTP. This endocrine stress during wet weather is added to the already existing one during dry weather and will increase, considering climate change with increased heavy rain events. Overall, as with the investigation and assessment of WWTPs, more studies should address the impact of stormwater dependent discharges from structures or diffuse sources.

5.6. Acknowledgements

Financial support for the graduate program Future Water by Ministry of Culture and Science of the Federal State of North Rhine-Westphalia (MKW NRW) is gratefully acknowledged.

Special thanks go to the city of Ratingen, Germany, in particular Mr. Römermann and Mr. Tempel, for providing information on the sewer network and the investigated stormwater structures.

5.7. References

- Alygizakis N., Ng K., Maragou N., Alirai S., Behnisch P., Besselink H., Oswald P., Čirka L., Thomaidis N. S., Slobodnik J., 2023. Battery of In Vitro Bioassays: A Case Study for the Cost-Effective and Effect-Based Evaluation of Wastewater Effluent Quality. *Water*, 15 (4), 619. <https://doi.org/10.3390/w15040619>.
- Argolo A. D. S., Gomes G., Bila D. M., 2021. Insights into total estrogenic activity in a sewage-impacted urban stream assessed via ER transcriptional activation assay: Distribution between particulate and dissolved phases. *Ecotoxicology and Environmental Safety*, 208, 111574. <https://doi.org/10.1016/j.ecoenv.2020.111574>.
- Baetz N., Rothe L., Wirzberger V., Sures B., Schmidt T. C., Tuerk J., 2021. High-performance thin-layer chromatography in combination with a yeast-based multi-effect bioassay to determine endocrine effects in environmental samples. *Analytical and Bioanalytical Chemistry*, 413 (5), 1321–1335. <https://doi.org/10.1007/s00216-020-03095-5>.
- Baetz N., Schmidt T. C., Tuerk J., 2022. High-performance thin-layer chromatography in combination with an acetylcholinesterase-inhibition bioassay with pre-oxidation of organothiophosphates to determine neurotoxic effects in storm, waste, and surface water. *Analytical and Bioanalytical Chemistry*, 414 (14), 4167–4178. <https://doi.org/10.1007/s00216-022-04068-6>.

- Bell A. M., Keltsch N., Schweyen P., Reifferscheid G., Ternes T., Buchinger S., 2021. UV aged epoxy coatings - Ecotoxicological effects and released compounds. *Water Research X*, 12, 100105. <https://doi.org/10.1016/j.wroa.2021.100105>.
- Brack W., Aissa S. A., Backhaus T., Dulio V., Escher B. I., Faust M., Hilscherova K., Hollender J., Hollert H., Müller C., Munthe J., Posthuma L., Seiler T.-B., Slobodnik J., Teodorovic I., Tindall A. J., De Aragão Umbuzeiro G., Zhang X., Altenburger R., 2019. Effect-based methods are key. The European Collaborative Project SOLUTIONS recommends integrating effect-based methods for diagnosis and monitoring of water quality. *Environmental Sciences Europe*, 31 (1), 5423. <https://doi.org/10.1186/s12302-019-0192-2>.
- Brückner I., Classen S., Hammers-Wirtz M., Klaer K., Reichert J., Pinnekamp J., 2020. Tool for selecting indicator substances to evaluate the impact of wastewater treatment plants on receiving water bodies. *Science of the Total Environment*, 745, 140746. <https://doi.org/10.1016/j.scitotenv.2020.140746>.
- Burkhardt M., Zuleeg S., Vonbank R., Schmid P., Hean S., Lamani X., Bester K., Boller M., 2011. Leaching of additives from construction materials to urban storm water runoff. *Water Science and Technology*, 63 (9), 1974–1982. <https://doi.org/10.2166/wst.2011.128>.
- Chamas A., Pham H. T. M., Jähne M., Hettwer K., Uhlig S., Simon K., Einspanier A., Baronian K., Kunze G., 2017. Simultaneous detection of three sex steroid hormone classes using a novel yeast-based biosensor. *Biotechnology and Bioengineering*, 114 (7), 1539–1549. <https://doi.org/10.1002/bit.26249>.
- De Souza R. M., Seibert D., Quesada H. B., De Jesus Bassetti F., Fagundes-Klen M. R., Bergamasco R., 2020. Occurrence, impacts and general aspects of pesticides in surface water: A review. *Process Safety and Environmental Protection*, 135, 22–37. <https://doi.org/10.1016/j.psep.2019.12.035>.
- Deutsches Institut für Normung (DIN), 2008. Chemical analysis - Decision limit, detection limit and determination limit under repeatability conditions - Terms, methods, evaluation. Beuth, Berlin. DIN 32645.
- Dopp E., Pannekens H., Itzel F., Tuerk J., 2019. Effect-based methods in combination with state-of-the-art chemical analysis for assessment of water quality as integrated approach. *International Journal of Hygiene and Environmental Health*, 222 (4), 607–614. <https://doi.org/10.1016/j.ijheh.2019.03.001>.
- Dührkop K., Fleischauer M., Ludwig M., Aksenov A. A., Melnik A. V., Meusel M., Dorrestein P. C., Rousu J., Böcker S., 2019. SIRIUS 4: a rapid tool for turning tandem mass spectra into metabolite structure information. *Nature Methods*, 16 (4), 299–302. <https://doi.org/10.1038/s41592-019-0344-8>.
- Finckh S., Buchinger S., Escher B. I., Hollert H., König M., Krauss M., Leekitratapanisan W., Schiwy S., Schlichting R., Shuliakovich A., Brack W., 2022. Endocrine disrupting chemicals entering European rivers: Occurrence and adverse mixture effects in treated wastewater. *Environment International*, 170, 107608. <https://doi.org/10.1016/j.envint.2022.107608>.
- Gehrmann L., Bielak H., Behr M., Itzel F., Lyko S., Simon A., Kunze G., Dopp E., Wagner M., Tuerk J., 2018. (Anti-)estrogenic and (anti-)androgenic effects in wastewater during advanced treatment: comparison of three in vitro bioassays. *Environmental Science and Pollution Research International*, 25 (5), 4094–4104. <https://doi.org/10.1007/s11356-016-7165-4>.
- Hashmi M. A. K., Krauss M., Escher B. I., Teodorovic I., Brack W., 2020. Effect-Directed Analysis of Progestogens and Glucocorticoids at Trace Concentrations in River Water. *Environmental Toxicology and Chemistry*, 39 (1), 189–199. <https://doi.org/10.1002/etc.4609>.

- Helmus R., Ter Laak T. L., Van Wezel A. P., De Voogt P., Schymanski E. L., 2021. patRoom: open source software platform for environmental mass spectrometry based non-target screening. *Journal of Cheminformatics*, 13 (1), 1. <https://doi.org/10.1186/s13321-020-00477-w>.
- IPCC, 2021. *Climate Change 2021. The Physical Science Basis. Contribution of Working Group I to the Sixth Assessment Report of the Intergovernmental Panel on Climate Change*. IPCC, Cambridge, UK and New York, NY, USA. <https://doi.org/10.1017/9781009157896>.
- IPCC, 2022. *Climate Change 2022. Impacts, Adaptation and Vulnerability. Contribution of Working Group II to the Sixth Assessment Report of the Intergovernmental Panel on Climate Change*. IPCC, Cambridge, UK and New York, NY, USA. <https://doi.org/10.1017/9781009325844>.
- Itzel F., Baetz N., Hohrenk L. L., Gehrman L., Antakyali D., Schmidt T. C., Tuerk J., 2020. Evaluation of a biological post-treatment after full-scale ozonation at a municipal wastewater treatment plant. *Water Research*, 170, 115316. <https://doi.org/10.1016/j.watres.2019.115316>.
- Itzel F., Gehrman L., Teutenberg T., Schmidt T. C., Tuerk J., 2019. Recent developments and concepts of effect-based methods for the detection of endocrine activity and the importance of antagonistic effects. *TrAC Trends in Analytical Chemistry*, 118 (21), 699–708. <https://doi.org/10.1016/j.trac.2019.06.030>.
- Janex-Habibi M.-L., Huyard A., Esperanza M., Bruchet A., 2009. Reduction of endocrine disruptor emissions in the environment: the benefit of wastewater treatment. *Water Research*, 43 (6), 1565–1576. <https://doi.org/10.1016/j.watres.2008.12.051>.
- Kasonga T. K., Coetzee M. A. A., Kamika I., Ngole-Jeme V. M., Benteke Momba M. N., 2021. Endocrine-disruptive chemicals as contaminants of emerging concern in wastewater and surface water: A review. *Journal of Environmental Management*, 277, 111485. <https://doi.org/10.1016/j.jenvman.2020.111485>.
- Kay P., Hughes S. R., Ault J. R., Ashcroft A. E., Brown L. E., 2017. Widespread, routine occurrence of pharmaceuticals in sewage effluent, combined sewer overflows and receiving waters. *Environmental Pollution*, 220 (Pt B), 1447–1455. <https://doi.org/10.1016/j.envpol.2016.10.087>.
- Kiefer K., Du L., Singer H., Hollender J., 2021. Identification of LC-HRMS nontarget signals in groundwater after source related prioritization. *Water Research*, 196, 116994. <https://doi.org/10.1016/j.watres.2021.116994>.
- Kirk L. A., Tyler C. R., Lye C. M., Sumpter J. P., 2002. Changes in estrogenic and androgenic activities at different stages of treatment in wastewater treatment works. *Environmental Toxicology and Chemistry*, 21, 972–979.
- Lefrancq M., Jadas-Hécart A., La Jeunesse I., Landry D., Payraudeau S., 2017. High frequency monitoring of pesticides in runoff water to improve understanding of their transport and environmental impacts. *Science of the Total Environment*, 587-588, 75–86. <https://doi.org/10.1016/j.scitotenv.2017.02.022>.
- Masoner J. R., Kolpin D. W., Cozzarelli I. M., Barber L. B., Burden D. S., Foreman W. T., Forshay K. J., Furlong E. T., Groves J. F., Hladik M. L., Hopton M. E., Jaeschke J. B., Keefe S. H., Krabbenhoft D. P., Lowrance R., Romanok K. M., Rus D. L., Selbig W. R., Williams B. H., Bradley P. M., 2019. Urban Stormwater: An Overlooked Pathway of Extensive Mixed Contaminants to Surface and Groundwaters in the United States. *Environmental Science & Technology*, 53 (17), 10070–10081. <https://doi.org/10.1021/acs.est.9b02867>.
- Mehl A., Schwack W., Morlock G. E., 2021. On-surface autosampling for liquid chromatography-mass spectrometry. *Journal of Chromatography A*, 1651, 462334. <https://doi.org/10.1016/j.chroma.2021.462334>.

- Menger F., Celma A., Schymanski E. L., Lai F. Y., Bijlsma L., Wiberg K., Hernández F., Sancho J. V., Ahrens L., 2022. Enhancing spectral quality in complex environmental matrices: Supporting suspect and non-target screening in zebra mussels with ion mobility. *Environment International*, 170, 107585. <https://doi.org/10.1016/j.envint.2022.107585>.
- Morlock G. E., 2021. High-performance thin-layer chromatography combined with effect-directed assays and high-resolution mass spectrometry as an emerging hyphenated technology: A tutorial review. *Analytica Chimica Acta*, 1180, 338644. <https://doi.org/10.1016/j.aca.2021.338644>.
- Müller A., Österlund H., Marsalek J., Viklander M., 2020. The pollution conveyed by urban runoff: A review of sources. *Science of the Total Environment*, 709, 136125. <https://doi.org/10.1016/j.scitotenv.2019.136125>.
- Neale P. A., Braun G., Brack W., Carmona E., Gunold R., König M., Krauss M., Liebmann L., Liess M., Link M., Schäfer R. B., Schlichting R., Schreiner V. C., Schulze T., Vormeier P., Weisner O., Escher B. I., 2020. Assessing the Mixture Effects in In Vitro Bioassays of Chemicals Occurring in Small Agricultural Streams during Rain Events. *Environmental Science & Technology*, 54 (13), 8280–8290. <https://doi.org/10.1021/acs.est.0c02235>.
- Nissen K. M. and Ulbrich U., 2017. Increasing frequencies and changing characteristics of heavy precipitation events threatening infrastructure in Europe under climate change. *Natural Hazards and Earth System Sciences*, 17 (7), 1177–1190. <https://doi.org/10.5194/nhess-17-1177-2017>.
- NORMAN. 2023. NORMAN Substance Database – NORMAN SusDat. <https://www.norman-network.com/nds/susdat/>. Accessed 7 Jul 2023.
- Paijens C., Bressy A., Frère B., Tedoldi D., Mailler R., Rocher V., Neveu P., Moilleron R., 2021. Urban pathways of biocides towards surface waters during dry and wet weathers: Assessment at the Paris conurbation scale. *Journal of Hazardous Materials*, 402, 123765. <https://doi.org/10.1016/j.jhazmat.2020.123765>.
- Parajulee A., Lei Y. D., De Silva A. O., Cao X., Mitchell C. P. J., Wania F., 2017. Assessing the Source-to-Stream Transport of Benzotriazoles during Rainfall and Snowmelt in Urban and Agricultural Watersheds. *Environmental Science & Technology*, 51 (8), 4191–4198. <https://doi.org/10.1021/acs.est.6b05638>.
- Phillips P. J., Chalmers A. T., Gray J. L., Kolpin D. W., Foreman W. T., Wall G. R., 2012. Combined sewer overflows: an environmental source of hormones and wastewater micropollutants. *Environmental Science & Technology*, 46 (10), 5336–5343. <https://doi.org/10.1021/es3001294>.
- Pironti C., Ricciardi M., Proto A., Bianco P. M., Montano L., Motta O., 2021. Endocrine-Disrupting Compounds: An Overview on Their Occurrence in the Aquatic Environment and Human Exposure. *Water*, 13 (10), 1347. <https://doi.org/10.3390/w13101347>.
- R Core Team, 2020. R: A language and environment for statistical computing. <https://www.R-project.org/>.
- Riegraf C., Bell A. M., Ohlig M., Reifferscheid G., Buchinger S., 2022. Planar chromatography-bioassays for the parallel and sensitive detection of androgenicity, anti-androgenicity and cytotoxicity. *Journal of Chromatography A*, 1684, 463582. <https://doi.org/10.1016/j.chroma.2022.463582>.
- Schreiner T. and Morlock G. E., 2021. Non-target bioanalytical eight-dimensional hyphenation including bioassay, heart-cut trapping, online desalting, orthogonal separations and mass spectrometry. *Journal of Chromatography A*, 1647, 462154. <https://doi.org/10.1016/j.chroma.2021.462154>.
- Schymanski E. L., Jeon J., Gulde R., Fenner K., Ruff M., Singer H. P., Hollender J., 2014. Identifying small molecules via high resolution mass spectrometry: communicating confidence. *Environmental Science & Technology*, 48 (4), 2097–2098. <https://doi.org/10.1021/es5002105>.

- Shi Q., Guo W., Shen Q., Han J., Lei L., Chen L., Yang L., Feng C., Zhou B., 2021. In vitro biolayer interferometry analysis of acetylcholinesterase as a potential target of aryl-organophosphorus flame-retardants. *Journal of Hazardous Materials*, 409, 124999. <https://doi.org/10.1016/j.jhazmat.2020.124999>.
- Shuliakovich A., Schroeder K., Nagengast L., Wolf Y., Brückner I., Muz M., Behnisch P. A., Hollert H., Schiwy S., 2022. Extensive rain events have a more substantial impact than advanced effluent treatment on the endocrine-disrupting activity in an effluent-dominated small river. *Science of the Total Environment*, 807 (Pt 2), 150887. <https://doi.org/10.1016/j.scitotenv.2021.150887>.
- Spahr S., Teixidó M., Sedlak D. L., Luthy R. G., 2020. Hydrophilic trace organic contaminants in urban stormwater: occurrence, toxicological relevance, and the need to enhance green stormwater infrastructure. *Environmental Science: Water Research & Technology*, 6 (1), 15–44. <https://doi.org/10.1039/C9EW00674E>.
- Stütz L., Schulz W., Winzenbacher R., 2020. Identification of acetylcholinesterase inhibitors in water by combining two-dimensional thin-layer chromatography and high-resolution mass spectrometry. *Journal of Chromatography A*, 1624, 461239. <https://doi.org/10.1016/j.chroma.2020.461239>.
- Ternes T. A., Stumpf M., Mueller J., Haberer K., Wilken R. D., Servos M., 1999. Behavior and occurrence of estrogens in municipal sewage treatment plants—I. Investigations in Germany, Canada and Brazil. *Science of the Total Environment*, 225 (1-2), 81–90. [https://doi.org/10.1016/S0048-9697\(98\)00334-9](https://doi.org/10.1016/S0048-9697(98)00334-9).
- Tian Z., McMinn M. H., Fang M., 2023. Effect-directed analysis and beyond: how to find causal environmental toxicants. *Exposome*, 3 (1), osad002, 617. <https://doi.org/10.1093/exposome/osad002>.
- Weyrauch P., Matzinger A., Pawlowsky-Reusing E., Plume S., Von Seggern D., Heinzmann B., Schroeder K., Rouault P., 2010. Contribution of combined sewer overflows to trace contaminant loads in urban streams. *Water Research*, 44 (15), 4451–4462. <https://doi.org/10.1016/j.watres.2010.06.011>.
- Wicke D., Matzinger A., Sonnenberg H., Caradot N., Schubert R.-L., Dick R., Heinzmann B., Dünnbier U., Von Seggern D., Rouault P., 2021. Micropollutants in Urban Stormwater Runoff of Different Land Uses. *Water*, 13 (9), 1312. <https://doi.org/10.3390/w13091312>.
- Willkommen S., Pfannerstill M., Ulrich U., Guse B., Fohrer N., 2019. How weather conditions and physico-chemical properties control the leaching of flufenacet, diflufenican, and pendimethalin in a tile-drained landscape. *Agriculture, Ecosystems & Environment*, 278, 107–116. <https://doi.org/10.1016/j.agee.2019.03.017>.
- Wilson I. D. and Poole C. F., 2023. Planar chromatography - Current practice and future prospects. *Journal of Chromatography B*, 1214, 123553. <https://doi.org/10.1016/j.jchromb.2022.123553>.
- Wolf Y., Oster S., Shuliakovich A., Brückner I., Dolny R., Linnemann V., Pinnekamp J., Hollert H., Schiwy S., 2022. Improvement of wastewater and water quality via a full-scale ozonation plant? - A comprehensive analysis of the endocrine potential using effect-based methods. *Science of the Total Environment*, 803, 149756. <https://doi.org/10.1016/j.scitotenv.2021.149756>.
- Zwart N., Jonker W., Ten Broek R., De Boer J., Somsen G., Kool J., Hamers T., Houtman C. J., Lamoree M. H., 2020. Identification of mutagenic and endocrine disrupting compounds in surface water and wastewater treatment plant effluents using high-resolution effect-directed analysis. *Water Research*, 168, 115204. <https://doi.org/10.1016/j.watres.2019.115204>.

5.8. Appendix

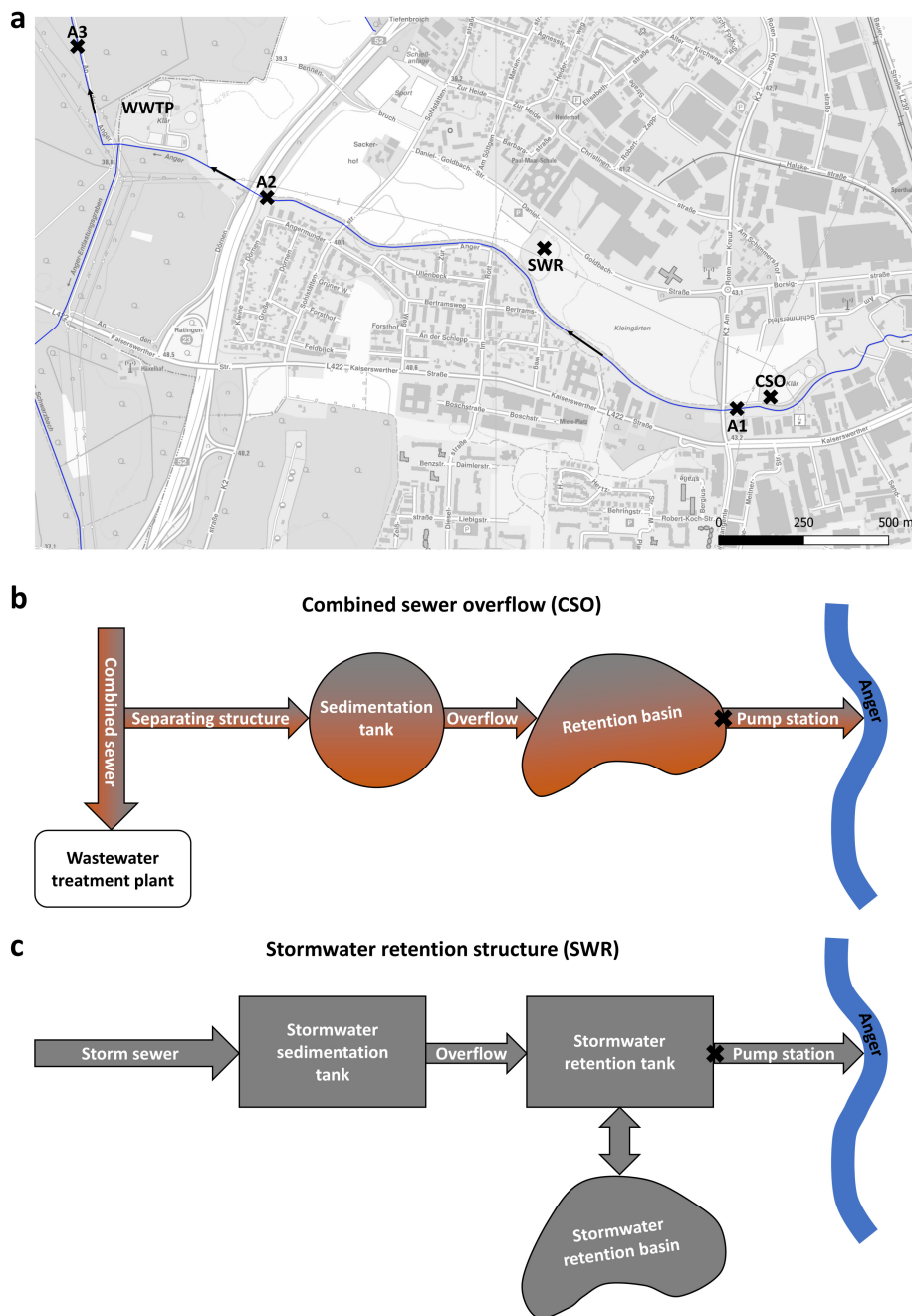


Figure 5-4 Sampling site 1 at the Anger in Ratingen, Germany (a). Samples were taken at following sampling points: combined sewer overflow (CSO), downstream the CSO and upstream storm sewer outlets (A1), a stormwater retention structure (SWR) connected to the storm sewer, downstream the storm sewer outlets (A2), and downstream the wastewater treatment plant Ratingen, Germany (A3). The crosses and the arrows represent the sampling points and the flow direction, respectively. Simplified structure of the CSO (b) and the SWR (c). Mixed water (waste- and stormwater) is discharged over a separating structure into the sedimentation tank of the CSO, when the hydraulic capacity of the combined sewer is exceeded. After passing the sedimentation tank the mixed water is discharged into a retention basin. From the retention basin, water can be pumped into the Anger or back into the combined sewer, depending on the load. Stormwater from the storm sewer is discharged into the sedimentation tank of the SWR. After passing the sedimentation tank, stormwater is discharged into the connected retention structures. From there it is pumped into the Anger. Samples were taken at the outlets of the retention structures prior to the pumping stations (black crosses).

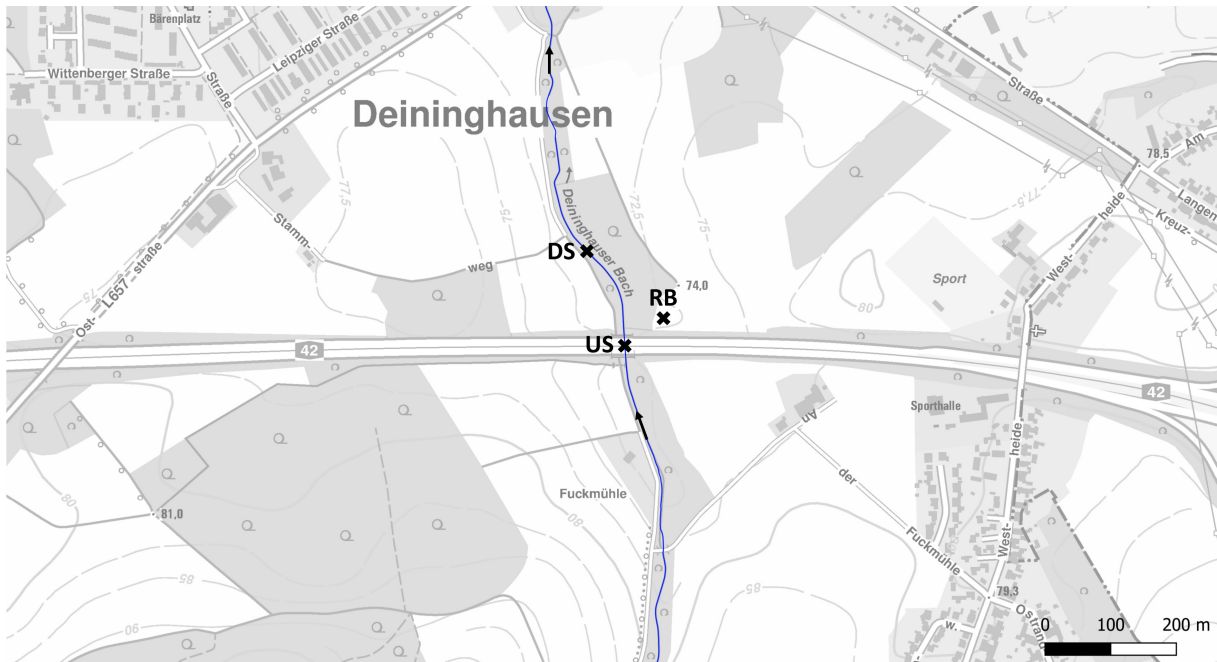


Figure 5-5 Sampling site 2 at the Deininghauser Bach in Deininghausen, Germany, next to the highway A42. Samples were taken at following sampling points: stormwater retention basin (RB), which is connected to a highway nearby, and up- and downstream the receiving stream Deininghauser Bach (US and DS). The crosses and the arrows represent the sampling points and the flow direction, respectively.

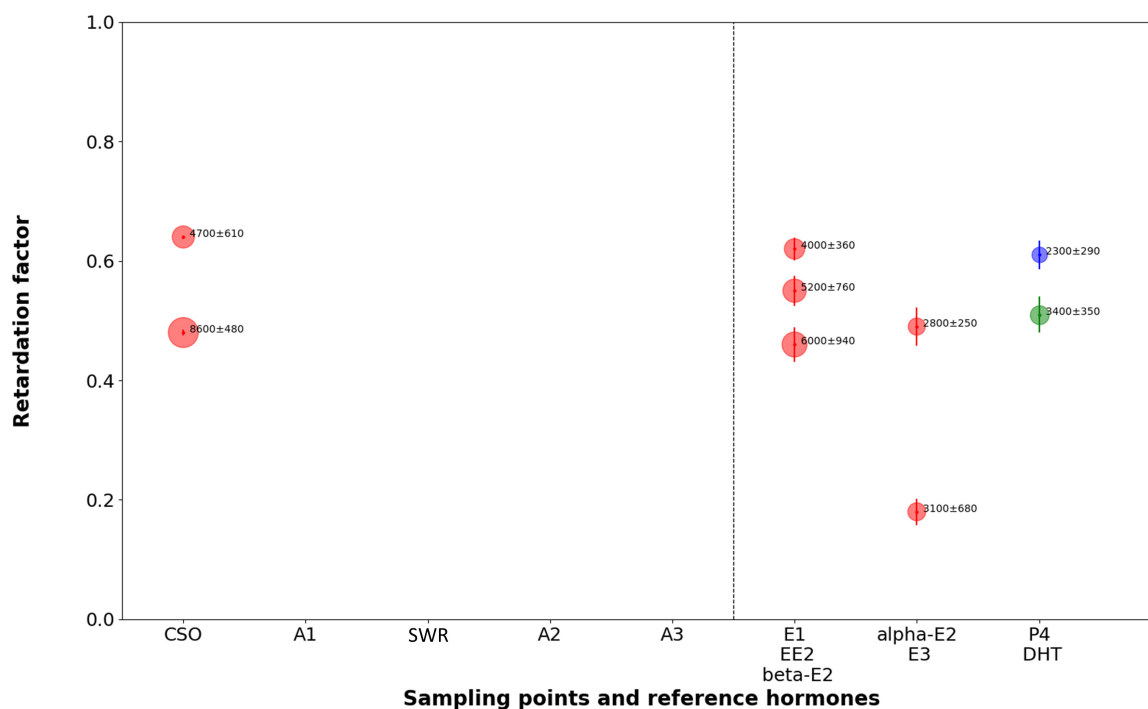


Figure 5-6 Estrogenic effects detected in samples from stormwater structures and the receiving river Anger in Ratingen, Germany (first sampling site). The sampling was performed in August 2020 during dry weather conditions. The samples were taken from a combined sewer overflow (CSO), downstream the CSO and upstream storm sewer outlets (A1), a stormwater retention structure (SWR) connected to the storm sewer, downstream the storm sewer outlets (A2), and downstream the wastewater treatment plant Ratingen, Germany (A3). A mix of 1000 pg E1 (40 µg/L), 100 pg EE2 (4 µg/L), and 100 pg 17β-E2 (4 µg/L), a mix of 250 pg 17α-E2 (10 µg/L), and 250 pg E3 (10 µg/L), and a mix of 250 pg P4 (10 µg/L) and 100 pg DHT (4 µg/L) were applied (right side). The red, green, and blue dots represent estrogenic, androgenic, and gestagenic effects, respectively. The mean peak area (AU) ± standard deviation of the effects (n = 4) and the reference hormones (n = 4) are presented next to the dots. The size of the dots also represents the peak area. The y-axis shows the retardation factor (R_f). The position of the dots highlights the mean R_f s and the error bars show the standard deviations of the effects (n = 4) and the reference hormones (n = 4). The samples were 1000-fold enriched by SPE. The application volume on the HPTLC plate was 25 µL. The samples were separated by HPTLC and measured with the yeast multi-endocrine effect screen (YMEES) for the detection of estrogenic, androgenic, and gestagenic effects.

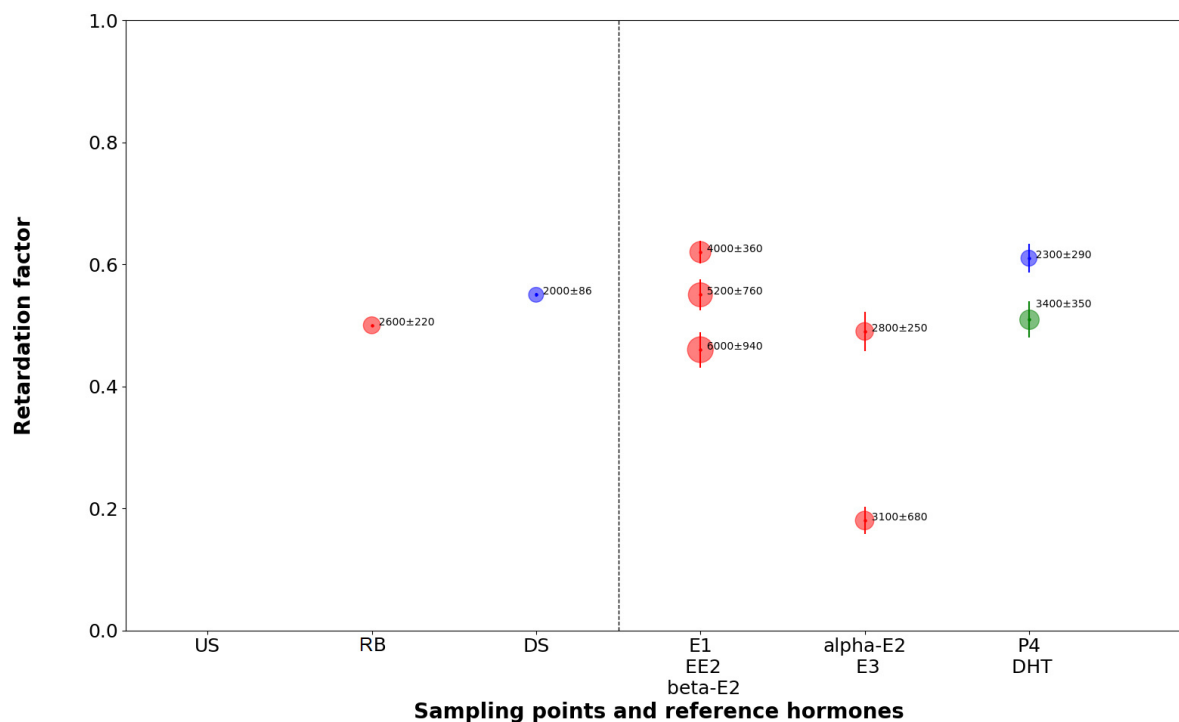


Figure 5-7 Estrogenic and gestagenic effects detected in samples from a stormwater retention basin, draining a highway, and the receiving small stream Deininghauser Bach near Deininghausen, Germany (second sampling site). The sampling was performed in August 2020 during dry weather conditions. The samples were taken from a stormwater retention basin (RB), which is connected to a highway nearby, and up- and downstream the receiving stream Deininghauser Bach (US and DS). A mix of 1000 pg E1 (40 µg/L), 100 pg EE2 (4 µg/L), and 100 pg 17β-E2 (4 µg/L), a mix of 250 pg 17α-E2 (10 µg/L), and 250 pg E3 (10 µg/L), and a mix of 250 pg P4 (10 µg/L) and 100 pg DHT (4 µg/L) were applied (right side). The red, green, and blue dots represent estrogenic, androgenic, and gestagenic effects, respectively. The mean peak area (AU) ± standard deviation of the effects (n = 4) and the reference hormones (n = 4) are presented next to the dots. The size of the dots also represents the peak area. The y-axis shows the retardation factor (R_F). The position of the dots highlights the mean R_F s and the error bars show the standard deviations of the effects (n = 4) and the reference hormones (n = 4). The samples were 1000-fold enriched by SPE. The application volume on the HPTLC plate was 25 µL. The samples were separated by HPTLC and measured with the yeast multi-endocrine effect screen (YMEES) for the detection of estrogenic, androgenic, and gestagenic effects.

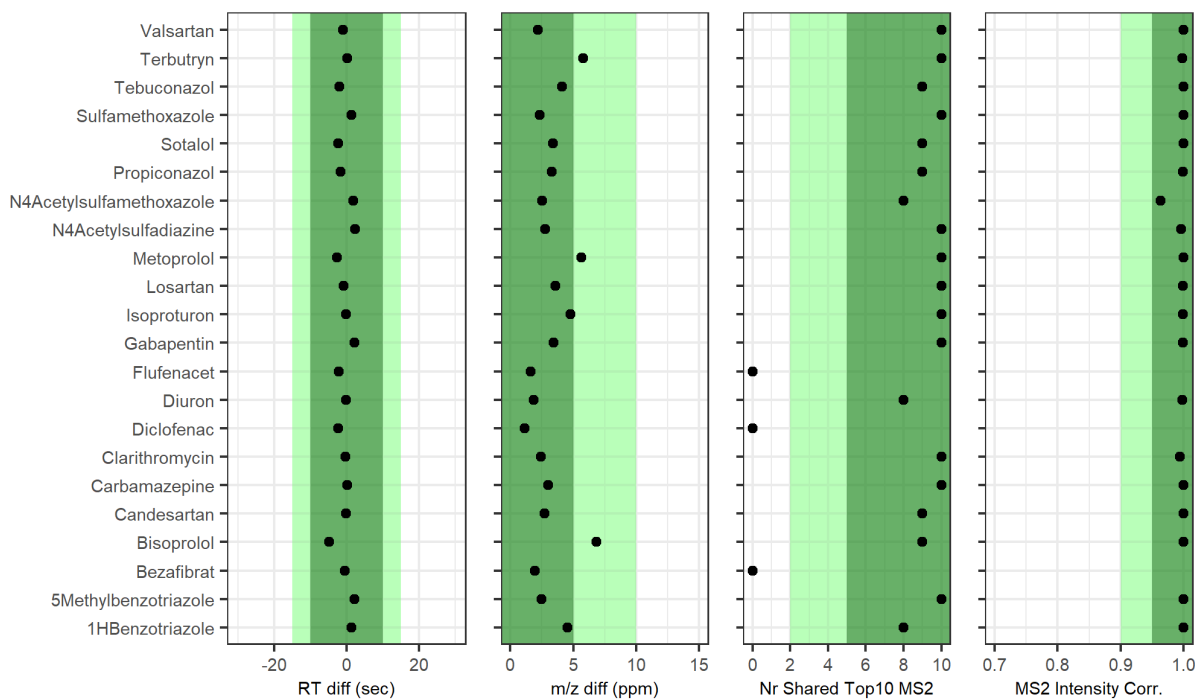


Figure 5-8 Retention time difference (sec), m/z difference (ppm), number of shared top 10 MS² fragments, and MS² intensity correction of substances used for quality control for LC-HRMS measurement.

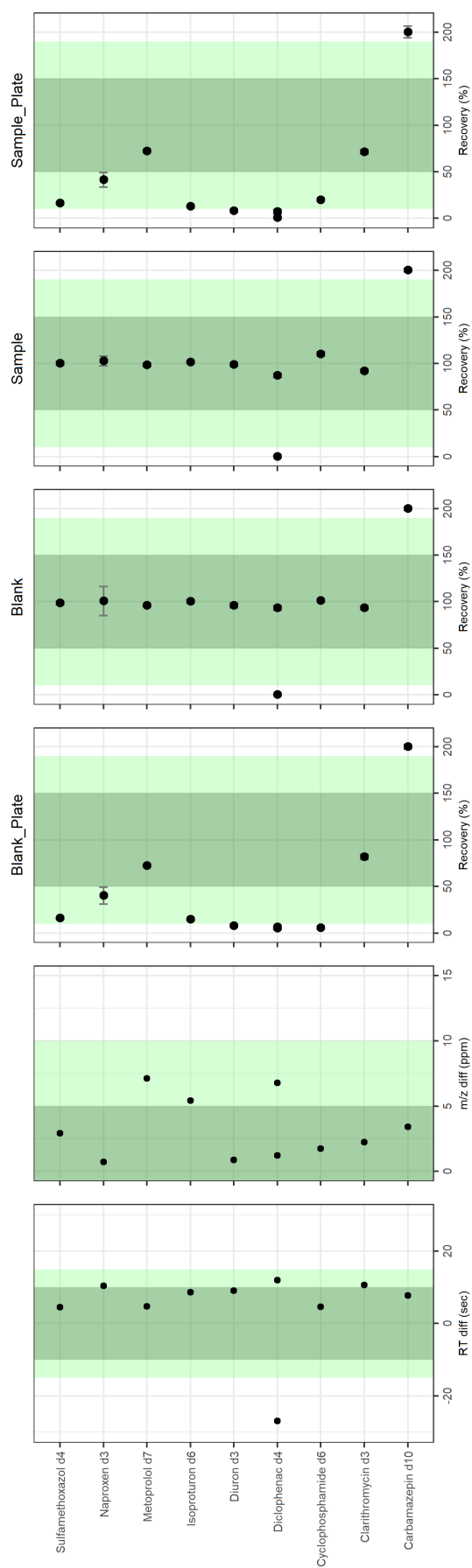


Figure 5-9 Retention time difference (sec), m/z difference (ppm), and recovery (%) of internal standards spiked into the samples before LC-HRMS measurement.

Table 5-2 Analytes and internal standards analyzed with HPTLC-YMEES, GC-MS/MS, LC-MS/MS, or LC-HRMS.

Substance	CAS	Sum formula	Monoisotopic mass	logP	Method
Estrone (E1)	53-16-7	C ₁₈ H ₂₂ O ₂	270.1620		HPTLC-YMEES, GC-MS/MS
17 α -Estradiol (17 α -E2)	57-91-0	C ₁₈ H ₂₄ O ₂	272.1776		HPTLC-YMEES, GC-MS/MS
17 β -Estradiol (17 β -E2)	50-28-2	C ₁₈ H ₂₄ O ₂	272.1776		HPTLC-YMEES, GC-MS/MS
17 β -Ethinylestradiol (EE2)	4717-38-8	C ₂₀ H ₂₄ O ₂	296.1776		HPTLC-YMEES, GC-MS/MS
Estriol (E3)	50-27-1	C ₁₈ H ₂₄ O ₃	288.1726		HPTLC-YMEES, GC-MS/MS
5 α -Dihydrotestosterone (DHT)	521-18-6	C ₁₉ H ₃₀ O ₂	290.2246		HPTLC-YMEES
Progesterone (P4)	57-83-0	C ₂₁ H ₃₀ O ₂	314.2246		HPTLC-YMEES
Estrone-d ₄ (E1-d ₄)	53866-34-5	C ₁₈ H ₁₈ D ₄ O ₂	274.1871		GC-MS/MS
17 β -Estradiol-d ₃ (17 β -E2-d ₃)	79037-37-9	C ₁₈ D ₃ H ₂₁ O ₂	275.1965		GC-MS/MS
17 α -Ethinylestradiol-d ₄ (EE2-d ₄)	350820-06-3	C ₂₀ H ₂₀ D ₄ O ₂	300.4288		GC-MS/MS
10,11-Dihydroxy-10,11-dihydrocarbamazepine	58955-93-4	C ₁₅ H ₁₄ N ₂ O ₃	270.1004		LC-MS/MS
Ciprofloxacin	85721-33-1	C ₁₇ H ₁₈ FN ₃ O ₃	331.1332		LC-MS/MS
Ibuprofen	15687-27-1	C ₁₃ H ₁₈ O ₂	206.1307		LC-MS/MS
Sotalol	3930-20-9	C ₁₂ H ₂₀ N ₂ O ₃ S	272.1195	0.13	LC-MS/MS, LC-HRMS
Gabapentin	60142-96-3	C ₉ H ₁₇ NO ₂	171.1259	1.39	LC-MS/MS, LC-HRMS
1H-Benzotriazole	95-14-7	C ₆ H ₅ N ₃	119.0483	0.58	LC-MS/MS, LC-HRMS
N(4)-Acetylsulfadiazine	127-74-2	C ₁₂ H ₁₂ N ₄ O ₃ S	292.0630	-1.39	LC-MS/MS, LC-HRMS
Metoprolol	37350-58-6	C ₁₅ H ₂₅ NO ₃	267.1834	0.70	LC-MS/MS, LC-HRMS
5-Methylbenzotriazole	136-85-6	C ₇ H ₇ N ₃	133.0640	NA	LC-MS/MS, LC-HRMS
Sulfamethoxazole	723-46-6	C ₁₀ H ₁₁ N ₃ O ₃ S	253.0521	0.89	LC-MS/MS, LC-HRMS
Bisoprolol	66722-44-9	C ₁₈ H ₃₁ NO ₄	325.2253	1.24	LC-MS/MS, LC-HRMS
N(4)-Acetylsulfamethoxazole	21312-10-7	C ₁₂ H ₁₃ N ₃ O ₄ S	295.0627	0.33	LC-MS/MS, LC-HRMS

Substance	CAS	Sum formula	Monoisotopic mass	logP	Method
Carbamazepine	298-46-4	C ₁₅ H ₁₂ N ₂ O	236.0950	0.79	LC-MS/MS, LC-HRMS
Terbutryn	886-50-0	C ₁₀ H ₁₉ N ₅ S	241.1361	3.74	LC-MS/MS, LC-HRMS
Clarithromycin	81103-11-9	C ₃₈ H ₆₉ NO ₁₃	747.4769	1.66	LC-MS/MS, LC-HRMS
Losartan	114798-26-4	C ₂₂ H ₂₃ ClN ₆ O	422.1622	4.64	LC-MS/MS, LC-HRMS
Candesartan	139481-59-7	C ₂₄ H ₂₀ N ₆ O ₃	440.1597	4.79	LC-MS/MS, LC-HRMS
Isoproturon	34123-59-6	C ₁₂ H ₁₈ N ₂ O	206.1419	2.87	LC-MS/MS, LC-HRMS
Diuron	330-54-1	C ₉ H ₁₀ Cl ₂ N ₂ O	232.0170	2.68	LC-MS/MS, LC-HRMS
Bezafibrate	41859-67-0	C ₁₉ H ₂₀ ClNO ₄	361.1081	1.59	LC-MS/MS, LC-HRMS
Valsartan	137862-53-4	C ₂₄ H ₂₉ N ₅ O ₃	435.2271	4.41	LC-MS/MS, LC-HRMS
Tebuconazole	107534-96-3	C ₁₆ H ₂₂ ClN ₃ O	307.1451	NA	LC-MS/MS, LC-HRMS
Diclofenac	15307-86-5	C ₁₄ H ₁₁ Cl ₂ NO ₂	295.0167	2.22	LC-MS/MS, LC-HRMS
Propiconazol	60207-90-1	C ₁₅ H ₁₇ Cl ₂ N ₃ O ₂	341.0698	NA	LC-MS/MS, LC-HRMS
Flufenacet	142459-58-3	C ₁₄ H ₁₃ F ₄ N ₃ O ₂ S	363.0665	NA	LC-MS/MS, LC-HRMS
Carbamazepine-d ₁₀	132183-78-9	C ₁₅ D ₁₀ H ₂ N ₂ O	246.1577		LC-MS/MS, LC-HRMS
Clarithromycin-d ₃	959119-17-6	C ₃₈ H ₆₆ D ₃ NO ₁₃	750.4957		LC-MS/MS, LC-HRMS
Cyclophosphamide-d ₆	951173-63-0	C ₇ H ₉ D ₆ Cl ₂ N ₂ O ₂ P	266.0625		LC-MS/MS, LC-HRMS
Diclofenac-d ₄	153466-65-0	C ₁₄ H ₇ D ₄ Cl ₂ NO ₂	299.0418		LC-MS/MS, LC-HRMS
Diuron-d ₆	1007536-67-5	C ₉ H ₄ D ₆ Cl ₂ N ₂ O	238.0547		LC-MS/MS, LC-HRMS
Ibuprofen-d ₃	121662-14-4	C ₁₃ D ₃ H ₁₅ O ₂	209.2999		LC-MS/MS
Metoprolol-d ₇	51384-51-1	C ₁₅ H ₁₈ D ₇ NO ₃	274.2274		LC-MS/MS, LC-HRMS
Sulfamethoxazole-d ₄	1020719-86-1	C ₁₀ H ₇ D ₄ N ₃ O ₃ S	257.0772		LC-MS/MS, LC-HRMS
Naproxen d ₃	958293-77-1	C ₁₄ H ₁₁ D ₃ O ₃	233.1131		LC-HRMS
Isoproturon d ₆	217487-17-7	C ₁₂ H ₁₂ D ₆ N ₂ O	212.1796		LC-HRMS

Table 5-3 Recovery rates of E1, α -E2, β -E2, EE2, E3, DHT, and P4 in the SPE quality controls (QCs) in relation to the positive controls (PCs). The QCs were 1000-fold enriched by SPE. The application volume on the HPTLC plate was 25 μ L. The SPE QCs and PCs contain a mix of 1000 pg E1 (40 μ g/L), 100 pg β -E2 (4 μ g/L), and 100 pg EE2 (4 μ g/L), and a mix of 250 pg α -E2 (10 μ g/L) and 250 pg E3 (10 μ g/L), and a mix of 100 pg DHT (4 μ g/L) and 250 pg P4 (10 μ g/L). No QC with the α -E2 and E3 mix was measured for the first sampling. The samples were separated by HPTLC and measured with the yeast multi-endocrine effect screen (YMEES) for the detection of estrogenic, androgenic, and gestagenic effects. The tested mean peak areas of the SPE QCs were divided by the mean peak areas of the PCs (100%). The recovery rates \pm standard deviations (%) are shown.

Sampling	Recovery \pm standard deviation (%)	
	First (n = 6)	Second (n = 3)
Substance		
E1	140 \pm 19	117 \pm 24
α -E2	-	93 \pm 15
β -E2	57 \pm 15	132 \pm 18
EE2	62 \pm 15	119 \pm 24
E3	-	123 \pm 17
DHT	71 \pm 10	101 \pm 6
P4	103 \pm 12	109 \pm 7

Table 5-4 Parameters for the GC-MS/MS analysis of estrogens.

Injector	Temperature ($^{\circ}$ C)	270		
	Injection type	Splitless		
	Injection volume (μ L)	3		
	Rinse solution	Toluol		
Gas chromatograph	Heating rate ($^{\circ}$ C/min)	25	10	
	Time (min)	0	2	11.5
	Temperature ($^{\circ}$ C)	150	200	315
	Hold time (min)	0	0	3
Column	Type	Zebron ZB-5MSi		
	Size	30 m x 0.25 mm x 0.25 μ m		
	Manufacturer	Phenomenex, Torrance, USA		
Interface	Temperature ($^{\circ}$ C)	300		
Ion source	Temperature ($^{\circ}$ C)	250		
Ionization	EI (eV)	70		
Detector	Voltage (kV)	2,6		

Table 5-5 Analytes and internal standards with information for identification, verification, and quantification with GC-MS/MS. MRMs (m/z) are shown with the specific collision energy (CE).

Substance	MRM 1 m/z	CE (eV)	MRM 2 m/z	CE (eV)	MRM 3 m/z	CE (eV)	MRM 4 m/z	CE (eV)	LOD (ng/L)	LOQ (ng/L)
E1	342.2 → 257.2	18	342.2 → 218.2	18	342.2 → 244.2	18	-	-	0.002	0.006
17 α -E2	416.3 → 285.2	15	416.3 → 129.1	21	285.2 → 205.1	18	-	-	0.003	0.009
17 β -E2	416.3 → 285.2	18	416.3 → 129.1	21	285.2 → 205.1	18	-	-	0.002	0.005
EE2	425.2 → 193.1	21	425.2 → 167.1	27	425.2 → 231.1	18	-	-	0.002	0.006
E3	504.3 → 311.1	21	504.3 → 386.2	9	311.2 → 282.1	18	311.2 → 267.0	24	0.001	0.003
E1-d ₄	346.2 → 261.2	15	346.2 → 205.2	30	346.2 → 246.1	18	-	-	-	-
17 β -E2-d ₃	419.3 → 285.2	15	419.3 → 131.2	21	419.3 → 232.2	24	-	-	-	-
EE2-d ₄	429.3 → 233.2	27	429.3 → 169.1	18	429.3 → 195.2	15	-	-	-	-

Table 5-6 Concentrations of the hormones E1, 17 α -E2, 17 β -E2, EE2, and E3 detected with GC-MS/MS in the field blank, SPE blank, and quality control (QC) samples. The sampling was performed in March 2020. Both blank sample types and the QCs were prepared with LC-MS grade water. The field blank was used to wash the sampling vessel and opened at the sampling points. The SPE blank was deployed for the sample preparation. The blanks and QCs were spiked with 1 ng of the internal standards E1-D4, 17 β -E2-D3, and EE2-D4. The QC sample was also spiked with 1 ng of E1, 17 α -E2, 17 β -E2, EE2, and E3. The substance concentrations are shown in ng/L \pm confidence interval (95%).

Substance	Concentration (ng/L)				
	E1	17 α -E2	17 β -E2	EE2	E3
Sample					
Field blank	0.31 \pm 0.17	0.17 \pm 0.05	< 0.035*	0.58 \pm 0.24	0.33 \pm 0.15
SPE blank	0.26 \pm 0.18	0.10 \pm 0.05	< 0.035*	0.42 \pm 0.24	< 0.066*
QC	1.1 \pm 0.2	0.93 \pm 0.05	0.91 \pm 0.07	1.2 \pm 0.2	1.6 \pm 0.2

* Sample specific LOD (S/N = 3)

Table 5-7 Recovery rates (%) of the internal standards E1-d4, 17 β -E2-d3, and EE2-d4 used for GC-MS/MS analysis in samples from stormwater structures and the receiving river Anger in Ratingen, Germany (first sampling site) and from a stormwater retention basin, draining a highway, and the receiving small stream Deininghauser Bach near Deininghausen, Germany (second sampling site). The sampling was performed in March 2020. At the first sampling site the samples were taken from a combined sewer overflow (CSO), downstream the CSO and upstream storm sewer outlets (A1), a stormwater retention structure (SWR) connected to the storm sewer, downstream the storm sewer outlets (A2), and downstream the wastewater treatment plant Ratingen, Germany (A3). At the second sampling site the samples were taken from a stormwater retention basin (RB), which is connected to a highway nearby, and up- and downstream the receiving stream Deininghauser Bach (US and DS). The recoveries in the field blank, SPE blank and quality control (QC) samples are also shown.

Substance	Recovery rate (%)		
	E1-d4	17 β -E2-d3	EE2-d4
Sample			
Field blank	90	92	87
SPE blank	83	81	81
QC	99	98	94
CSO	84	76	77
A1	46	50	82
SWR	67	76	82
A2	30	34	35
A3	86	98	147
US	66	77	176
RB	70	74	74
DS	74	82	96

Table 5-8 Parameters for the LC-MS/MS analysis.

Injection volume (μL)	50					
Temperature oven ($^{\circ}\text{C}$)	40					
Pre-column	Raptor ARC-18, 5 x 2.1 mm, 2.7 μm , Restek GmbH, Bad Homburg, Germany					
Column	Raptor ARC-18, 50 x 2.1 mm, 2.7 μm , Restek GmbH, Bad Homburg, Germany					
Flow rate ($\mu\text{L}/\text{min}$)	500					
A	Water + 0.1% formic acid					
B	Acetonitrile + 0.1% formic acid					
Total time (min)	0	8	8.1	10	10.1	13
A (%)	99	33	1	1	99	99
B (%)	1	67	99	99	1	1
Ion source temperature ($^{\circ}\text{C}$)	550					
Ionization IS (eV)	5500					

Table 5-9 Analytes and internal standards with information for identification, verification, and quantification with LC-MS/MS. MRMs (m/z) are shown for verification (V) and quantification (Q) with the specific collision energy (CE).

Substance	MRM (V) m/z	CE (eV)	MRM (Q) m/z	CE (eV)	LOD ($\mu\text{g}/\text{L}$)	LOQ ($\mu\text{g}/\text{L}$)
10,11-Dihydroxy-10,11-dihydrocarbamazepine	271 \rightarrow 180	54	271 \rightarrow 210	23	0.005	0.016
1H-Benzotriazole	120 \rightarrow 65	31	120 \rightarrow 92	23	0.004	0.013
4N-Acetylsulfadiazin	293 \rightarrow 134	33	293 \rightarrow 65	59	0.007	0.023
4N-Acethylsulfamethoxazole	296 \rightarrow 134	31	296 \rightarrow 65	63	0.007	0.022
Bezafibrate	362 \rightarrow 139	31	362 \rightarrow 121	37	0.002	0.007
Bisoprolol	326 \rightarrow 116	20	326 \rightarrow 121	35	0.0002	0.001
Candesartan	441 \rightarrow 263	20	441 \rightarrow 423	20	0.001	0.002
Carbamazepine	237 \rightarrow 194	28	237 \rightarrow 193	43	0.001	0.002
Ciprofloxacin	332 \rightarrow 231	54	332 \rightarrow 288	26	0.010	0.032
Clarithromycin	749 \rightarrow 158	35	749 \rightarrow 83	50	0.0003	0.001
Diclofenac	296 \rightarrow 214	50	296 \rightarrow 250	17	0.004	0.015
Diuron	233 \rightarrow 72	31	233 \rightarrow 160	33	0.017	0.056
Flufenacet	364 \rightarrow 194	25	364 \rightarrow 152	17	0.002	0.008
Gabapentin	172 \rightarrow 137	20	172 \rightarrow 154	19	0.004	0.015
Ibuprofen	207 \rightarrow 161	17	207 \rightarrow 119	33	1.378	4.592
Isoproturon	207 \rightarrow 72	29	207 \rightarrow 165	19	0.001	0.004
Losartan	423 \rightarrow 207	35	423 \rightarrow 405	20	0.001	0.003
Σ 4+5-Methylbenzotriazole	134 \rightarrow 77	10	134 \rightarrow 79	10	0.205	0.682

Substance	MRM (V) <i>m/z</i>	CE (eV)	MRM (Q) <i>m/z</i>	CE (eV)	LOD ($\mu\text{g/L}$)	LOQ ($\mu\text{g/L}$)
Metoprolol	268 → 133	35	268 → 103	50	0.012	0.039
Propiconazole	342 → 159	46	342 → 123	46	0.004	0.014
Sotalol	273 → 255	20	273 → 133	40	0.003	0.011
Sulfamethoxazole	254 → 156	23	254 → 92	40	0.030	0.099
Tebuconazole	308 → 70	39	308 → 125	51	0.001	0.004
Terbutryn	242 → 186	25	242 → 68	57	0.001	0.002
Valsartan	436 → 207	35	436 → 291	20	0.004	0.014
Carbamazepine-d ₁₀	-		247 → 204	29	-	-
Clarithromycin-d ₃	-		752 → 593	29	-	-
Cyclophosphamide-d ₆	-		267 → 140	31	-	-
Diclofenac-d ₄	-		300 → 218	41	-	-
Diuron-d ₆	-		239 → 78	35	-	-
Ibuprofen-d ₃	-		210 → 164	15	-	-
Metoprolol-d ₇	-		275 → 123	27	-	-
Sulfamethoxazole-d ₄	-		258 → 96	46	-	-

Table 5-10 Concentrations of substances detected with LC-MS/MS in samples from stormwater structures and the receiving river Anger in Ratingen, Germany (first sampling site) and from a stormwater retention basin, draining a highway, and the receiving small stream Deininghauser Bach near Deininghausen, Germany (second sampling site). The sampling was performed in March 2020 during rainy weather conditions. At the first sampling site the samples were taken from a combined sewer overflow (CSO), downstream the CSO and upstream storm sewer outlets (A1), a stormwater retention structure (SWR) connected to the storm sewer, downstream the storm sewer outlets (A2), and downstream the wastewater treatment plant Ratingen, Germany (A3). At the second sampling site the samples were taken from a stormwater retention basin (RB), which is connected to a highway nearby, and up- and downstream the receiving stream Deininghauser Bach (US and DS). The LOQ and concentrations of the analytes are shown in ng/L. Results which are lower than the LOQ or LOD are highlighted with < LOQ or < LOD, respectively.

Sample	Concentration (ng/L)										Method blank
	CSO	A1	SWR	A2	A3	US	RB	DS	Field blank		
Substance	LOQ										
10,11-Dihydroxy-10,11-dihydrocarbamazepine	90	72	< LOD	71	120	< LOQ	< LOQ	< LOQ	< LOQ	< LOQ	< LOQ
4N-Acetylsulfadiazine	< LOQ	< LOQ	< LOQ	< LOQ	< LOQ	< LOQ	< LOQ	< LOQ	< LOQ	< LOQ	< LOQ
4N-Acetylsulfamethoxazole	38	< LOQ	< LOQ	< LOQ							
Bezafibrate	90	58	< LOQ	51	71	< LOQ	< LOQ	< LOQ	< LOQ	< LOQ	< LOQ
Bisoprolol	23	27	< LOQ	24	35	< LOQ	< LOQ	< LOQ	< LOQ	< LOQ	< LOQ
Candesartan	210	260	< LOQ	240	350	< LOQ	< LOQ	< LOQ	< LOQ	< LOQ	< LOQ
Carbamazepine	60	63	< LOQ	60	75	< LOQ	< LOQ	< LOQ	< LOQ	< LOQ	< LOQ
Ciprofloxacin	< LOQ	< LOQ	< LOQ	< LOQ	< LOQ	< LOQ	< LOQ	< LOQ	< LOQ	< LOQ	< LOQ
Clarithromycin	62	23	< LOQ	26	44	< LOQ	< LOQ	< LOQ	< LOQ	< LOQ	< LOQ
Diclofenac	170	230	< LOQ	220	350	< LOQ	< LOQ	< LOQ	< LOQ	< LOQ	< LOQ
Gabapentin	940	720	18	650	1,000	< LOQ	< LOQ	< LOQ	< LOQ	< LOQ	< LOQ
Ibuprofen	980	< LOQ	< LOQ	< LOQ							
Losartan	48	< LOQ	< LOQ	< LOQ							
Metoprolol	210	94	< LOD	89	230	< LOQ	< LOQ	< LOQ	< LOQ	< LOQ	< LOQ
Sotalol	28	29	< LOQ	27	35	< LOQ	< LOQ	< LOQ	< LOQ	< LOQ	< LOQ
Sulfamethoxazol	15	25	< LOQ	36	30	< LOQ	< LOQ	< LOQ	< LOQ	< LOQ	< LOQ
Valsartan	720	250	< LOQ	230	470	< LOQ	< LOQ	< LOQ	< LOQ	< LOQ	< LOQ
∑ Pharmaceuticals	3,684	1,851	18	1,724	2,810	-	-	-	-	-	-
1H-Benzotriazole	580	430	59	370	730	< LOQ	< LOQ	< LOQ	< LOQ	< LOQ	< LOQ
∑ 4+5-Methylbenzotriazole	< LOQ	< LOQ	< LOQ	< LOQ	< LOQ	< LOQ	< LOQ	< LOQ	< LOQ	< LOQ	< LOQ
Diuron	< LOQ	< LOQ	< LOQ	< LOQ	< LOQ	< LOQ	< LOQ	< LOQ	< LOQ	< LOQ	< LOQ
Flufenacet	< LOQ	18	< LOQ	17	15	37	16	31	< LOQ	< LOQ	< LOQ
Isoproturon	< LOQ	< LOQ	< LOQ	< LOQ	< LOQ	< LOQ	< LOQ	< LOQ	< LOQ	< LOQ	< LOQ
Terbutryn	18	< LOQ	21	< LOQ	< LOQ	< LOQ					
Propiconazol	< LOQ	< LOQ	< LOQ	< LOQ	< LOQ	< LOQ	< LOQ	< LOQ	< LOQ	< LOQ	< LOQ
Tebuconazol	< LOQ	< LOQ	< LOQ	< LOQ	< LOQ	< LOQ	< LOQ	< LOQ	< LOQ	< LOQ	< LOQ

Table 5-11 Concentrations of substances detected with LC-MS/MS in samples from stormwater structures and the receiving river Anger in Ratingen, Germany (first sampling site) and from a stormwater retention basin, draining a highway, and the receiving small stream Deininghauser Bach near Deininghausen, Germany (second sampling site). The sampling was performed in August 2020 during dry weather conditions. At the first sampling site the samples were taken from a combined sewer overflow (CSO), downstream the CSO and upstream storm sewer outlets (A1), a stormwater retention structure (SWR) connected to the storm sewer, downstream the storm sewer outlets (A2), and downstream the wastewater treatment plant Ratingen, Germany (A3). At the second sampling site the samples were taken from a stormwater retention basin (RB), which is connected to a highway nearby, and up- and downstream the receiving stream Deininghauser Bach (US and DS). The LOQ and concentrations of the analytes are shown in ng/L. Results which are lower than the LOQ or LOD are highlighted with < LOQ or < LOD, respectively.

Sample	Concentration (ng/L)										Field blank	Method blank
	CSO	A1	SWR	A2	A3	US	RB	DS				
Substance	LOQ											
10,11-Dihydroxy-10,11-dihydrocarbamazepine	50	250	600	< LOQ	610	1,600	< LOQ	< LOQ				
4N-Acetylsulfadiazine	22.5	< LOQ	< LOQ	< LOQ	< LOQ	< LOQ	< LOQ	< LOQ				
4N-Acetylsulfamethoxazole	20	< LOQ	< LOQ	< LOQ	< LOQ	< LOQ	< LOQ	< LOQ				
Bezafibrate	20	< LOQ	< LOQ	< LOQ	< LOQ	33	< LOQ	< LOQ				
Bisoprolol	9	31	55	< LOQ	55	110	< LOQ	< LOQ				
Candesartan	22.5	1,300	1,900	< LOQ	1,900	4,200	< LOQ	< LOQ				
Carbamazepine	22.5	170	200	< LOQ	210	480	< LOQ	< LOQ				
Ciprofloxacin	50	< LOQ	< LOQ	< LOQ	< LOQ	< LOQ	< LOQ	< LOQ				
Clarithromycin	9	11	19	< LOQ	18	32	< LOQ	< LOQ				
Diclofenac	50	85	510	< LOQ	490	2,700	< LOQ	< LOQ				
Gabapentin	20	3,000	460	< LOQ	< LOQ	< LOQ	< LOQ	< LOQ	< LOQ	< LOQ	< LOQ	< LOQ
Ibuprofen	2,000	< LOQ	< LOQ	< LOQ	< LOQ	< LOQ	< LOQ	< LOQ				
Losartan	9	180	< LOQ	< LOQ	< LOQ	65	< LOQ	< LOQ				
Metoprolol	9	660	320	< LOQ	300	1,300	< LOQ	< LOQ				
Sotalol	9	< LOQ	56	< LOQ	60	240	< LOQ	< LOQ				
Sulfamethoxazol	9	< LOQ	110	< LOQ	120	300	< LOQ	< LOQ				
Valsartan	9	2,500	57	13	55	270	< LOQ	18	< LOQ	< LOQ	< LOQ	< LOQ
Σ Pharmaceuticals	-	8,247	4336	13	3,818	12,530	-	18	11	-	-	-
1H-Benzotriazole	20	1,600	1,900	1,200	2,000	5,700	40	92	36	120	< LOQ	< LOQ
Σ 4+5-Methylbenzotriazole	500	1,200	760	< LOQ	670	2,300	< LOQ	< LOQ				
Diuron	200	< LOQ	< LOQ	< LOQ	< LOQ	< LOQ	< LOQ	< LOQ				
Flufenacet	20	< LOQ	< LOQ	< LOQ	< LOQ	< LOQ	< LOQ	< LOQ				
Isoproturon	9	< LOQ	< LOQ	< LOQ	21	23	< LOQ	< LOQ	9.7	< LOQ	< LOQ	< LOQ
Terbutryn	9	83	44	58	19	21	< LOQ	11	< LOQ	< LOQ	< LOQ	< LOQ
Propiconazol	20	36	26	< LOQ	< LOQ	< LOQ	< LOQ	< LOQ	< LOQ	< LOQ	< LOQ	< LOQ
Tebuconazol	9	42	30	17	13	170	15	< LOQ	< LOQ	20	< LOQ	< LOQ

Table 5-12 Suspect transformation fragment (TF) list used for suspect target analysis with LC-HRMS.

Fragment	Sum formula	Monoisotopic mass
Phosphoric acid	H3PO4	97.9769
Thiophosphoric acid	H3PO3S	113.9540
Dithiophosphoric acid	H3PO2S2	129.9312
OP pesticide fragment 1	C3H9PO3S	156.001
OP pesticide fragment 2	PS2O2C3H9	171.9782
OP pesticide fragment 3	PO4C2H7	126.0082
OP pesticide fragment 4	PO4C3H9	140.0238
OP pesticide fragment 5	C6H15PO2S2	214.0251
OP pesticide fragment 6	C4H11PO2S2	185.9938
OP pesticide fragment 7	C4H11PO3S	170.0167
OP pesticide fragment 8	C2H7PO2S2	157.9625
OP pesticide fragment 9	C2H7PO3S	141.9854
Carbamic acid	CH3NO2	61.0164
TCEP, V6 fragment 1	OHC2H4Cl	80.0029
TCEP, V6 fragment 2	C4H9Cl2O4P1	221.9616
TCEP, V6 fragment 3	C2H6Cl1O4P1	159.9692
TEP fragment 1	OHC2H5	46.0419
TEP fragment 2	C4H11O4P	154.0395
TEP fragment 3	C2H7O4P	126.0082
TCIPP fragment 1	OHC3H6Cl	94.01854
TCIPP fragment 2	C6H13Cl2O4P	249.9929
TCIPP fragment 3	C3H8Cl1O4P	173.9849
TPP fragment 1	OHC3H7	60.0575
TPP fragment 2	C6H15O4P	182.0708
TPP fragment 3	C3H9O4P	140.0238
TDCIPP fragment 1	OHC3H5Cl2	127.9796
TDCIPP fragment 2	C6H11Cl4O4P	317.9149
TDCIPP fragment 3	C3H7Cl2O4P	207.9459
TBP fragment 1	OHC4H9	74.0732
TBP, TEHP fragment 2	C8H19O4P	210.1021
TBP fragment 3	C4H11O4P	154.0395
TEHP fragment 1	OHC8H17	130.1358
TEHP fragment 3	C16H35O4P	322.2273
Phenol	C6H6O	94.0419
TPHP, EHDPP, BDP, RDP, IDDP fragment 1	C12H11O4P	250.0395
TPHP, EHDPP, BDP, RDP, IDDP fragment 2	C6H7O4P	174.0082
Kresol, TCP fragment 1	C7H8O	108.0575
TCP fragment 2	C14H15O4P	278.0708
TCP fragment 3	C7H9O4P	188.0238
TBMP fragment 1	C7H7OBr	185.9680
TBMP fragment 2	C14H13Br2O4P	433.8918
TBMP fragment 3	C7H8BrO4P	265.9344
TBOEP fragment 1	OHOC6H13	118.0994
TBOEP fragment 2	C12H27O6P	298.1545
TBOEP fragment 3	C6H15O5P	198.0657
TTBPP fragment 1	OHC5H8Br3	321.8204
TTBPP fragment 2	C10H17Br6O4P	705.5965
TTBPP fragment 3	C5H10Br6O4P	638.5417
EHDPP fragment 3	C8H18O	130.1358
EHDPP fragment 4	C8H19PO4	210.1021
T246MPP fragment 1	C9H12O	136.0888

Fragment	Sum formula	Monoisotopic mass
T246MPP fragment 2	C18H23PO4	334.1334
T246MPP fragment 3	C9H13PO4	216.0551
BDP fragment 3	C15H16O2	228.1150
BDP fragment 4	C33H30O8P2	616.1416
BDP fragment 5	C27H26O8P2	540.1103
BDP fragment 6	C21H22O8P2	464.0790
BDP fragment 7	C15H18O8P2	388.0477
BDP fragment 8	C27H25PO4	444.1490
BDP fragment 9	C21H21PO4	368.1177
BDP fragment 10	C15H17PO4	292.0864
V6 fragment 4	C11H21Cl5O8P2	517.9154
V6 fragment 5	C9H18Cl4O8P2	455.9231
V6 fragment 6	C7H15Cl3O8P2	393.9308
V6 fragment 7	C5H12Cl2O8P2	331.9384
V6 fragment 8	C5H11Cl2O4P	235.9772
V6 fragment 9	C7H14Cl3O4P	297.9695
V6 fragment 10	C9H17Cl4O4P	359.9619
V6 fragment 11	C5H10O2Cl2	172.0058
T4TBPP fragment 1	C10H14PO5	245.0579
T4TBPP fragment 2	C20H27O4P	362.1647
T4TBPP fragment 3	C10H15O4P	230.0708
RDP fragment 3	C24H20O8P2	498.0633
RDP fragment 4	C18H16O8P2	422.0320
RDP fragment 5	C12H12O8P2	346.0007
RDP fragment 6	C6H8O8P2	269.9694
RDP fragment 7	C18H15O5P	342.0657
RDP fragment 8	C12H11O5P	266.0344
RDP fragment 9	C6H7O5P	190.0031
IDDP fragment 3	C16H27O4P	314.1647
IDDP fragment 4	C10H23O4P	238.1334
IDDP fragment 5	C10H22	142.1722

Table 5-13 Suspect target list used for suspect target analysis with LC-HRMS. Representative substances used in a reference mix are highlighted in bold.

Substance	CAS	Sum formula	Monoisotopic mass	logP
Azinphos-ethyl	2642-71-9	C12H16N3O3PS2	345.0371	3.51
Azinphos-methyl	86-50-0	C10H12N3O3PS2	317.0058	2.53
Azinphos-methyl oxon	961-22-8	C10H12N3O4PS	301.0286	0.77
Carbophenothion	786-19-6	C11H16ClO2PS3	341.9739	5.44
Methyl Trithion (Carbophenothion-methyl)	953-17-3	C9H12ClO2PS3	313.9426	
Chlorethoxyfos	54593-83-8	C6H11Cl4O3PS	333.8921	4.17
Chlorfenvinphos	470-90-6	C12H14Cl3O4P	357.9695	4.15
Chlorpyrifos	2921-88-2	C9H11Cl3NO3PS	348.9263	5.11
Chlorpyrifos-methyl	5598-13-0	C7H7Cl3NO3PS	320.8950	4.13
Chlorpyrifos oxon	5598-15-2	C9H11Cl3NO4P	332.9491	
Coumaphos	56-72-4	C14H16ClO5PS	362.0145	4.47
Coumaphos oxon	321-54-0	C14H16ClO6P	346.0373	2.71
Cruformate	299-86-5	C12H19ClNO3P	291.0791	3.3
Cyanophos	2636-26-2	C9H10NO3PS	243.0119	2.76
Demephion-O	682-80-4	C5H13O3PS2	216.0044	1.74
Demephion-S	2587-90-8	C5H13O3PS2	216.0044	0.52
Demeton-S-methyl	919-86-8	C6H15O3PS2	230.0200	1.01
Demeton-O-methyl	867-27-6	C6H15O3PS2	230.0200	2.23
Demeton-O	298-03-3	C8H19O3PS2	258.0513	3.21
Demeton-S	126-75-0	C8H19O3PS2	258.0513	1.99
Oxydemeton-methyl	301-12-2	C6H15O4PS2	246.0149	-1.03
Demeton-S-methylsulphon	17040-19-6	C6H15O5PS2	262.0099	-0.91

Substance	CAS	Sum formula	Monoisotopic mass	logP
Dialifor	10311-84-9	C14H17ClNO4PS2	393.0025	4.14
Diazinon	333-41-5	C12H21N2O3PS	304.1011	3.86
Dichlorvos	62-73-7	C4H7Cl2O4P	219.9459	0.6
Dicrotophos	141-66-2	C8H16NO5P	237.0766	-0.1
Diisopropyl fluorophosphate	55-91-4	C6H14FO3P	184.0665	1.2
Dimefox	115-26-4	C4H12FN2OP	154.0671	-0.36
Dimethoate	60-51-5	C5H12NO3PS2	228.9996	0.72
Phosphoric acid dimethyl 4-(methylthio)phenyl ester	6552-13-2	C10H15O5PS	278.0378	0.15
Dioxathion	78-34-2	C12H26O6P2S4	456.0087	3.45
Disulfoton	298-04-4	C8H19O2PS3	274.0285	4.07
Disulfoton sulfone	2497-06-5	C8H19O4PS3	306.0183	1.83
Oxydisulfoton		C8H19O3PS3	290.0234	1.72
Endothion	2778-04-3	C9H13O6PS	280.0170	-0.31
Ethion	563-12-2	C9H22O4P2S4	383.9876	5
Ethoprop	13194-48-4	C8H19O2PS2	242.0564	3.14
Carboxyfenitrothion	54812-31-6	C9H10N1O7PS	306.9916	2.29
Fenitrothion	122-14-5	C9H12N1O5PS	277.0174	3.3
Fensulfothion-oxon	6552-21-2	C11H17O5PS	292.0534	0.58
Fensulfothion sulfone	14255-72-2	C11H17O5PS2	324.0255	2.48
Fensulfothion	115-90-2	C11H17O4PS2	308.0306	2.35
Fenthion	55-38-9	C10H15O3PS2	278.0200	4.08
Dichlofenthion	97-17-6	C10H13Cl2O3PS	313.9700	5.2
Fenthion oxon sulfone	14086-35-2	C10H15O6PS	294.0327	0.28
Fenthion oxon	6552-12-1	C10H15O4PS	262.0429	2.31
Fenthion sulfone	3761-42-0	C10H15O5PS2	310.0099	2.05
Fenthion-ethyl	1716-09-2	C12H19O3PS2	306.0513	5.06
Fonofos	944-22-9	C10H15OPS2	246.0302	4.02
Fosthiazate	98886-44-3	C9H18NO3PS2	283.0466	2.47
Formothion	2540-82-1	C6H12N1O4PS2	256.9945	1.26
Hexaethyl tetraphosphate	757-58-4	C12H30O11P4	474.0739	-2.35
Isoxathion	18854-01-8	C13H16NO4PS	313.0538	3.9
Leptophos	21609-90-5	C13H10BrCl2O2PS	409.8700	6.34
Malathion	121-75-5	C10H19O6PS2	330.0361	2.29
Malathion dicarboxylic Acid	1190-28-9	C6H11O6PS2	273.9735	0.15
Malaoxon	1634-78-2	C10H19O7PS	314.0589	0.52
Methamidophos	10265-92-6	C2H8N1O2PS	141.0013	-0.93
Methidathion	950-37-8	C6H11N2O4PS3	301.9619	1.58
Phenkapton	2275-14-1	C11H15Cl2O2PS3	375.9349	6.09
Trichlorfon	52-68-6	C4H8Cl3O4P	255.9226	0.42
Mevinphos	7786-34-7	C7H13O6P	224.0450	-0.24
Mipafox	371-86-8	C6H16FN2OP	182.0984	0.36
Monocrotophos	6923-22-4	C7H14NO5P	223.0610	0.28
Naled	300-76-5	C4H7Br2Cl2O4P	377.7826	1.6
Omethoate	1113-02-6	C5H12NO4P1S	213.0225	-0.79
Oxydemeton-methyl	301-12-2	C6H15O4PS2	246.0149	-1.03
Parathion	56-38-2	C10H14NO5PS	291.0330	3.73
Methyl parathion	298-00-0	C8H10NO5PS	263.0017	2.75
Paraoxon	311-45-5	C10H14NO6P	275.0559	1.97
Methylparaoxon	950-35-6	C8H10NO6P	247.0246	0.98
Phorate oxon	2600-69-3	C7H17O3PS2	244.0357	2.05
Phorate	298-02-2	C7H17O2PS3	260.0128	3.62
Phorate-sulfoxide	2588-05-8	C7H17O3PS3	276.0077	1.83
Phorate sulfone	2588-04-7	C7H17O4PS3	292.0027	1.94
Phorate oxon sulfoxide	2588-05-8	C7H17O4PS2	260.0306	1.76
Phorate oxon sulfone	2588-06-9	C7H17O5PS2	276.0255	
Phosalone	2310-17-0	C12H15ClNO4PS2	366.9869	4.29
Mephosfolan	950-10-7	C8H16NO3PS2	269.0309	1.58
Phosfolan	99910-17-5	C7H14NO3PS2	255.0153	1.17
Phosmet	5104-30-3	C11H12NO4PS2	316.9945	2.48
Phosphamidon	13171-21-6	C10H19ClNO5P	299.0689	1.38
Phoxim	14816-18-3	C12H15N2O3PS	298.0541	4.39
Chlorphoxim	14816-20-7	C12H14ClN2O3PS	332.0151	5.03
Profenofos	41198-08-7	C11H15BrClO3PS	371.9351	4.82
Propetamphos	31218-83-4	C10H20N1O4PS	281.0851	3.51
Prothoate	2275-18-5	C9H20N1O3PS2	285.0622	2.61
Quinalphos	13593-03-8	C12H15N2O3PS	298.0541	3.04
Schradan	152-16-9	C8H24N4O3P2	286.1324	-1.01
Sulfotep	3689-24-5	C8H20O5P2S2	322.0227	3.98
Tebupirimfos	96182-53-5	C13H23N2O3PS	318.1167	4.19
Temephos	3383-96-8	C16H20O6P2S3	465.9897	6.17
Terbufos sulfone	56070-16-7	C9H21O4PS3	320.0340	2.46
Terbufos sulfoxide	10548-10-4	C9H21O3PS3	304.0390	2.35

Substance	CAS	Sum formula	Monoisotopic mass	logP
Terbufos	13071-79-9	C9H21O2PS3	288.0441	4.49
Terbufos oxon sulfoxide	56165-57-2	C9H21O4PS2	288.0619	2.63
Tetrachlorvinphos	22248-79-9	C10H9Cl4O4P	363.8993	3.81
Triazophos	24017-47-8	C12H16N3O3PS	313.0650	3.37
Trichloronat	327-98-0	C10H12Cl3O2PS	331.9361	5.86
Aldicarb	116-06-3	C7H14N2O2S	190.0776	1.36
Aldicarb sulfoxide	1646-87-3	C7H14N2O3S	206.0725	-0.78
Aminocarb	2032-59-9	C11H16N2O2	208.1212	1.9
Bendiocarb	22781-23-3	C11H13NO4	223.0845	2.55
Bendiocarb phenol	22961-82-6	C9H10O3	166.0630	3.15
Butocarboxim	34681-10-2	C7H14N2O2S	190.0776	1.21
Butocarboxim-sulfoxide	34681-24-8	C7H14N2O3S	206.0725	-0.93
Carbaryl	63-25-2	C12H11NO2	201.0790	2.35
Carbofuran	1563-66-2	C12H15NO3	221.1052	2.3
3-Hydroxycarbofuran	16655-82-6	C12H15NO4	237.1001	0.76
Carbosulfan	55285-14-8	C20H32N2O3S	380.2134	5.57
m-Cumenyl methylcarbamate	64-00-6	C11H15NO2	193.1103	2.63
Dimetilan	644-64-4	C10H16N4O3	240.1222	0.27
Ethiofencarb	29973-13-5	C11H15NO2S	225.0823	2.04
Ethiofencarb sulfone	5427-28-1	C11H15NO4S	257.0722	0.01
Ethiofencarb sulfoxide	53380-22-6	C11H15NO3S	241.0773	-0.1
Fenobucarb	3766-81-2	C12H17NO2	207.1259	2.86
Fenoxycarb	72490-01-8	C17H19NO4	301.1314	4.24
Formetanate	22259-30-9	C11H15N3O2	221.1164	0.88
Methiocarb	2032-65-7	C11H15NO2S	225.0823	2.87
Methiocarb sulfoxide	2635-10-1	C11H15NO3S	241.0773	0.7
Methiocarb sulfone	2179-25-1	C11H15NO4S	257.0722	0.84
Methomyl	16752-77-5	C5H10N2O2S	162.0463	0.61
Metolcarb	1129-41-5	C9H11NO2	165.0790	1.72
Mexacarbate	315-18-4	C12H18N2O2	222.1368	2.44
Oxamyl	23135-22-0	C7H13N3O3S	219.0678	-1.2
Oxamyl-oxime	30558-43-1	C5H10N2O2S	162.0463	-0.71
Pirimicarb	23103-98-2	C11H18N4O2	238.1430	1.4
Desmethyl-pirimicarb	30614-22-3	C10H16N4O2	224.1273	0.85
pirimicarb-desmethyl formamido	27218-04-8	C11H16N4O3	252.1222	0.91
Promecarb	2631-37-0	C12H17NO2	207.1259	3.18
Propoxur	114-26-1	C11H15NO3	209.1052	1.9
Thiofanox	39196-18-4	C9H18N2O2S	218.1089	2.16
Thiofanox-sulfone	39184-59-3	C9H18N2O4S	250.0987	0.13
Thiofanox-sulfoxide	39184-27-5	C9H18N2O3S	234.1038	0.02
Tris(2-chlorethyl)phosphat (TCEP)	115-96-8	C6H12Cl3O4P	283.9539	1.63
Tris(2-chlorisopropyl)phosphat (TCIPP)	13674-84-5	C9H18Cl3O4P	326.0008	2.89
Tris(1,3-dichlorisopropyl)phosphat (TDCIPP)	13674-87-8	C9H15Cl6O4P	427.8839	3.65
Tris(2-ethylhexyl)phosphat (TEHP)	78-42-2	C24H51O4P	434.3525	9.49
Tricresyl phosphate (TCP)	78-30-8	C21H21O4P	368.1177	5.1
Triphenylphosphat (TPHP)	115-86-6	C18H15O4P	326.0708	4.7
Triethyl phosphate (TEP)	78-40-0	C6H15O4P	182.0708	0.87
Tripropyl phosphate (TPP)	513-08-6	C9H21O4P	224.1177	
Tributyl phosphate (TBP)	126-73-8	C12H27O4P	266.1647	
Tris(3-bromo-4-methylphenyl) phosphate (T3B4MPP)	35656-01-0	C21H18Br3O4P	601.8493	
Tris(2-butoxyethyl) phosphate (TBOEP)	78-51-3	C18H39O7P	398.2433	3
2-Ethylhexyl diphenyl phosphate (EHDPP)	1241-94-7	C20H27O4P	362.1647	6.3
Tri(2,4,6-trimethylphenyl) phosphate (T246MPP)	56444-79-2	C27H33O4P	452.2116	
Tris(tribromoneopentyl)phosphate (TTBPP)	19186-97-1	C15H24Br9O4P	1009.4063	8.05
Bisphenol A bis(diphenyl phosphate) (BDP)	5945-33-5	C39H34O8P2	692.1729	
Tris(4-tert-butylphenyl) phosphate (T4TBPP)	78-33-1	C30H39O4P	494.2586	
2,2-Bis(chloromethyl)trimethylene	38051-10-4	C13H24Cl6O8P2	579.9078	
bis(bis(2-chloroethyl)phosphate) (V6)				
Isodecyl diphenyl phosphate (IDDP)	29761-21-5	C22H31O4P	390.1960	7.4
Resorcinol bis(diphenylphosphate) (RDP)	57583-54-7	C30H24O8P2	574.0946	

Table 5-14 Limit of detection (LOD) (DIN, 2008) in $\mu\text{g/L}$ for representative substances used in a reference mix for LC-HRMS.

Substance	LOD ($\mu\text{g/L}$)
Chlorfenvinphos	2.0
Chlorpyrifos	1.1
Chlorpyrifos oxon	7.3
Diazinon	19
Dichlorvos	2.1
Disulfoton	-
Malathion	7.0
Malaoxon	3.9
Parathion	46
Methyl parathion	-
Paraoxon	2.3
Methiocarb	7.3
Thiofanox	-
Thiofanox-sulfoxide	-
Tris(2-chlorisopropyl)phosphat (TCIPP)	0.74

Table 5-15 Description of rule set for the identification levels adapted from patRoom and based on SCHYMANSKI et al. (2014).

Cat.	Description	Rule
1	Target match (<i>m/z</i> , retention time and MS/MS from reference standard)	The <i>m/z</i> deviates below 5 ppm, retention time deviates < 10 seconds and there are at least 3 fragments (or all if the suspect list contains less) that match the suspect list.
2	<i>m/z</i> and in silico MS/MS match	The <i>m/z</i> deviates below 5 ppm and more than 40% of the fragments explain the expected formula by in silico fragmentation.
3	<i>m/z</i> and retention time match	The <i>m/z</i> deviates below 5 ppm and the retention time deviates < 10 seconds from the suspect list.
4	Only <i>m/z</i> match	The <i>m/z</i> deviates below 5 ppm.

Table 5-16 Features detected with LC-HRMS and suspect transformation fragments (TF) in a stormwater retention basin (RB) at the second sampling site before and after extraction from a HPTLC plate after separation and AChE-I assay. The category levels were taken and adapted using the criteria described in Table 5-15.

Feature	Suspect TF	Retention time (sec)	m/z	Deviation (ppm)	HPTLC blank	Sample blank	Sample	HPTLC extract	Cat.
M127_R83_1080	OP pesticide fragment 3	83	127.0151	2.8	0	0	1,692	1,710	4
M127_R83_1080	TEP fragment 3	83	127.0151	2.8	0	0	1,692	1,710	4
M137_R1245_1360	T246MPP fragment 1	1,245	137.0962	1.0	1,106	582	1,855	1,590	4
M137_R1439_1358	T246MPP fragment 1	1,439	137.0960	1.1	777	420	1,657	839	4
M137_R638_1361	T246MPP fragment 1	638	137.0963	1.8	7,453	399	2,309	13,853	4
M212_R578_4336	EHDPP fragment 4	578	212.1182	4.8	70,928	11,953	255,261	98,098	4
M212_R627_4337	EHDPP fragment 4	627	212.1174	1.0	871	0	827	2,619	4
M279_R638_9130	TCP fragment 2	638	279.0778	1.1	10,490	174	1,502	757	4
M299_R1292_11015	TBOEP fragment 2	1,292	299.1626	2.8	97,035	348	2,844	110,796	4
M315_R1032_12439	IDDP fragment 3	1,032	315.1710	3.1	678	311	2,025	548	4
M315_R721_12441	IDDP fragment 3	721	315.1733	4.1	2,714	642	2,796	2,523	4
M315_R890_12438	IDDP fragment 3	890	315.1713	2.1	3,465	257	1,242	6,650	4
M323_R682_13202	TEHP fragment 3	683	323.2332	4.4	7,118	138	891	22,376	4
M323_R746_13205	TEHP fragment 3	746	323.2336	3.0	65,358	0	5,938	174,300	2
M95_R468_479	Phenol	468	95.0488	3.5	879	164	581	3,481	4

Table 5-17 Features detected with LC-HRMS and suspect targets in a stormwater retention basin (RB) at the second sampling site before and after extraction from a HPTLC plate after separation and AChE-assay. The category levels were taken and adapted using the criteria described in Table 5-15.

Feature	Suspect	Retention time (sec)	m/z	Deviation (ppm)	HPTLC blank	Sample blank	Sample	HPTLC extract	Cat.
M167_R245_2319	Bendiocarb phenol	246	167.0702	0.5	399	225	245	2,028	4
M210_R582_4218	Propoxur	582	210.1118	3.1	3,962,996	11,153	811,072	4,578,327	4
M222_R533_4876	Carbofuran	533	222.1125	0.2	76,612	584	7,944	253,839	4
M223_R320_4966	Mexacarbate	320	223.1435	3.0	0	139	398	6,196	4
M223_R356_4967	Mexacarbate	356	223.1445	1.7	0	155	0	6,548	4
M223_R403_4965	Mexacarbate	403	223.1442	0.1	0	178	176	1,691	4
M223_R550_4963	Mexacarbate	550	223.1435	2.9	260,833	2,963	22,439	686,127	4
M224_R354_4994	Monocrotophos	354	224.0686	1.6	735	163	2,814	2,973	4
M238_R575_5896	3-Hydroxycarbofuran	575	238.1066	3.6	16,534	261	3,551	52,454	4
M289_R711_10044	Terbufos	711	289.0523	2.9	0	112,625	112,121	37,313	4
M299_R723_10977	Phoxim	723	299.0605	2.9	358	273	146	1,475	4
M299_R723_10977	Quinalphos	723	299.0605	2.9	358	273	146	1,475	4
M302_R779_11264	Fenoxycarb	779	302.1374	4.2	572	156	384	2,704	4
M399_R771_20053	TBOEP	771	399.2487	4.9	2,610	0	823	5,227	4
M435_R1142_23178	TEHP	1,142	435.3584	3.2	8,335	136	2,970	10,161	4
M453_R993_24640	T246MPP	993	453.2177	2.7	5,765	234	776	2,807	4
M495_R854_27860	T4TBPP	854	495.2646	2.6	0	190	415	5,385	4

6 General Conclusions and Outlook

In this work, an effect-directed analysis (EDA) was established and applied to investigate stormwater-dependent pollution of surface waters. The focus was on estrogenic, androgenic, and gestagenic effects and acetylcholinesterase inhibition (AChE-I). In order to be able to make a well-founded statement about the pollution situation in a study area, an EDA should be able to detect low concentrations of relevant substances in a repeatable and effective manner.

The sensitivity of high-performance thin-layer chromatography in combination with the yeast multi-endocrine effect screen (HPTLC-YMEES) to the reference hormones estrone (E1), estradiol (E2), 17 α -ethinylestradiol (EE2), 5 α -dihydrotestosterone (DHT), and progesterone (P4) was investigated and optimized. Compared to the planar yeast estrogen screen (p-YES), which in combination with HPTLC allows the determination of estrogenic activity, the HPTLC-YMEES is not as sensitive to the three estrogens E1, E2, and EE2 (SCHOENBORN et al., 2017; BERGMANN et al., 2020). However, a different transgenic yeast strain is used in the p-YES, in which the enzyme β -galactosidase is formed after binding of an estrogen to the estrogen receptor, and the determination of estrogenic activity is realized indirectly by conversion and measurement of a chromogenic or fluorogenic substrate, rather than measuring a directly formed fluorescent protein as in the YMEES. Compared to the limits of detection (LODs) of 40 and 60 pg/spot for E2 and E1, respectively, in a simultaneous detection of estrogenic and androgenic effects reported by MOSCOVICI et al. (2020), the ED of 1.4 pg/spot for E2 shown in this work was lower, while the ED of 95 pg/spot for E1 was higher. The dose-response studies showed that with appropriate prior enrichment, e.g., as in this work using solid phase extraction (SPE), the LODs of the 2018 EU watch list and environmental quality standards (EQS) of 400 pg/L for E1 and E2 and 35 pg/L for EE2 (EU, 2012, 2018) can be achieved with HPTLC-YMEES. For E1 and EE2, however, very high enrichment factors, a high application volume and/or multiple applications must be selected for various reasons. Both the enrichment factor with SPE and the volume applied, including the possibility of multiple applications, to the HPTLC plate can be varied. Due to the very low required LOD of 35 pg/L for EE2, the sensitivity of the test system, which was almost a factor of 10 better for EE2 than for low receptor affine E1, is nevertheless insufficient to avoid a high enrichment factor and application volume.

Compared to the planar yeast androgen screen (p-YAS), the HPTLC-YMEES showed a higher sensitivity to DHT. The ED of DHT was 7.4 pg/spot, whereas RIEGRAF et al. (2019) described an ED of 46 pg/spot. In the simultaneous measurement of androgenic and estrogenic effects, MOSCOVICI et al. (2020) determined a LOD of 400 pg/spot for DHT. Depending on sample enrichment and application volume, HPTLC-YMEES can detect the androgenic effect of DHT in the double-digit pg/L range. Based on the ED₂₀ of 17 pg/spot for DHT, 170 pg/L can be reliably detected with a 1000-fold enrichment and an

application volume of 100 μL . Thus, the concentrations of DHT in a range of 1.1 – 17 ng/L measured by GONZÁLEZ et al. (2020) in a lake influenced by a wastewater treatment plant (WWTP) can also be determined by HPTLC-YMEES.

Comparable studies on the sensitivity of a combination of HPTLC and yeast gestagen screens could not be found or have not yet been published. Compared to CHAMAS et al. (2017) the sensitivity of HPTLC-YMEES to P4 was increased. With appropriate enrichment, it is possible to detect concentrations in the triple-digit pg/L range with HPTLC-YMEES. Using the ED_{20} of 19 pg/spot for P4 as an example, 190 pg/L can be reliably detected with an application volume of 100 μL and prior 1000-fold enrichment. As demonstrated with the ED_{10} of 15 pg/spot, concentrations below this level are detectable, especially if a higher enrichment and application volume are chosen. Concentrations of P4 measured in a lake by GONZÁLEZ et al. (2020) and in surface waters compiled by FENT (2015) range from 2.6 to 7.5 ng/L and 0.1 to 38 ng/L, respectively, and are thus detectable by HPTLC-YMEES. Since gestagens with corresponding effects play a role in the aquatic environment, further studies investigating gestagenic effects using effect-based methods (EBMs) are appropriate. The combination of yeast gestagen screens with HPTLC, also in a mixture with other endocrine endpoints as shown in this work, is also quite reasonable. A comparison with the results of the HPTLC-YMEES determined here would be possible and further conclusions could be drawn.

In summary, the HPTLC-YMEES can be used to detect the effects of the reference hormones E1, E2, EE2, DHT, and P4 in an environmentally relevant pg/L range, and the performance in terms of sensitivity is comparable to other similar test systems. However, a further increased sensitivity of HPTLC-YMEES, especially towards EE2, is appropriate and should definitely be considered for further optimization of the overall method to avoid a high enrichment of a sample. This could be accomplished in several ways. One way might be to look for other non-human hormone receptors (HRs) for which the reference hormones have a higher binding affinity than for the human HRs. If different species-specific HRs were used, species-specific ecotoxicological statements on endocrine effects would also be possible to a certain extent. It needs to be clarified which HR from which species should be used and which reference hormone or endocrine-disruptive compound (EDC) is crucial, since the binding affinity differs depending on the ligand and receptor (BLAIR et al., 2000; DENNY et al., 2005; OJOGHORO et al., 2021). For example the binding affinity of E2 for human estrogen receptors is higher than for the rainbow trout estrogen receptor (PETIT et al., 1995). However, if the focus is on the analytical aspect, which is the main purpose of *in vitro* EBMs, it makes more sense to continue to use human receptors in order to maintain comparability between different yeast assays for the determination of endocrine effects. A better way to increase the sensitivity of HPTLC-YMEES to all substances that bind to one of the HRs would be to increase the brightness of the formed proteins.

The use of new or optimized fluorescent proteins (BALOBAN et al., 2017; SHEMETOV et al., 2017; MO et al., 2020), whose emitted light has a higher intensity, could allow detection with a lower amount of molecules binding to the receptors, thus making it possible to detect lower concentrations. Another possibility to increase sensitivity would be to use a different type of HPTLC plate, such as LiChrosphere plates, which, as shown in this work, allow narrower peaks of the hormones studied than on the SIL G-25 plates used for the dose-response studies. This allows a clearer demarcation to the baseline and a better differentiation of the hormones in a mixture and thus possibly a better detection with the subsequent YMEES at lower concentrations.

Mimicking the natural metabolism of organothiophosphates (OTPs) in the organism, where they are oxidized and thus acquire their strong inhibitory effect on AChE, is a good way to increase the sensitivity of AChE-I assays to OTPs. One approach is to use *n*-bromosuccinimide (NBS) as an oxidant, but this has never been tested in combination with HPTLC. The oxidation of the three OTPs tested works on HPTLC plates, also in the application with surface and stormwater. The sensitivity of the HPTLC-Ox-AChE-I to OTPs could significantly be increased compared to the unoxidized forms. Biological activation of OTPs on HPTLC plates, e.g., with enzymes, comes closer to the actual metabolism in organisms (AZADNIYA et al., 2020). Ultimately, this is also only a mimic and serves primarily to increase the sensitivity of the assay to OTPs. Oxidation with NBS is more efficient in terms of time and materials and is therefore more suitable for routine use. The sensitivity to chlorpyrifos and parathion after oxidation with NBS was, with an IC_{10} of 0.35 and 0.75 ng/spot, respectively, in a comparable range to AZADNIYA et al. (2020), who determined LODs of 0.28 and 0.20 ng/spot, respectively, after oxidation with a S9 mixture. Concentrations of chlorpyrifos and malathion detected in surface waters worldwide compiled by DE SOUZA et al. (2020) ranged from 0.32 and 3100 ng/L and 0.24 and 1800 ng/L, respectively. These concentrations can be detected by the HPTLC-Ox-AChE-I with appropriate prior enrichment and application volume. However, using the IC_{20} of 0.48 ng/spot for malathion as an example, an enrichment of 10,000 and an application volume of 200 μ L would have to be selected for the lowest malathion concentration (0.24 ng/L) shown by DE SOUZA et al. (2020) in order to detect it reliably. Since the AChE-I assay can only detect the effects of AChE inhibitors, additional assays with other neurotoxic endpoints, e.g., developmental neurotoxicity (LEE et al., 2022a), should be used to provide a comprehensive picture of neurotoxicity in water samples with EDA (LEE et al., 2022b).

Adjustments to the workflow of an EDA can increase sensitivity, but also precision. For this purpose, a comparison was made between two application methods, spraying and immersion, for the biosensors in both the HPTLC-YMEES and the HPTLC-Ox-AChE-I. The spray method was similar and, in some cases, slightly more sensitive to the hormones tested by HPTLC-YMEES. The comparison of the two methods of applying AChE solution to HPTLC plates, which had not been done before, resulted in a slightly higher

sensitivity of the HPTLC-Ox-AChE-I to the reference OTPs parathion, chlorpyrifos, and malathion oxidized with NBS when using the spray method. This raises the question why the spray method has the potential to be more sensitive, since blurred spots as shown by SCHOENBORN et al. (2017) were not observed and could be excluded as a cause in both studies. One assumption is that substances applied to the HPTLC plate are dissolved in the suspension or solution during the immersion process. This would have to be verified in further studies by analyzing the yeast suspension and AChE solution after immersion for substances previously bound to the HPTLC plate. Since the sensitivity differences between the two application techniques are small, this more in-depth analysis of the method was not performed in this work. The optimized spray method (including 180° plate rotation) resulted in the most uniform yeast distribution on the HPTLC plate and the highest precision. A subsequent question is whether automated spraying of yeast cells, as used by other authors (BERGMANN et al., 2020; RIEGRAF et al., 2021), can lead to even more homogeneous distribution and thus further increase of precision. Overall, a spray method for applying yeast cells onto HPTLC plates has the potential to achieve better sensitivity and precision than an immersion method, which is one reason that it is now common practice (MOSCOVICI et al., 2020; FINCKH et al., 2022; RIEGRAF et al., 2022; SCHREINER AND MORLOCK, 2023). Higher sensitivity and precision increase the likelihood of repeatable identification of effects in environmental samples triggered by substances at low concentrations. In addition, a spray method requires significantly less yeast suspension per HPTLC plate, so the only argument in favor of immersion is that it takes less time. Therefore, it is recommended to spray yeast cells onto HPTLC plates. For the AChE solution, no clear trend in precision was observed for the two application methods. In addition to the slightly higher sensitivity of the spray technique to OTPs, which can be used as a basis for decision making, efficiency may be a decisive factor, especially in routine use. The immersion method can be considered a more efficient application technique in this case due to substantially shorter time and AChE solution required compared to manual spraying. The AChE solution could be reused for up to 6 months without complications, unlike the yeast suspension of the YMEES. The actual consumption of AChE solution per HPTLC plate was therefore less than the volume required for each spray procedure. Therefore, it should be preferred to immerse HPTLC plates in the AChE solution in practical applications. If a spray method is to be used in future applications, an automated technique should be applied as in AZADNIYA AND MORLOCK (2019) to approximate the efficiency of the immersion method. Due to the large volume required and the low durability of the solutions, the immersion method is not suitable for the application of the oxidation (NBS) and substrate (indoxylacetate) solutions to HPTLC plates. At the concentrations used for both solutions, the material consumption would be too high, so in this work they were sprayed on from the beginning.

In conclusion, when combining HPTLC with EBMs, spraying seems to have a greater potential in terms of higher sensitivity compared to immersion, but both spraying and immersion are techniques that have their justification and remain in use for the application of substances to HPTLC plates. It depends on the analytical method and the solution, suspension, or substance to be applied which of the two techniques acquires highest sensitivity, precision, and accuracy and which can be used more efficiently (VASTA AND SHERMA, 2008; SCHOENBORN et al., 2017; AZADNIYA AND MORLOCK, 2019). Other less commonly used options for applying biosensors or other substances to HPTLC plates such as rolling or pressing should not be ignored, as they may also be useful for certain applications (VASTA AND SHERMA, 2008; BAUMGARTNER et al., 2011). When new analytical methods, whether chemical or biological, are to be established in combination with HPTLC, it is advisable to first compare several application techniques in terms of sensitivity, precision, and efficiency.

In the highly complex and often time-consuming field of EDA, efficiency plays a key role when it comes to more widespread and routine applications in the future. The HPTLC-YMEES offers tremendous time and material savings compared to single effect assays. However further optimization of the HPTLC-YMEES is necessary to avoid detection of one effect in the scan of the other. More studies are needed to efficiently and validly exploit the advantages of simultaneous determination of multiple endocrine effects in routine operations. In addition to the possibility of detecting multiple effects at different wavelengths, the use of various fluorescent proteins eliminates the need for a substrate and the associated incubation and application. However, efforts should be made to reduce the incubation time of the yeast cells on the HPTLC plate and bring it in line with other comparable assay systems such as the p-YES (SCHOENBORN et al., 2017; BERGMANN et al., 2020) to further reduce the time required for a complete run. A reduction from 18 h to 3 h is possible, although this needs to be verified since the YMEES uses a different yeast strain with different transgenic modifications than the p-YES. This work and MOSCOVICI et al. (2020) have successfully demonstrated the simultaneous determination of multiple endocrine effects in aquatic environmental samples on a single HPTLC plate using fluorescent proteins. It is highly recommended to combine the detection of endocrine effects into one analysis to reduce the high workload of a comprehensive EDA with multiple endocrine endpoints (RIEGRAF et al., 2021). In particular, the study of gestagenic effects, which has rarely been conducted in the aquatic environment and which was realized for the first time with the YMEES in combination with HPTLC by CHAMAS et al. (2017) and in an optimized form in this work, requires further studies. For example, the detection of P4 needs improvement, as it proved difficult because the peak height remained low and only the width increased with increasing concentration. This complicates the identification of gestagenic effects due to insufficient differentiation from baseline, especially at low concentrations. Starting from the estrogenic and androgenic effects studied by MOSCOVICI et al. (2020) and the gestagenic effects additionally studied in this work, the range of endocrine effects should be expanded

to include, for example, glucocorticoid effects. A simultaneous determination of multiple effects on one HPTLC plate also allows the determination of not only agonistic but also antagonistic hormonal effects and, in addition, the exclusion of possible false-positive cytotoxic effects (KLINGELHÖFER et al., 2020; RIEGRAF et al., 2022; RONZHEIMER et al., 2022). Since antagonistic effects have been found to play a role in the endocrine contamination of rivers due to combined sewer overflow (CSO) events and inadequate elimination by advanced wastewater treatment (ITZEL et al., 2019; WOLF et al., 2022), the YMEES should be expanded to include a method for determining antagonistic endocrine effects.

HPTLC is an open system in which the HPTLC plate passes through several separate steps, from pretreatment and sample application to development, chemical or biological analytical methods, and detection. All of these steps can be partially or fully automated, up to a completely automated run of the HPTLC plate through each step, increasing efficiency through unattended operation (Colin F. Poole, 2023). Accordingly, the trend in HPTLC is toward increasing automation. Further automation of HPTLC, especially in combination with EBMs, should be pursued to reduce the effort of extensive EDA if studies demonstrate higher efficiency, sensitivity and precision than manual procedures. In addition to commercially available automated HPTLC instruments, the HPTLC is also suitable for in-house automated solutions, for example by using a robotic arm that can be intuitively trained via drag and drop to feed the HPTLC plate to the individual stations. The open-source, automated, and miniaturized HPTLC solutions shown by FICHOU AND MORLOCK (2018) and SCHADE et al. (2021) demonstrate the possibility of building systems with comparable performance to commercially available instruments and highlight the advantage of HPTLC as an open chromatographic method. In contrast to high-performance liquid-chromatography (HPLC), HPTLC works both offline and online, can be set up in a simple manual or more complex automated manner without specialized companies, and is directly combinable with bioanalytical methods. The use of easy-to-establish, low-cost techniques and materials, such as airbrushing used in this work for the application of yeast cells, illustrates the possibility of applying HPTLC also in combination with EBMs on a low budget. An airbrush gun costs more than ten times less than a reagent sprayer from the laboratory supplier. Independent of HPTLC vendors, 3D printing and open source software solutions makes it relatively easy to manufacture instruments and integrate them into an automated workflow (HÄBE AND MORLOCK, 2020; JAXEL et al., 2020; MEHL et al., 2021). Thin layers can be 3D printed (FICHOU AND MORLOCK, 2017), and even the 3D printer itself can be transformed into a sample application device (WOORTMAN et al., 2020). Depending on the method, not even a professional detector is required, just visual observation and documentation with a camera or mobile phone (YU et al., 2016; SIBUG-TORRES et al., 2019). Image processing tools can be used to evaluate color information on the HPTLC plate.

All of this provides the basis for widespread application of EDA based on HPTLC and EBM in the future, even in developing countries with low research and monitoring budgets. This would promote the research community in such states and contribute to a better global understanding of pollution of the aquatic environment.

The influence of stormwater depending discharges on endocrine and neurotoxic loads was investigated in two differently characterized rivers. Due to the expected land-use related sources of EDCs and neurotoxic substances from both surface runoff and wastewater influenced discharges (WICKE et al., 2021), and the variety of pharmaceuticals, pesticides and industrial chemicals detected by target analysis (TA) using liquid chromatography coupled to tandem mass spectrometry (LC-MS/MS), it was assumed that endocrine and neurotoxic effects would also be detectable in the sampling areas. Estrogenic, androgenic, and gestagenic effects as well as estrogens were detected in the CSO effluent and downstream during rainy weather using HPTLC-YMEES and gas chromatography coupled to tandem mass spectrometry (GC-MS/MS). Further in-depth investigations with event-dependent sampling of composite samples at the CSO and the stormwater retention structure (SWR) and a comparison with long-term composite samples at the WWTP are necessary to determine the actual pollution situation and the respective contribution of the point sources in the investigated river section. However, the CSO can be considered as a major contributor to the endocrine load when it discharges wastewater to the river, also compared to the sample site downstream of the WWTP. As shown by ELSKENS et al. (2023), the contribution of CSOs to the estrogenic load of a water body can be comparable to that of WWTPs. Estrogenic, but also antagonistic estrogenic and androgenic effects were detected downstream of a CSO after an overflow event by WOLF et al. (2022), with concentrations partly higher than in the effluent of a subsequent WWTP. In addition to determined concentrations induced by WWTPs, CSOs, and storm sewer outlets, annual loads would have to be considered for a good comparison between the different point sources (NICKEL AND FUCHS, 2019; NICKEL et al., 2021). Due to the endocrine stress on water bodies caused by CSOs, the need for further research, including antagonistic effects, and intensified monitoring of CSOs is evident, also in the light of climate change-induced increases in the intensity and frequency of heavy rainfall events and further growth of urbanization with the associated increase in overflow events. In this regard, the use of EDA can enable the identification of effect-causing EDCs discharged to surface waters by CSOs (PETRIE, 2021). The reference hormones and the estrogens detected give a strong indication of which hormones are at least partly responsible for the effects observed. TA using GC-MS/MS and the alternative method LC-MS/MS for the detection of estrogens (ISO, 2024) should be expanded to include other relevant hormones such as androgens and gestagens. GC-MS/MS and HPTLC-YMEES complement each other well because of the ability to determine known hormones responsible for effects and the potential to compensate for insufficient sensitivity of one method by the other.

Nevertheless, extraction of effect spots from the HPTLC plate and subsequent analysis with TA, suspect and non-target screening (SNTS) is useful to establish a more direct link and comparability of results within an EDA and also to allow determination of possible unknown effect-responsible substances. EDA is a useful tool to provide a more comprehensive picture of endocrine exposure and other pressures, such as neurotoxic effects, emanating from stormwater-dependent discharges. In this context, the identification of the substances responsible for the effects plays an essential role, as it allows not only better containment of possible sources of contamination, but also the derivation of regulatory and integrated environmental protection measures for individual substances. The AChE-I effect detected by HPTLC-Ox-AChE-I in a stormwater basin receiving highway runoff should therefore be attributed to the responsible substances to confirm the assumption that the highway runoff is the route of entry. The question was whether the EDA used, consisting of HPTLC-Ox-AChE-I followed by SNTS with high-resolution mass spectrometry (HRMS), could identify the responsible AChE inhibitors. To increase the efficiency of the entire workflow and thus reduce the overall effort, the effect spot was extracted directly from the HPTLC plate on which the oxidation and AChE-I assay were performed. When using this approach, care should be taken to avoid further alteration of the extract after extraction by substances from previous steps, such as oxidation on the HPTLC plate. In addition, methods should be used to prevent matrix components present in the extract, e.g., from previous oxidation or from the medium of the bioassay performed on the HPTLC plate, from entering the subsequent HRMS and causing ion suppression or signal overlay (SCHREINER AND MORLOCK, 2021). No AChE inhibitors could be identified in the extract of the effect spot by SNTS workflow used, probably due to the problems mentioned above. Nevertheless, in an EDA using HPTLC-EBM, samples can be focused on toxicologically relevant parts and the effect relevant features of a subsequent SNTS can be reduced compared to the original sample, making substance identification more likely (STÜTZ et al., 2020). In addition, the effects detected with the respective EBM, further meta-information from the sampling area, and properties of suspect target substances can lead to a narrowing of the relevant features and thus also increase the probability of identifying effect-causing substances.

Even if no AChE inhibitor could be identified, the AChE-I effect detected in a stormwater basin connected to a highway indicates that neurotoxic effects in the environment are not only caused by pesticides, but also by other groups of substances such as plasticizers or flame retardants (CHEN et al., 2021; SHI et al., 2021). Accordingly, the sensitivity of HPTLC-Ox-AChE-I to these substance groups should also be tested and, if necessary, increased by further adjustments to determine the occurrence of such AChE-I effects in the aquatic environment at relevant concentrations. Regarding endocrine effects, in addition to the reference hormones studied in this work, other natural hormones, such as the estrogens studied by TANG et al. (2021), which have received little scientific attention, as well as synthetic hormones (ROCHA AND ROCHA, 2022) are released into the aquatic environment.

In addition, EDCs such as industrial chemicals, pesticides or pharmaceuticals used for a variety of purposes, as well as metabolites and transformation products, pose a risk to aquatic systems that has not yet been adequately studied and assessed (GROBIN et al., 2022). The extent to which the sensitivity of the YMEES is sufficient to detect additional natural and synthetic hormones as well as other EDCs in the aquatic environment is not clear due to the large number of possible endocrine active substances and needs to be investigated for further relevant compounds, which are known to be continuously released to the aquatic environment, which are considered priority substances, for which environmental quality standards have been established, or which generally have a high (eco)toxicological potential. However, it is clear that the large number of known and unknown EDCs and neurotoxicants cannot be captured by conventional TA alone, highlighting the importance of EDA. EDA, for example the combination of HPTLC and YMEES or AChE-I assay, allows the targeted detection of endocrine or neurotoxic active sample components, reduces sample complexity and thus increases the likelihood of identifying effect-relevant compounds with further analytical methods.

As aptly described by WILSON AND POOLE (2023), HPTLC remains a relevant and justified technique as an open chromatographic format with possibilities for combination with EBMs and chemical analytical methods, and can be particularly useful in EDA approaches. Effect-causing substances have already been attributed to the observed effects, not only in water but also food analysis (STÜTZ et al., 2020; BELL et al., 2021; AGATONOVIC-KUSTRIN et al., 2023; SCHREINER AND MORLOCK, 2023). The optimized combinations of HPTLC with YMEES and AChE-I assay provide two HPTLC-EBM methods with good performance in terms of sensitivity, precision and efficiency for direct applicability in EDA approaches to monitor and assess endocrine and neurotoxic contamination of surface waters. The results of this work thus contribute to the field of investigating harmful inputs to the aquatic environment with efficient focused EDA methods to identify effects and responsible active substances. With EDA, a much more specific analysis can be achieved that is not limited to known analytes. A much broader range of substances and their effects in environmental matrices can be covered with different EBMs, various known and unknown substances can be addressed in combination with chemical-analytical methods, and the ecotoxicological relevance could subsequently be confirmed with *in vivo* methods (MUSCHKET et al., 2018; KIM et al., 2019; ZWART et al., 2020; LOPEZ-HERGUEDAS et al., 2022). In addition to studies of discharges from WWTPs, EDA can also provide a better understanding of sources, input and transformation pathways, effects, and efficiencies of potential treatment processes with regard to point or diffuse inputs to surface waters following heavy precipitation events. This can promote good chemical and ecological status as required by the Water Framework Directive (EU, 2000) and enhance the maintenance or establishment of ecosystem functions of water bodies and thus the provision of ecosystem services. Because of the far-reaching consequences of exposure to substances for

organisms and the potential effects on populations, communities, ecosystems, the entire biosphere, and ultimately humans, it is essential to understand the routes of entry, the occurrence in various environmental compartments, and the ecotoxicological effects of contaminants. The qualitative and quantitative determination of substances and their ecotoxicological potential in various environmental media such as surface water, groundwater and wastewater is therefore of great importance for the development and purposive implementation of integrated environmental protection measures for the sustainable production, use and disposal of chemicals as well as end-of-pipe technologies to reduce environmental pollution. EDA should be used to make targeted and meaningful statements about the sampling site, the substances responsible for the effects, and possible treatment and mitigation methods. This work will serve as a basis for establishing an EDA for further studies of surface water pollution from WWTPs and stormwater depending discharges. Further advanced treatment measures at WWTPs and more extensive treatment of stormwater discharges to protect surface waters from harmful substances, e.g. micropollutants, need to be established and evaluated (PISTOCCHI et al., 2022), also in the light of a new EU Urban Wastewater Treatment Directive (EU, 2022). Since these technical solutions are expensive and do not cover diffuse inputs, integrated environmental protection with renunciation or environmentally friendly substitution of hazardous substances is a real alternative, but more difficult to implement (EU, 2020; SCHOLZ et al., 2022).

Knowledge generated by intelligently linked analytical methods about the origin, occurrence, behavior, and effects of substances in the environment can help to better estimate the planetary boundary of novel entities described by ROCKSTRÖM et al. (2009), to link it to other global limits such as climate change or biosphere integrity, and to develop sustainable regulatory measures to prevent the release of chemicals into the environment in order to meet or regain the global chemical pollution limit (PERSSON et al., 2022; ARP et al., 2023; RICHARDSON et al., 2023). Ultimately, this contributes to the preservation and restoration of an environment that allows humanity to live and develop safely, now and in future generations.

6.1. References

- Agatonovic-Kustrin S., Wong S., Dolzhenko A. V., Gegechkori V., Ku H., Tucci J., Morton D. W., 2023. Evaluation of bioactive compounds from *Ficus carica* L. leaf extracts via high-performance thin-layer chromatography combined with effect-directed analysis. *Journal of Chromatography A*, 1706, 464241. <https://doi.org/10.1016/j.chroma.2023.464241>.
- Arp H. P. H., Aurich D., Schymanski E. L., Sims K., Hale S. E., 2023. Avoiding the Next Silent Spring: Our Chemical Past, Present, and Future. *Environmental Science & Technology*, 57 (16), 6355–6359. <https://doi.org/10.1021/acs.est.3c01735>.
- Azadniya E. and Morlock G. E., 2019. Automated piezoelectric spraying of biological and enzymatic assays for effect-directed analysis of planar chromatograms. *Journal of Chromatography A*, 1602, 458–466. <https://doi.org/10.1016/j.chroma.2019.05.043>.
- Azadniya E., Mollergues J., Stroheker T., Billerbeck K., Morlock G. E., 2020. New incorporation of the S9 metabolizing system into methods for detecting acetylcholinesterase inhibition. *Analytica Chimica Acta*, 1129, 76–84. <https://doi.org/10.1016/j.aca.2020.06.033>.
- Baloban M., Shcherbakova D. M., Pletnev S., Pletnev V. Z., Lagarias J. C., Verkhusha V. V., 2017. Designing brighter near-infrared fluorescent proteins: insights from structural and biochemical studies. *Chemical Science*, 8 (6), 4546–4557. <https://doi.org/10.1039/c7sc00855d>.
- Baumgartner V., Hohl C., Schwack W., 2011. Rolling--a new application technique for luminescent bacteria on high-performance thin-layer chromatography plates. *Journal of Chromatography A*, 1218 (19), 2692–2699. <https://doi.org/10.1016/j.chroma.2011.01.039>.
- Bell A. M., Keltsch N., Schweyen P., Reifferscheid G., Ternes T., Buchinger S., 2021. UV aged epoxy coatings - Ecotoxicological effects and released compounds. *Water Research X*, 12, 100105. <https://doi.org/10.1016/j.wroa.2021.100105>.
- Bergmann A. J., Simon E., Schifferli A., Schönborn A., Vermeirssen E. L. M., 2020. Estrogenic activity of food contact materials-evaluation of 20 chemicals using a yeast estrogen screen on HPTLC or 96-well plates. *Analytical and Bioanalytical Chemistry*, 412 (19), 4527–4536. <https://doi.org/10.1007/s00216-020-02701-w>.
- Blair R. M., Fang H., Branham W. S., Hass B. S., Dial S. L., Moland C. L., Tong W., Shi L., Perkins R., Sheehan D. M., 2000. The estrogen receptor relative binding affinities of 188 natural and xenochemicals: structural diversity of ligands. *Toxicological Sciences*, 54 (1), 138–153. <https://doi.org/10.1093/toxsci/54.1.138>.
- Chamas A., Pham H. T. M., Jähne M., Hettwer K., Gehrman L., Tuerk J., Uhlig S., Simon K., Baronian K., Kunze G., 2017. Separation and identification of hormone-active compounds using a combination of chromatographic separation and yeast-based reporter assay. *Science of the Total Environment*, 605-606, 507–513. <https://doi.org/10.1016/j.scitotenv.2017.06.077>.
- Chen X., Guo W., Lei L., Guo Y., Yang L., Han J., Zhou B., 2021. Bioconcentration and developmental neurotoxicity of novel brominated flame retardants, hexabromobenzene and pentabromobenzene in zebrafish. *Environmental Pollution*, 268 (Pt B), 115895. <https://doi.org/10.1016/j.envpol.2020.115895>.
- Colin F. Poole, 2023. Chapter 5. Instrument platforms for high-performance thin-layer chromatography. In: Colin F. Poole (ed.), *Handbooks in Separation Science, Instrumental Thin-Layer Chromatography*, 2nd ed., pp. 111–142. Elsevier.
- De Souza R. M., Seibert D., Quesada H. B., De Jesus Bassetti F., Fagundes-Klen M. R., Bergamasco R., 2020. Occurrence, impacts and general aspects of pesticides in surface water: A review. *Process Safety and Environmental Protection*, 135, 22–37. <https://doi.org/10.1016/j.psep.2019.12.035>.

- Denny J. S., Tapper M. A., Schmieder P. K., Hornung M. W., Jensen K. M., Ankley G. T., Henry T. R., 2005. Comparison of relative binding affinities of endocrine active compounds to fathead minnow and rainbow trout estrogen receptors. *Environmental Toxicology and Chemistry*, 24 (11), 2948–2953. <https://doi.org/10.1897/04-595r.1>.
- Elskens M., Van Langenhove K., Carbonnel V., Brion N., Eisenreich S. J., 2023. Dynamics of estrogenic activity in an urban river receiving wastewater effluents: effect-based measurements with CALUX. *Water Emerging Contaminants & Nanoplastics*, 2, 9–25. <https://doi.org/10.20517/wecn.2023.15>.
- EU, 2000. DIRECTIVE 2000/60/EC OF THE EUROPEAN PARLIAMENT AND OF THE COUNCIL of 23 October 2000 establishing a framework for Community action in the field of water policy (WFD). Official Journal of the European Communities.
- EU, 2012. Proposal for a DIRECTIVE OF THE EUROPEAN PARLIAMENT AND OF THE COUNCIL amending Directives 2000/60/EC and 2008/105/EC as regards priority substances in the field of water policy.
- EU, 2018. COMMISSION IMPLEMENTING DECISION (EU) 2018/ 840 - of 5 June 2018 - establishing a watch list of substances for Union-wide monitoring in the field of water policy pursuant to Directive 2008/ 105/ EC of the European Parliament and of the Council and repealing Commission Implementing Decision (EU) 2015/ 495 - (notified under document C(2018) 3362) (Watch List). Official Journal of the European Union.
- EU, 2020. COMMUNICATION FROM THE COMMISSION TO THE EUROPEAN PARLIAMENT, THE COUNCIL, THE EUROPEAN ECONOMIC AND SOCIAL COMMITTEE AND THE COMMITTEE OF THE REGIONS. Chemicals Strategy for Sustainability Towards a Toxic-Free Environment. <https://eur-lex.europa.eu/legal-content/EN/TXT/?uri=COM%3A2020%3A667%3AFIN>.
- EU, 2022. Proposal for a DIRECTIVE OF THE EUROPEAN PARLIAMENT AND OF THE COUNCIL concerning urban wastewater treatment (recast). <https://eur-lex.europa.eu/legal-content/EN/TXT/?uri=COM%3A2022%3A541%3AFIN>.
- Fent K., 2015. Progestins as endocrine disrupters in aquatic ecosystems: Concentrations, effects and risk assessment. *Environment International*, 84, 115–130. <https://doi.org/10.1016/j.envint.2015.06.012>.
- Fichou D. and Morlock G. E., 2017. Open-Source-Based 3D Printing of Thin Silica Gel Layers in Planar Chromatography. *Analytical Chemistry*, 89 (3), 2116–2122. <https://doi.org/10.1021/acs.analchem.6b04813>.
- Fichou D. and Morlock G. E., 2018. Office Chromatography: Miniaturized All-in-One Open-Source System for Planar Chromatography. *Analytical Chemistry*, 90 (21), 12647–12654. <https://doi.org/10.1021/acs.analchem.8b02866>.
- Finckh S., Buchinger S., Escher B. I., Hollert H., König M., Krauss M., Leekitratapanisan W., Schiwy S., Schlichting R., Shuliakovich A., Brack W., 2022. Endocrine disrupting chemicals entering European rivers: Occurrence and adverse mixture effects in treated wastewater. *Environment International*, 170, 107608. <https://doi.org/10.1016/j.envint.2022.107608>.
- González A., Kroll K. J., Silva-Sanchez C., Carriquiriborde P., Fernandino J. I., Denslow N. D., Somoza G. M., 2020. Steroid hormones and estrogenic activity in the wastewater outfall and receiving waters of the Chascomús chained shallow lakes system (Argentina). *Science of the Total Environment*, 743, 140401. <https://doi.org/10.1016/j.scitotenv.2020.140401>.
- Grobin A., Roškar R., Trontelj J., 2022. Multi-parameter risk assessment of forty-one selected substances with endocrine disruptive properties in surface waters worldwide. *Chemosphere*, 287 (Pt 2), 132195. <https://doi.org/10.1016/j.chemosphere.2021.132195>.

- Häbe T. T. and Morlock G. E., 2020. Open-source add-on kit for automation of zone elution in planar chromatography. *Rapid Communications in Mass Spectrometry*, 34 (7), e8631. <https://doi.org/10.1002/rcm.8631>.
- ISO (International Organization for Standardization), 2024. Water quality — Determination of selected estrogens in whole water samples — Method using solid phase extraction (SPE) followed by liquid chromatography (LC) or gas chromatography (GC) coupled to mass spectrometry (MS) detection. ISO/DIS 13646. 13.060.50.
- Itzel F., Gehrman L., Teutenberg T., Schmidt T. C., Tuerk J., 2019. Recent developments and concepts of effect-based methods for the detection of endocrine activity and the importance of antagonistic effects. *TrAC Trends in Analytical Chemistry*, 118 (21), 699–708. <https://doi.org/10.1016/j.trac.2019.06.030>.
- Jaxel J., Guggenberger M., Rosenau T., Böhmendorfer S., 2020. Unbreakable and customizable dipping chambers for TLC and HPTLC manufactured by fused deposition modelling. *Talanta*, 217, 121072. <https://doi.org/10.1016/j.talanta.2020.121072>.
- Kim J., Hong S., Cha J., Lee J., Kim T., Lee S., Moon H.-B., Shin K.-H., Hur J., Lee J.-S., Giesy J. P., Khim J. S., 2019. Newly Identified AhR-Active Compounds in the Sediments of an Industrial Area Using Effect-Directed Analysis. *Environmental Science & Technology*, 53 (17), 10043–10052. <https://doi.org/10.1021/acs.est.9b02166>.
- Klingelhöfer I., Hockamp N., Morlock G. E., 2020. Non-targeted detection and differentiation of agonists versus antagonists, directly in bioprofiles of everyday products. *Analytica Chimica Acta*, 1125, 288–298. <https://doi.org/10.1016/j.aca.2020.05.057>.
- Lee J., Escher B. I., Scholz S., Schlichting R., 2022a. Inhibition of neurite outgrowth and enhanced effects compared to baseline toxicity in SH-SY5Y cells. *Archives of Toxicology*, 96 (4), 1039–1053. <https://doi.org/10.1007/s00204-022-03237-x>.
- Lee J., Schlichting R., König M., Scholz S., Krauss M., Escher B. I., 2022b. Monitoring Mixture Effects of Neurotoxicants in Surface Water and Wastewater Treatment Plant Effluents with Neurite Outgrowth Inhibition in SH-SY5Y Cells. *ACS Environmental Au*, 2 (6), 523–535. <https://doi.org/10.1021/acsenvironau.2c00026>.
- Lopez-Herguedas N., González-Gaya B., Cano A., Alvarez-Mora I., Mijangos L., Etxebarria N., Zuloaga O., Olivares M., Prieto A., 2022. Effect-directed analysis of a hospital effluent sample using A-YES for the identification of endocrine disrupting compounds. *Science of the Total Environment*, 850, 157985. <https://doi.org/10.1016/j.scitotenv.2022.157985>.
- Mehl A., Schwack W., Morlock G. E., 2021. On-surface autosampling for liquid chromatography-mass spectrometry. *Journal of Chromatography A*, 1651, 462334. <https://doi.org/10.1016/j.chroma.2021.462334>.
- Mo G. C. H., Posner C., Rodriguez E. A., Sun T., Zhang J., 2020. A rationally enhanced red fluorescent protein expands the utility of FRET biosensors. *Nature Communications*, 11 (1), 1848. <https://doi.org/10.1038/s41467-020-15687-x>.
- Moscovici L., Riegraf C., Abu-Rmailah N., Atias H., Shakibai D., Buchinger S., Reifferscheid G., Belkin S., 2020. Yeast-Based Fluorescent Sensors for the Simultaneous Detection of Estrogenic and Androgenic Compounds, Coupled with High-Performance Thin Layer Chromatography. *Biosensors*, 10 (11), 169. <https://doi.org/10.3390/bios10110169>.
- Muschket M., Di Paolo C., Tindall A. J., Touak G., Phan A., Krauss M., Kirchner K., Seiler T.-B., Hollert H., Brack W., 2018. Identification of Unknown Antiandrogenic Compounds in Surface Waters by Effect-Directed Analysis (EDA) Using a Parallel Fractionation Approach. *Environmental Science & Technology*, 52 (1), 288–297. <https://doi.org/10.1021/acs.est.7b04994>.

- Nickel J. P. and Fuchs S., 2019. Micropollutant emissions from combined sewer overflows. *Water Science and Technology*, 80 (11), 2179–2190. <https://doi.org/10.2166/wst.2020.035>.
- Nickel J. P., Sacher F., Fuchs S., 2021. Up-to-date monitoring data of wastewater and stormwater quality in Germany. *Water Research*, 202, 117452. <https://doi.org/10.1016/j.watres.2021.117452>.
- Ojogoro J. O., Scrimshaw M. D., Sumpter J. P., 2021. Steroid hormones in the aquatic environment. *Science of the Total Environment*, 792, 148306. <https://doi.org/10.1016/j.scitotenv.2021.148306>.
- Persson L., Carney Almroth B. M., Collins C. D., Cornell S., De Wit C. A., Diamond M. L., Fantke P., Hassellöv M., MacLeod M., Ryberg M. W., Søggaard Jørgensen P., Villarrubia-Gómez P., Wang Z., Hauschild M. Z., 2022. Outside the Safe Operating Space of the Planetary Boundary for Novel Entities. *Environmental Science & Technology*, 56 (3), 1510–1521. <https://doi.org/10.1021/acs.est.1c04158>.
- Petit F., Valotaire Y., Pakdel F., 1995. Differential functional activities of rainbow trout and human estrogen receptors expressed in the yeast *Saccharomyces cerevisiae*. *European Journal of Biochemistry*, 233 (2), 584–592. https://doi.org/10.1111/j.1432-1033.1995.584_2.x.
- Petrie B., 2021. A review of combined sewer overflows as a source of wastewater-derived emerging contaminants in the environment and their management. *Environmental Science and Pollution Research International*, 28 (25), 32095–32110. <https://doi.org/10.1007/s11356-021-14103-1>.
- Pistocchi A., Alygizakis N. A., Brack W., Boxall A., Cousins I. T., Drewes J. E., Finckh S., Gallé T., Launay M. A., McLachlan M. S., Petrovic M., Schulze T., Slobodnik J., Ternes T., Van Wezel A., Verlicchi P., Whalley C., 2022. European scale assessment of the potential of ozonation and activated carbon treatment to reduce micropollutant emissions with wastewater. *Science of the Total Environment*, 848, 157124. <https://doi.org/10.1016/j.scitotenv.2022.157124>.
- Richardson K., Steffen W., Lucht W., Bendtsen J., Cornell S. E., Donges J. F., Drüke M., Fetzer I., Bala G., Von Bloh W., Feulner G., Fiedler S., Gerten D., Gleeson T., Hofmann M., Huiskamp W., Kummu M., Mohan C., Nogués-Bravo D., Petri S., Porkka M., Rahmstorf S., Schaphoff S., Thonicke K., Tobian A., Virkki V., Wang-Erlandsson L., Weber L., Rockström J., 2023. Earth beyond six of nine planetary boundaries. *Science Advances*, 9 (37), eadh2458. <https://doi.org/10.1126/sciadv.adh2458>.
- Riegraf C., Bell A. M., Ohlig M., Reifferscheid G., Buchinger S., 2022. Planar chromatography-bioassays for the parallel and sensitive detection of androgenicity, anti-androgenicity and cytotoxicity. *Journal of Chromatography A*, 1684, 463582. <https://doi.org/10.1016/j.chroma.2022.463582>.
- Riegraf C., Reifferscheid G., Belkin S., Moscovici L., Shakibai D., Hollert H., Buchinger S., 2019. Combination of yeast-based in vitro screens with high-performance thin-layer chromatography as a novel tool for the detection of hormonal and dioxin-like compounds. *Analytica Chimica Acta*, 1081, 218–230. <https://doi.org/10.1016/j.aca.2019.07.018>.
- Riegraf C., Reifferscheid G., Moscovici L., Shakibai D., Hollert H., Belkin S., Buchinger S., 2021. Coupling high-performance thin-layer chromatography with a battery of cell-based assays reveals bioactive components in wastewater and landfill leachates. *Ecotoxicology and Environmental Safety*, 214, 112092. <https://doi.org/10.1016/j.ecoenv.2021.112092>.
- Rocha M. J. and Rocha E., 2022. Synthetic Progestins in Waste and Surface Waters: Concentrations, Impacts and Ecological Risk. *Toxics*, 10 (4), 163. <https://doi.org/10.3390/toxics10040163>.

- Rockström J., Steffen W., Noone K., Persson Å., Chapin F. S. III, Lambin E., Lenton T. M., Scheffer M., Folke C., Schellnhuber H. J., Nykvist B., De Wit C. A., Hughes T., Van der Leeuw S., Rodhe H., Sörlin S., Snyder P. K., Costanza R., Svedin U., Falkenmark M., Karlberg L., Corell R. W., Fabry V. J., Hansen J., Walker B., Liverman D., Richardson K., Crutzen P., Foley J., 2009. Planetary Boundaries: Exploring the Safe Operating Space for Humanity. *Ecology and Society*, 14, 32. <https://www.ecologyandsociety.org/vol14/iss2/art32/>.
- Ronzheimer A., Schreiner T., Morlock G. E., 2022. Multiplex planar bioassay detecting estrogens, antiestrogens, false-positives and synergists as sharp zones on normal phase. *Phytomedicine*, 103, 154230. <https://doi.org/10.1016/j.phymed.2022.154230>.
- Schade F., Schwack W., Demirbas Y., Morlock G. E., 2021. Open-source all-in-one LabToGo Office Chromatography. *Analytica Chimica Acta*, 1174, 338702. <https://doi.org/10.1016/j.aca.2021.338702>.
- Schoenborn A., Schmid P., Bräm S., Reifferscheid G., Ohlig M., Buchinger S., 2017. Unprecedented sensitivity of the planar yeast estrogen screen by using a spray-on technology. *Journal of Chromatography A*, 1530, 185–191. <https://doi.org/10.1016/j.chroma.2017.11.009>.
- Scholz S., Brack W., Escher B. I., Hackermüller J., Liess M., Von Bergen M., Wick L. Y., Zenclussen A. C., Altenburger R., 2022. The EU chemicals strategy for sustainability: an opportunity to develop new approaches for hazard and risk assessment. *Archives of Toxicology*, 96 (8), 2381–2386. <https://doi.org/10.1007/s00204-022-03313-2>.
- Schreiner T. and Morlock G. E., 2021. Non-target bioanalytical eight-dimensional hyphenation including bioassay, heart-cut trapping, online desalting, orthogonal separations and mass spectrometry. *Journal of Chromatography A*, 1647, 462154. <https://doi.org/10.1016/j.chroma.2021.462154>.
- Schreiner T. and Morlock G. E., 2023. Investigation of the estrogenic potential of 15 rosé, white and red wines via effect-directed ten-dimensional hyphenation. *Journal of Chromatography A*, 1690, 463775. <https://doi.org/10.1016/j.chroma.2023.463775>.
- Shemetov A. A., Oliinyk O. S., Verkhusha V. V., 2017. How to Increase Brightness of Near-Infrared Fluorescent Proteins in Mammalian Cells. *Cell Chemical Biology*, 24 (6), 758-766.e3. <https://doi.org/10.1016/j.chembiol.2017.05.018>.
- Shi Q., Guo W., Shen Q., Han J., Lei L., Chen L., Yang L., Feng C., Zhou B., 2021. In vitro biolayer interferometry analysis of acetylcholinesterase as a potential target of aryl-organophosphorus flame-retardants. *Journal of Hazardous Materials*, 409, 124999. <https://doi.org/10.1016/j.jhazmat.2020.124999>.
- Sibug-Torres S. M., Padolina I. D., Cruz P., Garcia F. C., Garrovillas M. J., Yabillo M. R., Enriquez E. P., 2019. Smartphone-based image analysis and chemometric pattern recognition of the thin-layer chromatographic fingerprints of herbal materials. *Analytical Methods*, 11 (6), 721–732. <https://doi.org/10.1039/C8AY02698J>.
- Stütz L., Schulz W., Winzenbacher R., 2020. Identification of acetylcholinesterase inhibitors in water by combining two-dimensional thin-layer chromatography and high-resolution mass spectrometry. *Journal of Chromatography A*, 1624, 461239. <https://doi.org/10.1016/j.chroma.2020.461239>.
- Tang Z., Liu Z.-h., Wan Y.-p., Wang H., Dang Z., Liu Y., 2021. Far-Less Studied Natural Estrogens as Ignored Emerging Contaminants in Surface Water: Insights from Their Occurrence in the Pearl River, South China. *ACS ES&T Water*, 1 (8), 1776–1784. <https://doi.org/10.1021/acsestwater.1c00109>.

- Vasta J. V. and Sherma J., 2008. Comparison of spraying, dipping, and the derivapress for postchromatic derivatization with phosphomolybdic acid in the detection and quantification of neutral lipids by high-performance thin-layer chromatography. *Acta Chromatographica*, 20 (1), 15–23. <https://doi.org/10.1556/AChrom.20.2008.1.2>.
- Wicke D., Matzinger A., Sonnenberg H., Caradot N., Schubert R.-L., Dick R., Heinzmann B., Dünnbier U., Von Seggern D., Rouault P., 2021. Micropollutants in Urban Stormwater Runoff of Different Land Uses. *Water*, 13 (9), 1312. <https://doi.org/10.3390/w13091312>.
- Wilson I. D. and Poole C. F., 2023. Planar chromatography - Current practice and future prospects. *Journal of Chromatography B*, 1214, 123553. <https://doi.org/10.1016/j.jchromb.2022.123553>.
- Wolf Y., Oster S., Shuliakevich A., Brückner I., Dolny R., Linnemann V., Pinnekamp J., Hollert H., Schiwy S., 2022. Improvement of wastewater and water quality via a full-scale ozonation plant? - A comprehensive analysis of the endocrine potential using effect-based methods. *Science of the Total Environment*, 803, 149756. <https://doi.org/10.1016/j.scitotenv.2021.149756>.
- Woortman D. V., Haack M., Mehlmer N., Brück T. B., 2020. Additive Analytics: Easy Transformation of Low-Cost Fused Deposition Modeling Three-Dimensional Printers for HPTLC Sample Application. *ACS Omega*, 5 (19), 11147–11150. <https://doi.org/10.1021/acsomega.0c01096>.
- Yu H., Le H. M., Kaale E., Long K. D., Layloff T., Lumetta S. S., Cunningham B. T., 2016. Characterization of drug authenticity using thin-layer chromatography imaging with a mobile phone. *Journal of Pharmaceutical and Biomedical Analysis*, 125, 85–93. <https://doi.org/10.1016/j.jpba.2016.03.018>.
- Zwart N., Jonker W., Ten Broek R., De Boer J., Somsen G., Kool J., Hamers T., Houtman C. J., Lamoree M. H., 2020. Identification of mutagenic and endocrine disrupting compounds in surface water and wastewater treatment plant effluents using high-resolution effect-directed analysis. *Water Research*, 168, 115204. <https://doi.org/10.1016/j.watres.2019.115204>.

Appendix

List of Figures

Figure 1-1 Environmental fate, ecotoxicology and risk assessment of contaminants released to the environment from anthropogenic sources	2
Figure 1-2 The hypothalamic-pituitary axis.....	5
Figure 1-3 Genesis of the major classes of steroid hormones: progestagens, mineralocorticoids, glucocorticoids, androgens, and estrogens.....	7
Figure 1-4 Organophosphate pesticides inhibit acetylcholinesterase	14
Figure 1-5 Scheme of a transgenic modified <i>Arxula adenivorans</i> cell	17
Figure 1-6 Information content of the different analytical approaches target analysis, suspect and non-target screening, and effect-directed analysis in relation to their complexity and probability of identifying effect-causing substances	18
Figure 2-1 Scope and relationship of chapters 3, 4, and 5.....	35
Figure 3-1 Separation of E2, DHT, EE2, P4, and E1 on LiChrospher, RP-18W, and SIL G-25 plates	45
Figure 3-2 Dose-response curves of E1, E2, EE2, DHT, and P4. The HPTLC plates were either immersed into the yeast suspension or the cells were sprayed onto the plates by airbrush	47
Figure 3-3 Chromatogram of estrogenic and androgenic effects in the outlet of the ozonation	51
Figure 3-4 Estrogenic and androgenic effects detected in samples from the municipal WWTP in Schwerte, Germany	53
Figure 3-5 Estrogenic, androgenic, and gestagenic effects detected in a sample from the Anger in Ratingen, Germany.....	55
Figure 3-6 The automated eight-step HPTLC development process for separation of E1, E2, EE2, DHT, and P4 on SIL G-25, RP-18W and LiChrospher HPTLC plates	60
Figure 3-7 The automated eight-step HPTLC development process for the analysis of environmental samples on SIL G-25 plates.....	61
Figure 3-8 The used spraying scheme for yeast cell application on HPTLC plates.....	61
Figure 3-9 The used optimized spraying scheme for yeast cell application on HPTLC plates.....	62
Figure 3-10 Scheme of the municipal WWTP in Schwerte, Germany.....	62
Figure 3-11 Comparison of immersion, spray, and optimized spray application regarding the yeast cell dispersion of 20 evenly distributed E2 spots on SIL G-25 plates.....	63
Figure 3-12 Effects of 30 pg, 100 pg, and 250 pg P4 on a SIL G-25 plate.....	64
Figure 3-13 Recovery rates and standard deviations of E2 after multiple application in comparison to a one-time application on a SIL G-25 plate	65

Figure 3-14 Effects of E2, EE2, and E1 in the estrogen, androgen, and gestagen scan on a SIL G-25 plate.....	66
Figure 3-15 Effects of DHT and P4 in the estrogen, androgen, and gestagen scan on a SIL G-25 plate.....	67
Figure 4-1 Dose-response curves of malathion, parathion, and chlorpyrifos, and malaoxon, paraoxon, and chlorpyrifos-oxon. An AChE inhibition assay for the detection of inhibition effects was performed in 96-well plates	77
Figure 4-2 Dose-response curves of different organothiophosphates and their oxons. After chromatographic separation by HPTLC, an AChE inhibition assay was performed	80
Figure 4-3 AChE inhibition effect in the sample of a stormwater retention basin	83
Figure 4-4 Flow chart of the acetylcholinesterase inhibition assay in microtiter plates	89
Figure 4-5 The automated four-step HPTLC development process for separation of organothiophosphates and their oxons on LiChrospher HPTLC plates.....	90
Figure 4-6 Peak areas of positive controls containing malathion, parathion, and chlorpyrifos. After chromatographic separation by HPTLC, an AChE inhibition assay with and without prior oxidation by n-bromosuccinimide was performed	90
Figure 4-7 Results of dose-response investigations for malathion, malaoxon, parathion, paraoxon, chlorpyrifos, and chlorpyrifos-oxon	91
Figure 4-8 Separation of an enriched combined sewer overflow sample with HPTLC on LiChrosphere plates Two automatic development procedures were used	92
Figure 5-1 Workflow of the HPTLC-Ox-AChE-I analysis with subsequent suspect and non-target screening with LC-HRMS of suspect effect-responsible substances.....	103
Figure 5-2 Concentrations of substances detected with LC-MS/MS in samples from stormwater structures and the receiving river Anger in Ratingen, Germany and from a stormwater retention basin, draining a highway, and the receiving small stream Deininghauser Bach near Deininghausen, Germany	105
Figure 5-3 Estrogenic, androgenic, and gestagenic effects detected in samples from stormwater structures and the receiving river Anger in Ratingen, Germany. The sampling was performed in March 2020 during rainy weather conditions	108
Figure 5-4 Sampling site 1 at the Anger in Ratingen, Germany	117
Figure 5-5 Sampling site 2 at the Deininghauser Bach in Deininghausen, Germany	118
Figure 5-6 Estrogenic effects detected in samples from stormwater structures and the receiving river Anger in Ratingen, Germany. The sampling was performed in August 2020 during dry weather conditions.....	119

Figure 5-7 Estrogenic and gestagenic effects detected in samples from a stormwater retention basin, draining a highway, and the receiving small stream Deininghauser Bach near Deininghausen, Germany. The sampling was performed in August 2020 during dry weather conditions	120
Figure 5-8 Retention time difference, m/z difference, number of shared top 10 MS^2 fragments, and MS^2 intensity correction of substances used for quality control for LC-HRMS measurement.....	121
Figure 5-9 Retention time difference, m/z difference, and recovery of internal standards spiked into the samples before LC-HRMS measurement.	122

List of Tables

Table 3-1 The mean retardation factors \pm standard deviations of E2, DHT, EE2, P4, and E1 on different HPTLC plate types.....	44
Table 3-2 Results of dose-response investigations. A mix of E1, E2, and EE2, and a mix of DHT and P4 were applied with different concentrations on SIL G-25 plates. The HPTLC plates were either immersed into the yeast suspension or the cells were sprayed onto the plates by airbrush	48
Table 3-3 Recovery rates of E1, E2, EE2, DHT, and P4 in the SPE quality controls in relation to the positive controls	52
Table 3-4 Composition of the used cultivation medium and test medium for the yeast multi-endocrine effect screen.....	68
Table 3-5 Concentrations and applied masses of E1, E2, and EE2 used for the dose-response investigations	68
Table 3-6 Concentrations and applied masses of DHT and P4 used for the dose-response investigations	69
Table 3-7 Comparison of immersion, spray, and optimized spray application regarding the yeast cell dispersion using the relative standard deviation of the peak areas of 20 evenly distributed E2 spots on SIL G-25 plates	69
Table 4-1 The mean retardation factor (R_F), standard deviation, calculated relative R_F , and resolution of malaoxon, paraoxon, chlorpyrifos-oxon, malathion, parathion, and chlorpyrifos on the LiChrospher HPTLC plate. After chromatographic separation, using a four step HPTLC development process the plates were measured with an AChE inhibition assay	78
Table 4-2 Recovery rates of the effect peak area of malathion, parathion, and chlorpyrifos. The mean peak areas of the spiked samples were related to the mean peak areas of the positive controls.....	82
Table 4-3 Concentrations of parathion, chlorpyrifos, and malathion used for dose-response investigations	93

Table 4-4 Concentrations of parathion, chlorpyrifos, malathion, paraoxon, chlorpyrifos-oxon, and malaoxon used for dose-response investigations.....	93
Table 4-5 Results of dose-response investigations for malathion, malaoxon, parathion, paraoxon, chlorpyrifos, and chlorpyrifos-oxon. An AChE assay for the detection of inhibition effects was performed in 96-well plates	94
Table 4-6 Results of dose-response investigations for malathion, malaoxon, parathion, paraoxon, chlorpyrifos, and chlorpyrifos-oxon. After chromatographic separation by HPTLC, an AChE inhibition assay was performed.....	95
Table 4-7 The mean retardation factor (R_f), standard deviation, calculated relative R_f , and resolution of malaoxon, paraoxon, chlorpyrifos-oxon, malathion, parathion, and chlorpyrifos on the LiChrospher HPTLC plate. After chromatographic separation, using a one-step HPTLC development process, the plates were measured with an AChE inhibition assay	96
Table 4-8 Limits of detection for malathion, oxidized malathion, malaoxon, chlorpyrifos, oxidized chlorpyrifos, chlorpyrifos-oxon, parathion, oxidized parathion, and paraoxon	96
Table 5-1 Concentrations of E1, 17 α -E2, 17 β -E2, EE2, and E3 detected with GC-MS/MS in samples from stormwater structures and the receiving river Anger in Ratingen, Germany and from a stormwater retention basin, draining a highway, and the receiving small stream Deininghauser Bach near Deininghausen, Germany	107
Table 5-2 Analytes and internal standards analyzed with HPTLC-YMEES, GC-MS/MS, LC-MS/MS, or LC-HRMS.	123
Table 5-3 Recovery rates of E1, α -E2, β -E2, EE2, E3, DHT, and P4 in the SPE quality controls in relation to the positive controls	125
Table 5-4 Parameters for the GC-MS/MS analysis of estrogens.....	125
Table 5-5 Analytes and internal standards with information for identification, verification, and quantification with GC-MS/MS	126
Table 5-6 Concentrations of E1, 17 α -E2, 17 β -E2, EE2, and E3 detected with GC-MS/MS in the field blank, SPE blank, and quality control samples	127
Table 5-7 Recovery rates of the internal standards E1-d4, 17 β -E2-d3, and EE2-d4 used for GC-MS/MS analysis in samples from stormwater structures and the receiving river Anger in Ratingen, Germany and from a stormwater retention basin, draining a highway, and the receiving small stream Deininghauser Bach near Deininghausen, Germany.....	127
Table 5-8 Parameters for the LC-MS/MS analysis.....	128
Table 5-9 Analytes and internal standards with information for identification, verification, and quantification with LC-MS/MS	128

Table 5-10 Concentrations of substances detected with LC-MS/MS in samples from stormwater structures and the receiving river Anger in Ratingen, Germany and from a stormwater retention basin, draining a highway, and the receiving small stream Deininghauser Bach near Deininghausen, Germany. The sampling was performed in March 2020 during rainy weather conditions.....	130
Table 5-11 Concentrations of substances detected with LC-MS/MS in samples from stormwater structures and the receiving river Anger in Ratingen, Germany and from a stormwater retention basin, draining a highway, and the receiving small stream Deininghauser Bach near Deininghausen, Germany. The sampling was performed in August 2020 during dry weather conditions.....	131
Table 5-12 Suspect transformation fragment list used for suspect target analysis with LC-HRMS....	132
Table 5-13 Suspect target list used for suspect target analysis with LC-HRMS.....	133
Table 5-14 Limit of detection in µg/L for representative substances used in a reference mix for LC-HRMS.....	136
Table 5-15 Description of rule set for the identification levels adapted from patRoos.....	136
Table 5-16 Features detected with LC-HRMS and suspect transformation fragments in a stormwater retention basin.....	137
Table 5-17 Features detected with LC-HRMS and suspect targets in a stormwater retention basin.....	138

List of Abbreviations

ACh	Acetylcholine
AChE	Acetylcholinesterase
AChE-I	Acetylcholinesterase inhibition
ACN	Acetonitrile
ACTH	Adrenocorticotrophic hormone
ADH	Antidiuretic hormone
AOP	Advanced oxidation process
ATCL	Acetylthiocholine
BEQ	Bioanalytical equivalent concentration
BSTFA	N,O-bis(trimethylsilyl)trifluoroacetamide
CFP	Cyan fluorescent protein
CSO	Combined sewer overflow
DHT	5 α -dihydrotestosterone
DTNB	5,5'-dithiobis(2-nitrobenzoic acid)
E1	Estrone
E2	Estradiol
E3	Estriol
EBM	Effect-based method
EDA	Effect-directed analysis
EDC	Endocrine-disruptive/disrupting compound/chemical
ED _x	Effect dose at which X% effect is observed
EE2	17 α -ethinylestradiol
EHDPP	2-ethylhexyldiphenylphosphat
EQS	Environmental quality standard
FSH	Follicle-stimulating hormone
GC-MS/MS	Gas chromatography coupled to tandem mass spectrometry
GFP	Green fluorescent protein
GH	Growth hormone
HPA	Hypothalamic-pituitary-adrenal
HPG	Hypothalamic-pituitary-gonadal
HPLC	High-performance liquid-chromatography
HPT	Hypothalamic-pituitary-thyroid
HPTLC	High-performance thin-layer chromatography
HPTLC-AChE-I	Combination of high-performance thin-layer chromatography and acetylcholinesterase inhibition assay
HPTLC-Ox-AChE-I	Combination of high-performance thin-layer chromatography, oxidation, and acetylcholinesterase inhibition assay
HPTLC-YMEES	Combination of high-performance thin-layer chromatography and yeast multi-endocrine effect screen
HR	Hormone receptor
HRE	Hormone response element
HRMS	High-resolution mass spectrometry
IC _x	Inhibition concentration at which X% inhibition is observed
LC-HRMS	Liquid chromatography coupled to high resolution mass spectrometry
LC-MS	Liquid chromatography coupled to mass spectrometry
LC-MS/MS	Liquid chromatography coupled to tandem mass spectrometry

LH	Luteinizing hormone
LOD	Limit of detection
LOQ	Limit of quantification
MeOH	Methanol
MoA	Mode of action
NBS	N-bromosuccinimide
OP	Organophosphate
OTP	Organothiophosphate
P4	Progesterone
PBDE	Polybrominated diphenyl ether
PBT	Persistent bioaccumulative toxic
PC	Positive control
PCB	Polychlorinated biphenyl
PCDD	Polychlorinated dibenzodioxin
PCDF	Polychlorinated dibenzofuran
PFC	Perfluorinated chemical
PMOC	Persistent mobile organic compound
PMT	Persistent, mobile and toxic
POP	Persistent organic pollutant
PRL	Prolactin
p-YAS	Planar yeast androgen screen
p-YES	Planar yeast estrogen screen
QC	Quality control
RB	Stormwater retention basin
REACH	Registration, Evaluation, Authorisation and Restriction of Chemicals
R_F	Retardation factor
RSD	Relative standard deviation
SD	Standard deviation
SNTS	Suspect and non-target screening
SoA	Site of action
SPE	Solid-phase extraction
SWR	Stormwater retention structure
T3	Triiodothyronine
T4	Thyroxine
TA	Target analysis
TCIPP	Tris(2-chlorisopropyl)phosphat
TEHP	Tris(2-ethylhexyl)phosphat
TF	Transformation fragment
TP	Transformation product
TRIS	Tris(hydroxymethyl)aminomethane
TSH	Thyroid-stimulating hormone
vPvB	Very persistent and very bioaccumulative
vPvM	Very persistent and very mobile
WFD	Water Framework Directive
WWTP	Wastewater treatment plant
YMEES	Yeast multi-endocrine effect screen

List of publications

Publications in peer-reviewed journals

- Hohrenk L. L., Itzel F., Baetz N., Tuerk J., Vosough M., Schmidt T. C., 2020. Comparison of Software Tools for Liquid Chromatography-High-Resolution Mass Spectrometry Data Processing in Nontarget Screening of Environmental Samples. *Analytical Chemistry*, 92 (2), 1898–1907. <https://doi.org/10.1021/acs.analchem.9b04095>.
- Itzel F., Baetz N., Hohrenk L. L., Gehrman L., Antakyali D., Schmidt T. C., Tuerk J., 2020. Evaluation of a biological post-treatment after full-scale ozonation at a municipal wastewater treatment plant. *Water Research*, 170, 115316. <https://doi.org/10.1016/j.watres.2019.115316>.
- Baetz N., Rothe L., Wirzberger V., Sures B., Schmidt T. C., Tuerk J., 2021. High-performance thin-layer chromatography in combination with a yeast-based multi-effect bioassay to determine endocrine effects in environmental samples. *Analytical and Bioanalytical Chemistry*, 413 (5), 1321–1335. <https://doi.org/10.1007/s00216-020-03095-5>.
- Baetz N., Schmidt T. C., Tuerk J., 2022. High-performance thin-layer chromatography in combination with an acetylcholinesterase-inhibition bioassay with pre-oxidation of organothiophosphates to determine neurotoxic effects in storm, waste, and surface water. *Analytical and Bioanalytical Chemistry*, 414 (14), 4167–4178. <https://doi.org/10.1007/s00216-022-04068-6>.
- Kontchou J. A., Baetz N., Grabner D., Nachev M., Tuerk J., Sures B., 2023. Pollutant load and ecotoxicological effects of sediment from stormwater retention basins to receiving surface water on *Lumbriculus variegatus*. *Science of the Total Environment*, 859 (Pt 2), 160185. <https://doi.org/10.1016/j.scitotenv.2022.160185>.

Publications in non-peer-reviewed journals

- Stricker M., Schmid C., Bätz N., in Vertretung des Forschungskollegs Future Water, 2021. Starkregenereignisse in der wissenschaftlichen Forschung. Eine bibliometrische Analyse zur Interdisziplinarität. *gwf - Wasser|Abwasser*, 05.
- Bätz N., Klein M., Itzel F., Schmidt T. C., Türk J., 2021. Hormonelle Belastung im Fließgewässer während eines Regenereignisses. *GDCh, Mitteilungen Umweltchemie Ökotoxikologie*, 27 (3).
- Bätz N., Itzel F., Klein M., Türk J., Schmidt T. C., 2021. Der Blick aufs Ganze. Mit der wirkungsbezogenen Analytik anthropogene Einträge in Oberflächengewässer bewerten. *GDCh, Fachgruppe Analytische Chemie, Mitteilungsblatt*, 3.

Oral Presentations

- Baetz N., Rothe L., Wirzberger V., Schmidt T. C., Tuerk J. High Performance Thin-Layer Chromatography in Combination with a Yeast-Based Bioassay to Determine Endocrine Effects. 11th Micropol & Ecohazard Conference, Seoul, Korea, 20.10. – 24.10.2019.

Poster Presentations

- Bätz N., Itzel F., Gehrman L., Schmidt T. C., Türk J. Agonistic and Antagonistic Effects. Ozonation and Biological Post-Treatment. MWAS, Mülheim an der Ruhr, 12.09. – 13.09.2018.
- Bätz N., Itzel F., Gehrman L., Schmidt T. C., Türk J. Agonistic and Antagonistic Effects. Ozonation and Biological Post-Treatment. XENOWAC, Limassol, Zypern, 10.10. – 12.10.2018. Auszeichnung: 1. Platz.
- Bätz N., Schmidt T. C., Türk J. Kombination aus HPTLC und Bioassay zur Bestimmung von drei hormonellen Effekten. ANAKON, Münster, 25.03. - 28.03.2019.

Declaration of Scientific Contributions

This thesis includes work that was published in cooperation with co-authors. My own contributions are declared in the following:

Chapter 3: Conceptualization, Methodology, Validation, Formal analysis, Investigation, Writing - Original Draft, Writing - Review & Editing, Visualization

Chapter 4: Conceptualization, Methodology, Validation, Formal analysis, Investigation, Writing - Original Draft, Writing - Review & Editing, Visualization

Chapter 5: Conceptualization, Methodology, Validation, Formal analysis, Investigation, Writing - Original Draft, Writing - Review & Editing, Visualization

Curriculum Vitae

Der Lebenslauf ist in der Online-Version aus Gründen des Datenschutzes nicht enthalten.

Danksagung

“Over every mountain there is a path, although it may not be seen from the valley” (THEODORE ROETHKE, 1908 – 1963). In diesem Sinne habe ich es geschafft im Laufe meiner Promotion und bei der Erstellung dieser Arbeit ganze Bergketten zu überwinden. Dies wäre mir ohne einige wichtige Menschen nicht möglich gewesen, denen ich hier meinen Dank ausprechen möchte.

Zunächst bin ich dankbar, dass ich im Rahmen des Forschungskollegs FUTURE WATER mit öffentlichen Mitteln promovieren und diese Arbeit anfertigen konnte. Außerdem denke ich gerne an die Zeit mit den FuWa Kollegiaten, insbesondere während der gemeinsamen Reisen, zurück. Vielen Dank für die schöne Zeit.

Meinem Doktorvater, Prof. Dr. Torsten C. Schmidt, und meinem Betreuer, Dr. Jochen Türk, möchte ich an dieser Stelle ganz herzlich danken. Ihr habt mir den Beginn meiner Promotion ermöglicht, meine Arbeit mit Euren wissenschaftlich analytischen Blicken begleitet und mir durch Euer Vertrauen geholfen, meine Dissertation zu einem erfolgreichen Abschluss zu bringen.

Mein Dank gilt auch allen Kolleginnen und Kollegen am IUTA, die mich bei meiner praktischen Arbeit im Labor unterstützt haben. Außerdem danke ich allen Koautorinnen und Koautoren für ihre Beiträge zu meinen Veröffentlichungen.

Prof. Dr. Dr. h.c. Henner Hollert danke ich ganz herzlich für die Übernahme des Zweitgutachtens.

Mein besonderer Dank gilt meinem Mentor Prof. Dr. Thomas Grünebaum. Bei unseren regelmäßigen Treffen während der gesamten Promotionszeit bis zum Abschluss der Dissertation haben Sie meine Motivation immer wieder neu geweckt und mir darüber hinaus wertvolle Hinweise für meinen Berufsalltag vermittelt.

Ihr habt mich auf meinem bisherigen Lebensweg mit all seinen Höhen und Tiefen begleitet und unterstützt. Liebe Mama, lieber Papa, danke, dass Ihr bei mir seid.

Abschließend möchte ich zum Ausdruck bringen, dass ich dankbar bin, in einem Land zu leben, in dem Wissenschaft frei und offen betrieben werden kann und wo Ideen, Methoden, Ergebnisse und Schlussfolgerungen öffentlich präsentiert und diskutiert werden können.